# Adsorption Study of Block Copolymers at Solid/Liquid Interfaces

JABIR ALI SHAR


A thesis submitted in partial fulfilment of the requirements for the degree of Doctor of Philosophy.

School of Chemistry Faculty of Science
University of Bristol, Bristol.

November 1998.

# Declaration

Except in cases where acknowledged the work presented in this thesis is the sole work of the author. This work has been carried out at the University of Bristol, between May 1994 and November 1998 and has not previously been submitted, either wholly or in part, for this or any other degree.

Jabir Ali Shar

November 1998

## Publications

*As a result of this study, the following publications have been made;*

1) Cosgrove, T., Shar, J., Obey, T., Richardson, T., Clifton, B., Griffiths, P.C., Booth, C., Yu, G.E., "The adsorption of tri-block copolymers at the solid-liquid and liquid-liquid interface";*Abstracts of Papers of the American Chemical society*, 1996 Vol.212, No. Pt1, pp.153-COLL.

2) Shar, J.A, Obey, T. and Cosgrove, T., "Adsorption studies of polyethers, part I: "Adsorption onto hydrophobic surfaces"; *Colloids and Surfaces, A: Physicochem. and Eng. Aspects*, 1998, Vol. 136, pp 21-33.

3) Griffiths, P. C., Cosgrove, T., Shar, J., King, S. M., Yu, G. E., Booth, C., and Malmsten, M., "Role of copolymer architecture on adsorption at the solid/liquid interface"; *LANGMUIR*, 1998, Vol.14, No.7, pp.1779-1785.

4) Shar, J. A, Obey, T., and Cosgrove, T., "Adsorption studies of polyethers part II: Adsorption onto hydrophilic surfaces;" C*olloids and Surfaces, A: Physicochem. and Eng. Aspects*, Paper in press.

5) Shar, J. A., Cosgrove, T., Obey, T., and Wedlock, D., "Adsorption studies of AB-type diblock copolymers at cyclohexane/carbon black interface";
Paper submitted to Langmuir.

6) Shar, J. A, Obey, T. and Cosgrove, T., "Adsorption studies of reverse Pluronics, part III: Adsorption onto hydrophobic surface;"
Paper in preparation.

7) Shar, J. A, Obey, T. and Cosgrove, T., "Adsorption studies of reverse Pluronics, part IV: Adsorption onto hydrophilic surface;"
Paper in preparation.

8) Shar, J. A., Cosgrove, T. and Obey, T., "Adsorption studies of PEO homopolymers and PEO-PBO block copolymers, part V: Adsorbed onto hydrophobic and hydrophilic surfaces;"
Paper in preparation.

# Dedication

This work is dedicated to my parents, who sadly didn't live long enough to see me finish my Ph D., Mahran, my dear little son, who has suffered a lot in his young age and tried all his best to divert my attention. Finally, to my family for their co-operation and encouragement.

# Acknowledgements

I would like to thank Professor Terry Cosgrove for his advice, support and encouragement on all aspects of this work. Special thanks should go to Tim Obey for his guidance and encouragement throughout. Also thanks to all of the old and new players of TC Empire, BV kingdom, and J Eastoe estate.

Also, thanks will go to Shah Abdul Latif University, Khairpur, Sindh, Pakistan, for providing funds and granting study leave, which enabled me to carry out this work.

Finally, my thanks must go to my parents, family and the Tee family without whom I would haven't been able to carry out this work.

Jabir Ali Shar

# Table of Contents

# Chapter 1

# *INTRODUCTION*

Over the last few decades the adsorption of polymers at the solid-liquid interface has become the focus of attention for both theoretical and experimental studies, in both natural and synthetic systems.[1,2,3,4,5,6] In the latter case various technical areas employ the presence of macromolecular species at an interface to modify the physical characteristics of a particular system. These areas include the stability of colloidal dispersions,[7] adhesion,[8] corrosion inhibition,[9] lubrication[10] and composite materials.[11] Natural processes where polymer adsorption has been found to be important include the antibody/antigen reaction,[12] cell cohesion[13] and bacterial aggregation.[14]

Polymers are used widely in industrial and pharmaceutical applications as stabilisers in the field of colloidal systems. Polymer stabilisation strongly depends upon the inter-particle energy,[15] which, in turn strongly depends on the structure of the adsorbed polymer layer. The adsorbed polymer configuration may be determined by a number of factors, for example, the adsorbed amount, $\Gamma$, and the hydrodynamic thickness, $\delta_H$. $\Gamma$ and $\delta_H$ are expected to depend strongly on polymer molar mass (chain length), polymer architecture[16,17] and the nature of the polymer-surface and polymer-solvent interaction energies. A detailed knowledge of the polymer adsorbed layer conformation is essential for predicting the stability of a colloidal dispersion.[18]

A good steric stabiliser attaches firmly to a particle surface and hence gives a high level of polymer adsorption, which, results in a thick polymer adsorbed layer (in good solvency conditions). This prevents polymer desorption as well as polymer aggregation in the system.[19] It is difficult to fulfil all these requirements simultaneously with a homopolymer; however, these requirements may be met simultaneously by using the AB or ABA- type block copolymers.[20] For the case of block copolymers one of the blocks, which has a strong surface affinity but is partially soluble in the bulk solution acts as an "*anchor*". This strong segment-surface interaction can be expressed in terms of the surface-Flory parameter, $\chi_s$, and is

equivalent to the net exchange energy required for displacing an adsorbed solvent molecule with a polymer segment from the surface. The second block which is highly soluble in the bulk solution and possesses a lower particle-surface affinity ($\chi$, Flory-Huggins parameter < 0.5) as compared to *anchor* block is called "*buoy*" block. This *buoy* block is mainly responsible for forming the steric barrier in the system.

The stabilisation of paints is considered as one of the oldest processes to employ polymer adsorption in ancient times. It is generally found in many practical systems that 'charge stabilisation', described by the classic Deryagin-Landau-Verwey-Overbeek (DLVO) theory[21] for the overlap of the electrical double layers around the particles, and steric stabilisation operate simultaneously in aqueous systems. Dispersions containing polymer stabilisers have a wide variety of applications in the pharmaceutical, cosmetic, paint, paper, agriculture and processed foodstuffs industries. Therefore, an understanding of the fundamental principles governing polymer adsorption and the interactions taking place at the interface is of great technological importance.[17,20,22,23]

Polymer adsorption is considered as an important aspect of adhesion[8,24] and it covers both synthetic as well as naturally occurring polymers. Due to strong adhesive and stabilising properties the polymers like poly(vinyl alcohol) (PVA), starch, soybean extract, poly(acrylates), polyesters and rubber *etc.* are widely used[8] in the paper industry. PVA, due to its high solubility in water, has achieved a very important place in the paper industry for binding and sticking purposes. Also, adsorbed polymers are widely used as strong adhesives in certain industrial composite materials. A composite material of the required physical properties can be obtained by varying the strength of various interaction energies taking place in the system.[11]

It is predicted that the layer conformation adopted by an adsorbed polymer layer at an interface depends upon various factors, for example, polymer composition, polymer structure, surface-segment interactions, concentration and the temperature. The polymer conformation plays a vital role in understanding polymer adsorption in various systems; hence it is necessary to have knowledge of adsorbed layer conformation. In an adsorbed layer the adsorbed polymers are considered to adopt a conformation consisting of '*trains*', the polymer segments closely linked to the surface, whereas "*loops*" and "*tails*" are the segments extending out into the bulk

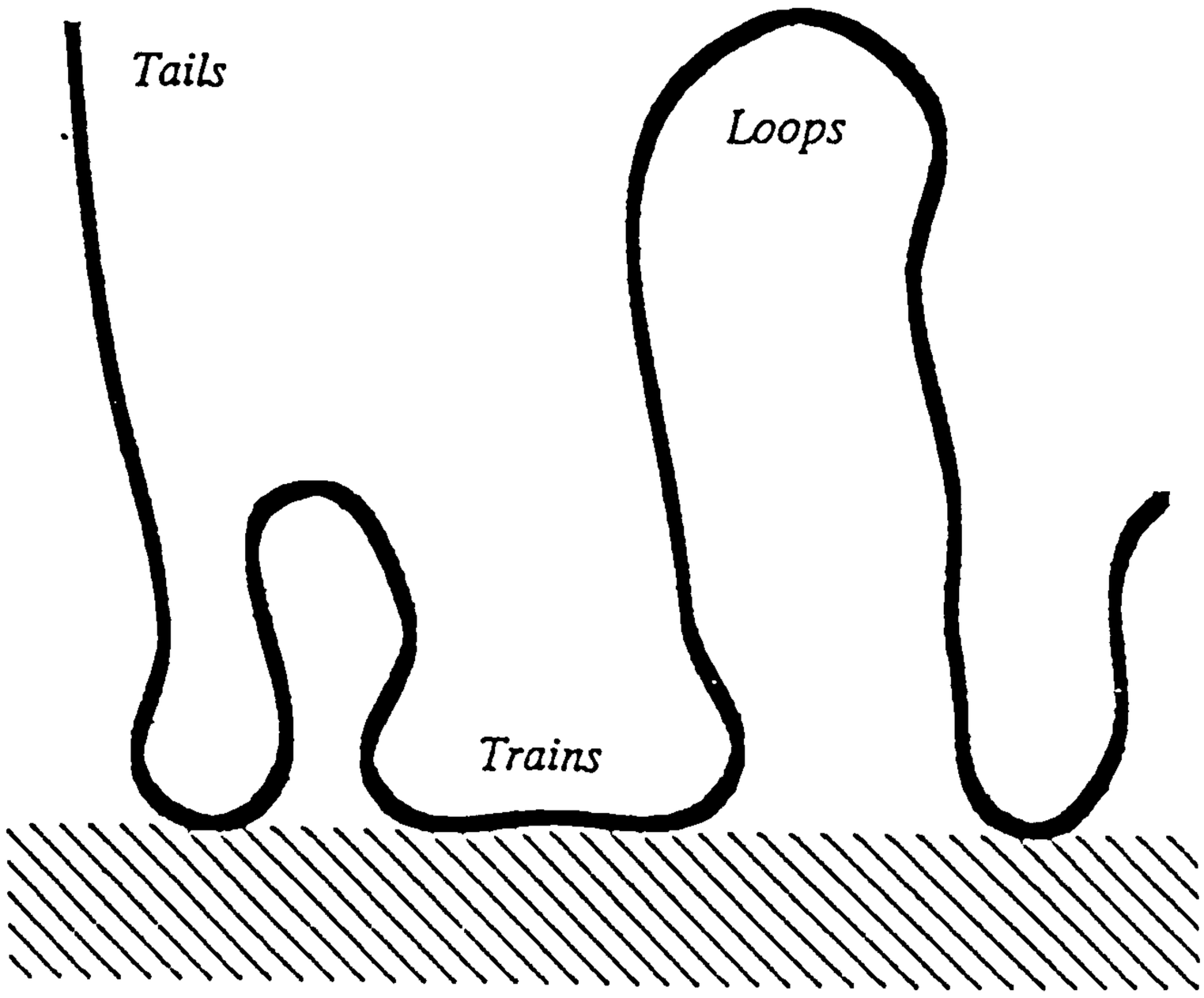


*Figure 1.1: Schematic diagram showing trains, loops and the tails of a polymer.*

solution[25], *see* for instance, Figure 1.1. A loop is a string of segments between any two segments bound to the surface and tails extend into the bulk.

In this study we aim to obtain a better understanding of the role of the polymer composition and the molecular architecture on adsorption using a series of diblock and triblock copolymers, adsorbed at the solid/liquid interface. More specifically we aim to investigate the effects of the total copolymer molar mass, concentration, anchor and buoy block sizes on the level of adsorption and the layer thickness for a much more wider range of copolymers with varying composition than has so far been studied.[3,4,5,6,26]

We have selected a range of AB diblock, and BAB and ABA-type triblock copolymers, since they are readily obtainable in a wide range of molar masses in relatively pure form and have commercial relevance. Also, for comparison purposes, a set of PEO, poly(ethyl oxide), homopolymers was studied, since the data obtained for PEO may be helpful in understanding the influence of PEO-PPO, PEO-PBO block ratios on the polymer adsorption, where PPO and PBO stand for poly(propylene oxide) and poly(butylene oxide), respectively. The macromolecules used in this study can be classified as;

1) PEO homopolymers;

2) BA type diblock copolymers; where, B stands for *buoy* and A for *anchor* blocks;

   (a) $PS_m$-$HPIP_n$ diblock copolymers; where, PS stands for polystyrene and HPIP for hydrogenated-polyisoprene blocks, where m and n are the monomer number of the respective segments.

   (b) $PEO_m$-$PBO_n$ diblock copolymers; the copolymers used were of both linear as well as cyclic structures.

3) BAB type triblock copolymers;

   (a) Pluronic copolymers with the general structure $PEO_m$-$PPO_n$-$PEO_m$.

   (b) $PEO_m$-$PBO_n$-$PEO_m$ copolymers having linear and ring structures.

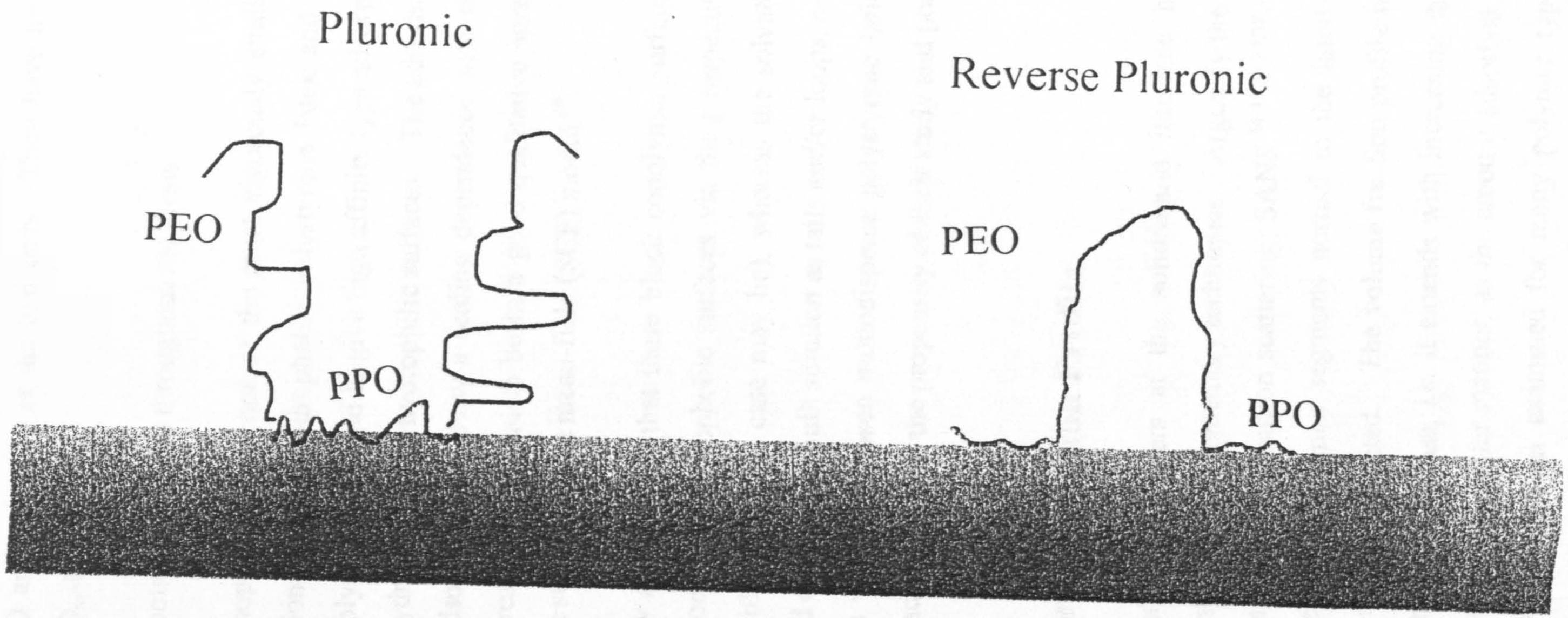


*Figure 1.2: Schematic diagram for the adsorption of triblock copolymers at an aqueous/hydrophobic interface*

4) ABA type triblock copolymers; Reverse Pluronic copolymers are the inverse of the normal Pluronics with a PEO block in the middle and two PPO anchor blocks at the two ends. They have the general structure $PPO_m$-$PEO_n$-$PPO_m$.

All these symbols will be used throughout the thesis.

The PEO homopolymers are one of the most vigorously studied polymers with respect to adsorption on both hydrophobic polystyrene latex and hydrophilic silica surfaces. These polymers are found to give high affinity type adsorption isotherms for the cases of both hydrophobic and hydrophilic surfaces. The adsorbed amount and the thickness of the adsorbed layer show a scaling dependence with the polymer molar mass.[27,28,44] The results are found to be in a good qualitative agreement with those calculated using the self-consistent mean-field (SCF) model.[29]

It is generally assumed[30,31] that these block copolymer surfactants adsorb from polymer solutions onto the hydrophobic surfaces via their respective *anchor* blocks (PPO, PBO or PS blocks, as the case may be), whereas the solvated *buoy* (PEO or HPIP) blocks extend out into the bulk solution as tails and/or loops, *see* Figure 1.2. As a model adsorbents we have chosen monodisperse polystyrene latices, Snowtex-YL silica and carbon black because of the propensity of their study and practical uses.[32,33]

## 1.1. The Volume Fraction Profile

The adsorption of polymers at the solid/liquid interface has been studied extensively by a number of complementary techniques. Arguably the most informative technique has been small-angle neutron scattering, SANS,[34,35,36,37,38,39] from which the concentration profile of the polymer segments normal to the interface - the *volume fraction profile* ($\phi$)- can be extracted. The volume fraction profile has been found to depend on the polymer molar mass, *i.e.* it extends with increasing the polymer molar mass.[40] It also extends in a similar manner, as the amount adsorbed increases.[41] The volume fraction profile has been examined for many polymer types ranging from simple homopolymers to complex block copolymers.[42] It is predicted theoretically that the homopolymers adopt an exponentially shaped volume fraction profile, mainly for

the segments forming the loops. The adsorbed amount, which is the integral under the volume fraction profile, depends on the equilibrium polymer concentration and molecular weight of the polymer and the relative magnitudes of the segment-solvent, solvent-solvent, segment-segment and segment-surface interaction energies (the Flory parameters). Previous studies also show a strong dependence of the polymer adsorption on molecular weight, particularly at low values of molar mass. It was observed that both of the adsorption parameters, the adsorbed amount[40,43] and the hydrodynamic thickness of the polymer adsorbed layer, increase with increasing molar mass up to a limiting value, when a plateau value is observed. Furthermore, it was also observed that the molar mass effect becomes weaker for the case of high molar mass polymers having high PEO content (and hence low anchor fraction) and will be stronger for low molar mass and high anchor fraction polymers. Several investigations have also reported this trend for Pluronics, Synperonics and random copolymers of PEO and PPO blocks adsorbed onto hydrophobic polystyrene latex.[5,6,44] Cohen-Stuart *et al*[44] have shown a very strong dependence of the adsorbed amount on polymer molar mass for PEO homopolymer/polystyrene latex systems and compared them with the data calculated using Scheutjen-Fleer theory.

## 1.2. Adsorbed Amount

The influence of the PEO:PPO block ratio of the copolymers on the adsorbed amount has also been determined for the triblock copolymers on both silica and latex systems. Kayes *et al.*[45] and Baker *et al.*[5] in their separate works have investigated the adsorption of PEO homopolymers and the PEO-PPO-PEO block copolymers adsorbed on latices. Baker *et al* predicted an increase in both adsorbed amount and the adsorbed layer thickness with increasing the PEO block size and the polymer solution concentration. Kayes *et al.* and Baker *et al* have also predicted the firm attachment of the PPO blocks with the surface in trains /loops, whilst, the PEO blocks remain extended out in the solution in loops or tails, and are mainly responsible for the thickness of the polymer adsorbed layer.

Overall the triblock copolymers adsorb at lower level on silica than the latex and show an increase in the adsorbed amount with increasing the total polymer molar mass

of the samples. Malmsten *et al.*[26] have shown that for the case of triblock copolymers adsorbed on silica both the adsorbed amount and the adsorbed layer thickness are independent of the total polymer molar mass (up to 15000). Schroen *et al.*[30] have shown that for PPO-PEO block copolymers adsorbed on hydrophilic surface, both the PPO and PEO blocks interact with the surface through hydrogen bonds and are firmly attached to the surface. This gives rise to a flat "pancake" configuration for the adsorbed layers, which corresponds to the formation of thin adsorbed layers and hence very low adsorbed amounts are obtained. Killmann *et al.*[3] and Lucie *et al.*[46] in their separate works have also presented relatively lower adsorption of PEO homopolymers and the block copolymers, respectively, for hydrophilic surfaces than hydrophobic surfaces. Lucie *et al.*[46] have studied the same set of triblock copolymers on two different surface chemical gradients (*i.e.* one more hydrophobic and the other more hydrophilic) and have found lower adsorption of the polymers for the more hydrophilic surface than that observed for the more hydrophobic surface.

It has been shown that high molar mass polymers preferentially adsorb over those having lower molar mass, and hence any polydispersity in the polymers used will lead to difficulty in the interpretation of the results obtained.[47,48] Mallagh[49] has shown that the polydispersity in the polymer molar mass or in the polymer composition makes the bulk concentration required for plateau adsorption much higher than that required for the monodisperse systems.

For adsorbing homopolymers, the adsorbed amount derived from the plateau region of the adsorption isotherm depends on the logarithm of molecular weight for $\theta$ solvents, but has a weaker dependence for good solvents. However, for the case of copolymers, it is rather complex to understand the adsorption process, since many different interactions can lead to more complex shapes for the polymer configuration and the volume fraction profile. Typical functional forms invoked to discuss adsorbed layers include Gaussian (end-grafted polymers)[1] and rectangle plus exponential (AB block copolymers).[50] For a selective solvent, a melt of the insoluble block can be formed at the surface whilst the soluble block forms a highly extended "mushroom" or "brush" type conformation.[18,51]

Polymer adsorption has also been found to be affected by variations made in the

"system temperature" and that the adsorption may increase or decrease with increasing temperature.[52] This effect may be due to any possible changes brought about in the solvency and flexibility of the polymer as a result of the temperature variations.

The adsorption of diblock copolymers at interfaces has been widely examined, mainly by varying the copolymer composition (*e.g.* the length of one block) but with the same (linear) architecture. Commonly studied systems include diblock copolymers of dimethyl-aminoethyl-methacrylate and n-butyl methacrylate adsorbed from 2-propanol onto mica[53], ethylene oxide and styrene[54], as well as 2-vinyl pyridine and styrene (and its derivatives)[55] on mica from toluene. All these data are well described by the theoretical predictions. However, there have been far fewer experimental studies of the role of copolymer architecture in adsorption at the solid/liquid interface, where the architecture of the copolymer is varied but its composition is unchanged. This is primarily due to difficulties in chemical synthesis although the poly(ethylene oxide)-poly(propylene oxide) PEO-PPO series has been studied extensively.[56] Many of these studies, however, do not compare copolymers at constant chain compositions.

Recently, a study of the adsorption of a similar series of PEO-PBO copolymers ($E_{41}B_8$, $E_{21}B_8E_{21}$ and $B_4E_{40}B_4$) from aqueous solution onto methylated silica has been presented[57]. The diblock was found to have the greatest adsorbed amount due to the fact that the diblocks are attached to the adsorbent surface more strongly and more efficiently than the triblocks of the corresponding molar masses. The two triblocks exhibited comparable adsorbed amounts, which were significantly less than that of the diblock. The adsorption data were well described by mean-field theory provided the polydispersity of the PBO block was accounted for, but no cyclic polymer was studied.

## 1.3. Cyclic Copolymers

Cosgrove and van Lent[58] have used the self-consistent mean-field theory to compare the adsorption of cyclic and linear homopolymers and predicted that for low molar mass, cyclic polymers would adsorb more than linear chains with the same number of monomers. However, they predicted an adsorption energy dependent crossover for the polymers with intermediate chain lengths. In a series of experiments these effects were substantiated.[59,60] Subsequently, Joanny and Johner[61] presented a

mean-field description of the adsorption from very dilute solution of homopolymers with other architectures, cyclic, star and comb polymers. Close to the particle surface, the segment density ρ(z), has the same scaling behaviour as for the equivalent linear homopolymer system. Here the z-axis is taken to be normal to the interface whilst the x and y axis parallel to the interface. The segment density governs the interactions between approaching particles in a dispersion.[62] Towards the periphery of the polymer layer, the segment density is dominated by the tail fraction (of which the cyclic homopolymer has none), and thus the linear homopolymer forms a thicker layer. The parameters like fraction of segments in contact with the surface, bound fraction, and the layer thickness, rms. though are not experimentally measurable, but can be derived from the segment density distribution values of the adsorbed polymer. In the limit of infinite molecular weight, Joanny and Johner[61] predict that the adsorbed amount would be higher for a linear polymer compared to an equivalently sized cyclic. Furthermore, the thickness of the polymer adsorbed layers formed from star and comb homopolymers are the same as that formed by a linear homopolymer after correcting to an equivalent number of segments.

## 1.4. Reverse Pluronic Copolymers

Very little work is available for the study of adsorption of the reverse Pluronics at the solid/liquid interface. Balazs *et al*[63] predicted an *end-to-end* interaction of the *anchor-anchor* blocks of the two neighbouring molecules for the case of generic ABA - type copolymers. The interactions of that type result in a continuous increase in the adsorbed amount without reaching any plateau level. It is also predicted that the *end-to-end* type interactions (through hydrophobic bonding with the PPO groups) increase with increasing the total polymer molar mass, *anchor:buoy* ratio and the polymer solution concentration in the bulk. Overall, the level of polymer adsorption has been predicted to depend on the total polymer molar mass, however, this effect weakens for the case of more hydrophilic polymers. Baker *et al.*[5] have studied the adsorption of the reverse Pluronics of the same series (10R8, 25R2 and 25R8) adsorbed from aqueous solution onto the latex surface. As predicted they also have shown an approximate linear dependence of the plateau levels of the adsorption isotherms on the polymer molar mass and the equilibrium concentration. Killmann *et al.*[64] have presented a

strong dependence of the adsorbed amount derived from the pseudo-plateau levels of the adsorption isotherms on the total polymer molar mass for the similar series of reverse Pluronics adsorbed onto aerosol 200 from CCl4 and CHCl3 solvents, using the infra red (IR) spectroscopy. They also discussed the influence of PEO:PPO block ratio present in the reverse Pluronics on the adsorbed amount and the adsorbed layer thickness: the polymers with low PEO content (PEO≤10%) behave more like a PPO homopolymer of the same molar mass, whilst, those having higher PEO content (PEO ≥80%) behave more like PEO homopolymers. However, no such *anchor-anchor* attachments between the end blocks of the neighbouring polymers, as predicted by Balazs *et al.*[63] have been so far presented in the literature.

In this work, the role of copolymer architecture and polymer composition in adsorption was also investigated by comparing SANS, adsorption isotherms and photon correlation spectroscopy, PCS, results for a series of poly(ethylene oxide) - poly(butylene oxide) and poly(ethylene oxide) - poly(propylene oxide) copolymers; adsorbed from aqueous solution onto polystyrene latices and silica. The study presented here involves a more extensive range of copolymers and in particular the block polymers with different architectures but the same monomer composition. The experimental data are compared with theoretical calculations.

# References


[1] Cosgrove, T., *J. Chem. Soc., Faraday Trans-1* 1990, **86**,1323.

[2] Cosgrove, T., Mallagh, L. M., Ryan, K., and Scheutjens, J. M. H. M., *J. Surface Sci. Technol.* 1988, **4**, 81.

[3] Killmann, E., Maier, H., and Baker, J. A. ,*Colloids & Surf.* 1988, **31**, 51.

[4] Baker, J. A., Pearson, R. A., and Berg, J. C., *Langmuir* 1989, **5**, 339.

[5] Baker, J. A. and Berg, J. C., *Langmuir* 1988, **4**, 1055.

[6] Tadros, Th. F.,and Vincent, B., *J. Phys. Chem.* 1980, **84**, 1575.

[7] Mateau, L., Tardieu, A., Luzzati, V., Aggerbeck, L., and Schanu, M., *J. Molec. Biol.*, 1972, **70**, 105.

[8] Toyoshima, K., in "Polyvinyl Alcohol, Properties and Applications" Ed. Finch, C. A., John Wiley, London.

[9] Kennedy, P., Petronio, M., and Gisser, H., *J. Phys. Chem.* 1971, **75**, 1975.

[10] Forbes, E. S., Groszek, A.J., and Neustadter, E. L., *J. Colloid & Intf. Sci.*, 1970, **33**, 629.

[11] Kenyon, A. S., *J. Colloid. & Intf. Sci.*, 1968, **27**, 761.

[12] Goldberg, R. J., *J. Am. Chem.* Soc., 1952, **74**, 5715.

[13] Pethica, B. A., *Expt. Cell. Res. Suppl.*, 1961, **8**, 123.

[14] Busch, P. L., and Stumm, W., *Environ. Sci., Technol.* 1968, **2**, 49.

[15] Luckham, P. F., *Curr. Opin. Coll. Int. Sci.* 1996, **1**,(1) 37.

[16] Sato, T., and Ruch, R., "Stabilization of Colloidal Dispersions by Polymer Adsorption" Marcel Dekker, New York, 1980.

[17] Napper, D. H., "Polymeric Stabilization of Colloidal Dispersions", Academic, London, 1983.

[18] Fleer, G. J., Cohen Stuart M. A., Scheutjens, J. M. H. M., Cosgrove, T. and Vincent, B., "Polymers at Interfaces" 1st Ed. Chapman and Hall, London, 1993.

[19] Clifton B., Ph.D. Thesis, University of Bristol, Bristol, 1996.

[20] Vincent, B. and Whittington, S. G., in E. Matijevic Ed., "Surface and Colloid Sci.", Vol. **12** Plenum Press, New York, 1982, p 1-117.

[24] Schrader, M. E., and Block, A., *J. Polym., Sci.*, 1971, **C34**, 281..

[25] Jenkel, E. And Rumbach, B., Z. Electrochem., 1951, **55**, 612.

[26] Malmsten, M., Linse, P., and Cosgrove, T., *Macromolecules*, 1992, **25**, 2474.

[27] Cohen-Stuart, M. A., Cosgrove, T., and Vincent, B., *Adv. Coll. Int. Sci.* 1986, **24**, 143.

[28] van der Beek, G. P., and Cohen-Stuart, M. A., *Langmuir*, 1991, **7**, 327.

[29] Evers, O. A., Scheutjens, J. M. H. M., and Fleer, G. J., *J. Chem. Soc. Faraday Trans.I*, 1990, **86** (9), 1333.

[30] Schroen, C. G. P. H., Cohen-Stuart, M. A., van der voort Maarschalk, K., van der Padt, A., and van't Riet, K., *Langmuir*, 1995, **11**, 3068.

[31] Alexandridis, P., and Halton, T. A., *Colloids and Surfaces A: Physicochemical and Engineering Aspects* 1995, **96**, 1.

[32] Pluronic and Tetronic Surfactants, "Technical Brochure, BASF Wyandotte Corporation", Parsippany, N. J., 1989.

[33] Goodwin, J. W., Hearn, J., Ho, C. C., and Ottewill, R. H., *Colloid and Polymer Sci.* 1974, **252**, 464.

[34] Cosgrove, T., Heath, T. G., and Ryan, K., *Langmuir* 1994, **10**, 350.

[35] Auroy, P., and Auvray, L., *Macromolecules* 1996, **29**, 337.

[36] Auroy, P., and Auvray, L., *J Phys II* 1993, **3**, 227.

[37] Auroy, P., Auvray, L., and Leger, L., *Macromolecules* 1991, **24**, 2523.

[38] Auroy, P., Auvray, L., and Leger, L., *Physica A* 1991, **172**, 269

[39] Auvray, L., and Cotton, J. P., *Macromolecules* 1987, **20**, 202.

[40] Kawaguchi, M., Hayakawa, K., and Takahashi, A., *Polymer, J.*, 1980, **12**, 265.

[41] Day, J. C., and Robb, I. D., *Polymer*, 1980, **21**, 408.

[42] Milner, S. T., *J Polym Sci , Part B: Polym. Phys.* 1994, **32**, 2743.

[43] Van der Linden, C., and Van Leemput, R., *J. Colloid & Intf. Sci.*, 1978, **67**, 48.

[44] Cohen-Staurt, M. A., Waajen, F. W. H., Cosgrove, T., Vincent, B. and Crowley, T. L., *Macromolecules*, 1984, **17**, 1825.

[45] Kayes, J. B., and Rawlins, D. A., *Colloid Polym. Sci.* 1979, **257**, 622.

[46] Lucie, M. A., Van de Steeg and Carl-Gustaf Golander, *Colloid & Surf.* 1991, **55**, 105.

[47] Cohen Stuart, M. A., Scheutjens, J. M. H. M., and Fleer, G. J, *J. Polym. Sci., Polym. Phys.*, 1980, **18**, 559.

[48] Koopal, L. K., *J. Colloid & Intf. Sci.*, 1981, **83**, 116.

[49] Mallagh, L. M., Ph.D. Thesis, Bristol, 1989.

[50] Griffiths, P. C., Cosgrove, T., and Hair, M. L., *Macromolecules* 1996, *submitted.*

[51] Marques, C. M., Joanny, J. F., and Leibler, L., *Macromolecules*, 1988, **21**, 1051.

[52] Gilliland, E. R., and Gutoff, E., B., *J. Appl. Polym. Sc.*, 1960, 3, 26.

[53] Wu, D. T., Yokohama, A., and Setterquist, R. L., *Polymer Journal* 1991, **23**, 711.

[54].Guzonas, D., Boils, D., Hair, M. L., and Tripp, C., *Macromolecules* 1992, **24**, 2434, and Lai, D., and Toprakcioglu, C., *Europhys. Lett.* 1991, **16**, 331.

[55] (a) Parsonage, E., Tirrell, M., Watanabe, H., and Nuzzo, R. G., *Macromolecules* 1991, **24**, 1987; (b) Webber, R. M., Anderson, J. S., and John, M. S., *Macromolecules* 1990, **23**, 1026; (c) Hadziiannou, G., Patel, S., Granick, S., and Tirrell, M., *J. A. C. S.*, 1986, **108**, 2869; (d) Guzonas, D., Hair, M. L., and Boil, D., *Macrocmolecules* 1991, **24**, 3383.

[56] Chu, B., In "Non-Ionic Surfactants" Nace, V. M.; Ed.; Marcel Dekker Inc.; New York, 1996.

[57] Schillen, K., Claeson, P. M., Malmsten, M., Linse, P., and Booth, C., *J. Phys. Chem. B* 1997, **101**, 4238.

[58] Cosgrove, T., van Lent, B., and Scheutjens, J. H. M. H., *Macromolecules* 1987, **20**, 366.

[59] Patel, A. Semlyen, A. J., and Cosgrove T., *Polymer* 1991, **32**, 1313.

[60] Cosgrove, T., Prestidge, C. A., King S. M., and Vincent, B., *J. Chem. Soc. Faraday Trans.* 1990 , **86**, 1377.

[61] Joanny, J. F., and Johner, A., *J. Phys. II,* 1996, **6**, 511.

[62] Vincent, B., Adv. *Colloid & Intf. Sci.*, 1974, **4**, 193.

[63] Balazs, A. C., and Lewandowski, S., *Macromolecules*, 1990, **23**, 839.

[64] Killmann, E., Fulka, C., and Reiner, M., *Chem. Soc. Faraday Trans.* 1990, **86**, 1389.

# Chapter 2

# *POLYMER SYSTEMS*

## 2.1. Introduction

Over the last 40 years, polymer adsorption has become a centre point for both academic and technological study. Both theoretical and experimental investigations have been carried out on the mechanism of polymer adsorption and on the conformation which polymers attain at interfaces. Polymers may now be found in most areas of colloid science; from polymers in solution through micelles, membranes, vesicles, to polymer stabilised emulsions and dispersions and have a wide variety of industrial applications as stabilisers in foams and suspensions, and as flocculating agents, adhesives, wetting agents and soil improvers, *etc.*

## 2.2. Polymer Chain Dimensions

Early theories of polymer conformation focused on the prediction of coil dimensions using simple physical models; volumeless, freely rotating segments which did not interact, coupled with the concept of a three dimensional random walk through space. These conditions led to the prediction of two useful parameters to describe polymer conformation: (I) the root-mean-square end to end distance $\langle r^2 \rangle^{1/2}$ and (ii) the radius of gyration, $R_g$. The chain dimensions can be determined by several methods; for example, light scattering measurements can be used to obtain the radius of gyration, $R_g$.

### 2.2.1. The Root-Mean-Square Dimensions (RMS) of a Polymer

The average of all possible conformations of the polymer chains gives the root-mean-square end-to-end distance "RMS" dimensions, $\langle r^2 \rangle^{1/2}$, where r is the end to end distance. If "N" is the number of segments present in a chain and "*l*" is the bond length

of each chain then;

for an ideal random walk

$$\underline{\langle r^2 \rangle = Nl^2} \qquad \text{Equation 2. 1}$$

$$RMS = \langle r^2 \rangle^{1/2} = (Nl^2)^{1/2} \qquad \text{Equation 2. 2}$$

This gives a Guassian distribution of end-to-end distance, r.

## 2.2.2. The Radius of Gyration, $R_g$

$R_g$ is defined as the root-mean-square distance of segments from the centre of mass of the coil, where there is a finite probability of finding a polymer segment at a certain distance from the centre of the mass. $R_g$ can be defined as;

$$R_g^2 = \frac{\sum_{i=1}^{N} m_i r_i^2}{\sum_{i=1}^{N} m_i} \qquad \text{Equation 2. 3}$$

$$\text{And } \langle R_g^{\,2} \rangle = \frac{\langle r^2 \rangle}{6} \qquad \text{Equation 2. 4}$$

The radius of gyration $R_g$, of a chain is therefore proportional to the square root of the total polymer molar mass, M.

$$R_g = \frac{N^{1/2} l}{\sqrt{6}} \qquad \text{Equation 2. 5}$$

$$R_g \alpha M^{1/2} \qquad \text{Equation 2. 6}$$

## 2.2.3. Real Chains and Excluded Volume Effects

Since real molecules do interact with one another, their segments occupy a definite volume and the segments belonging to the same chain are not free enough to

rotate unhindered. Therefore, it is difficult to predict the accurate dimensions of polymer chains with the above model, and is presumed that in reality the polymer chains have sizes much larger than those predicted by the this model. Benoit[1] predicted that polymer coils due to their spatial mobility and preferred bond angles in the polymer chains are expected to expand by the factor;

$$\left(\frac{1-\cos\theta}{1+\cos\theta}\right)^{\frac{1}{2}}\sigma \qquad \text{Equation 2. 7}$$

Where, $\theta$ and $\sigma$ are bond angle and steric factor, respectively. In addition to these short-range interactions, which aid the polymer coil expansion in dilute solution there are some long-range interactions, which would have a similar effect. These interactions take place between segments in the same chain, here it is the general excluded volume of segments which causes the expansion; the obvious physical constraint that no two parts of the same chain may occupy the same space results in the expansion of the radius of gyration, $R_g$;

$$R_g^{\bullet} = \frac{N^{\frac{1}{2}}l}{\sqrt{6}}\left(\frac{1-\cos\theta}{1+\cos\theta}\right)^{\frac{1}{2}}\sigma \qquad \text{Equation 2. 8}$$

Where, $R^{\circ}_g$ is radius of gyration considering that there is no solvent or excluded volume effect, *i.e.* actual size of the coil. For the case of *freely rotating* chains the value of $\sigma$ is unity, whilst, for *rigid chains* it is higher than unity. Because of the solvent and excluded volume effects larger coil dimensions are predicted than those of ideal chains. The actual size is related to the $R_g$ by an expansion factor, $\alpha$;

$$R_g^2 = \alpha\, R_g^{\circ 2} \qquad \text{Equation 2. 9}$$

Where $\alpha$ are an experimentally measurable factor and its value depends upon the quality of the solvent and the system temperature. In a $\theta$ (theta) or an ideal solvent at the $\theta$-temperature the excluded volume effects are balanced by unfavourable solvent-segment interactions and the expansion factor, $\alpha$, is unity. When $\alpha$=1, the chain may be considered to be in an ideal thermodynamic state, hence, $R_g^2 = R_g^{\circ 2}$.

## 2.3. Polymers in Solution

There are three distinct concentration regimes in the theories of polymer chain conformation: (I) the regime where chains do not overlap and are well separated from each other by solvent, is defined as a very dilute solution (II) solutions with $c \geq c^*$, the concentration where the chains start to overlap, is defined as the intermediate concentrations or "semi-dilute" solution and (III) a solution where the fraction of solvent is small and the polymer chains overlap strongly, $c > c^*$, are defined as highly concentrated solutions.

### 2.3.1. Semi-Dilute Polymer Solutions

Consider the following three concentration regimes each of which regimes possesses different thermodynamic and configuratuional behaviours. For a system consisting of "m" number of chains with N segments per chain, a volume V with each chain having an excluded volume per chain of B;

(a) The concentrated regime;

$$\frac{mNB}{V} \approx 1.0 \qquad \text{Equation 2. 10}$$

(b) The semi-dilute regime

$$m\langle r^2 \rangle^{3/2} \geq B \qquad \text{Equation 2. 11}$$

© The dilute regime;

$$m\langle r^2 \rangle^{3/2} \leq B \qquad \text{Equation 2. 12}$$

### 2.3.2. The Flory-Huggins Theory of Concentrated Solutions

Flory-Huggins theory describes the thermodynamics of mixing of a polymer with a solvent, using the "mean field" approach. Flory and Huggins in their independent works developed a lattice model for polymers in solution. The "*mean field*" condition is that the polymer concentration is so high that segments are

distributed in a uniform fashion on the sites of a three dimensional lattice and each polymer segment contributes a *mean field* to the overall interactions. This theory is mainly based on the following assumptions: (I) the lattice is full with solvent or polymer molecules, (II) both the solvent and the polymer segments are of identical size, (III) the mean field approximation is valid, (IV) polymer-polymer, surface-polymer, surface-solvent and polymer-solvent interactions are present. The entropy of mixing can be calculated by the relation;

$$\Delta S_{mix} = -k(n_1 \ln\phi_1 + n_2 \ln\phi_2) \qquad \text{Equation 2. 13}$$

Where, k is Boltzmann constant, $n_1$ and $n_2$ are number of solvent and polymer molecules, respectively, placed on a three-dimensional lattice model, and $\phi_1$ and $\phi_2$ are the volume fractions of solvent and polymer respectively and are defined by the relations:

$$\phi_1 = \frac{n_1}{n_1 + n_2 x}, \quad \phi_2 = \frac{n_2}{n_1 + n_2 x} \qquad \text{Equation 2. 14}$$

where, $x$ is number of segments per chain of the polymer

Since, within a lattice model the enthalpy of mixing is related to the number of segment-solvent contacts, hence, the Flory-Huggins interaction parameter, $\chi$, gives the interaction energy of each such a contact by the relationship;

$$\chi = \frac{1}{kT}\left[E_{12} - \frac{1}{2}(E_{11} - E_{22})\right] \qquad \text{Equation 2. 15}$$

Where $E_{11}$, $E_{12}$ and $E_{22}$ are energies of solvent-solvent, solvent-polymer and polymer-polymer interactions, respectively.

The enthalpy of mixing, $\Delta H_{mix}$, can be determined after considering the effect of energies of such contacts (polymer-solvent) existing in the system by the following relation.

$$\Delta H_{mix} = kT\chi n_1\phi_2 \qquad \text{Equation 2. 16}$$

The enthalpies of solvent-solvent and polymer-polymer contacts yield the interaction parameter, $\chi$. Overall the free energy of mixing (of polymer segments and solvent molecules together), $\Delta F_{mix}$, may then be calculated by the relation;

$$\Delta F_{mix} = \Delta H_{mix} - T\Delta S_{mix} \qquad \text{Equation 2. 17}$$

By substitution from Equation 2. 13 and Equation 2. 16, the Equation 2. 17 becomes;

$$\Delta F_{mix} = kT[n_1 \ln\phi_1 + n_2 \ln\phi_2 + n_1\phi_2\chi] \qquad \text{Equation 2. 18}$$

Mixing also occurs if $\Delta F_{mix} < 0$, if $n_2\phi_2\chi$ is large and positive then phase separation occurs.

## 2.3.3. de Gennes Scaling Theory

de Gennes[2] proposed a scaling theory approach to investigate concentrated polymer solutions based on a continuum model in which the polymer chains are considered to be made up of statistical segments or groups called as "blobs". These blobs may contain several monomers. If "N" is the total number of polymer segments per chain, then the number of blobs will be equal to ~ N/n,

where, "n" is the number of monomer segments in each blob.

The radius of gyration can be determined with the help of scaling theory, since it considers the polymer chain as a series of blobs of diameter, $\xi$. If it is considered that inside the block the polymer undergoes a self-avoiding walk (SAW) and outside the blob it undergoes an ideal random walk then;

inside the blob

$$\xi \approx n^{3/5} \qquad \text{Equation 2. 19}$$

and outside the blob

$$R_g^2 \approx \left\langle \frac{N}{n} \right\rangle \xi^2 \qquad \text{Equation 2. 20}$$

hence, by combining the above two equations

$$R_g^2 \approx N n^{1/3} \qquad \text{Equation 2. 21}$$

After knowing the diameter of each blob, $\xi$ and the number of monomers present in a blob, n, many parameters, for example the osmotic pressure, etc. can be predicted.

## 2.4. Copolymers

Polymer chains composed of two or more different monomers (repeat units) are called as *copolymers*. The copolymers are grouped according to the sequence of repeat units (monomers) and their properties depend strongly on the backbone structure of the molecules. Copolymers composed of two different monomers (A and B) arranged alternately be called *alternating* copolymers (ABABAB). *Random* copolymers are composed of segments of one type randomly distributed amongst the others along the chain (AABABBABAB). Random block copolymers could be considered a subset of this class and includes those macromolecules in which the segments of either segment type always appear in blocks. An example of a random block copolymer is poly(vinyl alcohol-co-acetate). Another main class of copolymers is block copolymers containing diblocks (AB), *e.g.* PEO-PBO or triblock copolymers (ABA) *e.g.* PEO-PPO-PEO (Pluronics), as used in this study.

### 2.4.1. Micellization of Copolymers

Overall, the solution behaviour of copolymers is governed by similar rules followed by the homopolymers and may be described by the same models. However, for the case of copolymers there are many more interaction parameters ($\chi$) (for example solvent-segment, segment-segment, *etc.*) to be considered. As a consequence of the freedom to form copolymers from segments with very different solution properties, copolymer solutions can exhibit additional phenomena which are not encountered in

homopolymer solutions. Copolymers may form micelles, analogous to those formed by short chain conventional surfactants if they are dissolved in a selective solvent (the solvent in which one block or segment type is partially soluble or insoluble).

In micellar solutions, the "insoluble" segment forms a central core surrounded by the "soluble" monomers. The size and shape of these micelles and the concentration at which micellisation occurs (*cmc*) depends on the enthalpy-entropy balance and therefore on polymer-solvent interactions, the temperature, and the chain length and flexibility *i.e.* HLB value of a copolymer. HLB is defined as the "hydrophilic-lyophilic balance" and simply describes the relative solubility of the copolymers in aqueous and non-aqueous solution and/or their overall character. The aggregation (reversible or irreversible) of copolymers to form micelles also strongly depends on the glass transition temperature, $T_g$, of the polymeric inner core and the polymer below its $T_g$ may form an immobile glassy phase existing in the centre of the micelle. The micelles are often spherical in shape but may be of different shapes and sizes. Alexandridis, *et al.*[3] have given a detailed review of PEO-PPO triblock copolymers in aqueous solutions. While, choosing solvents and polymers used for adsorption studies it is very important to consider the CMC and $T_g$ of the polymers, before any study is carried out.

# References


[1] Benoit, J., *J. Chem. Phys.*, 1947, **44** 18.

[2] de Gennes, P. G., "Scaling Concepts in Polymer Physics", Cornell University Press,Ithaca, N. Y., 1979.

[3] Alexandridis, P., and Halton, T. A., *Colloids and Surfaces A: Physicochemical and Engineering Aspects* 1995, **96**, 1.

# Chapter 3

# *THE ADSORPTION OF POLYMERS*

## 3.1. General

The adsorption of macromolecules at solid/liquid interface involves polymer-surface, solvent-polymer, solvent-surface and polymer-polymer interactions. These interactions may be hydrogen bonding, chemical bonding, van der Waals attraction or a coulombic interaction. Various theories have been developed for predicting the conformational parameters of adsorbed polymers. These parameters include the thickness of the interfacial region, $\delta$, amount of adsorbed polymer per unit area, $\Gamma$, the segment density profile normal to the interface, $\rho(z)$, and the fraction of polymer segments in contact with the surface, (p). In general, these adsorption parameters depend strongly on polymer composition (*i.e.* polymer total molar mass and block molar mass, polymer architecture), polymer solution concentration, c, and nature of the particle surface, the solvent and the temperature, T, of the system.

This section is mainly concerned with polymer adsorption at the solid-liquid interface and covers the fundamental properties of solid-liquid interfaces, adsorption at the solid-liquid interface and in particular, polymer and copolymer adsorption and to interpret and understand the results of this study. Experimental investigations on solid-liquid systems are given and finally a review of recent theories of solid-liquid adsorption is discussed. Unlike the low molar mass molecules, the polymer segments can not all lie flat in close contact with the surface simultaneously. However, they accommodate themselves in configuration of "tails", "loops" and "trains" (Jenkel and Rumbach[1]). These configurations result from the balance of the net energy change on adsorption *i.e.* decrease in entropy of polymer and an increase in entropy of released solvent molecules. At an interface a polymer adopts a (dynamic) conformation of loops, tails and trains (segments in the surface layer). A schematic representation of a single molecule at a solid-liquid interface is given in Figure 1.1.

Although radial symmetry is lost, many segments are expected to lie in a solution-like environment. Consequently, the description of the adsorbed chains derives to a great extent from the solution models. The main difference is the concentration of segments at the interface, lateral interactions remaining very similar to the interaction of coils in solution.

The parameter $\chi_s$ most commonly used to describe surface adsorption energies was originally defined by Silberberg[2] and expresses the "preference" of the surface for a polymer segment over a solvent molecule. Strong adsorption is characterised by a high $\chi_s$ value. However, polymer molecules experience a much greater energetic attraction due to the large number of segments which may interact with the surface. The driving force for adsorption is the overall reduction in the free energy, $\Delta F_{ads}$, resulting from partition to the surface.

$$\Delta F_{ads} = \Delta H_{ads} - T\Delta S_{ads} \qquad \text{Equation 3. 1}$$

where, $\Delta H_{ads}$ and $\Delta S_{ads}$ are defined as changes in the adsorption enthalpy and adsorption entropy respectively, whilst, T is the system temperature.

So far, several approaches have been made in a wide range of models which attempt to describe the polymers in solution and at interfaces, the lattice models and scaling theory models for stiff chain polymers, dilute solution models and bridging models. Most theories may be grouped into two classes: (I) mean field[3] and (II) scaling theories.[4,5]

Macromolecules may adopt a very large number of conformations when present in solution, a polymer melt or even when associated with a solid-liquid interface. It is therefore essential to elucidate the entropic contributions to the free energy in order to understand the differences between the adsorption of small and polymeric molecules. The adsorption of any polymer chain will result in the loss of translational and rotational entropy. More importantly there will usually be a significant decrease in the very large number of conformations a chain may adopt. Thus, upon adsorption macromolecules lose substantial amounts of configurational entropy. This entropic contribution to the free energy opposes the attractive enthalpic forces between the polymer molecules and the surface.

The value of the actual adsorption energy of a polymer-surface system, relative to the critical value, leads to two distinct cases; adsorption or depletion.

I) When the value of the adsorption energy exceeds the critical value, the enthalpic term in Equation 3.1 becomes dominant and dictates the free energy of adsorption $\Delta F_{ads}$ : polymer is adsorbed at the interface.

ii) If the value of the adsorption energy is smaller than the critical value, then the entropic term becomes the controlling factor. This leads to a region near the surface from which polymer is excluded known as the depleted zone.

Four further factors must be considered when dealing with the comparison of small molecule adsorption with that of polymer chains:

I) The time taken for the attainment of equilibrium in polymer adsorption is much greater than that taken for the small molecules.

II Adsorbed amounts (mg $m^{-2}$)of polymeric molecules are much higher than those of smaller molecules.

III An adsorbed polymer molecule will have many contacts with the adsorbing interface and, hence, much larger adsorbed layer thickness.

## 3.2. Adsorbed systems

As discussed above four main parameters; the adsorbed amount, the bound fraction, the adsorbed layer thickness and the segment density profile characterize any adsorbed polymer layer.

### 3.2.1. Adsorbed Amount and Adsorption Isotherms

An adsorption isotherm relates the amount of polymer adsorbed at the interface to the equilibrium polymer concentration of the surrounding medium (bulk). The polymer adsorption experiments are usually conducted at a wide range of polymer solution concentrations (*i.e.* 0 ppm to 5,000 ppm) to obtain an adsorption isotherm. The adsorbed amount is the most basic parameter defining the adsorbed system and it is

the amount of polymer in the region of the interface in excess of the bulk concentration. The adsorbed amount can also be defined as "the maximum amount of polymer in close contact with the surface, $\Gamma_{max}$". The adsorbed amount of a polymer in the interfacial region can be separated into two components representing the excess adsorbed amount, $\Gamma_{ex}$, and the depleted adsorbed amount, $\Gamma_d$, but for the case of dilute polymer solutions, $\Gamma_d$ is negligible hence, $\Gamma_{max} \approx \Gamma_{ex}$, and will be symbolised as $\Gamma$. The adsorbed amount, $\Gamma$, (normally expressed in units of mg $m^{-2}$) can be calculated by the relationship;

$$\Gamma = \frac{\Delta c V}{S_A} \qquad \text{Equation 3. 2}$$

Where, $\Delta c$ is the change in the polymer concentration after adsorption has taken place, $V$ is the total solution volume and $S_A$ is the available surface area for adsorption.

In contrary to low-affinity, Langmuir-type adsorption isotherms generally obtained for small molecules, high-affinity adsorption isotherms are obtained for polymer molecules, as shown in Figure 3. 1.

There are three main regions of an adsorption isotherm; *see* (a), (b) and (c) given below. For the case of high affinity adsorption isotherms, initially every chain in the system finds its way to the surface and so the entire polymer is adsorbed from solution. This results in a rapid increase in the adsorbed amount with polymer concentration which can be observed in region "a" of the Figure 3.1, which can be attributed to more polymer molecules being accommodated at the surface. Whilst, beyond this point at position "b", a reduction in the surface area per polymer molecule is observed due to the lateral interactions between molecules. The polymer packing becomes tighter until a final plateau in the adsorbed amount is reached, *see* region "c" in Figure 3. 1.

The adsorbed amount is also related to the area bounded by the different volume fraction profiles and the volume fraction of the solution, $\phi_f(z)$. Figure 3. 2 shows these areas along with the adsorbed amounts they represent.

$$\Gamma = \rho_p \int_0^\infty \phi(z) dz \qquad \text{Equation 3. 3}$$

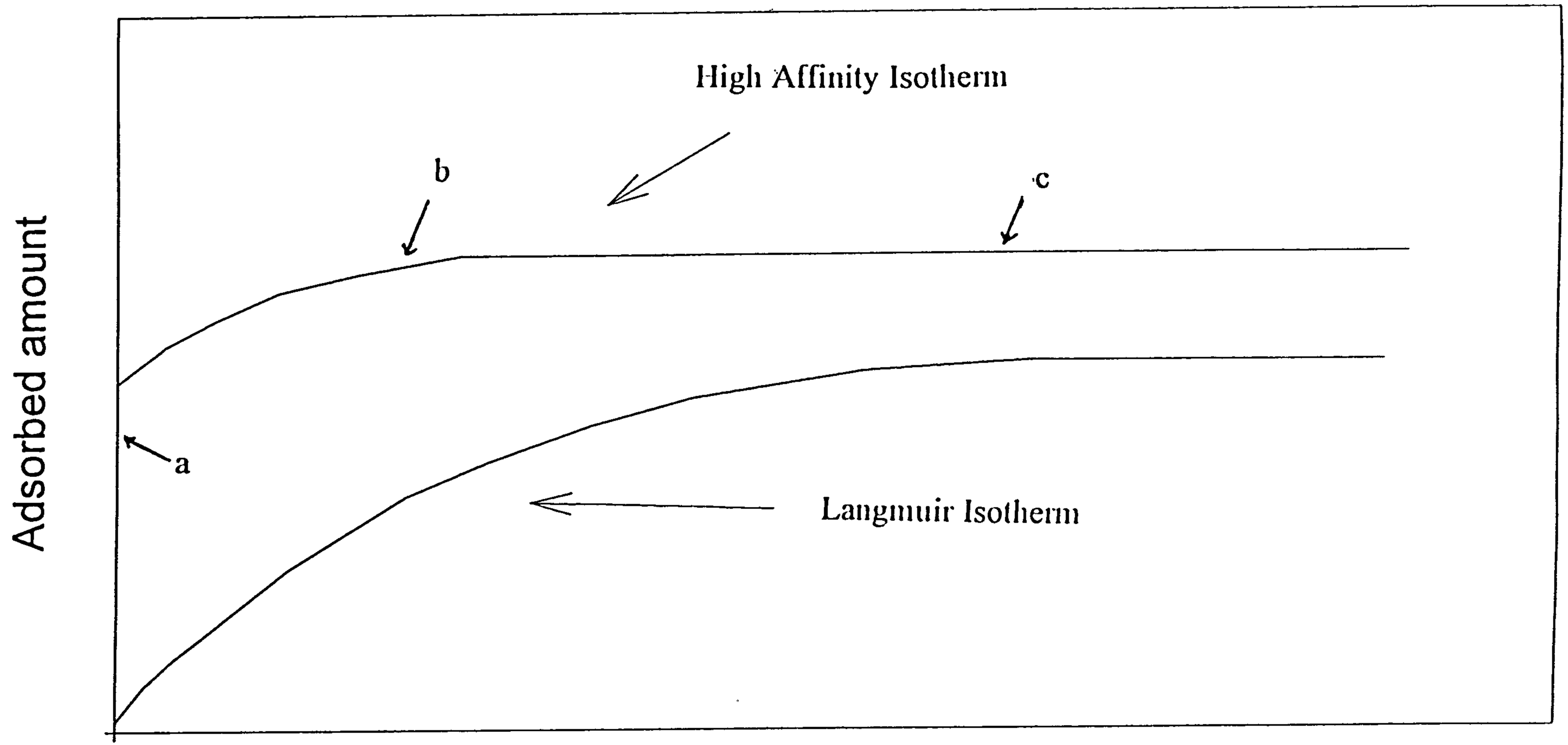


***Figure 3.1: Presents the schematic diagram for adsorption isotherms for the polymer molecules as a function of polymer solution concentration.***

Where, $\rho_p$ is the density of polymer.

### 3.2.2. Thermodynamics of the Polymer Adsorption

In order for adsorption to take place, $\Delta F_{ads}$, must be negative. Unlike mixing, in which entropy is the driving force, $\Delta U_{ads}$ is the main driving force for the polymer adsorption on the surfaces. $\Delta F_{ads}$ can be derived by the relationship;

$$\Delta F_{ads} = \Delta H_{ads} - T\Delta S_{ads} \qquad \text{Equation 3. 4}$$

Let us consider that as a result of adsorption the entropy of the system changes from three to two dimensions, which can be calculated by the relation;

$$\Delta S_{ads} = k \ln \Omega^{2D} - k \ln \Omega^{3D} \qquad \text{Equation 3. 5}$$

Where, $\Omega$ is the number of possible conformations in dimension x D.

By substitution $\Omega^{3D} = 3^m$ and $\Omega^{2D} = 2^m$ we get;

$$\Delta S_{ads} = mk \ln(2/3) \qquad \text{Equation 3. 6}$$

Where 'm' is the number of monomer units

The enthalpy of adsorption is given by;

$$\Delta U_{ads} = m\chi_s kT \qquad \text{Equation 3. 7}$$

where,

$$\chi_s = \frac{E_1^a - E_2^a}{kT} \qquad \text{Equation 3. 8}$$

where $E_1^a$ *and* $E_2^b$ are the adsorption energies of solvent and polymer, respectively.

At equilibrium,

$$\chi_s^{crit} kT = kT \ln(2/3) \qquad \text{Equation 3. 9}$$

$$\chi_s^{crit} \approx \ln(2/3) \qquad \text{Equation 3. 10}$$

This is the critical value of $\chi_s$ parameter. The adsorption will take place only when the value of $\chi_s$ is positive and higher than this critical value. A more detailed derivation gives;

$$\chi_s^{crit} = -\ln(1-\lambda_1) \qquad \text{Equation 3. 11}$$

where $\lambda_1$ is a lattice parameter, such that $\lambda_{1z}$ is the number of neighbours a site has in each of the adjacent layers.

### 3.2.3. Volume Fraction Profile

A volume fraction profile describes the volume fraction or segment density of the adsorbed polymer layer, $\phi$, as a function of distance normal to the surface, z. Knowledge of the volume fraction profile is helpful in deriving many of the other parameters of the adsorbed layer. The total volume fraction profile, $\phi(z)$, is described as sum of the volume fraction of free unadsorbed, $\phi^f(z)$, and that of the adsorbed, $\phi^a(z)$, chains, *see* Figure 3.2. The adsorbed chains are those, which at least have one of its segments closely attached to the surface.

$$\phi(z) = \phi^f(z) + \phi^a(z) \qquad \text{Equation 3. 12}$$

For the case of negative adsorption or depletion process a decrease in the total volume fraction, $\phi(z)$, is observed in the vicinity of the interface, exactly opposite to the adsorption process.

### 3.2.4. Adsorbed Layer Thickness

There are several methods for determining the thickness of the adsorbed layer but each of these techniques measure different aspects of it. Hence, the layer thickness measured by different methods may not necessarily be the same. For example, neutron

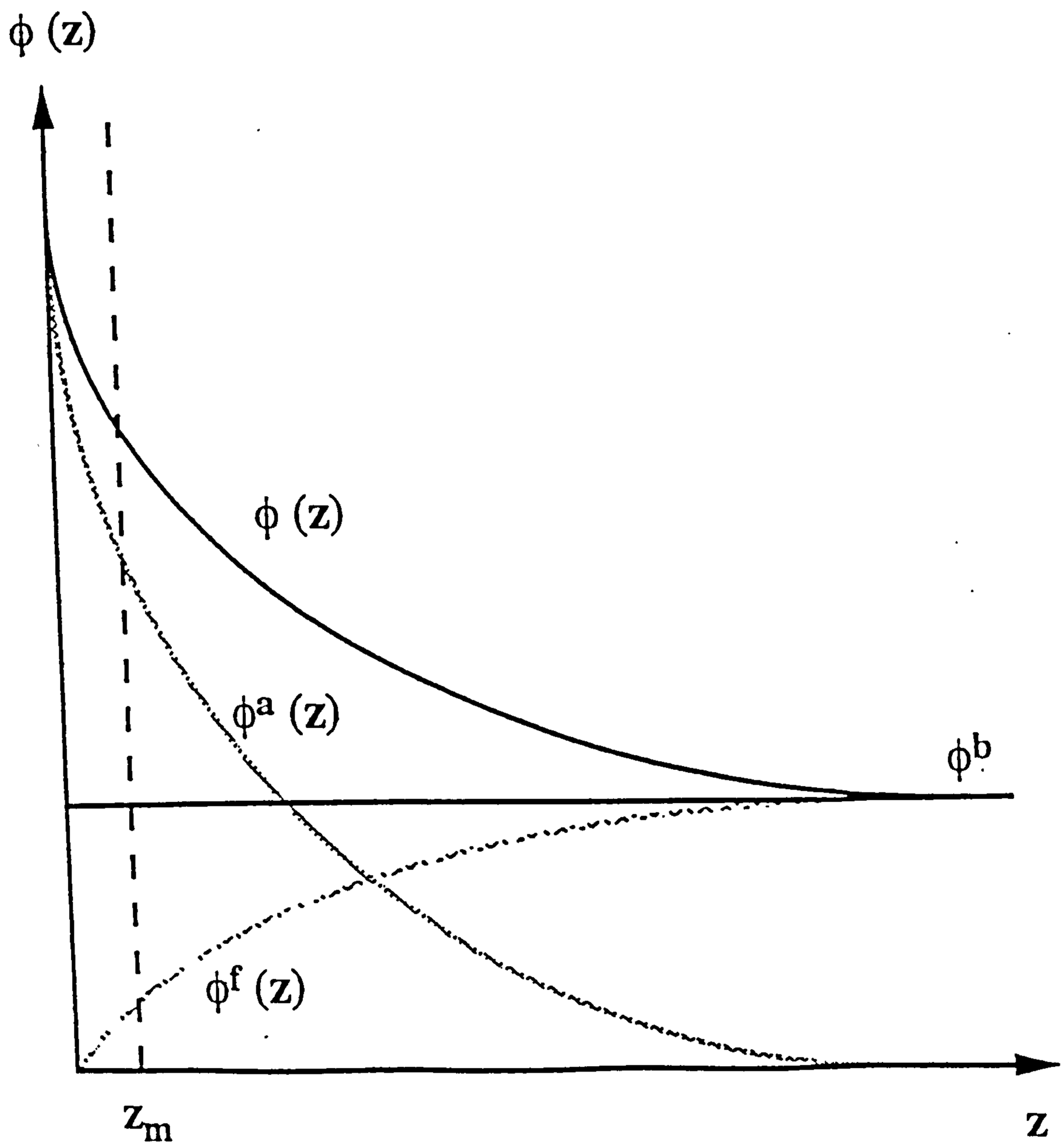


*Figure 3.2 presents the schematic diagram for polymer volume fraction profile near to the adsorbing surface as a function of distance from the surface.*

scattering and capillary flow probe a different aspect of the volume fraction profile. The first moment, $\delta_1$, can be defined as;

$$\delta_1 = \frac{\int_0^\infty \phi(z) z dz}{\int_0^\infty \phi(z) dz} \qquad \text{Equation 3. 13}$$

Whilst, the second moment, $\delta_2$, can be defined as;

$$\delta_2 = \frac{\int_0^\infty \phi(z) z^2 dz}{\int_0^\infty \phi(z) dz} \qquad \text{Equation 3. 14}$$

The square root of second moment is most commonly referred to as the root mean square thickness of the adsorbed layer, $\delta_{rms}$. Another quantity, *the second moment about the mean*, $\sigma^2$, is frequently used and related to the $\delta_1$ and $\delta_2$ by the relation;

$$\sigma^2 = \delta_2 - \delta_1^2 \qquad \text{Equation 3. 15}$$

### 3.2.5. Bound Fraction

The bound fraction, p, is equal to the fraction of total segments in close contact with the interface. The value of bound fraction may vary between *unity to* 1/N, where N is the total number of polymer segments present, and may also yield information about the gross conformation of the adsorbed layer. A higher bound fraction values suggests a *flat* conformation with many segments in trains, whilst a low bound fraction suggests that the major part of the adsorbed layer comprised of long loops and tails. In addition the bound fraction also gives an indication of how well anchored an adsorbed layer is at the interface.

### 3.2.6. The Effect of Polydispersity on Adsorption Isotherms

Theoretical calculations made for polymer adsorption often rely on the assumption that the adsorbing polymer is monodisperse, *i.e.* the polymer chains are of same size (N). This is never the case in practice; N varies about some mean value and the best that may be achieved is to minimise the variation. Most commercially available polymers formed by free radical polymerisation tend to be polydisperse. Cohen-Stuart *et al.*[6] and Koopal[7] have determined the effect of polydispersity in terms of the preferential adsorption of long molecules over shorter ones. They propose that at low coverage, molecules of all sizes can adsorb equally, however, as the surface becomes crowded smaller molecules are squeezed out allowing larger polymer molecules to adsorb minimising the entropy factors. The adsorption equilibrium is achieved in a shorter time for the case of monodisperse systems than the polydisperse systems (this is due to rearrangements of adsorbed chains and desorption of smaller polymer chains). Also, more "rounded" isotherms are observed as the result of the effect of polydispersity.

### 3.2.7. Multilayer Formation

In general, for the case of polymer adsorption on the solid surfaces the chances of multilayer formation are very small because of the shielding effect of the first adsorbed polymer layer, since the force of attraction of the surface for a second polymer layer is very small. However, such polymer multilayers can only be found (I) for the case of low molar mass polymers or (II) under conditions where the polymer in solution is close to the phase separation, or the cloud point[8] or for certain block copolymers as have been studied in this work.

### 3.2.8. Reversibility

Since a polymer is attached to the surface at more than one point ("multi-point" attachment) it is very unlikely that all segments can desorb completely, even, if individual polymer segments are reversibly adsorbed. Therefore, polymer adsorption as a whole is said to be an irreversible process. This is particularly true

for polydisperse systems.

### 3.2.9. Kinetics

As compared to the small molecules, which achieve the equilibrium state of adsorption after short times, the equilibrium adsorption of polymers is only achieved after relatively long times. This effect can be explained by two factors: (a) polymer molecules being larger entities possess much lower diffusion coefficients in solution than small molecules; (b) much more time is needed to the polymer molecules to change from their solution configuration to the adsorbed configuration. This first effect is concentration dependent, hence, the extent of it varies as a subject of the solution concentration *i.e.* at low concentrations its effect increases, whilst, at high concentrations it decreases.

For the case of polydisperse polymer systems it takes more time to achieve the equilibration of adsorption. This may be attributed to the replacement of more rapidly diffusing smaller molecules by the larger molecules, since; the larger molecules adsorb preferentially to the smaller molecules.[6]

## 3.3. Theories of Polymer Adsorption

### 3.3.1. Introduction

Polymer adsorption theories have been very much developed from the theories of polymer solutions. In recent years, with an increased interest in polymers due to their wide industrial applications as colloidal systems, the interest of the scientists to predict phase properties of the polymer solutions, and to develop better stabilising properties in the polymer systems has led to the development of' many new theories.

The early adsorption theories of Frisch, Simha and Eirich (FSE)[9,10,11] were based on the assumption of single chain adsorption at a surface and they did not take into account excluded volume effects. In these theories the polymer was treated purely as a random walk and the adsorbed polymer chains were assumed to be characterised by a Gaussian segment density distribution of end-to-end distances.

For real chains there exists an excluded volume but in early theories these solvent-segment and the segment-segment interactions, which, in reality play a very important role in determining the polymer conformation in the adsorbed layer were ignored. Inspite of these shortcomings these theories provided an excellent basic knowledge for polymer adsorption and considered detailed conformational statistics of the adsorbed segments and the assumption of segment-surface interactions. The polymer chains were also assumed to be anchored to the surface at one end *i.e.* the walk starts in the surface plane. This assumption simplifies the mathematics and allows the partition function for the system to be calculated and has been very helpful in calculating various parameters associated with the polymer. However, many theories have ignored important experimental aspects such as polydispersity of the polymer sample, adsorption from mixed solvents *etc.*

A more developed approach was later adopted by several workers in which all previously ignored segment-segment and segment-solvent interactions were taken into account. During the last two decades several different approaches to the problems facing to the adsorption processes have been developed. Out of those problems the main problem was the adequate theoretical treatment of the large number of the possible adsorption conformations that both free and adsorbed molecules may adopt. For this purpose different workers, each of whom resulted in a different adsorption theory, gave several different assumptions and treatments. A statistical mechanical formulation to the problem was investigated whereby a polymer chain of N units was assumed to have its individual segments in one of two states - adsorbed or desorbed. The length of the series of either completely desorbed (loops) or completely adsorbed (trains) segments then further specified the chain. This approach enabled the study of the average conformations, *e.g.* average length of trains and loops formed by the polymer segments in an adsorbed layer. The aim of any reasonable theory must be to give qualitative agreement (at least), with experimental data. The various theoretical approaches made to the development of the adsorption theories can be subdivided into three different classes.

**a)** Numerical methods; for example, exact numeration, Monte Carlo, *etc.*

**b)** Semi-analytical; for example, Roe, Scheutjens-Fleer, *etc.*

**c)** Analytical; for example, Hove, de Gennes scaling theory, *etc.*

Most of the methods will be described in the following section.

## 3.3.2. Adsorption of Homopolymers

### 3.3.2.1. Scheutjens and Fleer (SF)Theory

The Scheutjens and Fleer theory of polymers adsorption is a self-consistent approach and is an extension of the Flory-Huggins lattice theory for polymer solutions.[12,13] In this theory the polymer conformations are represented as step-weighted random walks on a lattice. Each step is weighted by an entropy factor dependent on the local entropy of mixing and an energy factor dependent on segment-segment interactions ($\chi$). In order to obtain the correct equilibrium between adsorbed and free polymer chains the number of polymer layers chosen must extend well into the bulk solution. The polymer segments placed in layers parallel to the interface and each segment may thus be assigned a layer number. The chains with similar conformations are grouped together in different sets. Similar non-interacting monomers are grouped together with a weighing factor. The partition function Q is then stated in terms of the concentration of chain conformations, it is minimised with each segment contributing a weighting factor, or free segment probability to the overall conformational probability. This weighting factor is defined as the probability of finding a certain polymer layer with respect to the bulk assuming that none of the monomers react with each other. Q is maximised by varying the number of chains in each subset. Once the partition function Q is maximised the number of chains in any conformation may be expressed in terms of the weighting factors. Thus the information concerning the set of chain conformations from which Q has been derived may be retained. Therefore the calculation of conformational probabilities, the free energy, the distribution of average tail loop and train size and the evaluation of the average layer thickness of the adsorbed polymer layer may be carried out.

This theory has some shortcomings; it does not incorporate self-avoiding walks, the case of two polymer segments occupying the same lattice site is therefore not explicitly forbidden. A polymer segment and a solvent molecule, occupying one lattice site are considered as necessarily of the same size. The major predictions of the SF theory are detailed as below.

a) A critical, non-zero, adsorption energy exists in the system ($\chi_{sc}^{crit}$) below which no adsorption is expected.

b) The high molar mass polymers give adsorption isotherms of high affinity.

c) Polymer adsorbed amount in θ -solvents increases linearly with increasing chain length up to a limiting value, whereafter it levels off.

d) Tails are considered to be important in determining the segment density in the region away from the interface.

e) A significant solvent effect is predicted where the both bound fraction and the adsorbed amount increase with increasing the adsorption energy.

f) Bound fraction decreases with increasing the solvent quality of the medium.

g) In a θ -solvent, the root-mean-square, RMS, layer thickness of the polymer is proportional to the square root of the polymer chain length.

h) Any increase in solution concentration decreases the train length and increases the length of tails and loops.

There are many examples when these predictions are matched with experimental results.

### 3.3.2.2. Scaling Theory

The de Gennes[4,14] scaling theory may be applied to polymer solutions and polymers at interfaces. This theory is based on an analytical approach and does not use any numerical methods.

Scaling theory proposes three distinct regimes of the adsorbed polymer layer normal to the surface:

a) *the proximal regime*, The region of adsorbed layer where polymer segments are in close contact with the surface, i.e. exist in trains

b) *the central regime*, the polymer is present as loops or tails which forms a fluctuating network of chain segments similar to that in solution

c) *the distal regime*, polymer exists in long loops only, and the polymer concentration falls quickly to the bulk value

The applications of scaling theory are restricted to the cases of weak adsorption, where $\chi_s<\chi_{sc}$ and for athermal solvents, $\chi_s = 0$. Both the real and excluded volumes are assumed to be equal, the adsorption energy being small and the results presented are non-numerical *i.e.* in the form of power laws. A single parameter, equilibrium constant, K, is utilised to account for interactions between the surface and the polymer chains, and may be related to $\chi_s$ by the relationship:

$$K=\frac{k\,T\chi_s}{S_A} \qquad \text{Equation 3. 16}$$

where K and k are equilibrium and the Boltzmann constants, respectively, whilst, $S_A$ is the area of the surface site.

This theory is unable to predict the ratio of segments in trains, loops and tails, but it may predict the volume fraction, $\phi(z)$, of a polymer at a distance, z, normal to the interface, by the relation;

$$\phi(z)\approx z^{-4/3} \qquad \text{Equation 3. 17}$$

### 3.3.3. Adsorption of Block Copolymers

The mean-field models and scaling predictions[15,16,17] describing the adsorption of block copolymers at the solid/liquid interface can be generalised as two cases: I) if both blocks are soluble, then the solvent is said to be "non-selective"; and II) if one block is insoluble the solvent is "selective".

The nature of the adsorption depends strongly on the anchor fraction ($\upsilon_A$) of the two respective blocks, $\upsilon_A=N_A/(N_A+N_B)$, where, $N_A$ and $N_B$ are the number of segments in the *anchor* and b*uoy* blocks. One of the basic ideas in the scaling models for block copolymer adsorption is that it is the relative size of the two blocks that determines the overall behaviour. When the *buoy* block ($N_B$) has a significantly greater size than the *anchor* block, $N_A$, the adsorption behaviour falls into the *buoy-dominated regime.*

However, as the *anchor fraction* ($\upsilon_A$) increases there is a transition to an a*nchor-dominated regime* and the adsorbed amount goes through a maximum. This can be understood in terms of a balance between the energy gained by adsorption of the *anchor* segments and the entropy loss in stretching the b*uoy* segments. For a selective solvent, this transition occurs when $\beta_n \sim N_A$, where $\beta_n$ is an asymmetry ratio and is defined as the ratio between the area occupied by the two respective blocks:[15,16] assuming the buoy block is swollen by the solvent and the anchor block is a polymer melt.

$$\beta_n \sim \frac{(1-\upsilon_A)^{6/5}}{\upsilon_A} \qquad \text{Equation 3. 18}$$

With increasing N (where $N = N_A + N_B$), this transition occurs at lower $\upsilon_A$ values. The maximum in the adsorbed amount with increasing $\upsilon_A$ is paralleled by changes in the polymer layer thickness.[15,16,18]

The adsorbed amount, $\sigma$, (the number of chains per unit area) can be described under the different conditions as:

1) in the buoy regime;

$$\sigma \sim \left(\frac{N_A}{N_B}\right)^{6/5} \qquad \text{Equation 3. 19}$$

2) in the anchor regime;

$$\sigma \sim \frac{1}{N_A} \qquad \text{Equation 3. 20}$$

A plot of $\sigma$ as a function of $N_A$ shows a crossover at the transition point between the buoy and anchor regimes. By combining the Equation 3. 19 and Equation 3. 20 we get;

$$\left(\frac{N_A}{N_B}\right)^{6/5} \sim \frac{1}{N_A} \qquad \text{Equation 3. 21}$$

$$\upsilon_A^{max} \sim \frac{1}{N_A}$$ Equation 3. 22

# References


[1] Jenkel, E., and Rumbach, B., *Z. Electrochem*, 1951, **55**, 612.

[2] Silberberg, A., *J. Chem. Phys.*, 1968, **48**, 2835.

[3] Fleer, G. J., Scheutjens, J. M. H. M., and Cohen Stuart, M. A., "Colloids and Surfaces", Elsevier Science Publishers B. V. Amsterdam, 1987.

[4] de Gennes, P. G., "Scaling Concepts in Polymer Physics", Cornell University Press, Ithaca, N. Y., 1979.

[5] de Gennes, P. G., *RSC Conference*, London, 1986

[6] Cohen Stuart, M. A., Scheutjens, J. M. H. M., and Fleer G. J., *J. Polym. Sci., Polym. Phys.*, 1980, **18**, 559.

[7] Koopal, L. K., *J. Colloid & Intf. Sci.*, 1981, **83**, 116.

[8] Silberberg, A., . *Colloid & Intf. Sci.*, 1972, **38**, 217.

[9] Frisch, H. L., and Simha, R., *J. Phys. Chem.*, 1954, **57**, 584.

[10] Frisch, H. L., *J. Phys. Chem.*, 1955, **59**, 633.

[11] Frisch, H. L., and Simha, R., *J. Chem. Phys.*, 1954, **58**, 507.

[12] Scheutjens, J. M. H. M., and Fleer, G. J., *J. Phys. Chem.*, 1979, **83** 1621.

[13] Scheutjens, J. M. H. M., and Fleer, G. J., *J. Phys. Chem.*, 1980, **84** 178.

[14] de Gennes, P. G., *Adv. Colliod and Int., Sci.*, 1987 **27** 189.

[15] Marques, C. M., Joanny, J. F., and Leibler, L., *Macromolecules* 1988, **21**, 1051.

[16] Marques, C. M., and Joanny, J. F., *Macromolecules* 1989, **22**, 1454.

[17] Evers, O. A., Scheutjens, J. M. H. M., and Fleer, G. J., *J. Chem. Soc. Faraday Trans.* 1990, **86**, 1333.

[18] Fleer, G. J., Cohen Stuart M. A., Scheutjens, J. M. H. M., Cosgrove, T., and Vincent, B., "Polymers at Interfaces" 1st Ed. Chapman and Hall, London, 1993.

# Chapter 4

# *EXPERIMENTAL*

## 4.1. Materials

### 4.1.1. Adsorbates

Block copolymers have wide industrial, pharmaceutical and cosmetic applications, for example as detergents, stabilisers, wetting agents, emulsifiers and flocculents.[1,2,3,4,5,6,7,8.9] Over the last few years copolymers have attracted a great deal of attention from both theoretical and experimental scientists. In this study we aim to understand the influence of polymer composition and architecture upon adsorption at the solid/liquid interface. For this purpose a range of poly(ethylene oxide), (PEO) homopolymers and poly(ethylene oxide)-poly(butylene oxide), (PEO-PBO) and poly(ethylene oxide)-poly(propylene oxide)-poly(ethylene oxide), (PEO-PPO-PEO) block copolymers with a range of total polymer molar mass and/or block molar masses were selected. A major part of our work was dedicated to studying the adsorption of Pluronic and Reverse Pluronic triblock copolymers hence more detail is included about these copolymers.

#### 4.1.1.1. Poly(ethylene oxide) Homopolymers

A range of poly(ethylene oxide), PEO, homopolymers of varying molar masses was supplied by Polymer Laboratories Limited, U.K. Since these polymers were of analytical grade, they were used as received. The characteristics of these polymers as stated by the manufacturers are given in Table 4.1[10] These polymers vary in molecular weight between 10,000 to 930,000 and have a very narrow molar mass distribution.

Table 4.1: characteristics of the PEO homopolymers as stated by the manufacturers.

| Polymer | 10K | 18.6K | 37.4K | 56K | 94K | 114K | 930K |
|---|---|---|---|---|---|---|---|
| $M_{wPEO}$ | 10,300 | 18,600 | 37,400 | 56,000 | 93,750 | 114,000 | 930.000 |
| $M_w/M_n$ | 1.03 | 1.06 | 1.02 | 1.05 | 1.04 | 1.05 | 1.02 |

### 4.1.1.2. Pluronic Copolymers

Pluronic copolymers are a range of commercially available BAB type triblock copolymers (BASF Wyandotte Corporation) with the general structure $PEO_m$-$PPO_n$-$PEO_m$, where PEO is poly(ethylene oxide) and PPO is poly(propylene oxide), (for these copolymers, the nomenclature $E_m$-$P_n$-$E_m$, will be used throughout the thesis, where E corresponds to an ethylene oxide unit and P to a propylene oxide unit). These copolymers are produced by copolymerisation of ethylene oxide and propylene oxide monomers. Several samples are available with varying composition, which were used without any further treatment (*see* Table 4.2). The hydrophobic nature of poly(propylene oxide) increases with increasing molar mass and PPO homopolymer samples with molar mass greater than 1000 are insoluble in water. PPO can be dispersed in water by copolymerising with a second block of hydrophilic PEO. Generally speaking the hydrophobicity (*i.e.* solubility in water) of Pluronic copolymers depends upon the PPO/PEO ratio (balance) of the molecule *i.e.* HLB (hydrophilic-lypophilic balance) value.[11] Griffin[11] has discussed in his work that a molecule with high HLB value (for example F38 with HLB~30) is considered to be a very strongly hydrophilic in nature and one with very low HLB (for example L61~3.0) is very strong hydrophobic in nature. Most of the samples chosen for this study being rich in PEO were considered to be more hydrophilic in nature, hence readily "soluble" in water below the critical micellization concentration (CMC).

Pluronics are readily soluble in water at low temperatures and concentrations and

Table 4.2: physicochemical properties of the non-ionic, water-soluble PEO-PPO triblock copolymers, Pluronics.

| Pluronics | $M_W$* | $M_{W_{PEO}}$* | $M_{W_{PPO}}$* | $E_m$-$P_n$-$E_m$ | PPO/PEO | $\nu_A$ | $R_{gPEO}$ =9.37x10$^{-4}$xM /nm[12] | Mw† | $M_w/M_n$† | CMC/% w/v /25°C[13,14] | CMT[14] | Polymer %w/w[13] |
|---|---|---|---|---|---|---|---|---|---|---|---|---|
| F38 | 4800 | 3850 | 950 | $E_{44}P_{16}E_{44}$ | 0.25 | 0.158 | 1.34 | 4580 | 1.2 | N/A | N/A | N/A |
| L62 | 2400 | 650 | 1750 | $E_7P_{30}E_7$ | 2.69 | 0.671 | 0.55 | 1630 | 1.25 | 3 /30°C | N/A | N/A |
| L64 | 2900 | 1150 | 1750 | $E_{13}P_{30}E_{13}$ | 1.52 | 0.536 | 0.73 | 2350 | 1.2 | 11 | 36.5 | 0.25 |
| F68 | 8350 | 6600 | 1750 | $E_{75}P_{30}E_{75}$ | 0.26 | 0.167 | 1.76 | 6620 | 1.1 | N/A | 52.5 | 0.5 |
| P75 | 4450 | 2400 | 2050 | $E2_7P_{35}E_{27}$ | 0.85 | 0.393 | 1.06 | 3420 | 1.2 | N/A | N/A | N/A |
| P85 | 4650 | 2400 | 2250 | $E_{27}P_{39}E_{27}$ | 0.94 | 0.416 | 1.06 | 3585 | 1.2 | 4 | 33.7 | 0.25 |
| F87 | 7700 | 5450 | 2250 | $E_{62}P_{39}E_{62}$ | 0.41 | 0.238 | 1.60 | 3700 | 1.1 | N/A | N/A | N/A |
| F88 | 11800 | 9550 | 2250 | $E_{108}P_{39}E_{108}$ | 0.23 | 0.152 | 2.12 | 11000 | 1.1 | N/A | 45.00 | 0.25 |
| F98 | 13000 | 10250 | 2750 | $E_{116}P_{47}E_{116}$ | 0.27 | 0.169 | 2.19 | 11500 | 1.1 | N/A | N/A | N/A |
| F108 | 14000 | 10750 | 3250 | $E_{122}P_{56}E_{122}$ | 0.3 | 0.186 | 2.24 | 11200 | 1.2 | 4.5 | 33.5 | 0.25 |

*Molar mass as quoted by manufacturers,[16] and † Molar mass as determined by RAPRA[17]

can exist in solution as individual coils. Wanka *et al.*[13] showed that Pluronic copolymers with relatively lower total polymer molar mass and high PEO content do not aggregate at low concentrations and at room temperature. However, these copolymers may form micelles in aqueous solutions at increased temperature and/or high concentration. Alexandridis *et al.*[14,15] have shown that any increase in PPO block mass and/or in total polymer molar mass of the copolymers, whilst the PEO block mass is maintained constant, brings about a dramatic decrease in the critical micellization concentration/temperature (CMC/CMT). A small decrease in the CMC and CMT of these copolymers in aqueous solution has been observed with increasing the total polymer molar mass as a function of PEO block mass. This shows that it is easier for the copolymers with a higher total polymer molar mass and high PPO content to form micelles and aggregates. At higher concentration gelation can also take place for certain Pluronic copolymers.[16] Table 4. 2 presents the physicochemical properties of the non-ionic, water-soluble PEO-PPO triblock copolymers as stated by manufacturers.[16] Also listed are their respective molar masses and polydispersity indices ($M_w/M_n$) as determined by gel permeation chromatography.(*see* Appendix II)[17]

#### 4.1.1.3. PEO-PBO Copolymers

These polymers were BA and BAB type diblock and triblock copolymers with general structure $PEO_m$-$PBO_n$ and $PEO_m$-$PBO_n$-$PEO_m$ comprising of Poly(ethylene oxide)-Poly(butylene oxide) copolymers of linear and ring structures. Yu, at the Department of Chemistry, University of Manchester kindly supplied these polymers. Since, they were well characterised and fairly monodisperse in total polymer molar mass and block molar mass composition, they were used as received. Bedells *et al*[18], Yang *et al.*[19] and Luo *et al.*[20] have previously described the characterisation of these copolymers using GPC and NMR methods. NMR was used to characterise the composition, the total polymer molar mass and the purity of the copolymer samples. They presented that these block copolymers have the advantage of greater composition and chain length uniformity over comparable PEO-PPO-PEO copolymers. Molecular characteristics of these polymers are detailed in Table 4.3. Relatively wide chain distributions were found for the triblock compared to the diblock copolymers. Nace *et al.*[21] and Yu *et al.*[22,23] have also investigated the copolymer chain length distribution

and it was observed that in the anionic polymerisation of epoxides, different rates of reaction of ethylene oxide with secondary butylene oxide, (BO) and primary ethylene oxide, (EO) oxyanions lead to a wide EO-block-length distribution if EO is added to a preformed BO block. This is necessarily the case for a triblock copolymer with a central BO block. Chu *et al.*[24] have found that the wider distribution in the polymer composition may have a stronger influence over the adsorption phenomena of these copolymers.

Luo *et al.*[20] have determined the critical micellization concentration (CMC) and temperature (CMT) for a range of PEO-PBO triblock copolymers. They have observed that the CMC of the triblock copolymers of PEO-PBO was lower than that of the PEO-PPO copolymers of the corresponding molar mass and PEO composition. Nicholas *et al.*[25] presented CMC and gel formation properties for a range of PEO-PBO triblock copolymers of the same PEO:PBO ratio but increasing chain length (total polymer molar mass). They observed that by doing so (*i.e.* increasing the total polymer molar mass whilst keeping PEO:PBO ratio constant) the critical micellization and gel concentration decrease significantly, whilst, the micellar weights and sizes were observed to increase. Sun *et al.*,[26] Kelarakis *et al.*[27] and Beddels *et al.*[18] have separately reported the synthesis and solution properties in dilute aqueous solutions of a range of PEO-PBO diblock copolymers of corresponding composition to those used in this work. Surface tension, light scattering and gel permeation chromatography methods were used to investigate the solutions at different temperatures over a wide range of polymer concentrations (*i.e.* up to 100 $gl^{-1}$). It was observed that a minimum PBO block size of ~ 6 monomers was required to place to give a CMC and a gelation concentration in the temperature range of 30 – 50 °C. Furthermore, it was also observed that both CMC and gelation concentration decrease with increasing the PBO block size. The solution properties of the polymers used in this work were not available but were extrapolated from the data available for the samples closest in polymer composition to the samples used in this study.

#### 4.1.1.4. Reverse Pluronic copolymers

The Reverse Pluronic copolymers were commercially available ABA type copolymers, which were supplied by BASF Wyandotte Corporation and have the

Table 4.3: molecular characteristics of the PEO-PBO block copolymers.

| Polymer | $M_w$ | $M_{wPEO}$ | $M_{wPBO}$ | $\varphi E^a$ (NMR) | $Mn/M_n$[19,20] /($gml^{-1}$) (NMR) | Formula[19,20] (NMR) | $\upsilon_A$ | $M_w/M_n$[19,20] (GPC) | CMC[27] ($mgdm^{-3}$) /20 °C |
|---|---|---|---|---|---|---|---|---|---|
| $E_{144}B_{27}$ | 8,280 | 6,336 | 1,944 | N/A | 8280 | $E_{144}B_{27}$ | 0.16 | 1.06 | N/A |
| $E_{72}B_{27}E_{72}$ | 8,280 | 6,336 | 1,944 | N/A | 8280 | $E_{72}B_{27}E_{72}$ | 0.16 | 1.04 | N/A |
| $E_{100}B_{15}$ | 5,480 | 4,400 | 1,080 | 77.8 | 5800 | $E_{106}B_{16}$ | 0.13 | 1.03 | 4.7 |
| $E_{200}B_{15}$ | 9,880 | 8,800 | 1,080 | 87.3 | 10400 | $E_{210}B_{16}$ | 0.07 | 1.03 | 3.8 |
| c-$E_{200}B_{15}$* | 9,880 | 8,800 | 1,080 | 88.0 | 10000 | c-$E_{206}B_{15}$ | 0.07 | 1.05 | N/A |
| $E_{100}B_{15}E_{100}$ | 9,880 | 8,800 | 1,080 | 88.0 | 10100 | $E_{103}B_{15}E_{103}$ | 0.07 | 1.1 | N/A |

* = cyclic-$E_{200}B_{15}$

---

[a] $\phi E$ = volume fraction of poly(ethylene oxide) (liquid state) based on densities at 20 °C of 1.12 g $cm^{-3}$ for poly(ethylene oxide) and 0.97 g $cm^{-3}$ for poly(butylene oxide).

general structure $PPO_m$-$PEO_n$-$PPO_m$, *i.e.* essentially inverted Pluronics. These also were used as received. In keeping with the notation for the Pluronic copolymers the nomenclature $P_mE_nP_m$ will be used through out this thesis. Shown in Table 4.4 are the stated characteristics of the Reverse Pluronic copolymers used in this study,[16] also listed are their GPC data (*see* Appendix II). These copolymers in aqueous solutions show different behaviour than the normal Pluronics of the corresponding molar mass; particularly low foaming and good wetting properties are observed. The R. Pluronic copolymers are widely used in body care products, cosmetic face creams, shampoos, and lotions and dispersing agents for printing inks, paints and coatings. These copolymers, due to the presence of two hydrophobic blocks at the either end, were expected to adsorb at higher levels than the normal Pluronic copolymers, on both hydrophobic and hydrophilic surfaces.[28]

These copolymers are presumed to adsorb on the hydrophobic surface via hydrophobic PPO blocks lying firmly attached to the particle, whilst, the hydrophilic PEO block was expected to extend away in the solution in short loops and as trains. However, for the hydrophilic surfaces both PPO and PEO blocks were presumed to adsorb. For the reverse Pluronics, it is likely that tails do not play such a major role, as do the normal Pluronics.

Very little work exists on the solution properties of Reverse Pluronics. Although, the work reported is not sufficient to make any firm conclusion about the behaviour of R. Pluronic copolymers dissolved in solutions it can be considered as a little help to understand them. Balazs *et al.*[28] have discussed with the help of Monte Carlo simulation that the copolymer chains having two anchor groups at the two either ends can aggregate through these ends. They also indicated that the aggregation of the polymers depends strongly on the total polymer molar mass and mass of the anchor (sticky) blocks. Balazs *et al.*[28] have also shown that the adsorption of Reverse Pluronics is relatively complicated in sense that the two hydrophobes of different macromolecules can form longer chains by associating with each other. This could give rise to multilayer formation and bridging flocculation.

PAGE

MISSING

IN

ORIGINAL

Table 4.4: characteristics of the Reverse Pluronic copolymers

| R.Pluronic | $M_w$* | $M_{wPEO}$* | $M_{wPPO}$* | $P_m$-$E_n$-$P_m$ | PPO/PEO | $\upsilon_A$ | $R_{gPEO}$ =9.37x10$^{-4}$xM /nm$^{12}$ | $M_{w/GPC}$† | $M_w/M_n$† |
|---|---|---|---|---|---|---|---|---|---|
| 17R1 | 1900 | 190 | 1710 | $P_{15}E_4P_{15}$ | 7.5 | 0.88 | 0.30 | 1510 | 1.1 |
| 25R1 | 2700 | 270 | 2430 | $P_{21}E_6P_{21}$ | 7.0 | 0.88 | 0.36 | 2580 | 1.2 |
| 31R1 | 3250 | 325 | 2925 | $P_{25}E_7P_{25}$ | 7.14 | 0.88 | 0.39 | 2240 | 1.2 |
| 17R2 | 2150 | 430 | 1720 | $P_{15}E_{10}P_{15}$ | 3.0 | 0.76 | 0.70 | 1830 | 1.1 |
| 25R2 | 3100 | 620 | 2480 | $P_{21}E_{14}P_{21}$ | 3.0 | 0.76 | 0.54 | 2690 | 1.2 |
| 12R3 | 1800 | 1260 | 540 | $P_5E_{29}P_5$ | 0.34 | 0.26 | 0.68 | 1525 | 1.1 |
| 17R4 | 2650 | 1060 | 1590 | $P_{13}E_{24}P_{13}$ | 1.1 | 0.54 | 0.45 | 2300 | 1.1 |
| 22R4 | 3350 | 1340 | 2010 | $P_{17}E_{30}P_{17}$ | 1.13 | 0.54 | 0.77 | 2865 | 1.1 |
| 25R4 | 3650 | 1440 | 2160 | $P_{18}E_{33}P_{18}$ | 1.1 | 0.54 | 0.79 | 3330 | 1.2 |
| 31R4 | 4150 | 1660 | 2490 | $P_{21}E_{38}P_{21}$ | 1.1 | 0.54 | 0.82 | 3850 | 1.2 |
| 10R5 | 1950 | 975 | 975 | $P_8E_{22}P_8$ | 0.77 | 0.44 | 0.88 | 1600 | 1.2 |
| 25R5 | 4250 | 2125 | 2125 | $P_{19}E_{48}P_{19}$ | 0.79 | 0.44 | 1.00 | 4050 | 1.2 |
| 25R8 | 8550 | 6840 | 1710 | $P_{15}E_{155}P_{15}$ | 0.19 | 0.16 | 1.79 | 11200 | 1.1 |
| 31R8†† | 4000 | 3200 | 800 | $P_7E_{73}P_7$ | 0.19 | 0.08 | 1.7 | n/a | n/a |
| 25R10†† | 10500 | 8800 | 1700 | $P_{15}E_{200}P_{15}$ | 0.15 | 0.13 | 2.9 | n/a | n/a |
| 25R15†† | 15000 | 13000 | 2000 | $P_{18}E_{295}P_{18}$ | 0.12 | 0.11 | 2.5 | n/a | n/a |

*Molar mass as quoted by manufacturers, †Molar mass as determined by RAPRA, ††Very low anchor fraction, PPO-PEO-PPO triblock polymers used for the SCF calculations

Altink, *et al*[29]. have studied the architectural effect of PPO-PEO-PPO copolymers on their solution properties and have found that the R. Pluronic 25R8 ($P_{19}E_{113}P_{19}$) cloud at high temperature (40 °C and 45 °C) and high concentration. However, the data presented in this work were determined at lower temperatures (room temperature) and concentrations (0-2500 ppm) than those given in the literature. Mortensen *et al.*[30] have observed that at lower temperatures/concentrations (*i.e.* at below 40 °C temperature and 20 wt.% concentration) the PPO-PEO-PPO copolymer (25R8) dissolve in aqueous solutions as independent entities, whilst, at higher temperatures and/or polymer concentrations these copolymers form large domains of networks of copolymer strands interconnected randomly through the hydrophobic end blocks. Zhou *et al.*[31] determined that R. Pluronic 17R4 can also form micelles at increased temperature. They also studied the dependence of the CMC of the copolymers on the solution temperature (by varying the latter from 25 °C to 40 °C), from measurements of the solution viscosity, and observed that there was no significant change in the magnitude of the CMC with temperature. However, the light scattering data for 17R4 measured between 25 °C and 40 °C show that at elevated temperature the copolymer 17R4 forms micelles at 0.9 mg $ml^{-1}$ (900 ppm) concentration.

### 4.1.1.5. Adsorbents

The use of monodisperse non-porous spherical particles as a substrate for the adsorption of polymers is of paramount importance since:

1) The surface area available for adsorption can be determined accurately.

2) The subsequent particle size analysis by transmission electron microscopy (TEM) and photon correlation spectroscopy (PCS) can be performed to a high degree of accuracy.

3) The particles are free from surfactants.

These requirements preclude the use of commercially available polystyrene latices. Therefore, a standard method described by Goodwin *et al.*[32] was applied to prepare small monodispersed polystyrene latices (see details in the section followed). Mears[33] has discussed the effect of presence of surfactants on polymer adsorption.

Commercially available Snowtex-YL silica was used as a hydrophilic substrate, since it is of the required size and polydispersity.

#### 4.1.1.6. Snowtex-YL Silica

Commercial Snowtex-YL silica (hereafter referred to as YL70) obtained from Nissan Chemical Industries Ltd. was used as a hydrophilic substrate for the adsorption isotherm and photon correlation spectroscopy experiments. Its diameter was 70 ± 10.0 nm as given in the data sheets supplied by the manufacturers[34] although the measured average diameter was 73.0 ±13.0 nm (TEM) and 100.0 ± 2.6 nm (PCS) (*see* Figure 4. 1). The PCS particle size results were used for the adsorption measurements. The silica was dialysed against deionised water to remove any impurities and diluted as per requirement with deionised water, prior to use.

## 4.2. Methods

### 4.2.1. Preparation of Polystyrene Latices

In the field of colloid science polymer latices with a spherical shape and a narrow size distribution are important as model systems for investigating fundamental colloidal phenomena.[35, 36, 37] For this study, 5 polystyrene latex samples were prepared by emulsion polymerisation according to the method of Goodwin *et al.*[32] Table 4.5 presents the physicochemical characteristics of the polystyrene latices produced. The TEM photographs of these latices are shown in Figure 4. 2.

#### 4.2.1.1. Materials

The water used in the preparation of all the polystyrene latices was purified using a Millipore Milli-Q filter system. Styrene and sodium styrene sulphate (SSS) monomers were obtained from B.D.H and are of "laboratory reagent" grade. In order to remove any inhibitors present, prior to use, both monomers were purified by distillation at 40 – 50 °C in a reduced nitrogen atmosphere pressure (approximately 5

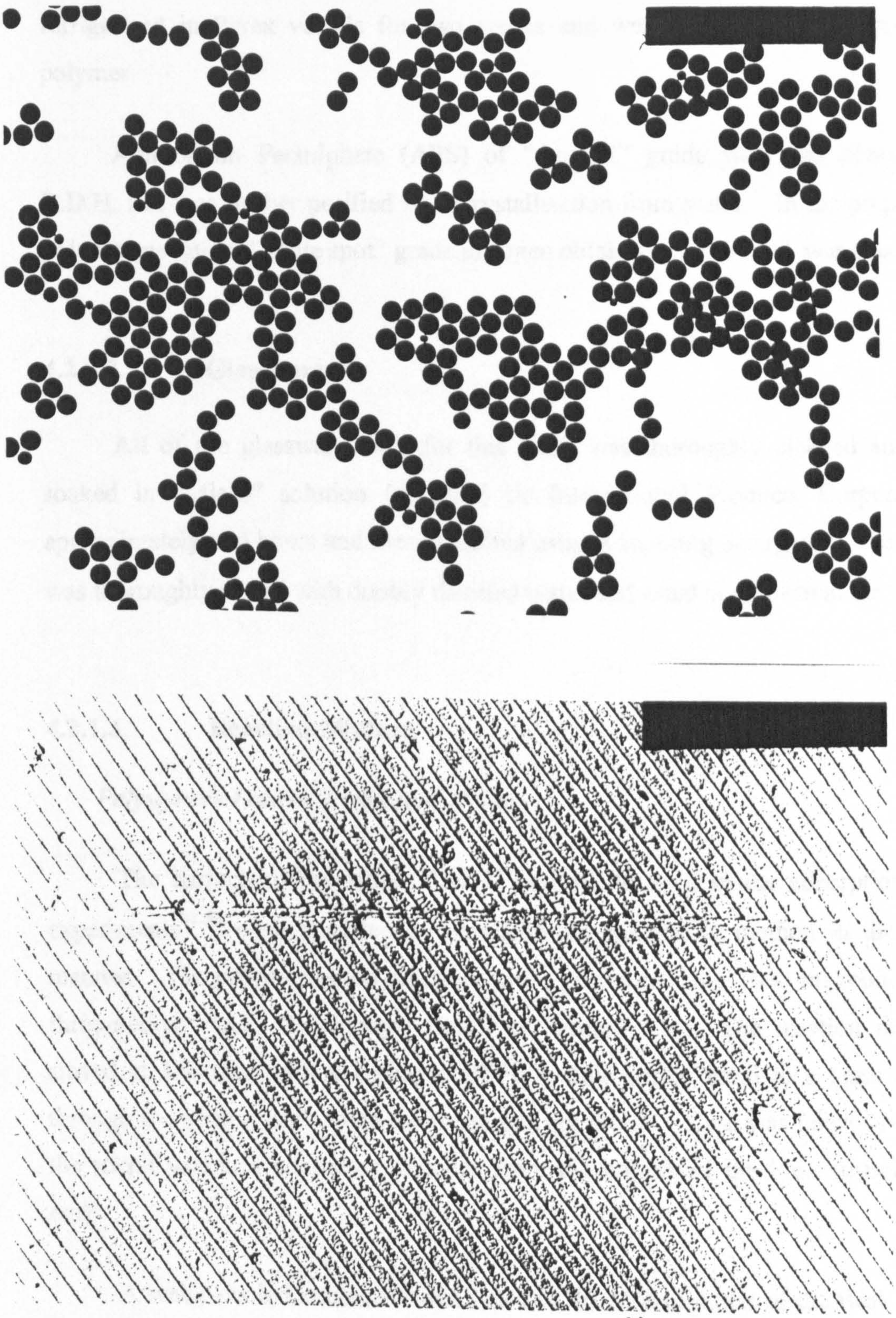


***Figure 4. 2 presents the TEM photograph of the polystyrene latex JS540 produced in this study.***

mm of mercury). After distillation both, styrene and sodium styrene sulphate were refrigerated in Pyrex vessels for two weeks and were checked for the presence of polymer.

Ammonium Persulphate (APS) of "AnalaR" grade was also obtained from B.D.H. and was further purified by recrystallisation from water. In the preparation of polystyrene latices "white spot" grade nitrogen obtained from B.O.C. was used.

### 4.2.1.2. Glassware

All of the glassware used for this work was thoroughly cleaned and initially soaked in "Micro" solution (supplied by International Products Corporation) for approximately two hours and then scrubbed using a scouring detergent. The glassware was thoroughly rinsed with doubly distilled water and dried in an oven at 80 °C.

### 4.2.1.3. Reaction Mixture

***Polystyrene Latices JS452 and JS540***

The surfactant free latices JS452* and JS540 used in the adsorption isotherm experiments[38,39] were prepared by emulsion polymerisation method in the following manner. The polymerisation reactions were performed in a 1000 ml round-bottomed three-necked flask, "Erlenmeyer flask" *see* Figure 4.3. The reaction mixture was stirred at 350 rpm with a T-shaped PTFE paddle stirrer fitted to a glass rod passed through the central neck to an overhead stirring motor. Care was taken to ensure that the stirrer was at a consistent distance from the bottom of the flask (usually about 1 cm).

A water-cooled condenser was fitted to the second outlet of the flask in order to prevent any loss of the solvent. To maintain the system at a constant temperature the flask was immersed up to its neck in a thermostated oil bath at 70 °C temperature.

---

* Prepared by Ian Weatherhead

Nitrogen gas was passed in through the water in the reaction vessel in order to remove any oxygen from the system using the second outlet of the flask. Hearn[40] has shown in his work that the presence of oxygen in the system inhibits the polymerisation process. The flow of nitrogen was controlled throughout the reaction but was maintained at a very low level in order to minimise the solvent evaporation. The water-cooled condenser was connected to the atmosphere through a wash-bottle containing water, which prevented back-flow of oxygen into the system.

Initially 620 ml of deionised water was added to the flask and stirred for 30 minutes in order to allow the contents of the system to reach thermal equilibrium and to expel any oxygen. Styrene monomer, 30 ml, was added and allowed to stir until thermal equilibrium was attained. Once equilibrium has been maintained 0.5 g of the reaction initiator, ammonium per sulphate (already dissolved in 30 ml of deionised water) was added to the reaction vessel and washed by the remaining portion (20 ml) of water. The reaction was left for 24 hours. After this time the reaction vessel was removed from the thermostat bath and allowed to cool. In order to remove the coagulum formed the latex was decanted through glass wool (B.D.H) packed into a glass filter funnel.

***Polystyrene Latices JS84, JS90 and JS100***

The polystyrene latices JS84, JS90 and JS100 used in the photon correlation spectroscopy experiments were prepared in the same manner as polystyrene latices JS452 and JS540, except that the monomer sodium styrene sulphate was also added. The addition of two monomers to the system makes the latex smaller and more monodisperse in size and shape. The recipe of the system was as follow.

| | |
|---|---|
| Deionised water | 678.15 ml |
| Styrene (monomer 1) | 21.00 g |
| Sodium styrene sulphate (monomer 2) | 0.41 g |
| Ammonium Persulphate | 0.45 g |
| System temperature | 75.00 ± 0.5 °C |

#### 4.2.1.4. Dialysis

In order to remove any unreacted soluble monomers or initiators, free ions and any side products formed in the reaction, the latices were put into Visking tubing (GallenKamp) and dialysed against singly distilled water in a 1:25 ratio.[41] Prior to use, the tubing was boiled in ten changes of singly-distilled water, in order to soften and to remove any free ions. The tubing was then filled with latex and placed inside a 5000 ml heavy-walled round-bottom Pyrex vessel and covered with distilled water. For the first day the dialysate (water) was changed after each hour and later on, three or four times a day. The dialysis was considered to be complete when the conductance of water and that of the dialysate was found to be nearly the same; this normally took two weeks. The tubing was removed from the apparatus and the latices taken out and stored in Pyrex vessels, in order to prevent any possible contamination by leaching of electrolytes or silicates from the surface of the glass vessel.

### 4.2.2. Characterisation of Substrates

The percentage solid concentration (% w/w) for each latex was determined by evaporating to dryness a known weight of latex and re-weighing the polymer residue. The latices were left to dry in an oven for overnight at 80 °C, well below the thermal decomposition temperature. The solid percentage (w/w) was calculated from the difference in the weights of the samples before and after drying.

Transmission Electron Microscopy (TEM) and Photon Correlation Spectroscopy, (PCS) were used to determine the size of the substrate particles. Ellen Howse kindly performed TEM of the substrates in the Transmission Electron Microscopy service of the School of Chemistry. Several electron micrographs of the dry particles (polystyrene latex and silica) were taken using a Hitachi HS7 transmission microscope.

The size and polydispersity of the latex were determined by analysing the micrographs using a SeeScan Image Analysis System connected to a Sony CCD camera which was calibrated with micrographs of a 468 nm diffraction grating taken at the same magnification.

#### 4.2.1.4. Dialysis

In order to remove any unreacted soluble monomers or initiators, free ions and any side products formed in the reaction, the latices were put into Visking tubing (GallenKamp) and dialysed against singly distilled water in a 1:25 ratio.[41] Prior to use, the tubing was boiled in ten changes of singly-distilled water, in order to soften and to remove any free ions. The tubing was then filled with latex and placed inside a 5000 ml heavy-walled round-bottom Pyrex vessel and covered with distilled water. For the first day the dialysate (water) was changed after each hour and later on, three or four times a day. The dialysis was considered to be complete when the conductance of water and that of the dialysate was found to be nearly the same; this normally took two weeks. The tubing was removed from the apparatus and the latices taken out and stored in Pyrex vessels, in order to prevent any possible contamination by leaching of electrolytes or silicates from the surface of the glass vessel.

### 4.2.2. Characterisation of Substrates

The percentage solid concentration (% w/w) for each latex was determined by evaporating to dryness a known weight of latex and re-weighing the polymer residue. The latices were left to dry in an oven for overnight at 80 °C, well below the thermal decomposition temperature. The solid percentage (w/w) was calculated from the difference in the weights of the samples before and after drying.

Transmission Electron Microscopy (TEM) and Photon Correlation Spectroscopy, (PCS) were used to determine the size of the substrate particles. Ellen Howse kindly performed TEM of the substrates in the Transmission Electron Microscopy service of the School of Chemistry. Several electron micrographs of the dry particles (polystyrene latex and silica) were taken using a Hitachi HS7 transmission microscope.

The size and polydispersity of the latex were determined by analysing the micrographs using a SeeScan Image Analysis System connected to a Sony CCD camera which was calibrated with micrographs of a 468 nm diffraction grating taken at the same magnification.

### 4.2.4. Molecular Weight and Polydispersity of the Copolymers

There are several techniques available for the determination of the composition of homopolymers; however, only a few of them can be used reliably for copolymers. One of the common techniques used is light scattering, which measures the weight average molecular weight (Mw), for copolymers. The method is subject to many difficulties, *eg.* micellisation and refractive indices increment *etc.* for the two blocks.

Another common method is viscometry where the viscosity (η) of the solution is measured as a function of polymer solution concentration. The Mark-Houwink theory[43] predicts that the dependence of the solution viscosity over the polymer solution concentration is strongly influenced by an approximate relationship between the polymer molar mass (M) and its hydrodynamic volume and is given by the Mark-Houwink equation.

$$\langle \eta \rangle \approx K M^{a} \qquad \text{Equation 4. 1}$$

where K and a are the Mark-Houwink parameters. Unfortunately, for copolymer chains, this semi-empirical relationship becomes much more approximate since many polymer-polymer and polymer-solvent interactions influence the hydrodynamic volume. Also, the uncertainty in the constancy of the monomer fraction in each chain will affect the relationship. Hence, in such conditions viscometry cannot be employed reliably for the characterisation of copolymers.

The most applicable technique used for the characterisation of the copolymers is gel permeation chromatography, GPC[43] (though it has still many problems regarding the determination of relative solubility, polymer concentration, diffusion rate and the polymer conformation). In this technique the rate of permeation of the polymer sample through a polymer gel of a particular pore size is inversely proportional to the polymer molar mass. The molar mass distribution within the sample can be ascertained by calibrating the distribution of times taken to arrive at the far end of the gel column (by a sample polydisperse in molar mass) with the time taken by samples of known, narrow distribution molar masses. This technique is very useful for homopolymers and may be used preparatively for the copolymers; however, it must be considered that

permeation rates may be dependent on both, copolymer composition and copolymer molar mass.

In this study, gel permeation chromatography was used to determine the molecular weight and polydispersity (molar indices) of the copolymers used. GPC traces for the Pluronic and R. Pluronic copolymers were determined by Rubber and Plastic Research Association (RAPRA)[17]. Dimethylformamide, DMF, being a common solvent for the copolymers was used as a solvent and PEO, being the structurally closest standard was used for the calibration of GPC traces (*see* Appendix I). The Tables 4.2 to 4.4 present the molecular weight distribution, molar indices, for the Pluronic copolymers, PEO-PBO block copolymers and the Reverse Pluronic copolymers, respectively. Data present that the samples have reasonably narrow molecular mass distribution with polydispersity indices ranging from 1.1 - 1.2.

After calibration, a series of varying molecular weight triblock copolymers were run in an attempt to establish a correlation between given molar mass and measured molar mass. From the GPC traces, following three important parameters can be derived:

I) The number average molar mass, $M_n$:

II) The weight average molar mass, $M_w$: $M_w$ is the average of the weight distribution curve.

III) The polydispersity factor, Q: where Q is given by $M_w/M_n$ and is a measure of the range of the molar masses in the sample. If Q = 1.0 the polymer is said to be monodisperse.

## 4.3. Techniques

### 4.3.1. Adsorption Isotherms

An accurate method for the quantitative analysis of very dilute copolymer solutions by the complexation/precipitation of the polymer with phosphomolybdic acid has been developed for this study. The complexation of the free polymer left in the

solution after adsorption is complete, is followed by spectrophotometric analysis. The absorption peaks obtained for supernatants containing a fixed amount of complexing reagent are observed to depend on the polymer concentration and the wavelength of the light used. Nuysink *et al.*[42] have shown that at 216 nm the reagent solutions give well-defined peak in both cases before and after the reaction with the polymer (before and after the adsorption of polymer on the particle surface), indicating that only free reagent is present in the solution. The polymer concentration is obtained from the difference in the peak of the reagent before and after the reaction with the polymer.

The polymer adsorption isotherms from aqueous solutions onto solid surfaces were determined as a function of bulk solution equilibrium polymer concentration using the depletion method.[44,45] Stock solutions (~ 3000 – 4000 ppm) of each polymer under study, were prepared by dissolving the required amounts of corresponding polymers into deionised water. A range of solution concentrations (10 – 3000 ppm) of different polymers was prepared from these stock solutions. The colloidal dispersion under study was then added to the relevant copolymer solutions in 1:1 ratio to give the required coverage. After end-to-end shaking for 30 minutes the dispersions were left for 24 hours to reach adsorption equilibrium. Special care was taken to prevent evaporation by sealing with parafilm. The free polymer was then separated from adsorbed polymer (dispersion) by centrifugation at 1300 rpm for 20 minutes using an MSE Microcentaur centrifuge. The equilibrium polymer concentration was determined by complexation of the polymer present in the supernatant with a freshly prepared phosphomolybdic acid solution. The phosphomolybdic acid solution was added to the supernatant in a 1:1 ratio and after end-to-end shaking left to stand for 15 minutes in order to reach a maximum level of the complexation. The mixtures were then centrifuged for 10 minutes at 1300 rpm and analysed at 216 nm using a Uvikon 940 UV spectrophotometer as discussed previously.[42] The path length of the quartz cell used was 1 cm and the temperature of the cell housing in the spectrophotometer was 25.0 ± 1.0 and the reference cell contained deionised water. The resultant absorption peaks were compared with calibration curves for the corresponding polymers previously obtained in the following manner. The absorption peaks were obtained for each solution concentration of each polymer and a plot of this data against initial polymer concentration yielded a straight line for the concentration range 0 - 1,000 ppm. It was therefore possible from this to analyse the polymer solutions in the range of 0 - 3,000

ppm. This range of concentration allows dilutions of sufficient accuracy within the scope of the analytical technique. Figure 4.4 shows a typical graph of UV absorbance as a function of initial polymer concentration. The adsorption isotherms for the PEO homopolymers and the block copolymers in different systems will be shown in the following chapters. The equilibrium polymer concentration of the original system was obtained. The adsorbed amount, $\Gamma$, of polymer was determined by measuring the difference between the polymer initial concentration, $C_i$, and the polymer equilibrium concentration, $C_{eq}$, (parts per million/ppm) upon exposure to a known surface area, $S_A$ ($m^2$ $mg^{-1}$) of the adsorbent and volume of the bulk solution (litres). The adsorbed amount, $\Gamma$, in mass per unit area (mg $m^{-2}$) is given by

$$\Gamma = \frac{(C_i - C_e) \times V}{S_A} \qquad \text{Equation 4. 2}$$

### 4.3.2 Hydrodynamic Layer Thickness

Photon correlation spectroscopy (PCS) was used to determine the hydrodynamic thickness ($\delta_H$ / nm) of the polymer adsorbed layers in dilute aqueous dispersion. PCS have been used extensively to determine the hydrodynamic thickness of the polymer-adsorbed layers.[46,47,48,49] This technique is considered to be highly sensitive to the presence of extended tail segments of the adsorbed chains.[6,42,44,50] The method involves the determination of the mean diffusion coefficient of "bare" and subsequently polymer-coated particles. By use of the Stokes-Einstein equation (Equation 4. 3), the hydrodynamic radii of these particles may be obtained.[51] Subtraction of the two radii yields $\delta_H$.

$$D = \frac{kT}{6\pi\eta a} \qquad \text{Equation 4. 3}$$

The equipment consisted of a Cambridge Lasers CL-4 argon ion laser operating at 514.5 nm and a Malvern PCS 100 spectrophotometer connected to a Malvern real-time multibit correlator K7027. The main components of the PCS spectrometer are shown in Figure 4.5. The correlator had a capacity of 128 data channels and a sample time ($\tau$) range of 0-32767 $\mu$s. The sample time was adjusted in such a way that a smooth

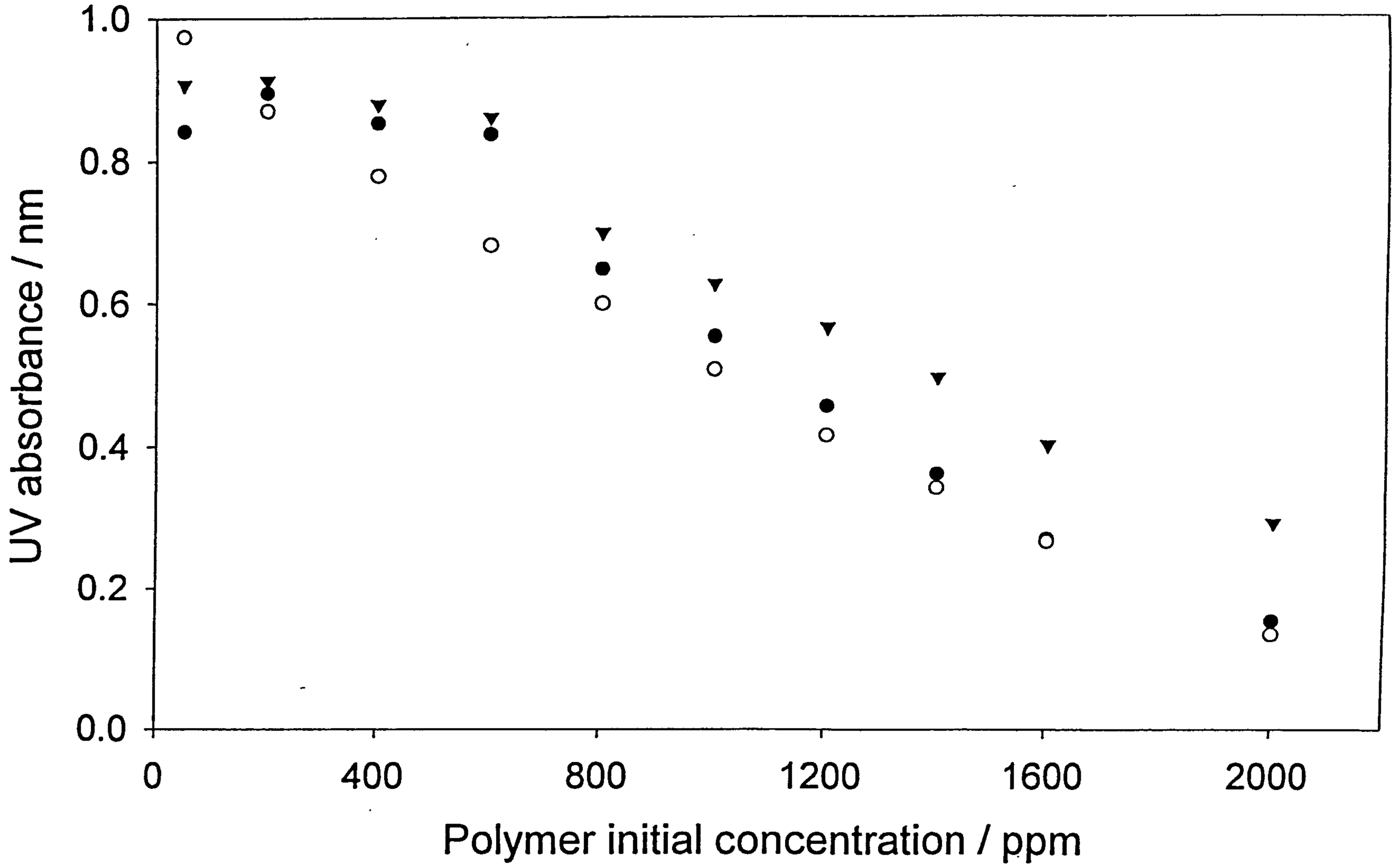


*Figure 4. 4 presents typical UV absorbance curves for block copolymers adsorbed on silica as a function of initial polymer solution concentration: O 12R3, ● 10R5 and ▼22R4.*

complete exponential correlation function that decayed over a maximum number of correlator channels. The rejection factor to eliminate dust selected for the data series was 0.003 and the experimental duration was 15 seconds. All measurements were performed at a scattering angle of 90° and the temperature of the system was controlled by a thermostated bath control unit at 25 °C and each size quoted is the average of several results. $\delta_H$ measurements were carried out as a function of polymer molecular weight at a fixed bulk polymer equilibrium concentration (800 - 1000 ppm) corresponding to plateau level adsorption for each copolymer sample. The dispersions were added to each sample and after end-to-end mixing was left for 24 hours to acquire the adsorption equilibrium. The polymer adsorption equilibrium was established after passing through certain stages. The samples containing sufficient number of particles were placed in a quartz PCS cell and analysed. Owing to the conflicting requirements[6] of the measuring techniques used to determine $\Gamma$ and $\delta_H$ the adsorption isotherms for polystyrene latex were determined using a larger diameter latex. It was considered that the low diameter particles were more difficult to separate from the supernatant by centrifugation. Thus the layer thicknesses were measured using the smaller diameter latices JS90 and JS100 to improve accuracy. Although these lattices have rather different particle diameters, their surface properties are similar; hence the adsorbed amounts may be used in conjunction with the hydrodynamic layer thickness determined using the smaller diameter particles. Both the adsorbed amount and the hydrodynamic thickness were determined using the same silica dispersion as the adsorbent.

### 4.3.2. Molecular Modelling[b]

The Molecular Modelling was performed for copolymer adsorption using the molecular mechanics approach, the conjugate gradient method implementing parameters and potentials specified in the Dreiding II force field.[52] Intermolecular interactions were cut off between 8.0 Å and 8.5 Å using a spline switching function.

---

[b] Mark, J. Warne performed the molecular modeling in the same group.

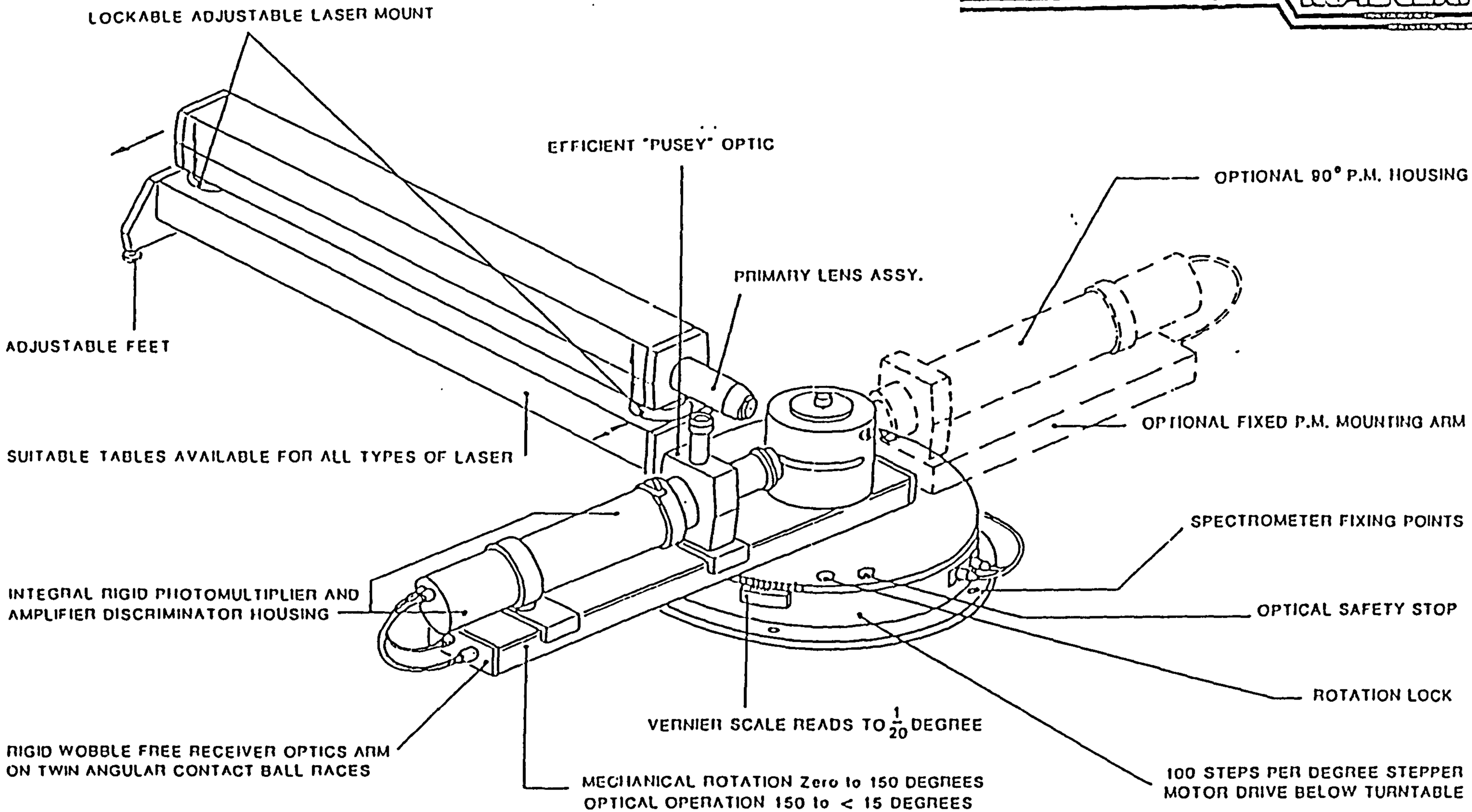


***Figure 4.5. shows the main components of the PCS spectrometer used in this study.***

# References


[1] Cosgrove, T. *J. Chem. Soc., Faraday Trans-1* 1990, 86,1323.

[2] Tiberg, F., Malmsten, M., Linse, P., Lindman, B. *Langmuir*, 1991, 7, 2723.

[3] Cosgrove, T., Mallagh, L.M., Ryan, K. and Scheutjens, J.M.H.M. *J. Surface Sci. Technol.* 1988, 4, 81.

[4] Killmann, E., Maier, H. and Baker, J.A. *Colloids Surf.* 1988, 31, 51.

[5] Baker, J.A., Pearson, R.A.and Berg, J.C. *Langmuir* 1989, 5, 339.

[6] Baker, J.A.and Berg, J.C. *Langmuir* 1988, 4, 1055.

[7] Kayes, J.B.and Rawlins, D.A. *Colloid Polym. Sci.* 1979, 257, 622

[8] Tadros, Th.F.and Vincent, B. *J. Phys. Chem.* 1980, 84, 1575.

[9] van de Steeg, L.M.A., Golander, C.G. *Colloids Surface* 1991, 55, 105.

[10] Technical Brochure, Polymer Laboratories Limited, UK.

[11] Griffin, W.C., *J. Soc. Cosmet. Chemists*, 1949, 1, 311.

[12] Brandrup, J., and Immergut, E. H., "Plymer Handbooks," 2nd, Ed. Wiley and Sons, Newyork, 1975.

[13] Wanka, G., Hoffmann, H. and Ulbricht, W. *Macromolecules*, 1994, 27, 4145.

[14] Alexandridis, P., Holzwarth, J.F. and Hatton, T.A., *Macromolecules* 1994, 27, 414.

[15] Alexandridis, P. and Halton, T.A. *Colloids and Surfaces A: Physicochemical and Engineering Aspects* 1995, 96, 1

[16] Pluronic and Tetronic Surfactants, "Technical Brochure, BASF Wyandotte Corporation", Parsippany, NJ, 1989.

[17] Data for the characterisation of the copolymers as determined by "RAPRA Technology Ltd.", 1995.

[18] Bedells, A. D., Arafeh, R. M., Yang, Z., Attwood, D., Heatley, F., Padget, J. C., Price, C., and Booth, C., *J. Chem. Soc., Faraday Trans.* 1993, 89, 1235.

[19] Yang, Z., Pickard, S., Deng, N. J., Barlow, R. J., Attwood, D., and Booth, C. *Macromolecules* 1994, 27, 2371

[20] Luo Y. Z, Nicholas, C. V., Attwood, D., Collet, J. H., Price, C., and Booth, C. *Colloid Polym Sci.*, 1992, 270, 1094.

[21] Nace, V. M., Whitmarsh, R. H., and Edens, M. W., *J. Amer. Oil Chem. Soc.* 1994, **71**, 777.

[22] Yu, G.-E., Yang, Y.-W., Yang, Z., Attwood, D., Booth, C., and Nace,V. M., *Langmuir* 1996, **12**, 3404.

[23] Yu, G.-E., Yang, Z., Ameri, M., Attwood, D. Collett, J. H., Price, C., and Booth, C., *J. Phys. Chem. B.* 1997, **101**, 4394.

[24] Chu, B., "In *Non-Ionic Surfactants"* Nace, V. M.; Ed.; Marcel Dekker Inc.; New York, 1996.

[25] Nicholas, C. V., Luo Y. Z, Deng, N. J., Attwood, D., Collet, J. H., Price, C., and Booth, C., *Polymer*, 1993, **34** 138.

[26] Sun, W. B., Ding, J. F., Mobbs, R. H., Heatly, F., Attwood, D., and Booth C., *Cooloids and Surfaces*, 1991, **54** 103.

[27] Kelarakis, A., Havredaki, V., Yu, Ga-Er, Derici, L., and Booth, C., *Macromolecules* 1989, **31**, 944.

[28] Balazs A. C., Anderson, C. and Muthukumar, M., *Macromolecules* 1987, **20**, 1999.

[29] Altinok, H., Yu, G. E., Nixon, S. K., Gorry, P.A., Attwood, D., and Booth, C., *Langmuir*, 1997, **13**, 5837.

[30] Mortensen, K., Brown, W., and Jorgensen, E., *Macromolecules*, 1994, **27**, 5654.

[31] Zhou, Z. and Chu, B., *Macromolecules,* 1994, **27**, 2025.

[32] Goodwin, J. W., Hearn, J., Ho, C. C., and Ottewill, R. H. *Colloid and Polymer Sci.* 1974, **252**, 464.

[33] Mears, S. J., Ph.D. Thesis, University of Bristol, 1996.

[34] Technical Data on Snowtex Silica, "Nissan Chemical Industries, Ltd., -Speciality Chemicals Division", Tokyo, Japan.

[35] Ottewill, R.H. and J.N. Shaw, Disc. *Faraday Soc.* 1966.**42**, 154.

[36] Watillon,A. and A.M. Joseph-petit, *Disc. Faraday Soc.* 1966 **42**, 143.

[37] Ottewill, R.H. and J.N. Shaw, *J. Electroanal. Chem.* 1972 **37**, 133.

[38] Turner, T.D., Ph.D. Thesis, Manchester,1981.

[39] Barnett, K.G., Ph.D. Thesis, Bristol, 1982.

[40] Hearn, J. Ph. D. Thesis, University of Bristol, Bristol, 1973.

[41] Hacchisu, S. and Kobayashi, Y.*J. Colloids Int. Sci.*, **46**, 470, 1974.

[42] Nuysink, J. and Koopal, L. K., *Talanta*, 1982, **29**, 495.

[43] Billingham, N.C., "Molar Mass Measurements in Polymer Science".

[44] Garvey, M.J., Tadros, Th.F. and Vincent, B. *J. Colloid and Interface Sci.*, 1974, **49**, 57.

[45] Boomgaard, V., Th., and King, T. A., J. *Colloid and Interface Sci.* 1978, **66**, 68.

[46] Malmsten, M., Linse, P. and Cosgrove, T. *Macromolecules*, 1992, **25**, 2474.

[47] Couture, L., and van de Ven, T. G. M., . *Colloids Surfaces*, 1991, **54**, 245.

[48] Killmann, E., Maier, H., Kaniut, P. and Gulling, N. *Colloids Surface*, 1985, **15**, 261.

[49] Cohen-Staurt, M. A., Waajen, F. W. H., Cosgrove, T., Vincent, B., and Crowley,T. L., *Macromolecules*, 1984, **17**, 1825.

[50] Vincent, B. and Whittington, S.G., in E. Matijevic Ed., "Surface and Colloid Sci"., Vol. **12**, Plenum Press, New York, 1982, p 1-117.

[51] Weiner, B. B., In "Modern methods of Particle Size Analysis", Barth, H.G., Ed. Wiley New York, 1984, P 1.

[52] Mayo, S. L., Olafson, B. D., and Goddard, W. A., *J. Phys. Chem.*, 1990, **94** 8897.

# Chapter 5

# *ADSORPTION OF R. PLURONICS ONTO POLYSTYRENE LATEX*

## 5.1. Introduction

This chapter concerns the adsorption of a series of Reverse Pluronic copolymers (PPO-PEO-PPO) listed in Table 4.4 adsorbed at the aqueous/hydrophobic polystyrene latex (JS452) interface. The data were measured and thereafter analysed in the same manner as described in Sections 4.3.1 and 4.3.2. The hydrodynamic layer thickness of the adsorbed layer determined from the decrease in the diffusion coefficient of the particles was measured as a function of the polymer solution equilibrium concentration corresponding to the plateau level of the adsorption isotherms. A strong influence of the polymer-surface interaction (segment-segment, segment-surface, segment-solvent, solvent-surface *etc.)* was anticipated. It can be observed from the data presented that the polymer composition (PPO:PEO block ratio) play a key role in the shape of the adsorption isotherms. In all cases the equilibrium polymer concentration was below the CMC[1,2,3] of these polymers, hence avoiding the problem of solution complexes. Although the polydispersity can affect the affinity of the adsorption isotherms this is not discussed here as all the polymers studied have $M_w/M_n$ between 1.05 and 1.2.

## 5.2. Adsorbed Amount

### 5.2.1. Adsorption Isotherms

Figure 5.1, Figure 5.2 and Figure 5.3 present the adsorption isotherms for a series of Reverse Pluronic copolymers adsorbed at the aqueous/polystyrene latex interface as a function of polymer equilibrium concentration. Overall, a rapid increase in the level of adsorption is observed at very low polymer concentration followed by a

gradual levelling off (in certain cases) until the so-called pseudo-plateau level is reached at approximately 150 ppm polymer solution equilibrium concentration. However, the level of adsorption for the majority of the polymers, 12R3, 22R4, 25R2, 25R4, 25R5 and 31R1, is observed to increases continuously with increasing the polymer solution equilibrium concentration. The adsorbed amounts for all of these polymers (since most of them do not show steady plateau levels in their isotherms) were measured at a polymer solution equilibrium concentration of 500 ppm. The data presented in Table 5.1 indicate relatively higher adsorbed amounts for the R. Pluronic copolymers than those for the normal polymers (of corresponding molar masses and anchor fractions) adsorbed on the same surface (*see* Chapters 7) and emphasises a strong influence of polymer architecture.[4,5]

Figure 5.1 presents the adsorption isotherms for the 17R1, 17R2 and 17R4 polymers adsorbed at aqueous/polystyrene latex interface as a function of polymer solution equilibrium concentration. The polymers in this figure are arranged in such a way that all these polymers have the same PPO block molar masses but varying PEO block molar mass. Rather unusually the adsorption isotherm for 17R1 shows a maximum which is reproducible. Although we have no explanation it is possible that a kinetically stable bilayer may be formed. At higher bulk concentration it adsorbs at a lower level than the high molar mass 17R2 and 17R4 polymers. This phenomena clearly requires more study and will not be pursued further here. These two polymers (17R2 and 17R4) with different molar masses and different PPO:PEO block ratios are observed to adsorb at a comparable level. This similarity in the adsorption behaviour is balance of anchor fraction and molecular weight effects, since, the adsorbed amount increases with increasing the molecular weight, whilst, it decreases with the polymer anchor fraction.[6]

Figure 5.2 presents the adsorption isotherms for 25R2, 22R4, 25R4 and 25R5 polymers as a function of polymer solution equilibrium concentration. The polymers in this figure are arranged in the order of increasing total polymer molar mass and the PEO block molar masses, consequently, there is a decrease in PPO:PEO block ratio (*i.e.* $\nu_A$ decreases. Initially, a rapid increase in the level of adsorption followed by a constant increase in the adsorbed amount with increasing polymer solution equilibrium concentration is observed. Balazs *et al*[7] have predicted that for the case of generic

**Table 5.1: experimental and theoretical data; adsorbed amounts and adsorbed layer thicknesses for the PPO-PEO-PPO block copolymers adsorbed onto polystyrene latex.**

| Polymer | $M_w$[a] | $\nu_A$ | $\Gamma/\pm 1.2\%$ /(mg $m^{-2}$) | $\delta_H/\pm 1.2$ %/ nm | Adsorbed Amount/θ | δ/layers |
|---|---|---|---|---|---|---|
| 17R1 | 1900 | 0.88 | 0.55 | 7.0 | 0.65 | 0.55 |
| 25R1 | 2700 | 0.88 | N/A | N/A | 0.7 | 0.6 |
| 31R1 | 3250 | 0.88 | 1.1 | 8.0 | 0.85 | 1.0 |
| 17R2 | 2150 | 0.76 | 0.8 | 8.0 | 0.65 | 0.8 |
| 25R2 | 3100 | 0.76 | 0.8 | 7.4 | 0.9 | 1.6 |
| 12R3 | 1800 | 0.26 | 0.5 | 8.0 | 0.2 | 0.9 |
| 17R4 | 2650 | 0.54 | 0.82 | 10.0 | 0.8 | 2.3 |
| 22R4 | 3350 | 0.54 | 0.9 | 8.0 | 0.95 | 2.6 |
| 25R4 | 3650 | 0.54 | 0.9 | 9.0 | 1.05 | 3.5 |
| 31R4 | 4150 | 0.54 | 1.4 | 9.0 | 1.2 | 3.7 |
| 10R5 | 1950 | 0.44 | 0.5 | 6.0 | 0.4 | 1.4 |
| 25R5 | 4250 | 0.44 | 1.3 | 10.0 | 1.4 | 4.7 |
| 25R8 | 8550 | 0.16 | N/A | 13.5 | 1.7 | 9.4 |
| 31R8[b] | 4000 | 0.08 | N/A | N/A | 0.37 | 3.0 |
| 25R10[b] | 10500 | 0.13 | N/A | N/A | 2.05 | 14.3 |
| 25R15[b] | 15000 | 0.11 | N/A | N/A | 0.83 | 12.0 |

[a] Molar mass as quoted by manufacturers,

[b] Very low anchor fraction, PPO-PEO-PPO triblock polymers used for the SCF calculations.

ABA - type copolymers, a free chain approaching the surface collides with an adsorbed short chain. In such cases it is possible (chances increase with increasing the polymer concentration) for the adsorbing chain to attach to the adsorbed chain rather than adsorbing on the surface through hydrophobic bonding with the PPO groups. This results in an *end-to-end* attachment of the *anchor-anchor* blocks of the two neighbouring molecules, which, gives rise to a continuous increase in the adsorbed amount. Furthermore, the level of adsorption for the different polymers is observed to depend on the total polymer molar mass, however, this effect is weaker for the case of more hydrophilic polymers. Hence a model of multilayer formation can qualitatively explain these data.

Figure 5.3 presents the adsorption isotherms for 10R5, 12R3, 31R1 and 31R4 polymers as a function of polymer solution equilibrium concentration. Similar trends in the patterns of the adsorption behaviour of these polymers to those shown in the Figure 5.1 are observed. The adsorption isotherms for low molar mass 10R5 and 12R3 are high affinity, whilst, more rounded shape adsorption isotherm are observed for the higher molar mass 31R4. This figure also shows a strong dependence of the level of polymer adsorption on the polymer composition and is similar to the patterns observed for the rest of the polymers studied (*see* Figures 5.1 and 5.2). An exception is polymer 31R1, where the level of polymer adsorption increases constantly with the polymer solution equilibrium concentration without reaching any plateau level as was found in Figure 5.2. The 31R1 being the largest (with high anchor fraction) in the range studied may tend to an *end-to-end* attachment of the *anchor-anchor* blocks of the two neighbouring molecules, hence giving elongated polymer adsorbed layer conformation.

The Reverse Pluronics are found to adsorb at relatively higher level than those of the normal Pluronics of the corresponding compositions (*see* Chapters 7 and 8), which, can be attributed to the increased hydrophobicity of these polymers. This results in the formation of thicker polymer adsorbed layers (*see* Section 5.2). The more hydrophobic polymers are very keen to attach to the hydrophobic surface, hence, more polymer segments are found on the surface, whilst, PEO blocks are presumed to lie in loops extending into the bulk solution, giving relatively dense adsorbed layers. Baker *et al.*[8] have measured the adsorption of 10R8, 25R2 and 25R8 polymers adsorbed on polystyrene latices. In contrast to our results (*i.e.* where the adsorbed amount increases

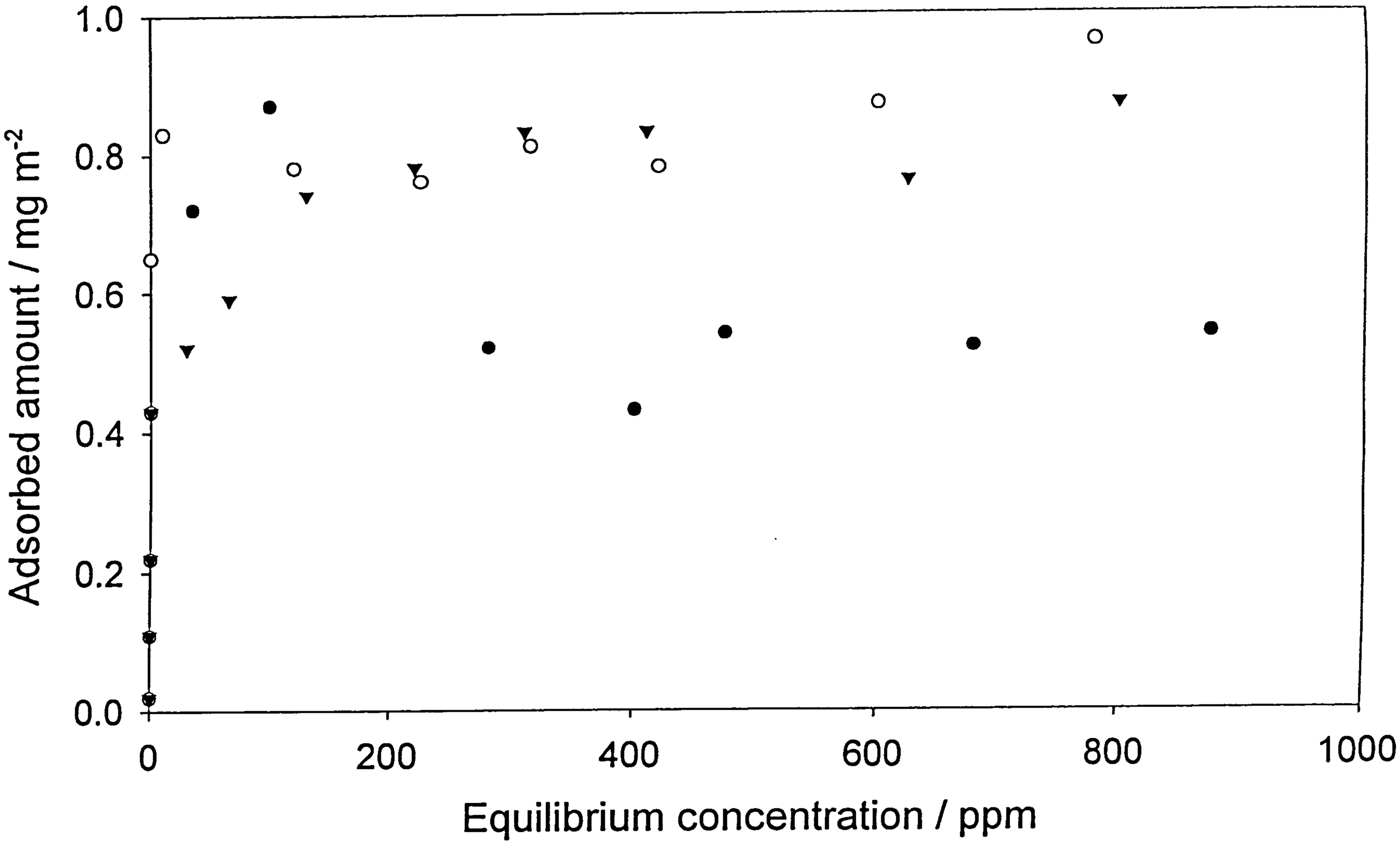


*Figure 5.1 presents the adsorption isotherms for the reverse Pluronics adsorbed at aqueous/polystyrene latex interface as a function of polymer solution equilibrium concentration: ● 17R1, O 17R2 and ▼17R4.*

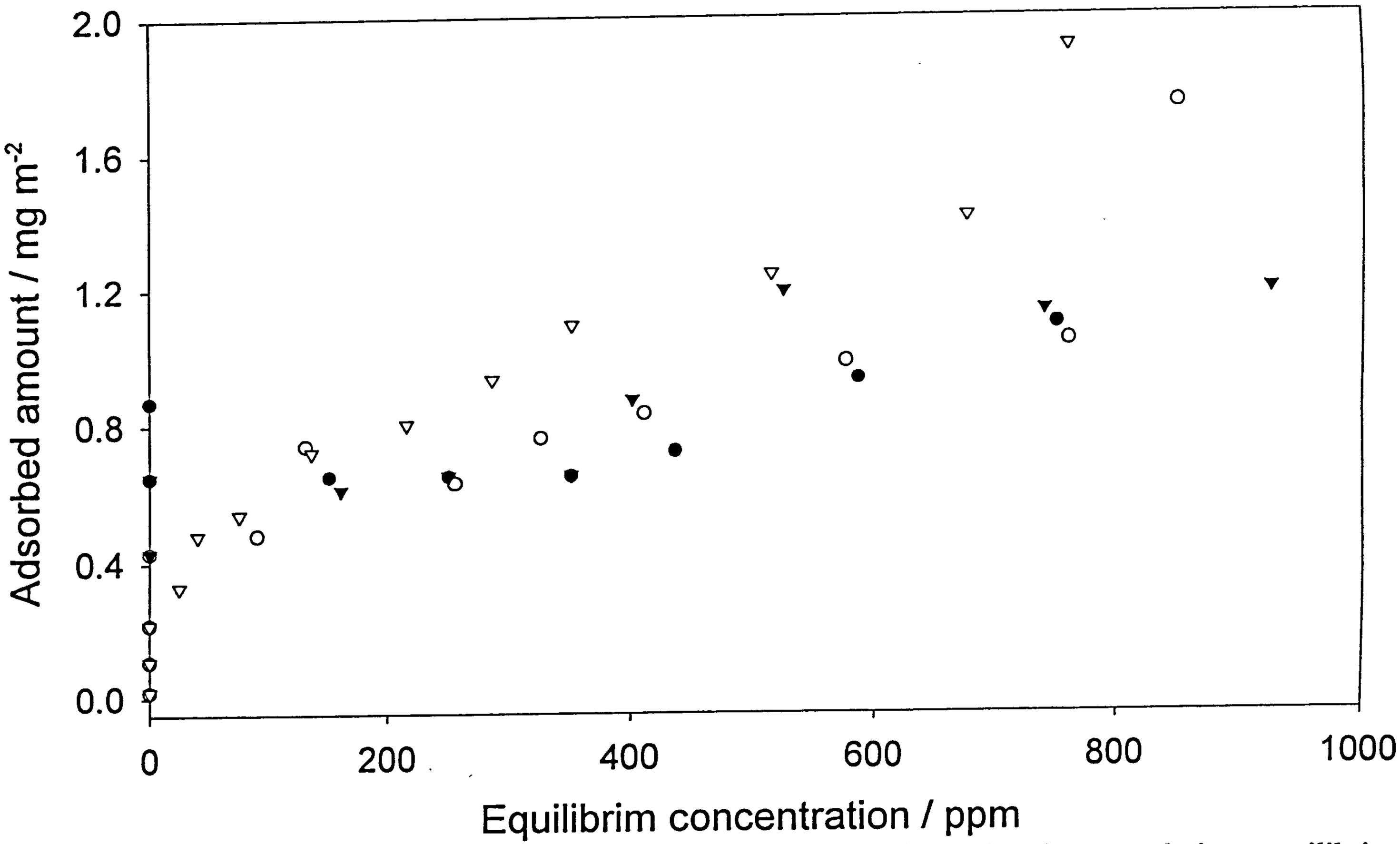


***Figure 5.2 presents the adsorption isotherms as a function of polymer solution equilibrium concentrations for polymers: ● 25R2, O 25R4, ▼22R4 and ▽ 25R5.***

constantly), they found normal adsorption isotherms for these polymers. However, similar to our findings, Baker *et al.*[8] have also found a strong dependence of the level of the polymer adsorption on the polymer molar mass. From these data they inferred a strong interaction between the particle surface and PPO blocks via hydrogen bonds. This makes the PPO blocks lie firmly to the surface in a flat configuration, whilst, the more hydrophilic PEO block would be extended out into the bulk solution in the form of loops.[9,10]

### 5.2.2. Molar Mass Dependence of the Adsorbed Amount

Figure 5.4 shows a strong dependence of the adsorbed amount on the logarithm of the total polymer molar mass for a series of the R.Pluronic copolymers adsorbed on polystyrene latex. The adsorbed amount in each case was derived from the adsorption level of each test polymer and/or from its so-called pseudo-plateau level of the adsorption isotherm taken at *500 ppm* polymer solution equilibrium concentration. The figure shows an approximately linear dependence of the adsorbed amount on the $\log_{10}$ of total polymer molar mass of the samples. Overall, this trend is also found for PEO homopolymers, the normal Pluronics (*see* Figures 7.7 and 8.7) and the Reverse Pluronic copolymers adsorbed onto silica (*see* Figure 6.4).

Figure 5.5(a) shows the dependence of the adsorbed amount of R. Pluronics on the logarithm of PEO block molar mass present. A complex dependence of the adsorbed amount on the $\log_{10}$ of PEO block molar mass, a steady behaviour is found up to a certain level (PEO block molar mass ~ 1250) afterwards a rapid rise in the adsorbed amount, is observed. An exception in this behaviour is found for 10R5 and 12R3, and 31R1. They deviate from the pattern giving, unexpectedly, a very low adsorption for former case, whilst, a very high adsorption in the latter case, respectively. This deviation in the adsorption behaviour of these polymers can be attributed to a very high PPO block mass (hydrophobic) present in the 31R1, which, results in the higher levels of adsorption. For 10R5 and 12R3 polymers, an unexpectedly lower polymer adsorption may be due to the lower PPO block fraction (higher polymer solubility in the bulk solution), which results in a lower level polymer adsorption. Similar trends in the

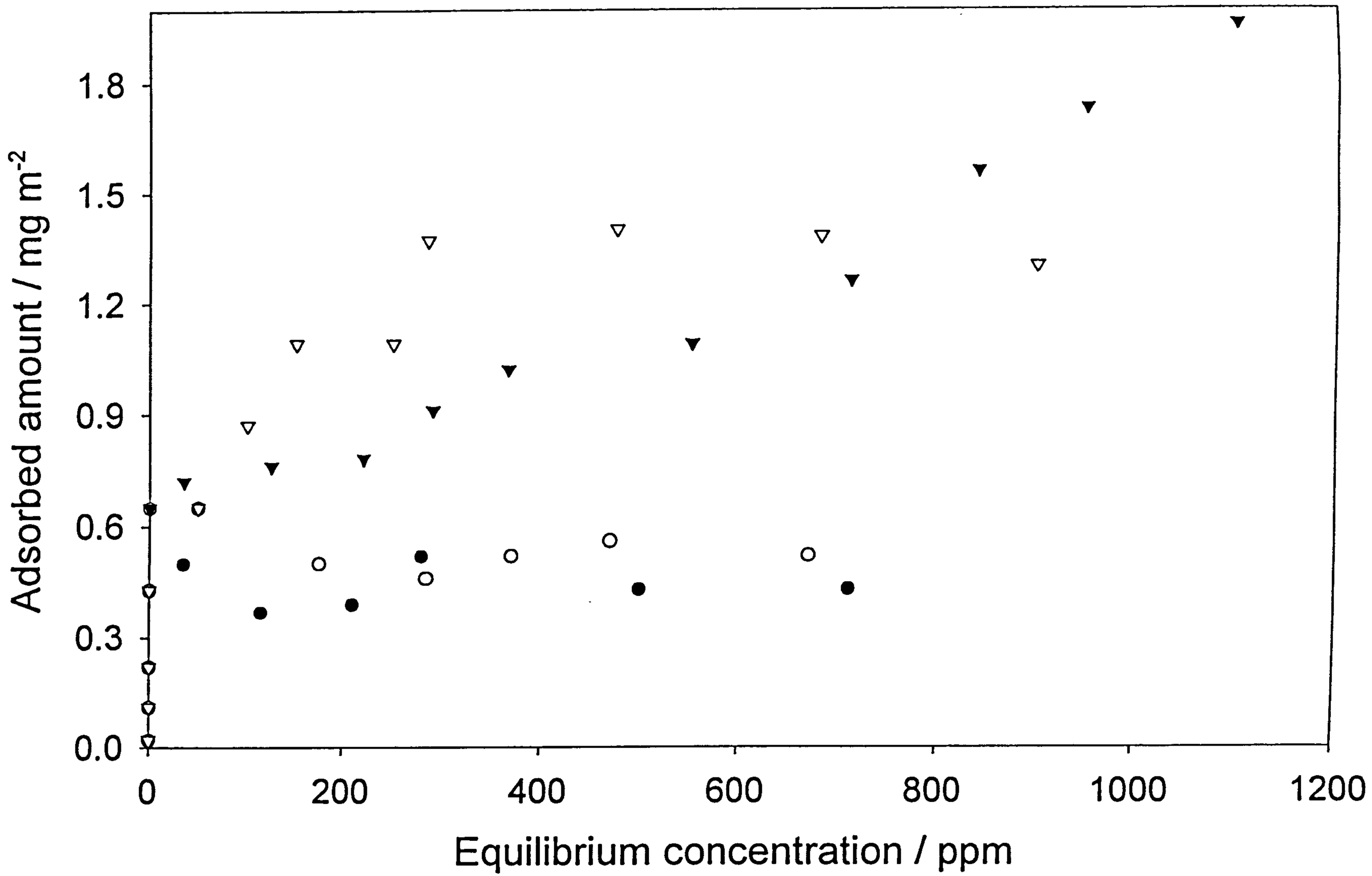


*Figure 5.3 presents the adsorption isotherms as a function of polymer solution equilibrium concentrations for: ● 10R5, O 12R3, ▼31R1 and ▽ 31R4.*

adsorption of 10R5, 25R10[c], 25R15[c] and 31R8[c] are observed from the adsorption data calculated using the SCF model (*see* Figure 5.9(a)). This may be attributed to the high PEO:PPO block ratio, where, a copolymer behaves more like a homopolymer rather than a copolymer.[11]

Figure 5.5 (b) shows the dependence of the measured adsorbed amount on the logarithm of PPO block molar mass present in the polymer. The figure shows that up to a certain level (at PPO block molar mass ~ 1350) the adsorbed amount increases slowly with increasing the PPO block mass (so the polymer molar mass increases), afterwards (*i.e.* at PPO block mass between 1350 and 2500) a tremendous increase in the adsorbed amount is observed. There are two effects influencing these data; adsorbed amount increases with increasing the total polymer molar mass but also it goes through a maximum with changing the anchor fraction (*see* Figures 5.4 and 5.7). These data are in consistent with a transition from *buoy* to the *anchor* regime. Interestingly, the transition occurs at the same molar mass for both PEO and PPO.

Figure 5.6 shows the dependence of the adsorbed amount on the hydrophilic PEO block mass while the hydrophobic PPO block is maintained constant. Two sets of data at two different PPO block masses are presented. A rapid increase in the adsorbed amount with increasing the variable block (PEO) molar mass is observed for the low molar mass polymers which slows down for the case of high molar mass (*and* high PEO content) polymers. It is presumed that the polymers with the lower PEO block content (with high $\nu_A$) lie flat on the surface and hence, giving much lower levels of adsorption. However, any increase in the PEO block molar mass makes the polymer more soluble (hydrophilic) in the bulk solution and tends to lead to the PEO blocks extending further into the bulk solution. In contrast to the behaviour observed for the normal Pluronics adsorbed on polystyrene latex (Δ, ▲) and on silica (for instance *see* Figures 7.9 & 8.9) this figure shows a weak dependence of the adsorbed amount on PPO block molar masses, whilst, the PEO block mass is maintained constant. Although, there is an indication of initial steep rise the results eventually suggest a linear increase in the adsorbed amount with increasing PEO content.

---

[c] Very low anchor fraction, PPO-PEO-PPO triblock polymers used for the SCF calculations.

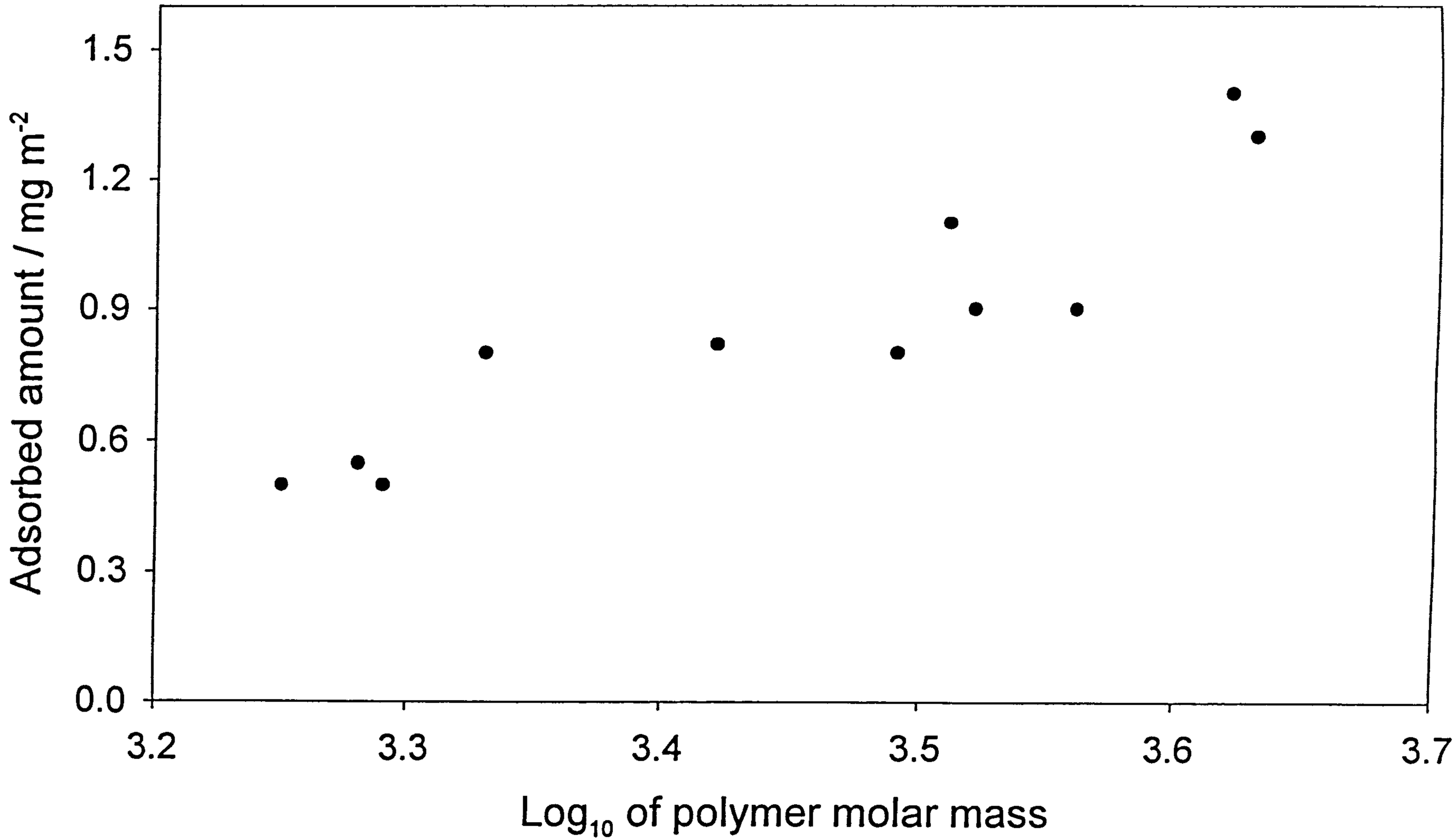


***Figure 5.4 shows the dependence of the measured adsorbed amount on the logarithm of the total polymer molar mass of the R. Pluronic copolymers adsorbed on latices.***

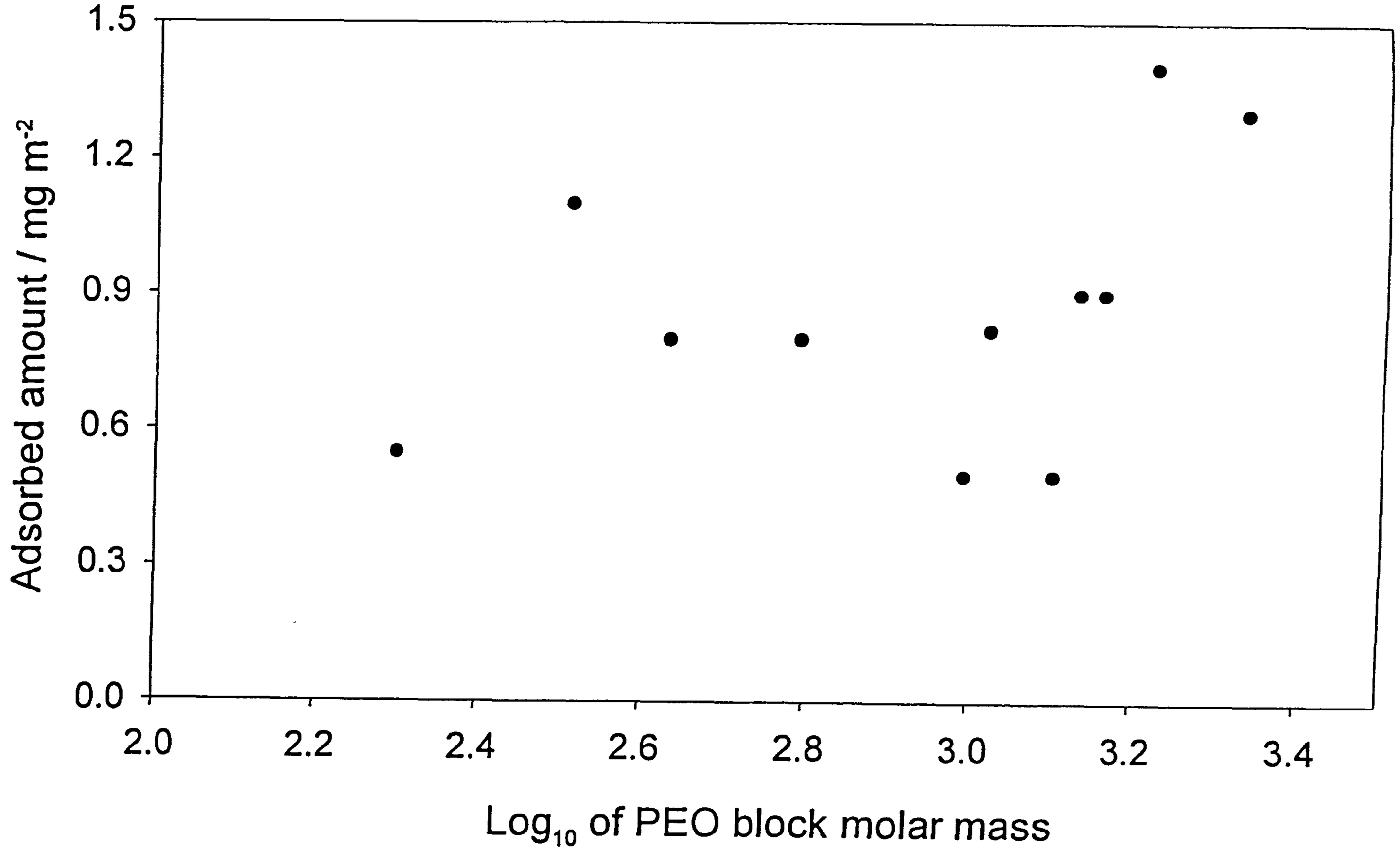


***Figure 5.5(a) shows the dependence of the measured adsorbed amount on the logarithm of the PEO block molar mass of the R. Pluronics adsorbed on latices.***

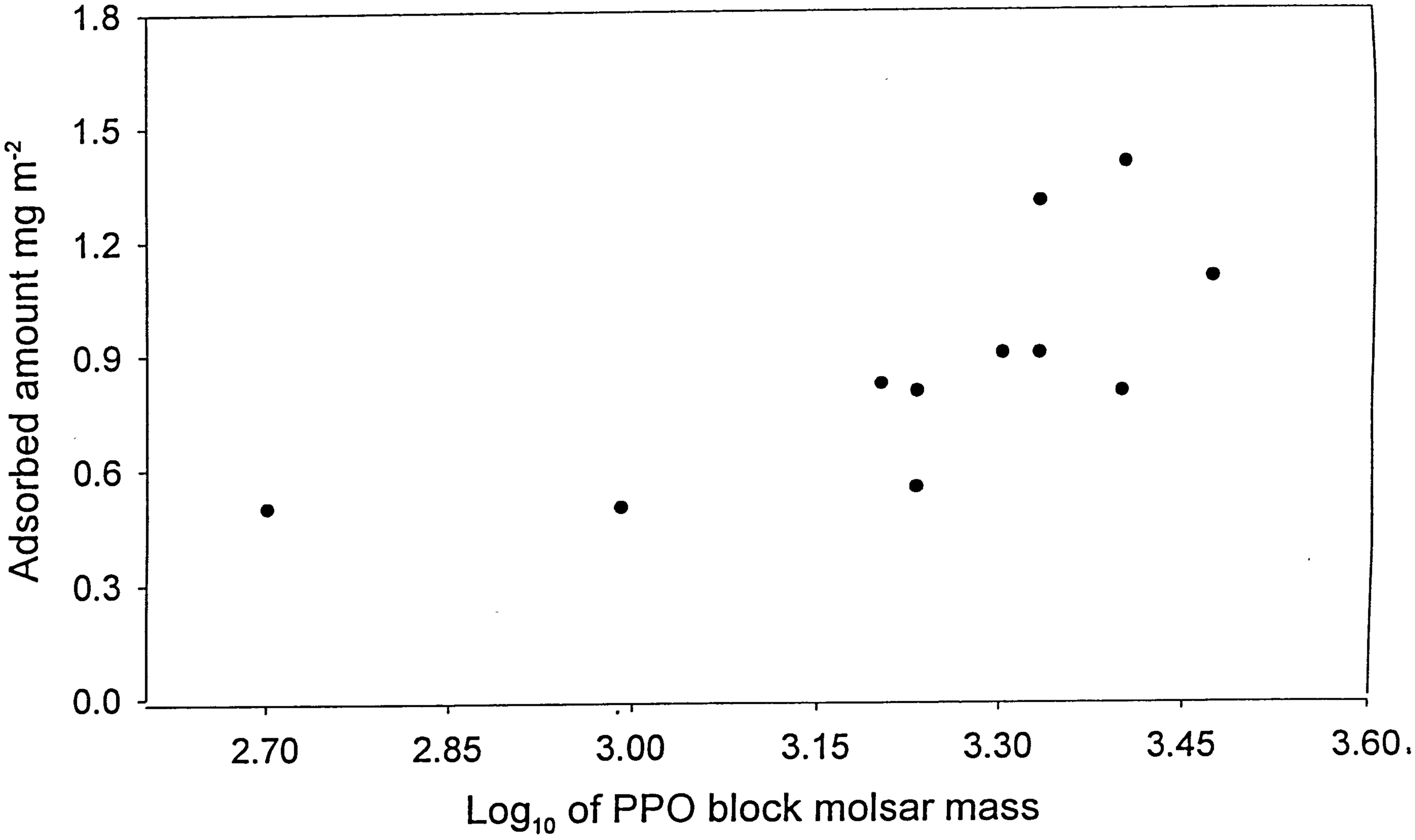


***Figure 5.5 (b) shows the dependence of the measured adsorbed amount on logarithm of the PPO block molar mass.***

### 5.2.3. Theoretical Predictions for the Adsorbed Amount

For the SCF[6,12] calculations polymer solution concentrations in the range 0 to 2000 ppm were used and 500 ppm polymer equilibrium concentration were chosen for comparison with experiment. For all the calculations related to the PEO-PPO adsorption on the hydrophobic surfaces, the Flory parameters were chosen as follows: $\chi_{PS} = -4.00$, $\chi_{ES} = -1.00$, $\chi_{EP} = 2.00$, $\chi_{EW} = 0.45$, $\chi_{PW} = 0.5$, and $\chi_{WS} = 0.00$, where E is ethylene oxide, P propylene oxide, W water and S is the surface of the polystyrene latex used. These parameters reflect the influence of solvent-surface, solvent-segment, surface-segment and segment-segment interactions,[13] their influence on polymer adsorption is detailed in Section 9.2.1, for this also see Figure 9.2(b). For the hydrophobic polystyrene latex substrate the PPO block due to its more hydrophobic nature was assumed to adsorb preferentially to the hydrophilic PEO block. Both of the polymer monomer types as well as the water solvent were considered to occupy a single lattice site.

The influence of the anchor fraction on the measured adsorbed amount is shown in Figure 5.7. The inset in this figure is the calculated data for the same series of polymers under study (*see* Table 4.4) determined using the SCF model.[6,12] A continuous decrease in the measured adsorbed amount in the range $\nu_A \sim 0.2$ to 1.0 is observed. The trends observed in the calculated data (*see* inset Figure) show a good qualitative agreement with the calculated adsorbed amounts. Interestingly the theoretical results for 12R3 and 10R5, which unexpectedly give a lower level of adsorption are also in a good agreement with the experimental. Extra theoretical points have been added at $\nu_A \sim 0.1$ and show that at $\nu_A \sim 0.2$ there is a maximum in the adsorbed amount. Unfortunately, no experimental samples were available in that range.

Figure 5.8 presents the strong dependence of the adsorbed amount on $\log_{10}$ of total polymer molar mass, as for the same series of R. Pluronic copolymers used in this study calculated using SCF model.[6,12] As for the measured adsorbed amount (*c.f.* Figure 5.4) a strong dependence of the adsorbed amount on the $\log_{10}$ of polymer molar mass is observed.

Figure 5.9 (a) shows the theoretical dependence of the adsorbed amount on the

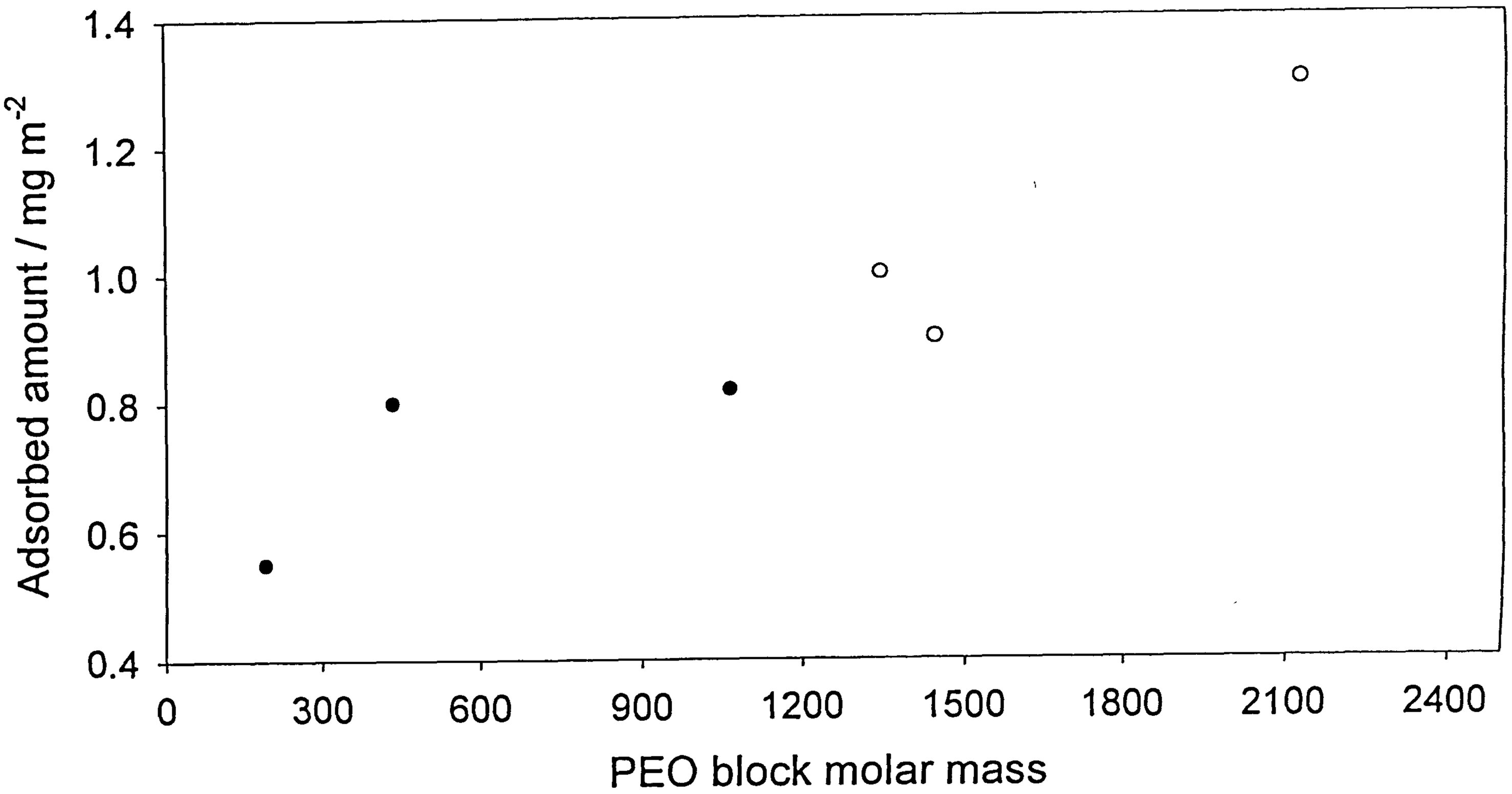


*Figure 5.6 shows the dependence of the adsorbed amount on the hydrophilic PEO block size while the hydrophobic PPO block is kept constant: reverse Pluronics, ● PPO≅1700 and O PPO≅2000.*

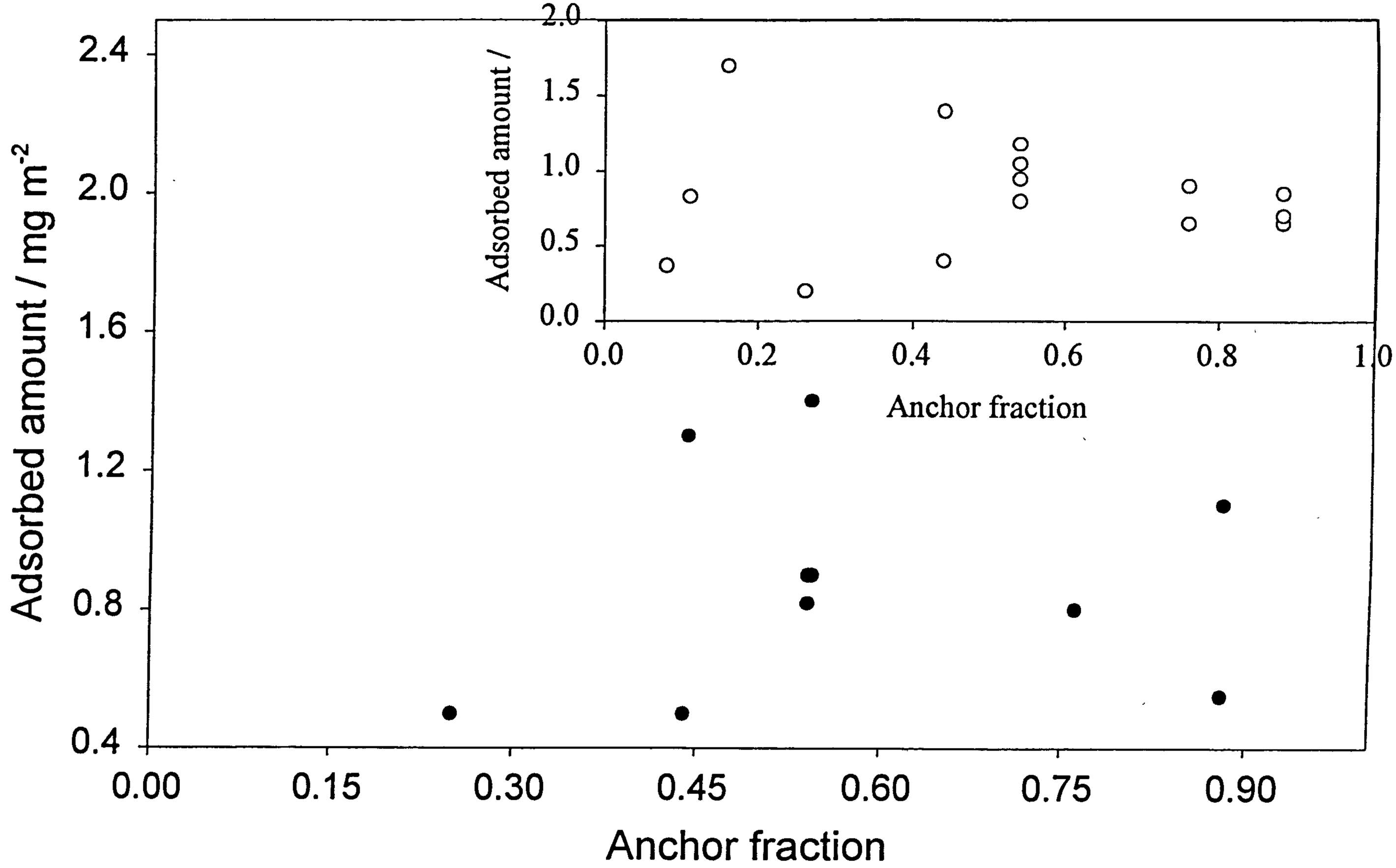


***Figure 5.7 shows the influence of anchor fraction on the adsorbed amount of R. Pluronic copolymers adsorbed on polystyrene latex: ● measured data and O (inset data) calculated data using the SCF model.***

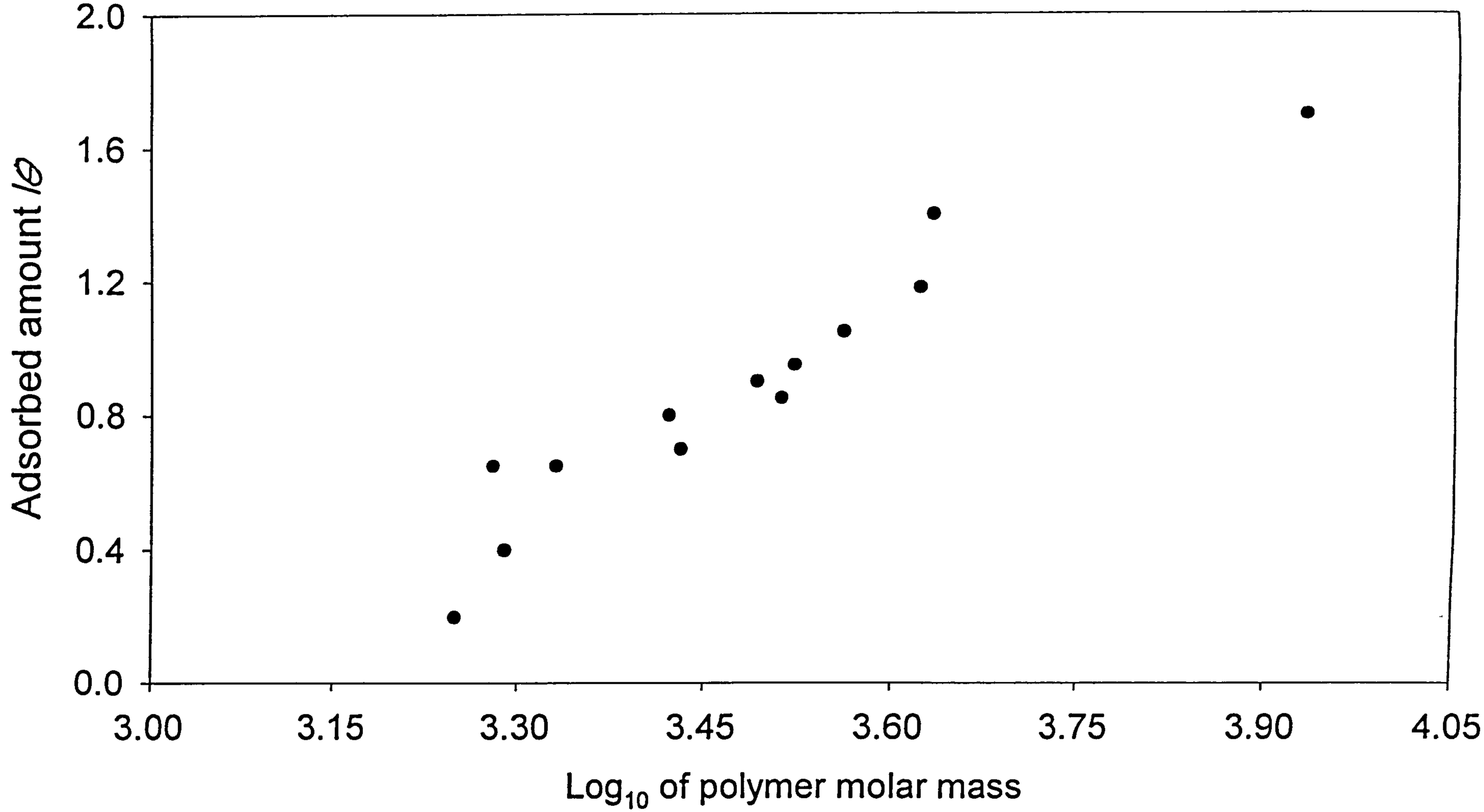


***Figure 5.8 presents the dependence of the adsorbed amount on $log_{10}$ of total polymer molar mass for a series of R. Pluronic copolymers adsorbed at aqueous/latex interface calculated using the SCF model.***

f PEO block molar mass. Overall, a very good qualitative agreement in the e adsorption behaviour is observed between the calculated and the measured igure 5.5(a)). As was also observed for the measured data the 10R5 and ıte from the pattern, adsorbing at relatively lower levels. Both these ıve a lower level of adsorption (both *measured* and *calculated*) and suggests ɔn of relatively small loops and hence thinner polymer adsorbed layers.

ıre 5.9(b)) shows the dependence of the adsorbed amount on the logarithm ck molar mass calculated using the SCF model[6,12] and compared with the ıl data in Figure 5.5(b). The trends highlight the importance of the higher rophobicity in the polymers with high anchor block ratios.

ıre 5.10 shows a linear dependence of the adsorbed amount determined SCF model[6,12] on the measured adsorbed amount for the same series of . Ideally, a slope of 1 would be expected (as shown) but this depends on ry to experiment. Overall, the similarity of the data is very convincing.

## drodynamic layer thickness

hydrodynamic thickness of the adsorbed polymer layer for the reverse ɔck copolymers (PPO-PEO-PPO) adsorbed at the aqueous/polystyrene latex as determined as a function of the polymer molar mass at a fixed bulk ncentration of 1000 ppm. All the measurements were performed using elation spectroscopy (PCS).

## lar Mass Dependence of the Hydrodynamic Layer Thickness

ıre 5.11 shows a double logarithmic plot of $\delta_H$ versus total polymer molar polymers under study (*see* Table 4.4). The figure shows a shallow increase $\delta_H$ with increase in $\log_{10}$ of polymer molar mass. Overall an approximately ıdence of $\log_{10}$ of $\delta_H$ on $\log_{10}$ of the polymer molar mass is observed which vith the behaviour observed for the adsorbed amount, though the rate of s faster (*see* Figure 5.4). This behaviour is rather different to that observed lymers where very long tails can be formed and increase observed for the

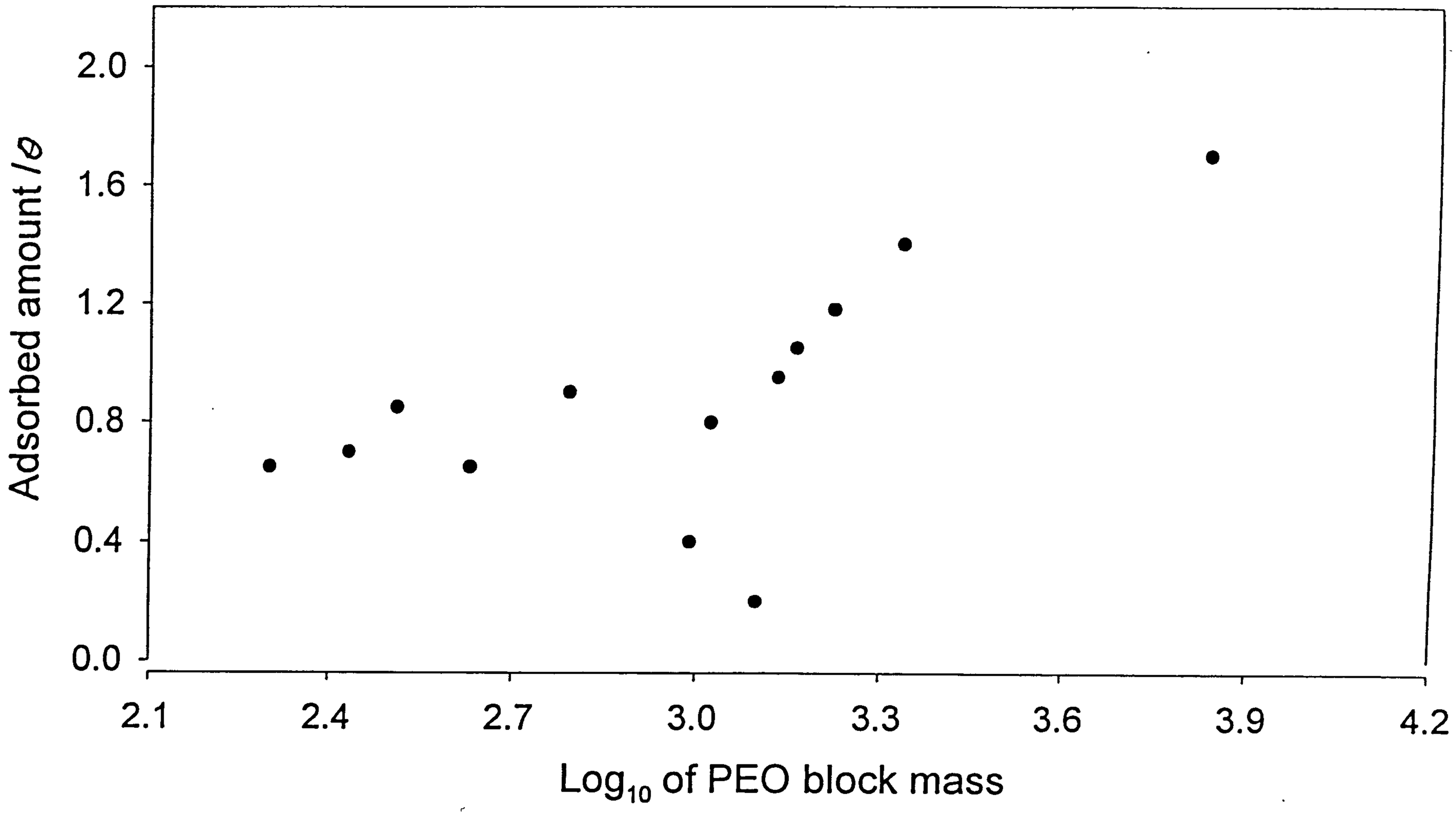


***Figure 5.9(a) shows the dependence of the adsorbed amount, calculated using SCF model, on logarithm of the PEO block molar mass.***

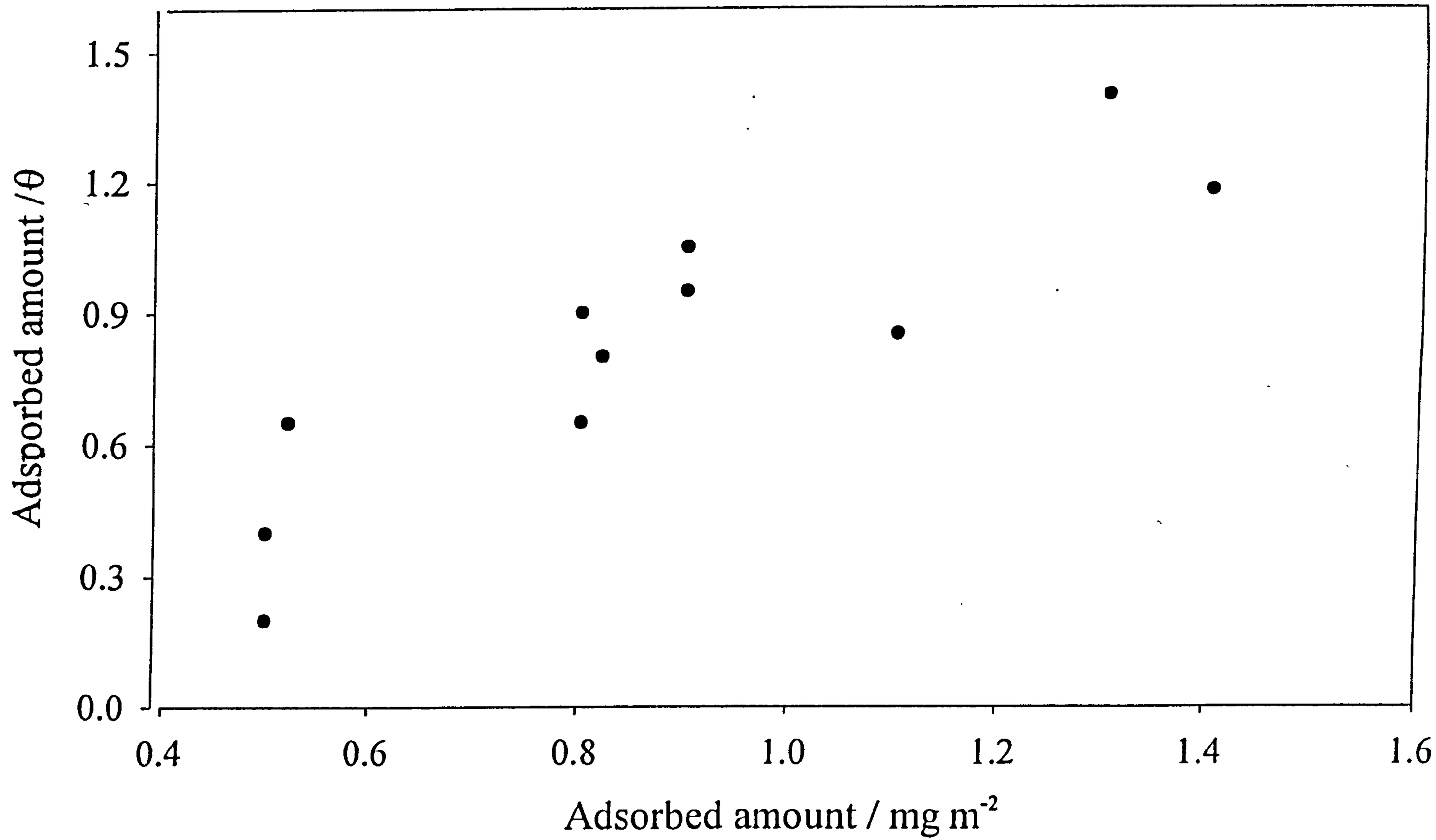


***Figure 5.10 shows the dependence of the calculated adsorbed amount on the measured adsorbed amount for R. Pluronic copolymers adsorbed on polystyrene latex.***

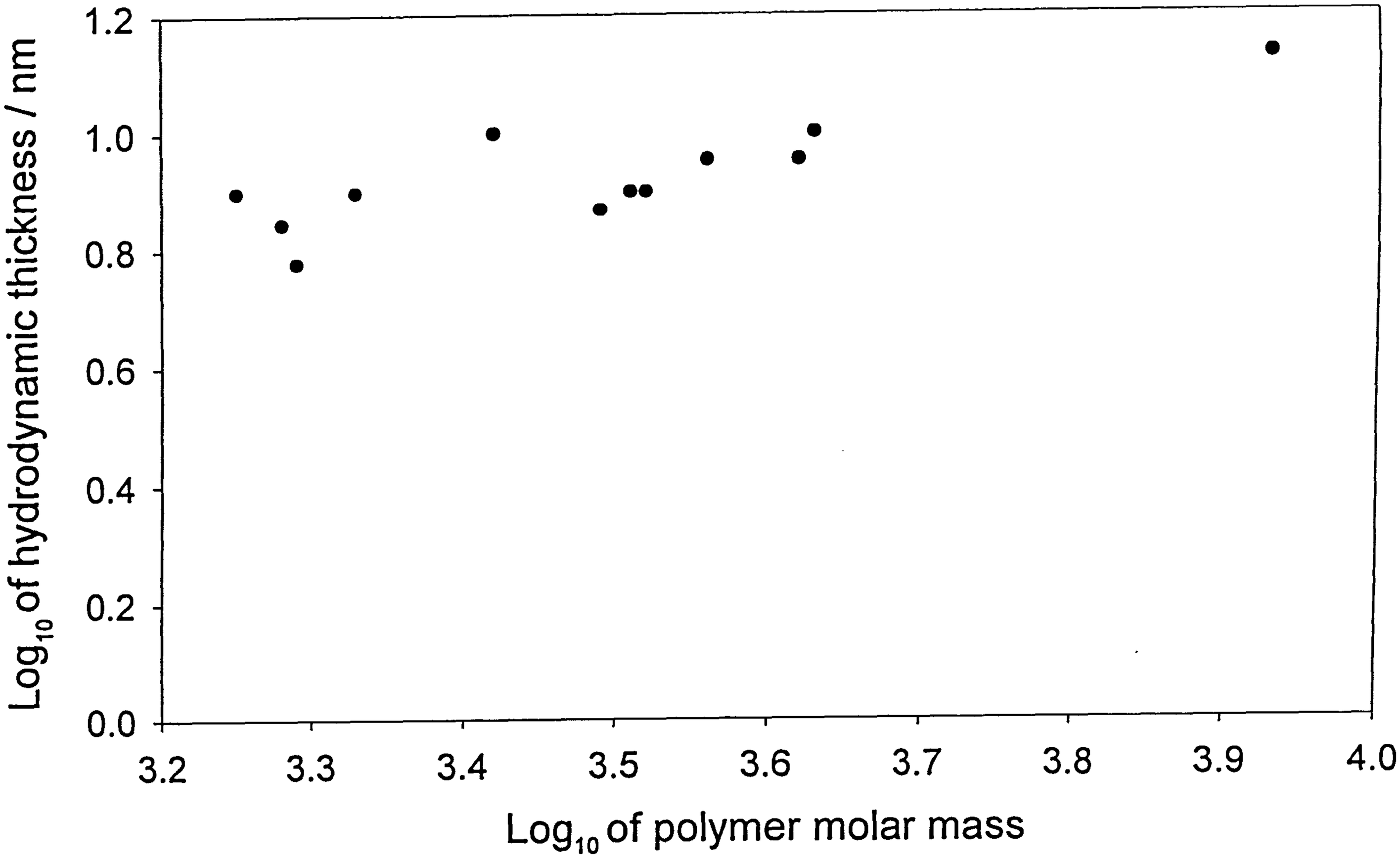


***Figure 5.11 presents the dependence of $log_{10}$ of the measured adsorbed layer thickness on $log_{10}$ of the total polymer molar mass.***

case of copolymers is in the propensity of loops. Applying the scaling relation $\delta_H \sim M^{\alpha}$, gives a value of $\alpha = 0.31$, which is much smaller than that obtained for the normal Pluronics (0.8) and PEO homopolymers ($\alpha = 0.4$). The values of $\alpha$ found in this work are much smaller than those presented for the PEO homopolymers (adsorbed on polystyrene latices), where, $\alpha$ varies between 0.4 and 0.8.[14,15,16]

Figure 5.12 shows double logarithmic plots of the dependence of the hydrodynamic thickness of the R. Pluronic adsorbed layer on PEO block molar mass. An approximately linear dependence is again observed suggesting a scaling relationship of the form $\delta_H \sim M^{\alpha}$, where $\alpha = 0.12$. However, $\alpha$ is smaller for this case than that observed in Figure 5.11 and is indicative of loop formation.

The influence of PEO block molar mass on $\delta_H$ of reverse polymers at *constant* PPO block content is shown in Figure 5.13. Two sets of data measured at two different fixed PPO block molar masses are presented. $\delta_H$ increases with increasing the PEO block molar mass at low values and slows down for higher values. An increase in PEO block size ultimately increases the number of PEO segments in loops, which, increase the adsorbed amount and hence in turn hydrodynamic thickness of the polymer adsorbed layer is increased. However, this effect is found to weaken for the high molar mass and more hydrophilic polymers. It has been predicted that the tails and/or loops contribute more towards the hydrodynamic thickness of the adsorbed polymer layer than they do to the adsorbed amount.[9,10] In addition, the dependence of $\delta_H$ on the PPO block molar mass is also presented, whilst, the PEO block is maintained constant. Contrary to the behaviour found for the normal Pluronic polymers (*see* Figures 7.13 and 8.14) any increase in the PPO block molar mass (at constant PEO block mass) decreases the thickness of the polymer adsorbed layer (*see* Figure 5.13). For the Reverse Pluronics any increase in the PPO block molar mass (at constant PEO block mass) increases the net interactive affinity between the polymer and the hydrophobic polystyrene latex surface, which results in increased number of trains (flat configuration). $\delta_H$ is also sensitive to the PPO block but this effect is not seen for the adsorbed amount.

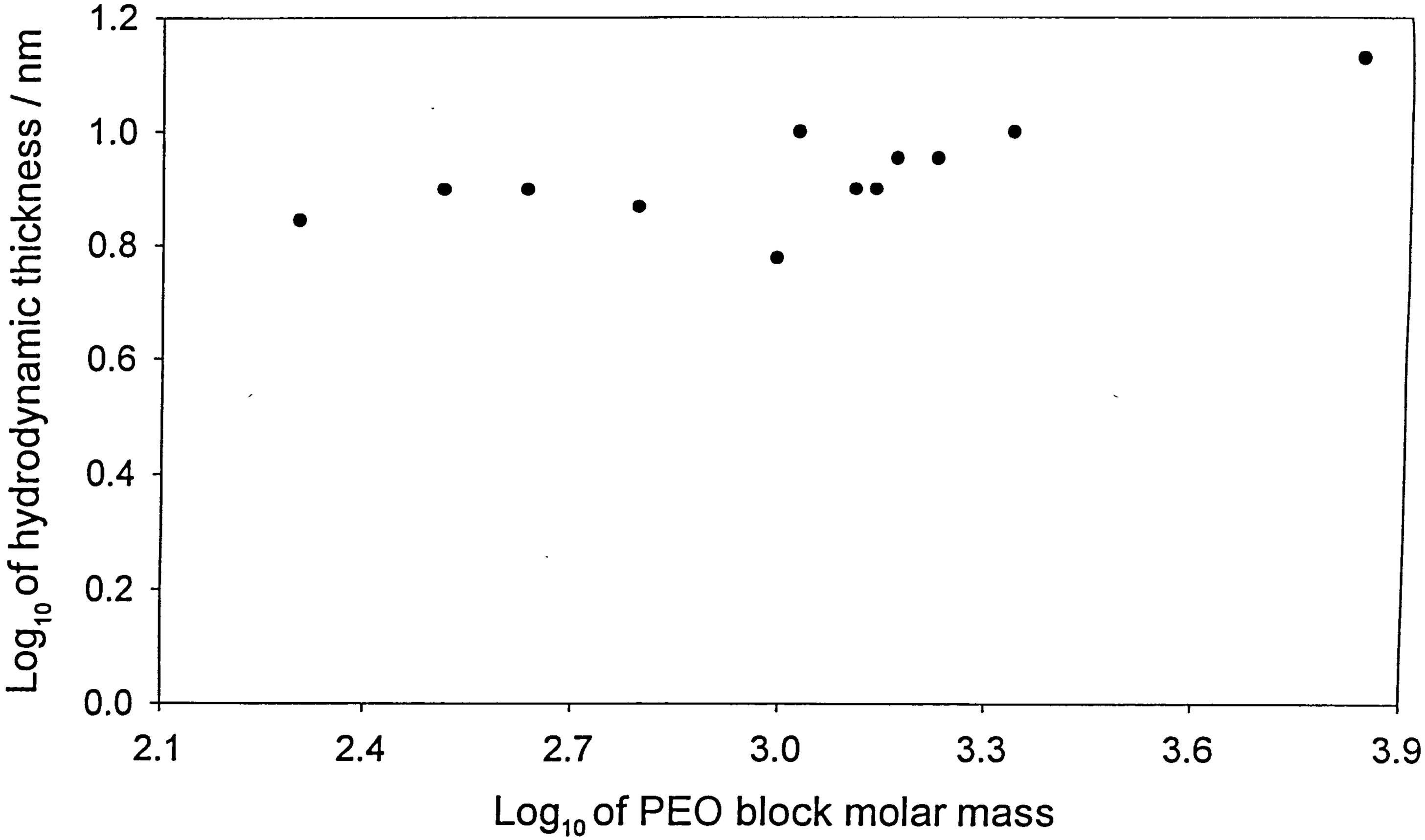


***Figure 5.12 presents the dependence of $log_{10}$ of the measured adsorbed layer thickness on $log_{10}$ of the PEO block molar mass.***

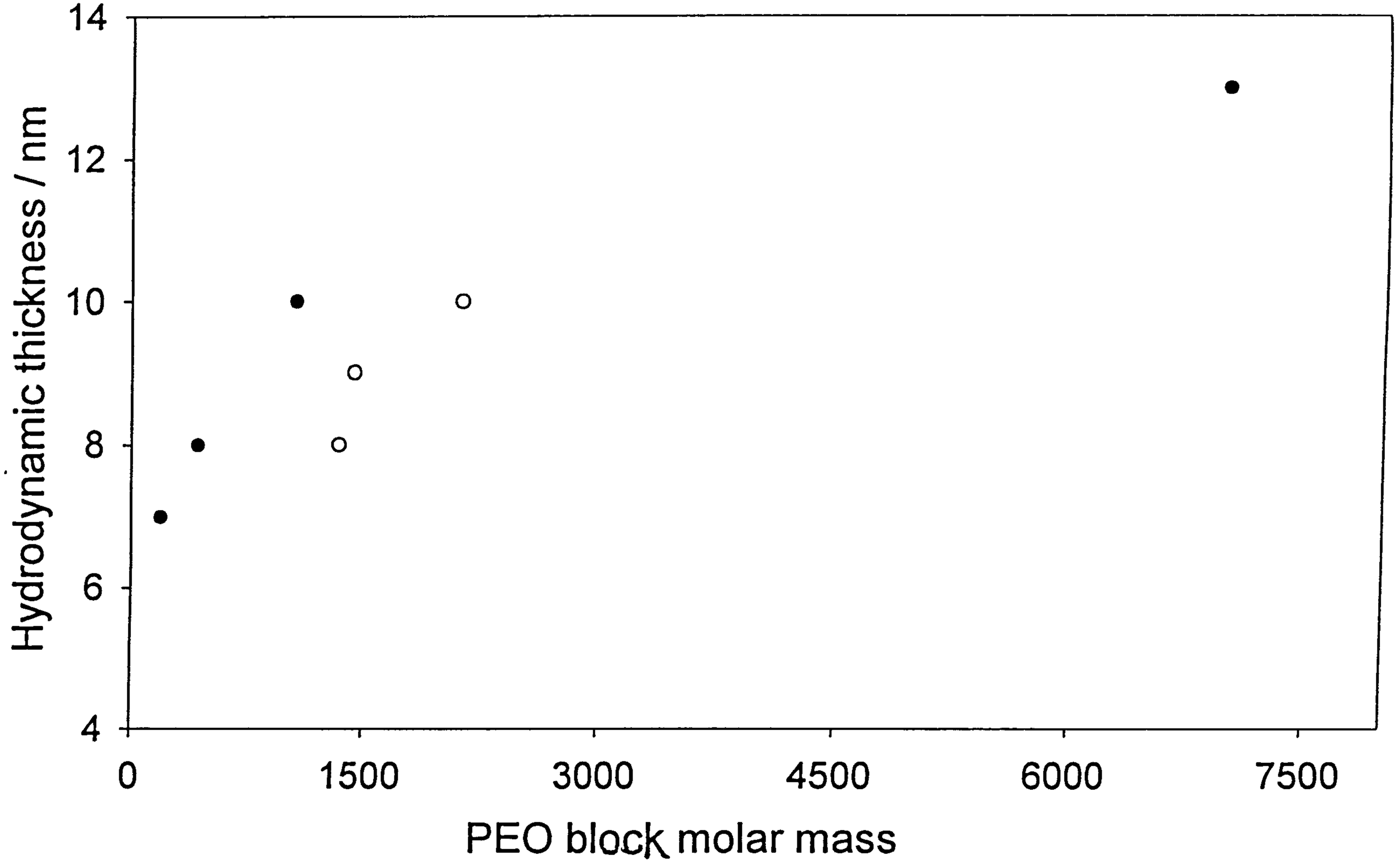


*Figure 5.13 shows the dependence of the measured hydrodynamic layer thickness on PEO block molar mass while the hydrophobic PPO block is kept constant for the reverse Pluronics: ● PPO≅1700 and O PPO≅2100*

### 5.3.2. Theoretical Predictions for Hydrodynamic Layer Thickness

Figure 5.14 shows the dependence of $\log_{10}$ of the calculated adsorbed layer thickness on $\log_{10}$ of the total polymer molar mass for the same set of polymers used in this study adsorbed at the aqueous/polystyrene latex interface. The data were determined using the SCF model[6,12] in a similar manner as described earlier. A shallow increase (which slows down in the region of high molar mass polymers) in the polymer adsorbed layer thickness with increasing the total polymer molar mass is observed. The trends observed in the patterns of the data are in a good qualitative agreement with those observed for the measured thickness determined for the same set of polymers. The apparent 'noise' in the data can be attributed to the fact that the polymer samples used for this study were of different total polymer molar mass and anchor fraction. They all belong to different "families" hence showing effects of total molar mass as well as that of the anchor fraction.

Figure 5.15 presents the dependence of $\log_{10}$ of the calculated adsorbed layer thickness on $\log_{10}$ of the PEO block molar mass for the same set of polymers used in this study. As observed from the measured data (*see* Figure 5.12(a)) this figure also shows a strong dependence of the adsorbed layer thickness on the size of the PEO block. This again emphasises an overwhelming contribution by the PEO block molar mass towards the loop formation. Also, a significant effect of the polymer molar mass and the PPO:PEO block ratio is clearly seen from this figure *i.e.* 12R3, 25R10,[c] 25R15[c] and 31R8[c] polymers with very high PEO fractions show relatively thin adsorbed layers which may be attributed to their higher solubility in the bulk. These polymers adsorb at lower levels and hence give thinner adsorbed layer thicknesses than those polymers having similar molar masses but low PEO fraction. It is presumed that the PEO block size gives a rough measurement of the hydrodynamic loop thickness of the adsorbed layer.[8]

Figure 5.16 shows the influence of the anchor-fraction on the measured adsorbed layer thickness of the PPO-PEO-PPO triblock copolymers. Inset into this figure is the adsorbed layer thickness data calculated using the SCF model[6,12] for the same set of polymers under study (*see* Table 4.4). A continuous increase in the

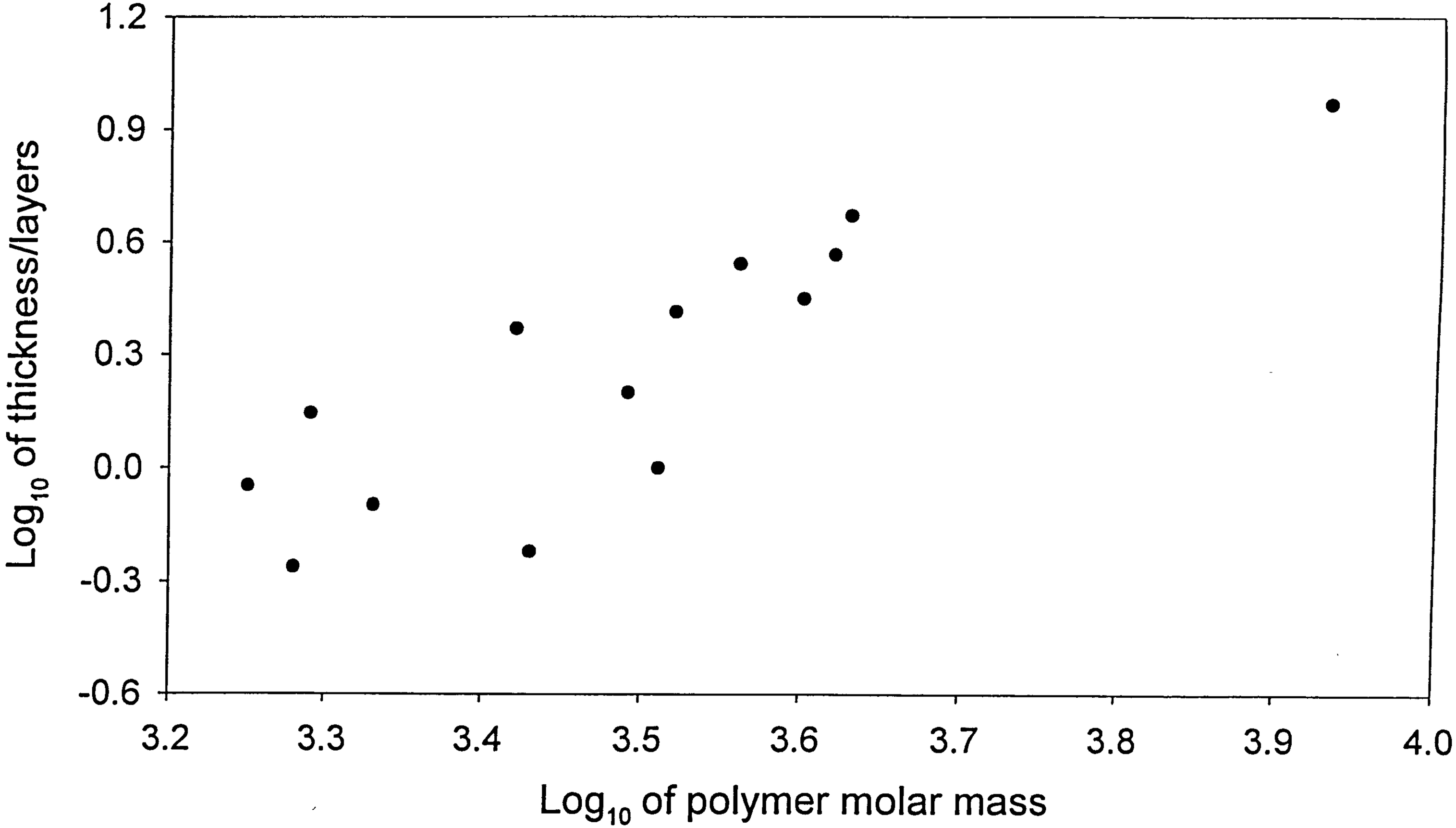


***Figure 5.14 shows the dependence of $log_{10}$ of the adsorbed layer thickness calculated using the SCF model on $log_{10}$ of total polymer molar mass.***

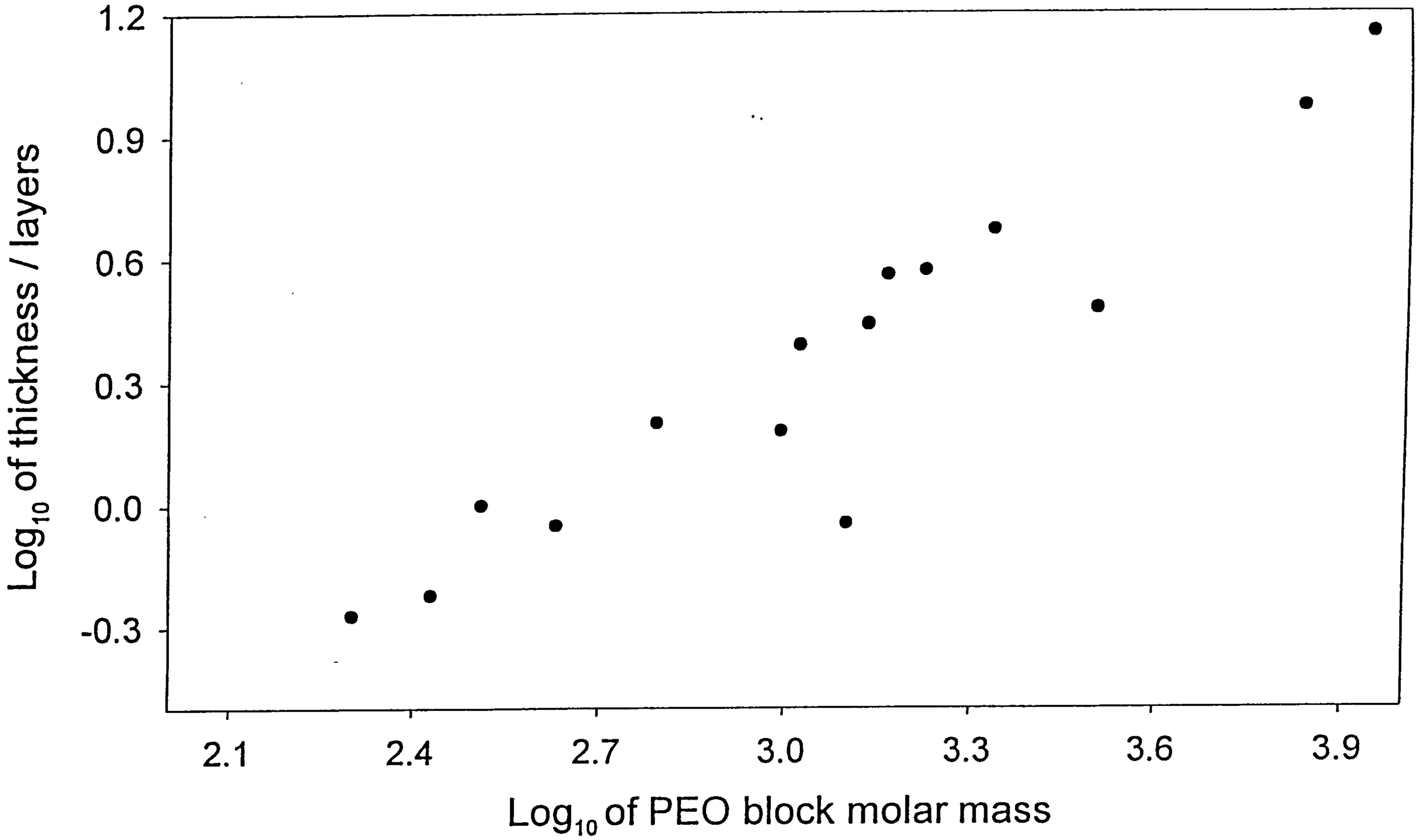


***Figure 5.15 presents the dependence of $log_{10}$ of the adsorbed layer thickness on $log_{10}$ of the PEO block molar mass, calculated using the SCF model.***

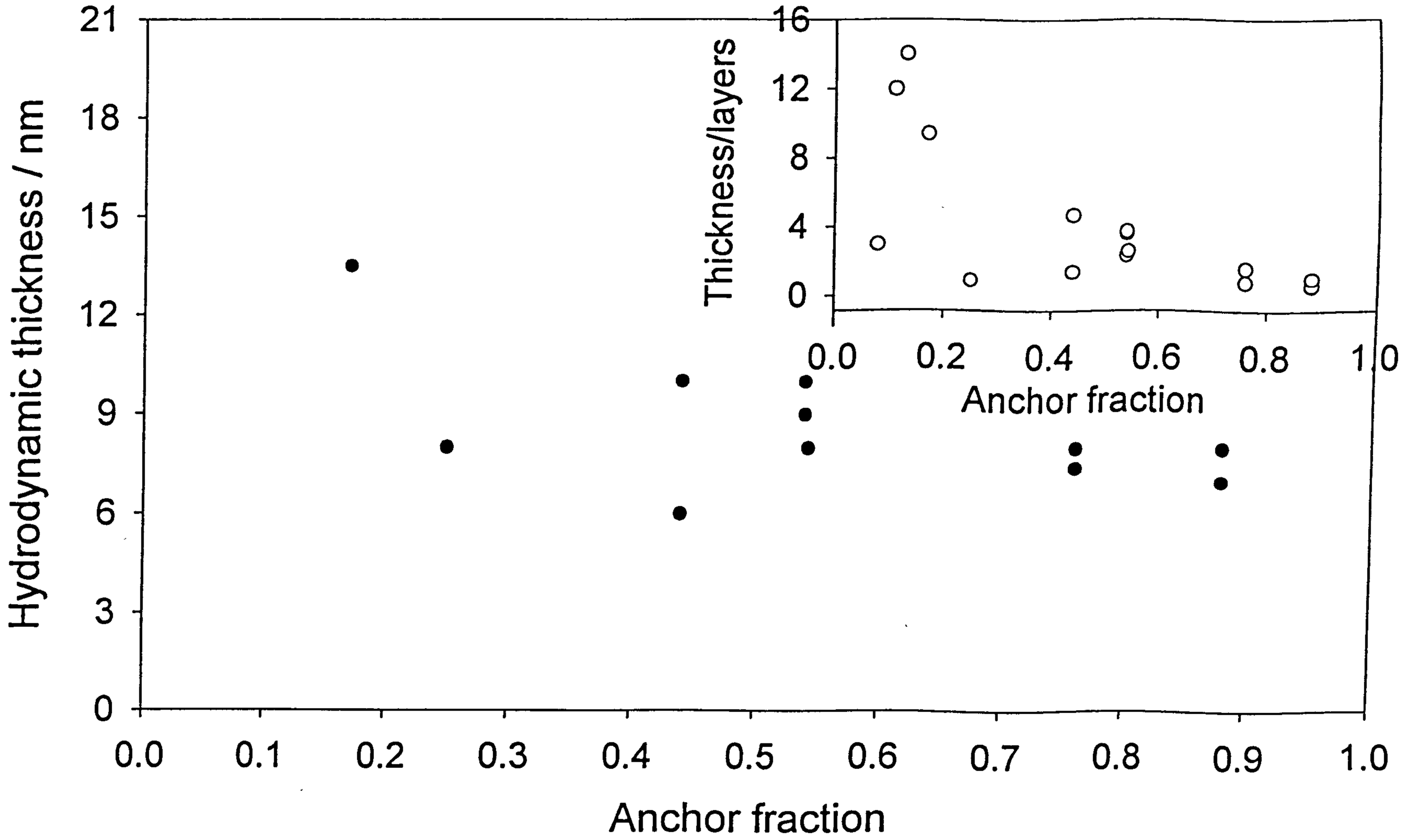


*Figure 5.16 shows the influence of anchor-fraction on the adsorbed layer thickness for the PPO-PEO-PPO triblock copolymers: ● measured and O calculated adsorbed layer thickness data.*

measured adsorbed layer thickness, with decreasing the anchor fraction is observed and compare favourably with the trends and patterns of the calculated data. Interestingly, the low molar mass and low anchor fraction polymers, 10R5 and 12R3, show lower level of adsorption (as was seen for the case of their adsorbed amounts, *see* Figure 5.7) and hence form thinner adsorbed layers.

Similar overall behaviour has also been observed with diblock copolymers[17] but this is the first time that this behaviour has been observed with a wide range of varying composition triblock copolymers having two hydrophobic ends and a hydrophilic block in the middle (*c.f.* Figure 5.7).

Figure 5.17 presents the dependence of the adsorbed layer thickness calculated using the SCF model[6,12] on the measured hydrodynamic thickness of the polymer adsorbed layer. The figure shows two sets of data for the polymers distinguished from each other by having different polymer molar mass ranges. The lower data set shows relatively thinner adsorbed layer thickness' for the low molar mass polymers, whilst, the upper data set (thicker adsorbed layer thickness) presents the polymers with relatively higher molar masses. The trends in the behaviour of the data indicate a strong influence of the polymer molar masses on the polymer adsorbed layer thickness. Overall, a very strong interdependence is observed between the two data sets *i.e.* the calculated and the measured adsorbed layer thickness'.

### 5.3.3. Dependence of Hydrodynamic Thickness on the Adsorbed Amount

Figure 5.18 shows the dependence of the measured hydrodynamic thickness of the adsorbed polymer layer on the adsorbed amount. An approximate linear increase in the hydrodynamic layer thickness with increasing the adsorbed amount is observed showing a strong interdependence of these two adsorption parameters. A close resemblance between the trends in the adsorption data presented in this figure is observed with those observed for the normal Pluronics (*see* Figure 8.18 (a)). However, for the case of latex system the R. Pluronics are observed to form relatively thicker adsorbed layers for the same adsorbed amounts than those observed for the normal

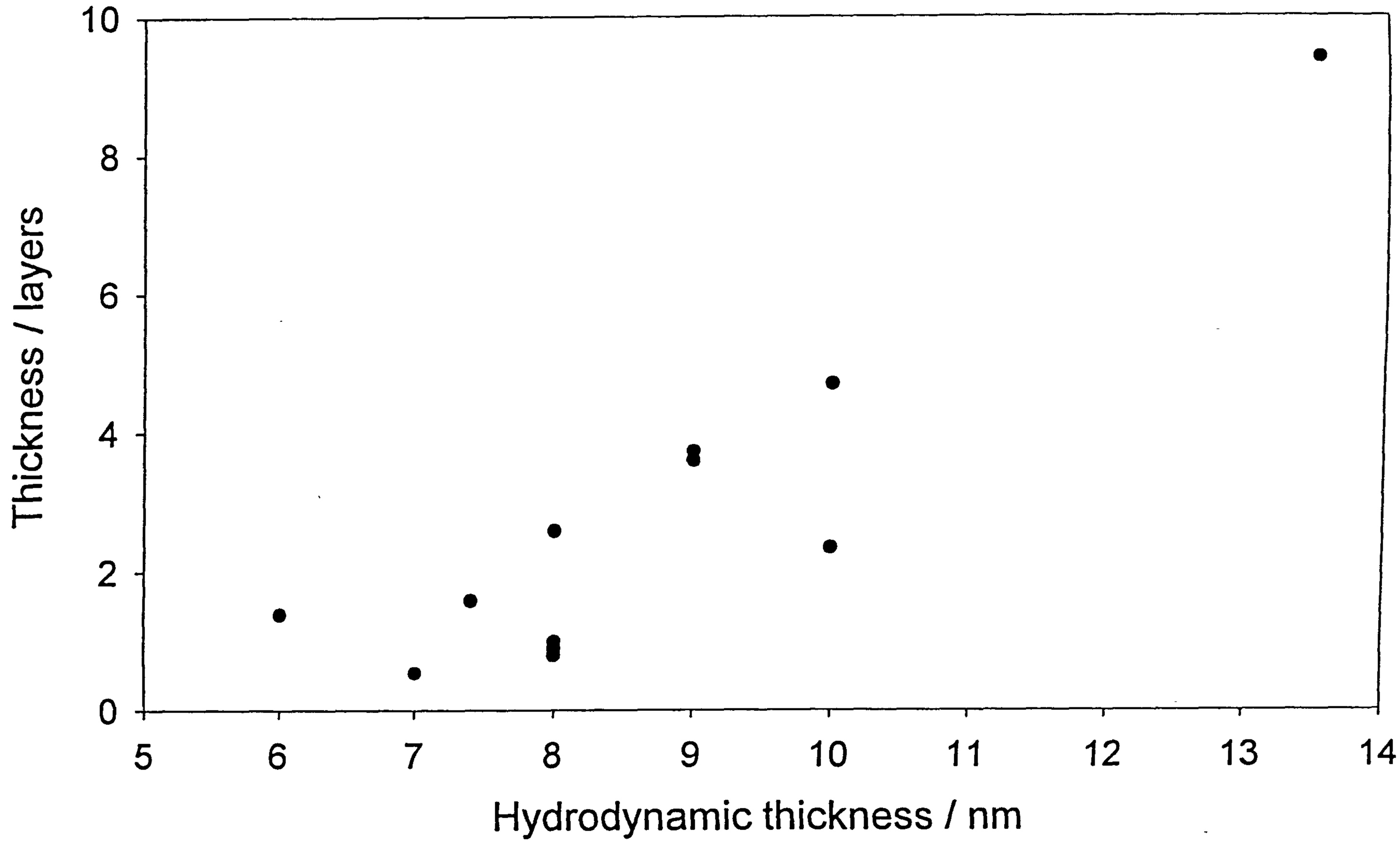


***Figure 5.17 shows the dependence of the calculated adsorbed layer thickness on the measured adsorbed layer thickness for a set of the reverse Pluronic copolymers under study.***

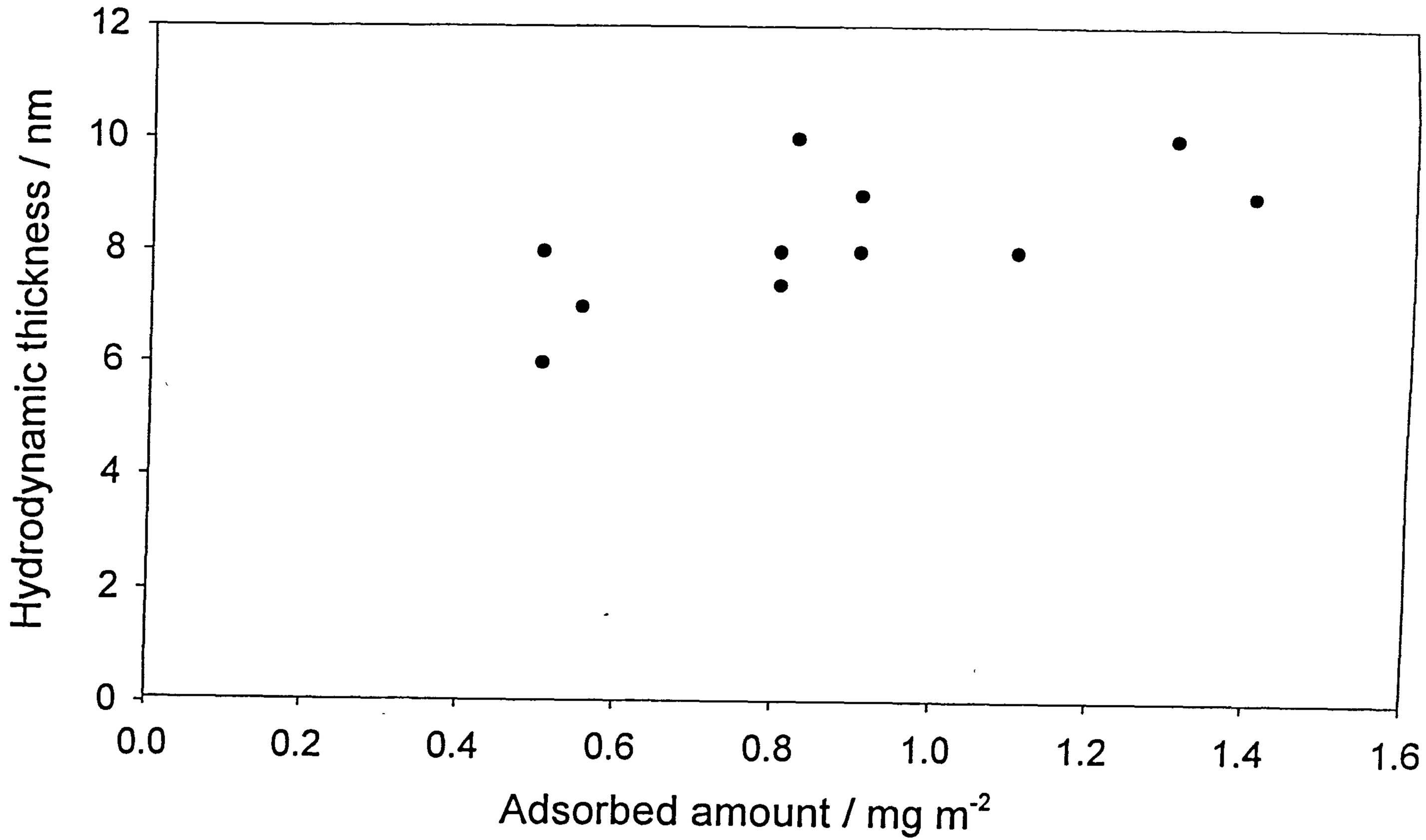


***Figure 5.18 presents the measured hydrodynamic thickness of the adsorbed polymer layer for the polymers adsorbed on polystyrene latex as a function of the measured adsorbed amount.***

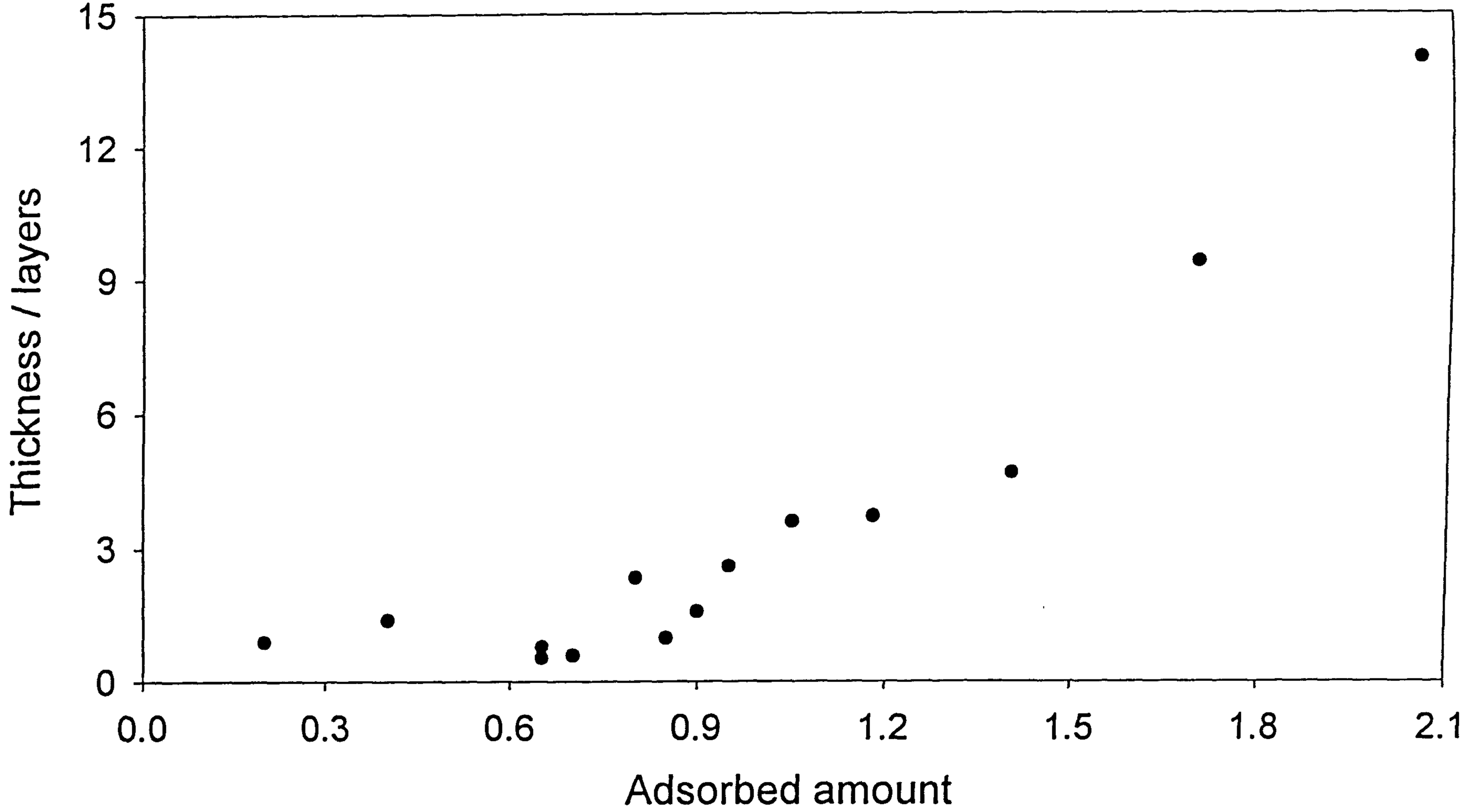


***Figure 5.19 shows the dependence of the adsorbed layer thickness on the adsorbed amount calculated using the SCF model.***

polymers (*see* Figure 7.18 (a)). This is reasonable as the reverse Pluronics can form more loops at expense of tails. This figure shows that for the case of reverse Pluronics even at low adsorbed amounts a reasonably thick adsorbed layer is evident, which becomes thicker with increasing the adsorbed amount. However, in contrast to the findings of Cohen-Stuart *et al.*[6] for PEO homopolymers adsorbed on polystyrene latex the rate of increase in the adsorbed layer thickness observed for the reverse polymers is found to be relatively weak and this is due to the formation of loops which are always considerably shorter than tails.

Figure 5.19 shows that the dependence of the adsorbed layer thickness on the adsorbed amount for the reverse copolymers (PPO-PEP-PPO) calculated using the SCF model.[6,12] Overall, a strong interdependence of these two adsorption parameters is observed. Relatively thicker adsorbed layers are found for given adsorbed amounts for the more hydrophilic polymers (10R5 and 12R3). This figure shows relatively thinner calculated adsorbed layers for corresponding adsorbed amounts than those measured experimentally. The comparison between the data shows a relatively higher rate of increase (in the hydrodynamic thickness as a function of the adsorbed amount) for the calculated data shown in this figure than those observed for the measured data (*see* Figure 5.18). Overall, a good qualitative agreement is evident between the data calculated using the SCF model and those measured for the same set of polymers.

## 5.4. Conclusion

1) In general, the level of polymer adsorption increases with increasing total polymer molar mass.

2) For the case of reverse Pluronics adsorbed on polystyrene latex most of the polymers studied do not reach any plateau level and hence a continuous increase in the adsorption with increasing the solution concentration is observed. This emphasises *end-to-end* interactions existing between the two anchor blocks of neighbouring molecules. These effects of *anchor-anchor* interactions may result in the bilayer/multilayer formation in the latex system.

3) The dependence of the adsorbed amount on the logarithm of PPO block molar

mass (present in the polymer) is weaker initially, but then a tremendous rise in the adsorbed amount with increasing the PPO block mass is observed.

4) The adsorbed amount also increases with increasing the PEO block molar mass but this dependence is weaker compared to that observed for the PPO block.

5) As for the case of normal Pluronics, a strong influence of PPO:PEO block ratios is observed. Polymers with similar total polymer molar masses but different anchor fractions (PPO:PEO block ratios) adsorb at different levels *i.e* following the trends suggested by SCF model passing through the maximum. At a very low anchor fraction the system will behave like that of the PEO homopolymer, whilst, at high $\nu_A$ values the surface seems to be saturated with the polymer segments hence a very low adsorbed amount is obtained at the two extreme values of the anchor fraction

6) A shallow increase in the polymer adsorbed layer thickness with increasing the total polymer molar mass is observed from both the measured data and those determined theoretically using the SCF model.

7) $\delta_H$ strongly depends on PEO block mass but less so on total polymer molar mass and the PPO block mass.

8) An approximately linear increase in the polymer adsorbed layer thickness with increasing the adsorbed amount is observed both theoretically and experimentally indicating a strong interdependence of the two-adsorption parameters.

9) Comparison of the data indicate that if adsorbed on similar surfaces, the R. Pluronic copolymers adsorb at higher levels than PEO homopolymers and the normal Pluronics (of corresponding molar masses and anchor fractions). This also results in the relatively higher adsorbed amounts and more thicker polymer adsorbed layers, for the reverse Pluronics.

# References


[1] Altinok, H., Yu, G. E., Nixon, S. K., Gorry, P. A.,Attwood, D., and Booth, C., *Langmuir*, 1997, **13**, 5837.

[2] Mortensen, K., Brown, W., and Jorgensen, E., *Macromolecules*, 1994, **27**, 5654.

[3] Zhou, Z. and Chu, B., *Macromolecules*, 1994, **27**, 2025.

[4] Sato, T. and Ruch, R. "Stabilization of Colloidal Dispersions by Polymer adsorption," Marcel Dekker, New York, 1980

[5] Lucie, M. A., Van de Steeg and Carl-Gustaf Golander, *Colloid & Surf.* 1991, **55**, 105.

[6] Cohen-Staurt, M. A., Waajen, F. W. H., Cosgrove, T., Vincent, B., and Crowley, T. L., *Macromolecules*, 1984, **17**, 1825.

[7] Balazs, A. C. and Lewandowski, S., *Macromolecules*, 1990, **23**, 839.

[8] Baker, J. A., and Berg, J. C. *Langmuir* 1988, **4**, 1055.

[9] Alexandridis, P., and Halton, T. A., Colloids and Surfaces A: Physicochemical and Engineering Aspects 1995, **96**, 1.

[10] Schroen, C. G. P. H., Cohen-Stuart, M. A., van der voort Maarschalk, K., van der Padt, A. and van't Riet, K., *Langmuir*, 1995, **11**, 3068.

[11] Killmann, E., Fulka, C. and Reiner, M. *Chem. Soc. Faraday Trans.* 1990, **86**, 1389.

[12] Evers, O. A., Scheutjens, J. M. H. M., and Fleer, G. J., *J. Chem. Soc. Faraday Trans.I*, 1990, **86** (9), 1333.

[13] Orwoll, R. A., *Rubber Chemistry and Technology*, 1977, **50**, 451.

[14] Cosgrove, T., Vincent, B., Crowley, T. L. and Cohen-Stuart, M. A., *ACS Symposium Ser.*, 1984, **240**, 147.

[15] Kato, T., Nakamura, K., Kawaguchi, M. and Takahashi, A., Polym. J., 1981, **13**, 1037.

[16] Fleer, G. J., Cohen-Stuart, M. A., Scheutjens, J. M. H. M, Cosgrove, T., and Vincent, B., "Polymers at Interfaces" London: Chapman and Hall, 1993, p 302.

[17] (a) Guzonas, D., Hair, M.,L., and Cosgrove, T., *American Chem. Soc.*, 1992, **20** 2777. (b) Wu, D. T., Yokohama, and Setterquist, *Polymer, J.*, 1991, **23**, 711.

# Chapter 6

# *ADSORPTION OF R. PLURONICS ONTO SILICA*

## 6.1. Introduction

This chapter is concerned with the adsorption of a series of Reverse Pluronic copolymers (PPO-PEO-PPO) (*see* Table 4.4) at the aqueous/hydrophilic silica interface. The adsorbed amount and the hydrodynamic layer thickness data have been measured at polymer solution concentrations corresponding to the plateau levels of the adsorption isotherms, *see* Section 4.3.

## 6.2. Adsorbed Amount

### 6.2.1. Adsorption Isotherms

Figures 6.1, 6.2 and 6.3 present the adsorption isotherms for a series of reverse Pluronic copolymers adsorbed at the aqueous/silica interface as a function of polymer equilibrium concentration. As for the normal Pluronics, the reverse Pluronics are found to show high affinity adsorption isotherms and also they do not show evidence of multilayer formation (Figures 6.1 to 6.3). In general, similar trends in the pattern of the adsorption isotherms to those determined for PEO homopolymers, PEO-PBO copolymers and the normal Pluronics adsorbed on polystyrene latices and on silica (*see* Figures 7.1 to 7.6 and 8.1 to 8.6, respectively) have been found. A rapid increase (high affinity) in the level of adsorption at very low copolymer concentration followed by a gradual levelling off until the so-called pseudo-plateau level is reached at an equilibrium concentration of approximately 150 ppm, has been observed for all of these polymers. The adsorbed amounts presented in this study (*see* Table 6.1) are about 3-4 times *lower* than those measured for the same set of polymers adsorbed on the

hydrophobic polystyrene latex substrate (*see* Section 5.2) which emphasises the strong influence of polymer-surface interactions.[1]

**Table 6.1: experimental and theoretical data; adsorbed amounts and adsorbed layer thicknesses for the PPO-PEO-PPO block copolymers adsorbed onto silica.**

| Polymers | $M_w$[a] | $\upsilon_A$ | $\Gamma$ / ± 1.2%/ (mg $m^{-2}$) | $\delta_H$ / ± 1.2%/ nm | Adsorbed Amount/θ | δ/ layers |
|---|---|---|---|---|---|---|
| 17R1 | 1900 | 0.88 | 0.15 | 2.5±1.0 | 0.05 | 0.06 |
| 25R1 | 2700 | 0.88 | N/A | N/A | 0.1 | 0.08 |
| 31R1 | 3250 | 0.88 | 0.14 | 1.25±1.0 | 0.13 | 0.3 |
| 17R2 | 2150 | 0.76 | 0.16 | 1.25±1.0 | 0.17 | 0.38 |
| 25R2 | 3100 | 0.76 | 0.24 | 0.5±1.0 | 0.9 | 1.61 |
| 12R3 | 1800 | 0.26 | 0.1 | 0.0±1.0 | 0.77 | 2.9 |
| 17R4 | 2650 | 0.54 | 0.18 | 0.0±1.0 | 0.7 | 2.24 |
| 22R4 | 3350 | 0.54 | 0.22 | 0.5±1.0 | 0.85 | 2.74 |
| 25R4 | 3650 | 0.54 | 0.25 | -1.0±1.0 | 1.0 | 3.63 |
| 31R4 | 4150 | 0.54 | 0.16 | 1.3±1.0 | 1.1 | 3.83 |
| 10R5 | 1950 | 0.44 | 0.11 | -1.0±1.0 | 0.45 | 1.83 |
| 25R5 | 4250 | 0.44 | 0.26 | -0.5±1.0 | 1.2 | 4.3 |
| 25R8 | 8550 | 0.16 | N/A | 0.0±1.0 | 1.4 | 5.9 |
| 31R8[b] | 4000 | 0.08 | N/A | N/A | 0.43 | N/A |

[a] Molar mass as quoted by manufacturers,

[b] Very low anchor fraction, PPO-PEO-PPO triblock polymers used for the SCF calculations.

Figure 6.1 presents the adsorption isotherms for the 17R1, 17R2 and 17R4 polymers adsorbed at aqueous/silica interface as a function of polymer solution equilibrium concentration. The polymers in this figure are arranged in such a way that they all have the same PPO block molar masses but varying PEO block molar mass. It is evident in this figure that the two polymers (17R1 and 17R2) with comparable molar masses and similar PPO:PEO block ratio adsorb at similar levels and give equally high affinity adsorption isotherms. However, the larger 17R4 polymer with a relatively lower anchor fraction adsorbs at a higher level than 17R1 and 17R2 but shows a lower affinity adsorption isotherm. This difference in the adsorption behaviour of these polymers emphasises a strong influence of the polymer composition.

Figure 6.2 presents the adsorption isotherms for 25R2, 22R4, 25R4 and 25R5 polymers. The polymers in this figure are also arranged in the order of increasing total polymer molar mass and PEO block molar mass, whilst, the PPO block mass is maintained approximately constant. Again, the level of adsorption is observed to increase in order of increasing total polymer molar mass.

Figure 6.3 presents the adsorption isotherms for 10R5, 12R3, 31R1 and 31R4 polymers. The polymers are arranged in such a way that both the blocks PPO and PEO vary along with the total polymer molar mass. The anchor fraction of the polymers present in this figure has also a wide range *i.e.* between 0.25 and 0.88. This figure shows similar trends in the adsorption behaviour of these polymers to those shown in Figures 6.1 and 6.2, *i.e.* an increase in the level of the adsorption isotherms with increasing the total polymer molar mass and the anchor fraction. An exception is the case of the polymer 31R1 where the level of polymer adsorption increases constantly with the polymer solution equilibrium concentration without reaching any plateau level. This can be attributed to the fact that 31R1 has the highest molar mass (with high anchor fraction) in the range studied. This may tend to an easy *end-to-end* attachment of the *anchor-anchor* blocks of neighbouring molecules leading to surface aggregation as predicted by Balazs *et al.*[2] They predict that at higher polymer concentrations there is more chance for a free anchoring end block to interact with another free anchor block belonging to a neighbouring macromolecule present in the solution and less chance to loop back to the particle surface. However, this needs more investigation before any final conclusions can be made.

These figures show that all of these polymers, except the polymers 17R1 and 17R4 give high affinity adsorption isotherms. This behaviour can be explained by the hydrophobic nature of these polymers; the high PPO content makes them less soluble in the bulk solution and hence more attractive to the particle surface. Furthermore, the low affinity adsorption isotherms for 17R1 and 17R4 may also be due to the polydispersity of the samples, in both the total polymer molar mass and/or the relative block masses, as the affinity changes with molar indices ($M_w/M_n$) of the polymers. Mallagh[3] predicted that the polydispersity in the polymer molar mass or in the polymer composition makes the bulk concentration required for plateau adsorption much higher. The Reverse Pluronics are found to adsorb at a lower level on the hydrophilic silica than on the hydrophobic polystyrene latex, which may be due to the flat adsorption configuration adopted by both PEO and PPO segments. Schroen *et al.*[4] have shown that the adsorption of PEO-PPO copolymers on a hydrophilic surface may involve both of PPO and PEO blocks via hydrogen bonds and hence both the polymer blocks may lie in a flat configuration. Killmann *et al.*[5] have presented adsorption data for 17R1, 25R1, 25R2, 31R1 and 31R4 from $CCl_4$ solvent onto pyrogenic silica. The data are in a good qualitative agreement with the trends observed in the patterns of the adsorption data presented in this work. In this study the adsorption isotherms were confined to concentrations below the CMC[6,7,8] of these polymers.

### 6.2.2. Molar Mass Dependence of the Adsorbed Amount

Figure 6.4 shows a strong dependence of the adsorbed amount on the logarithm of the total copolymer molar mass of the R.Pluronic copolymers adsorbed on silica (derived from the so-called pseudo-plateau levels of the adsorption isotherms). Exceptions are 31R1 and 31R4, which unexpectedly show low levels of adsorption, which is unusual and needs further investigation.[9] In contrast to data presented by Malmsten *et al.*[10] this figure shows a strong influence of polymer composition (also *see* Figure 6.5) on the adsorbed amount of the polymers. A comparison between the adsorption data measured for the same series of R. Pluronics on polystyrene latices (*see* Section 5.2) show that like normal Pluronics these copolymers adsorb at lower levels on silica than on polystyrene latices. Furthermore, the comparisons between the adsorption data determined for the reverse Pluronics and the normal Pluronics for the silica system (*see* Table 8.3 and Figure 8.7) show that the R.Pluronics adsorb at higher

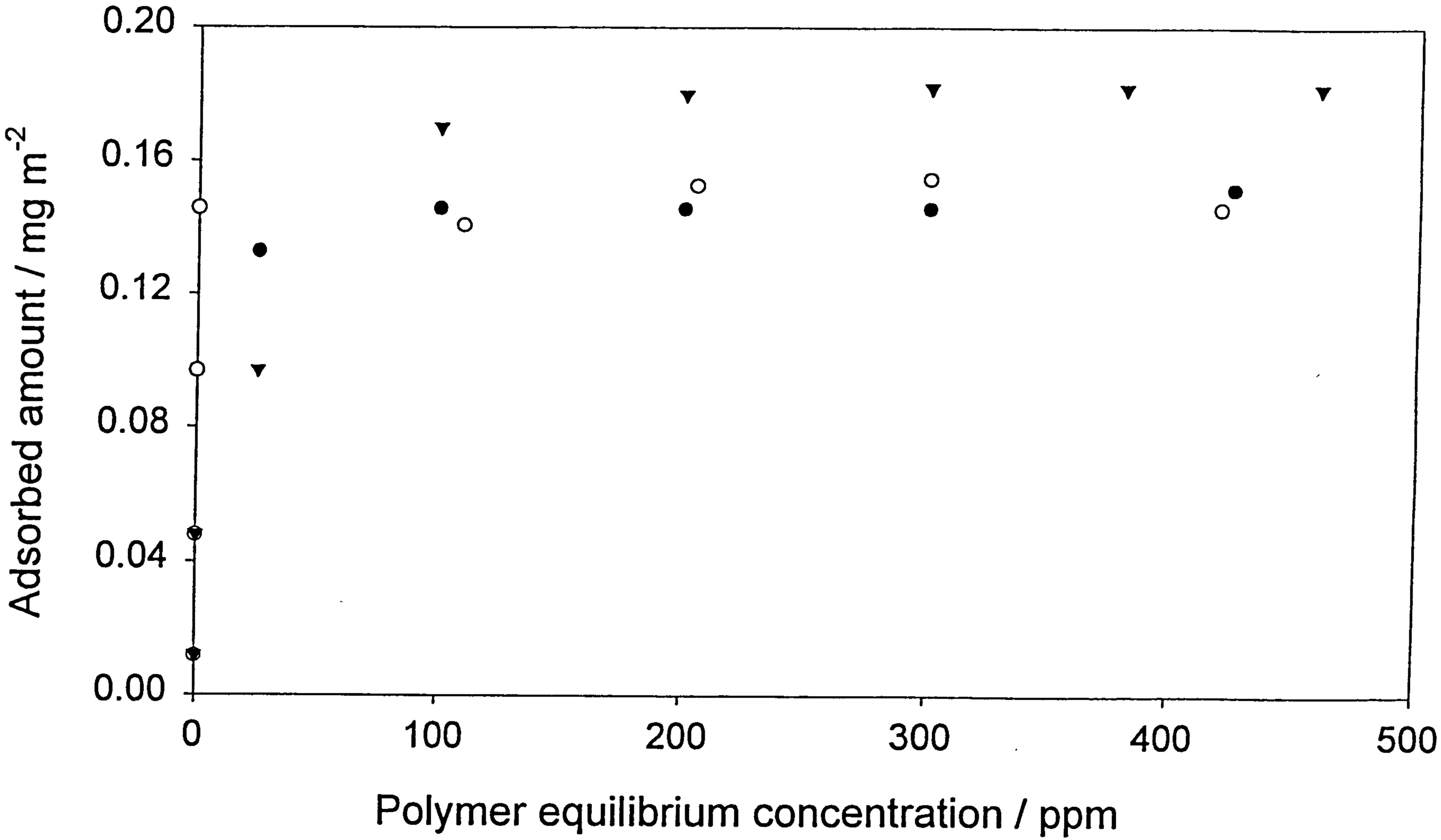


***Figure 6.1 presents the adsorption isotherms for the reverse Pluronics adsorbed at aqueous/silica interface as a function of polymer solution equilibrium concentration: ● 17R1, O 17R2 and ▼ 17R4.***

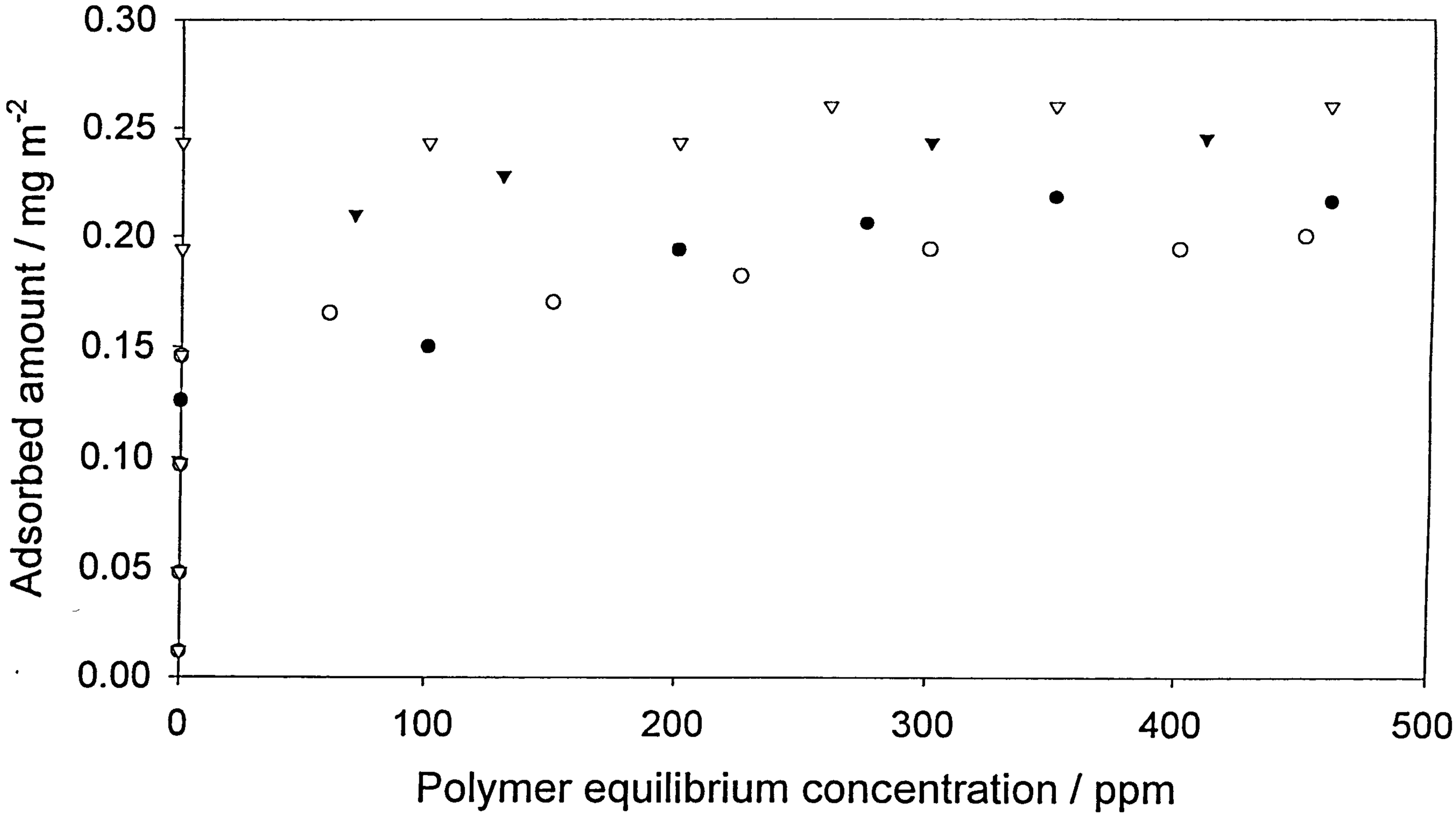


***Figure 6.2 presents the adsorption isotherms for the reverse Pluronics adsorbed at aqueous/silica interface as a function of polymer solution equilibrium concentration: ● 25R2, O 22R4, ▲ 25R4 and Δ 25R5.***

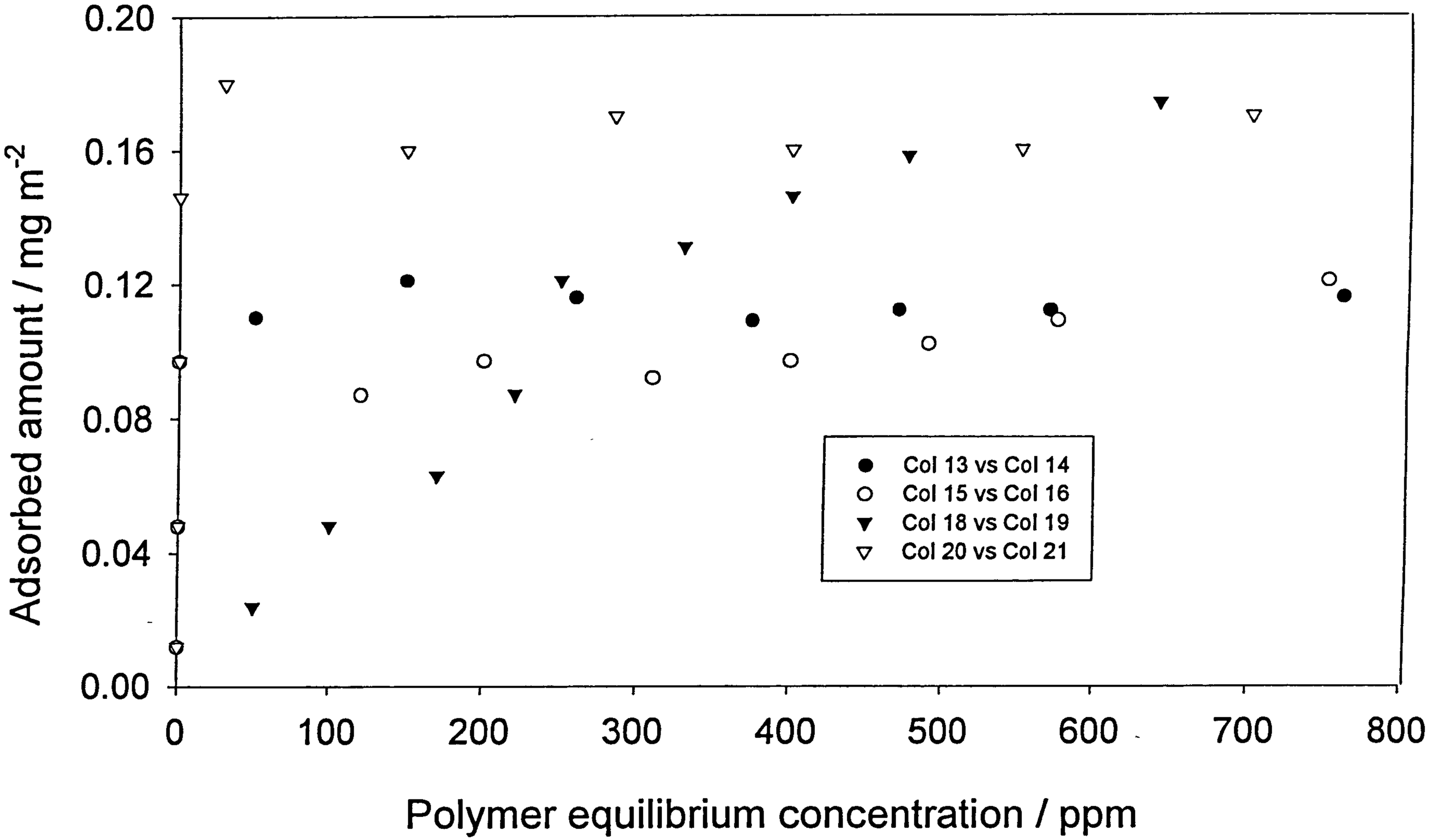


***Figure 6.3 presents the adsorption isotherms for the reverse Pluronics adsorbed at aqueous/silica interface as a function of polymer solution equilibrium concentration: ● 10R5, O 12R3, Δ 31R1 and ▲ 31R4 polymers.***

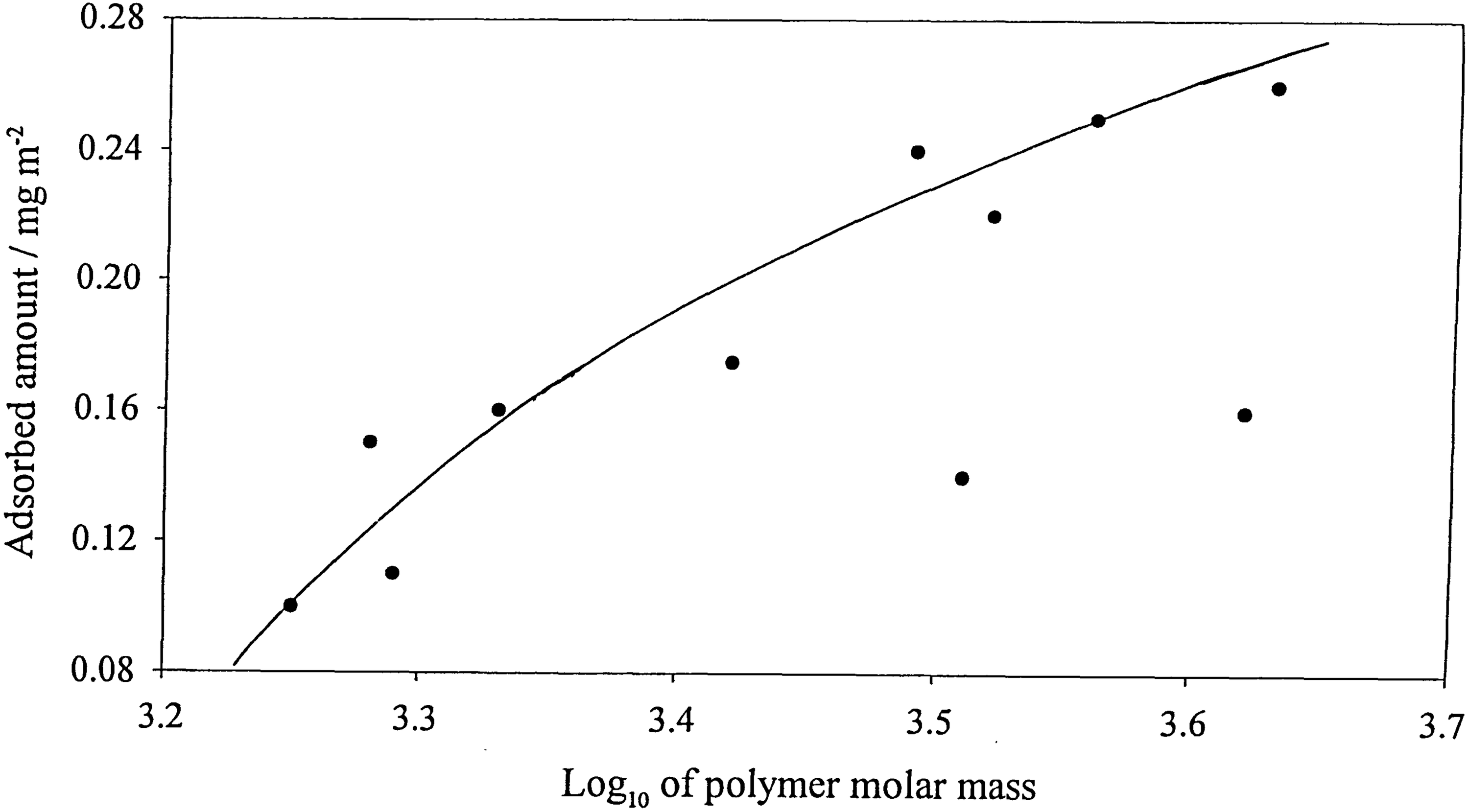


***Figure 6.4 shows the dependence of the adsorbed amount on the logarithm of the total copolymer molar mass of the R.Pluronic copolymers adsorbed on silica.***

levels than the normal Pluronics of the corresponding total polymer molar mass. This emphasises the role of polymer architecture on adsorption: the formation of tails for the normal Pluronics is favourable.

Figure 6.5 presents the dependence of the adsorbed amount on the hydrophilic PEO block size while the hydrophobic PPO block is kept constant. Two sets of data for two different PPO block masses are presented. A rapid increase in the adsorbed amount with increasing the variable block (PEO) molar mass is observed for the low molar mass polymers which slows for the high molar mass polymers. Copolymers with lower PEO block content (high $\nu_A$) lie flat on the surface, due to their more hydrophobic nature. However, any increase in the PEO block mass makes the polymer overall more soluble in the bulk solution.[11] The resultant conformation is a balance of these two effects. This figure also shows an increase in the adsorbed amount of the polymer with increasing PPO block size (for a constant PEO block content) of the sample. This indicates that the PPO block also contributes to the polymer adsorption at a substantial level; the adsorbed amount depends on both blocks. The trends in the adsorption behaviour of these polymers are similar to those observed for the other polymers having high PEO content and high total polymer molar mass, for instance *see* Figures 7.9 and 8.9, and are in a good agreement with those predicted in the literature.[12,13,14,15]

## 6.2.1. Theoretical Predictions for the Adsorbed Amount

The SCF[14,15,16] calculations were performed in each case for polymer solution concentrations of 0 to 2000 ppm and the pseudo-plateau level was presumed to occur at the polymer equilibrium concentration of 500 ppm. The block monomer number ($N_i$) is the molar mass of each individual block divided by the corresponding molecular mass of that block. The number of adsorbed layers was taken as the square root of number of PEO monomers ($N_B$) present in each sample. The Flory parameters for these calculations were taken as $\chi_{WS} = 0.00$, $\chi_{PS} = -1.00$, $\chi_{ES} = -4.00$, $\chi_{EP} = 2.00$, $\chi_{EW} = 0.45$ and $\chi_{PW} = 0.5$. Where W stands for water, (solvent), S for silica surface, (adsorbent surface) E for ethylene oxide and P for propylene oxide monomers. The $\chi$ values were selected bearing in mind the influence of solvent-surface, surface-segment, segment-segment and solvent-segment interactions.[1] Both the blocks were presumed to

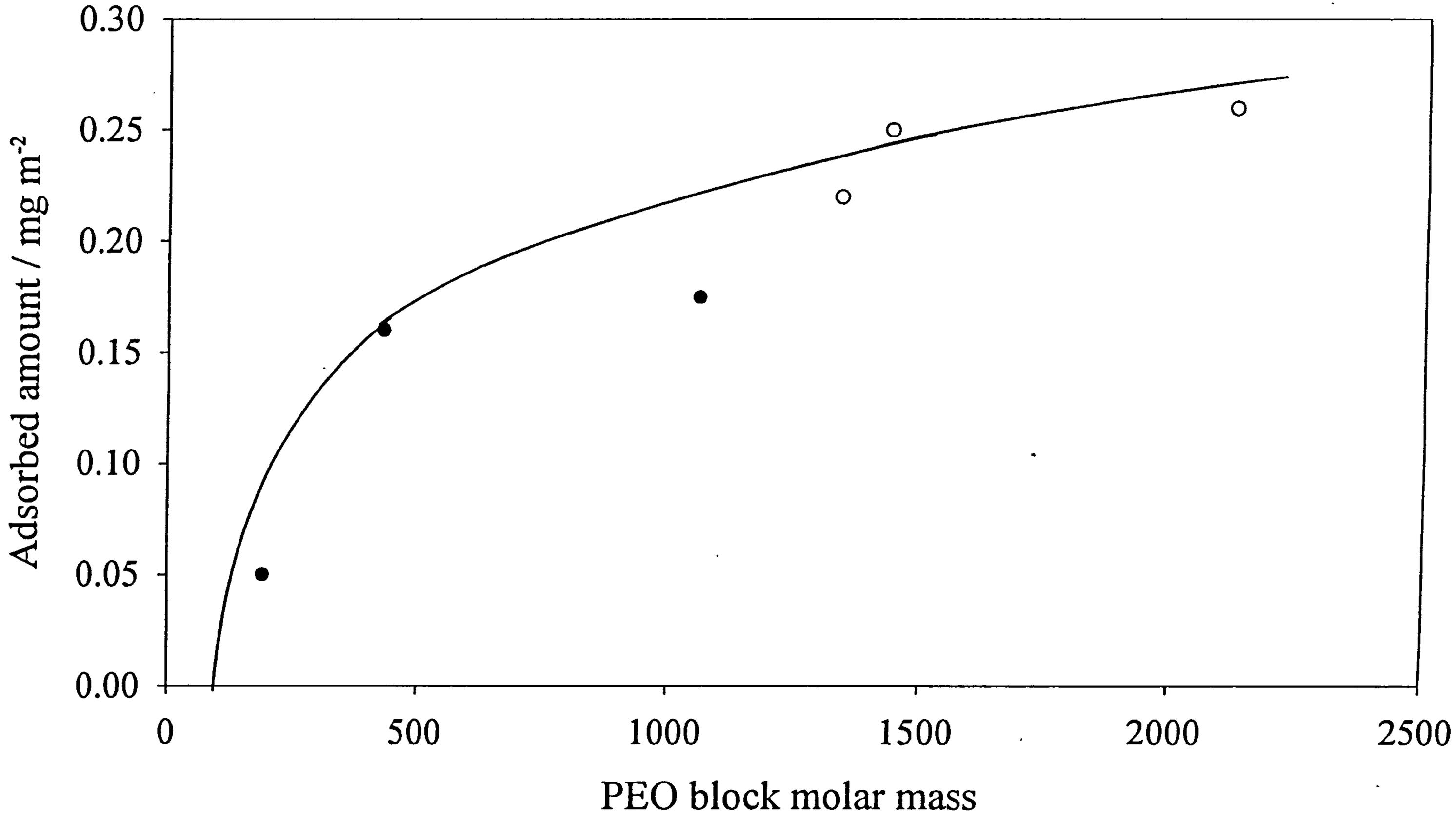


***Figure 6.5 shows dependence of the adsorbed amount on the hydrophilic PEO block size while the hydrophobic PPO block is kept constant: ● PPO≅1700 and O, PPO≅2000.***

adsorb onto the silica surface; the PEO block through hydrophilic nature and the PPO block through its insolubility in water.

The influence of anchor fraction on the adsorbed amount of R. Pluronic copolymers adsorbed on silica is shown in Figure 6.6. The inset into this figure is the calculated data for the same series of block copolymers under study (*see* Table 4.4) adsorbed on silica determined using the SCF model.[14,16] A continuous decrease in the measured adsorbed amount with increasing the anchor fraction is observed for $\nu_A >$ 0.16. A good qualitative agreement is observed between calculated and experimental values. Also, similar trends to those observed in the patterns of the adsorbed amount determined for the normal Pluronic copolymers adsorbed on polystyrene latices and silica (*see* Figures 7.10 and 8.10) can be clearly seen. Exceptions are the 12R3 and 10R5 polymers which unexpectedly adsorb at lower levels (both experimentally and theoretically) which may be attributed to the specific composition of these polymers *i.e.* having low molar mass and the low anchor fraction. It has also been shown that polymers with similar total polymer molar masses but different anchor fractions adsorb at different levels *i.e.* low anchor fraction polymers adsorb at lower levels than those of higher anchor fraction, hence, emphasising a strong influence PPO:PEO block ratio. The results suggest the transition between buoy and anchor regimes occur at anchor fraction, $\nu_A \sim 0.16$ for this inverted tripolymer.[12,13,14,15]

Figure 6.7 presents the strong dependence of the adsorbed amount on $\log_{10}$ of total polymer molar mass for a series of R. Pluronic copolymers adsorbed at aqueous/silica interface calculated using the SCF model.[14,16] As observed for the reverse Pluronics adsorbed on polystyrene latex (*see* Figure 5.8) an approximately linear dependence of the adsorbed amount on $\log_{10}$ of polymer molar mass has been observed for all the polymers with the exception of 31R1 and 12R3. These polymers show unexpectedly lower and higher adsorbed amounts, respectively. The high values of calculated adsorbed amount for 12R3 may be attributed to the formation of longer loops by the high PEO content, which, extends out into the bulk. The lower adsorbed amount given by 31R1 can be attributed to its high anchor fraction which makes the polymer lie flat on the surface hence, no significant loops are found. Overall, similar trends in the pattern of the measured data and those calculated using SCF[14,15] have been observed.

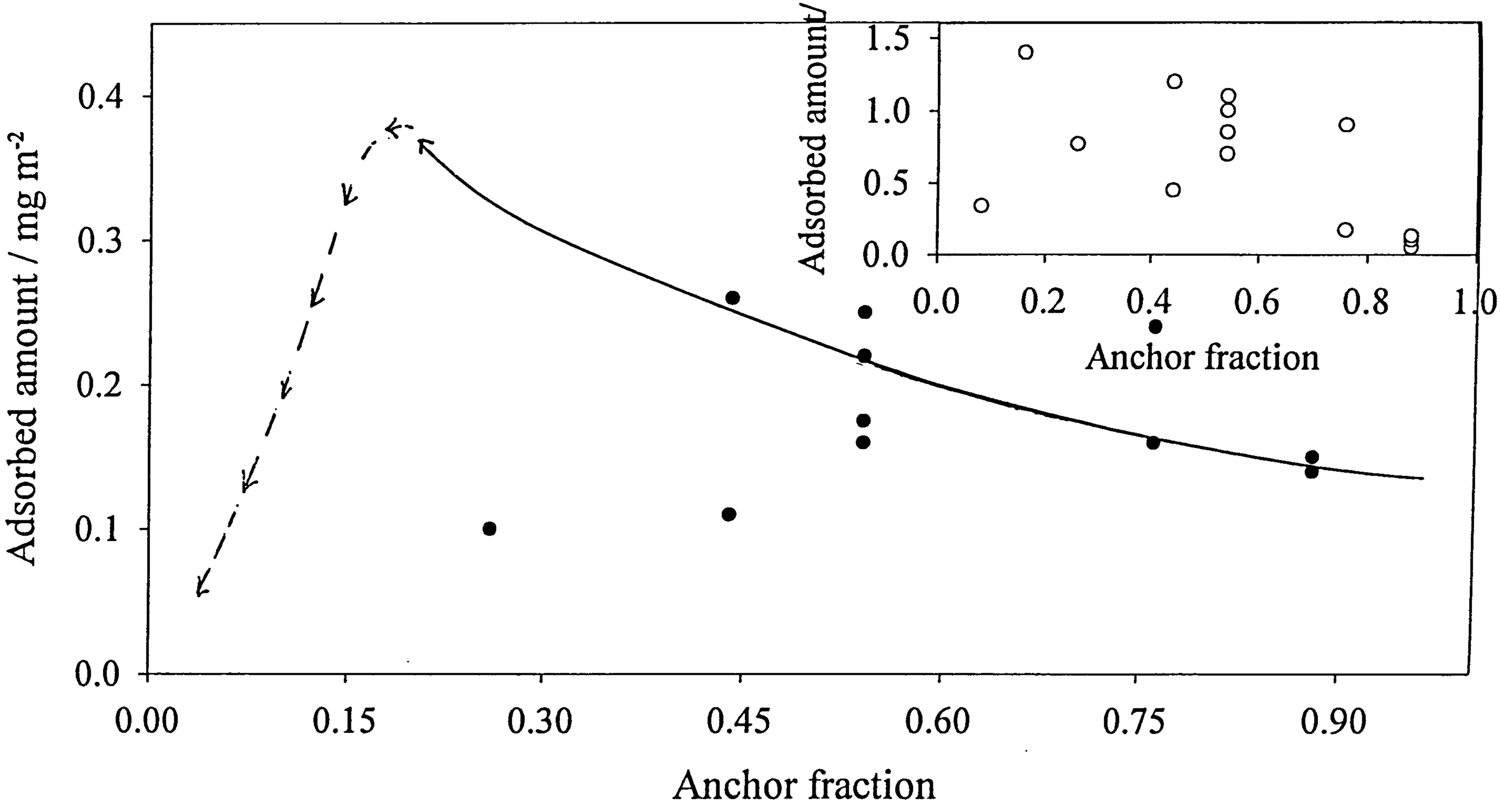


***Figure 6.6 shows the influence of anchor fraction on the adsorbed amount of R. Pluronic copolymers adsorbed on silica: ● measured data and O calculated data using the SCF model.***

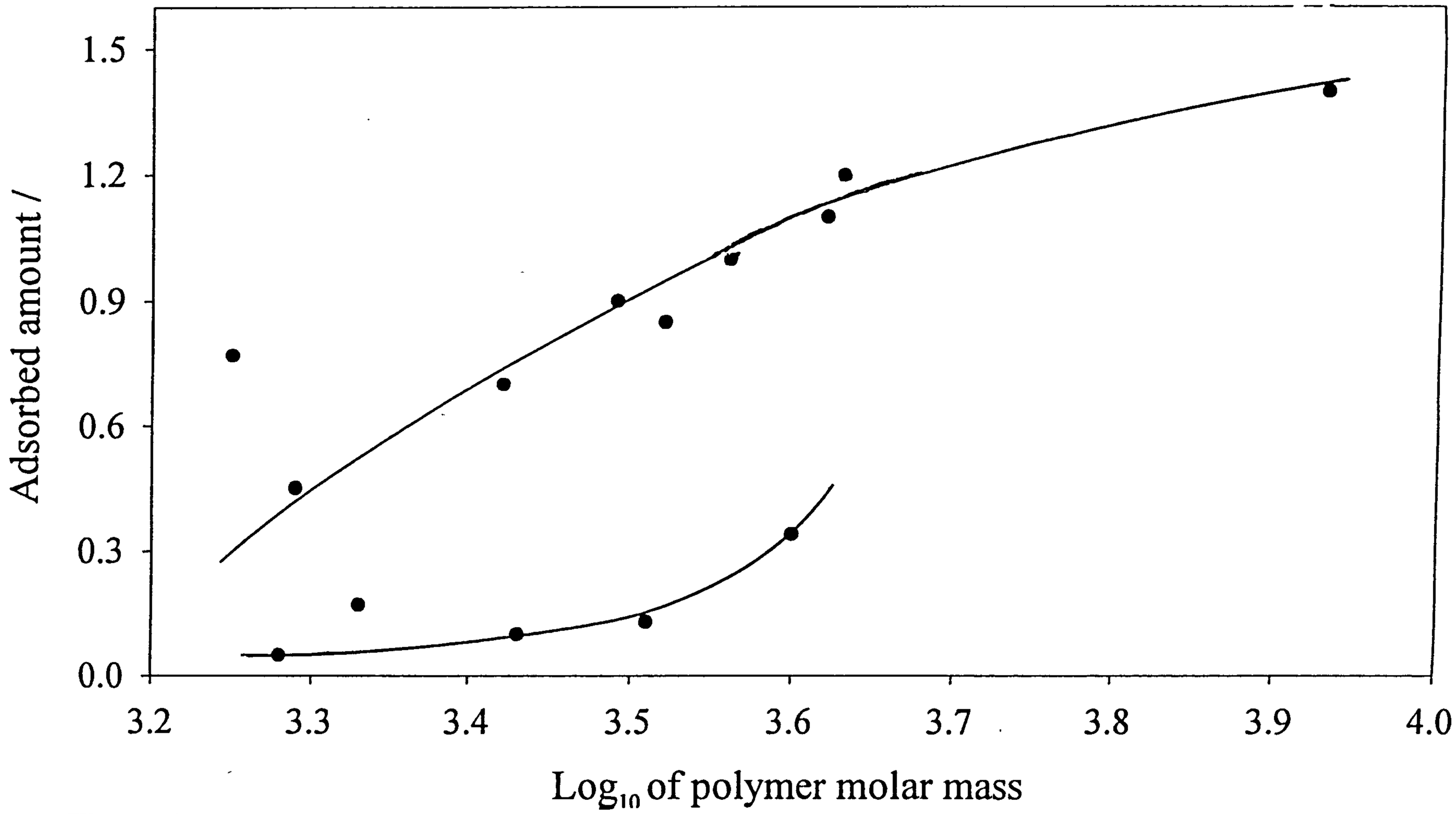


***Figure 6.7 presents the dependence of the adsorbed amount on $log_{10}$ of total polymer molar mass for a series of R. Pluronic copolymers adsorbed at aqueous/silica interface calculated using the SCF model.***

Figure 6.8 shows the dependence of the adsorbed amount calculated using the SCF model[14,16] on the logarithm of PEO block molar mass present in the samples. Similar trends to those observed for the same set of reverse Pluronics adsorbed on the hydrophobic latex surface are observed (*see* for instance Figure 5.9(a)). These data also show in the beginning, a slow increase in the adsorbed amount with increasing the $Log_{10}$ of PEO block molar mass followed by a rapid rise in the adsorption at PEO block mass of 1300. Interestingly, this transition occurs at a similar mass for both silica and the latex systems.

As for the case of normal Pluronics adsorbed on polystyrene latices and silica (*see* Figures 7.11(b) and 8.11(a)) and the reverse Pluronics adsorbed on PSL (*see* Figure 5.10), an approximately linear dependence of the calculated adsorbed amount ($\theta$) on the measured adsorbed amount is observed in Figure 6.9.

## 6.3. Adsorbed Layer Thickness

PCS was used to determine the hydrodynamic thickness of the adsorbed polymer layer in a similar manner as detailed in Section 4.3.2. The PCS measurement show that contrary to the data found for the same set of polymers adsorbed on polystyrene latex surface, very thin/insignificant adsorbed layers were formed on silica, since for this system, blocks of both types, PEO due to its hydrophilic nature, and PPO blocks due to their limited solubility in solution,[4] are expected to adsorb on the hydrophilic surface, giving a flat configuration which results in a very thin and /or insignificant adsorbed layer thickness (*see* Table 6.1). This can also be attributed to the extremely thin adsorbed layer, where adsorption of the polymers to the surface may "flatten" any extended particle "hairs".[17] This observation is consistent with the lower adsorbed amounts found on silica. However, adsorbed layer thicknesses determined using the SCF model[14,16] will be discussed in the following section

### 6.3.1. Theoretical Predictions for the Adsorbed Layer Thickness

Figure 6.10 presents the dependence of $log_{10}$ of the calculated adsorbed layer thickness on $log_{10}$ of the total polymer molar mass for the polymers used in this study. The theoretical data were determined in a similar manner as described in the Section

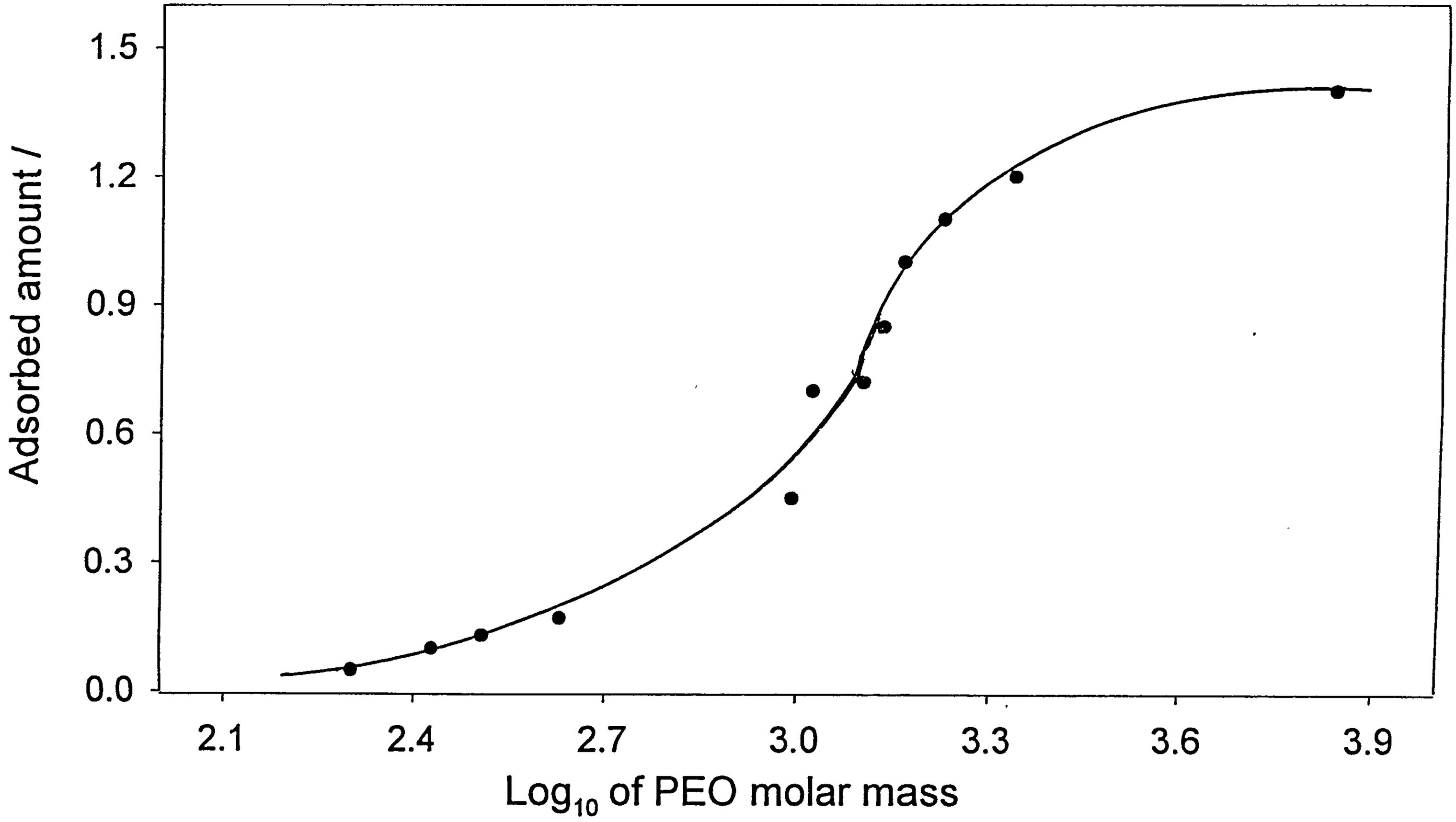


***Figure 6.8 shows the dependence of the adsorbed amount calculated using the SCF model on the logarithm of PEO block molar mass present in the samples.***

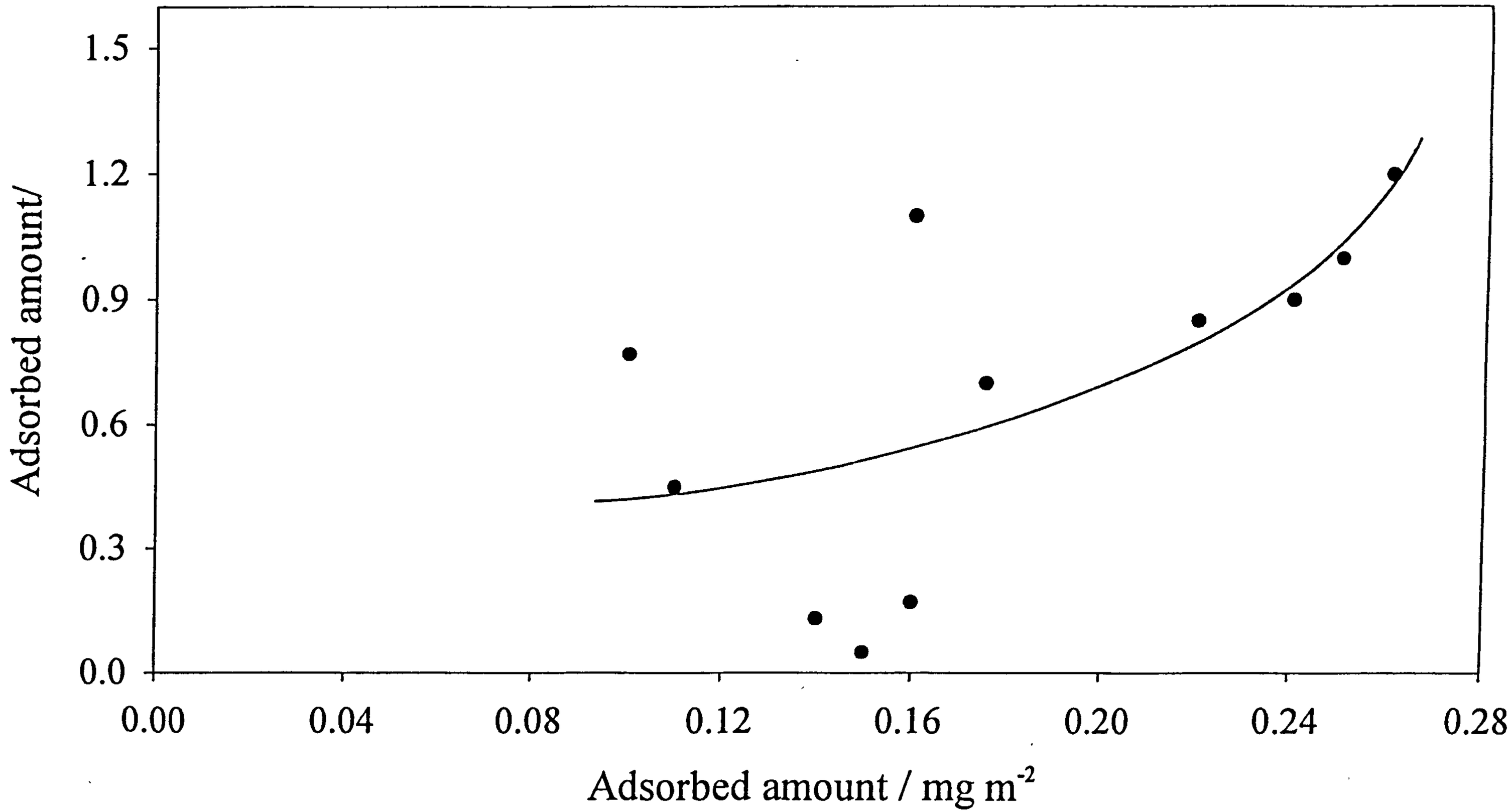


***Figure 6.9 shows the dependence of the calculated adsorbed amount on the measured adsorbed amount.***

6.2.4.[14,15,16] As observed for the reverse Pluronics adsorbed on polystyrene latex (*c.f.* Figure 5.14), a shallow increase (which slows down in the region of high molar mass polymers) in the polymer adsorbed layer thickness with increasing total polymer molar mass is observed.

Figure 6.11 shows a strong dependence of $\log_{10}$ of the calculated adsorbed layer thickness on $\log_{10}$ of the PEO block molar mass, which emphasises an overwhelming contribution by the PEO block molar mass towards loop formation. However, this dependence of the adsorbed layer thickness on the PEO block mass weakens for large PEO block sizes, which are more hydrophilic. This is again consistent with the fact that lower adsorbed amounts are obtained for low anchor fraction polymers.

The influence of anchor-fraction on the calculated adsorbed layer thickness of the PPO-PEO-PPO triblock copolymers is shown in Figure 6.12. Overall, similar trends to those observed for these polymers adsorbed on the polystyrene latex, *see* Figure 5.16, are observed.

### 6.3.2. Dependence of Adsorbed Layer Thickness on the Adsorbed Amount

Figure 6.13 shows an approximate linear dependence of the adsorbed layer thickness on the adsorbed amount calculated using the SCF model[14,15,16] and emphasises a strong interdependence of the two adsorption parameters as found previously.

## 6.4. Conclusion

1) In general, the level of polymer adsorption increases in order of increasing total polymer molar mass.

2) For the case of reverse Pluronics adsorbed on silica plateau levels are found, which emphasises monolayer adsorption rather than any end-to-end interaction between the two anchor blocks of the neighbouring molecules (as was observed for the case of latex surface). This emphasises that the reverse Pluronics

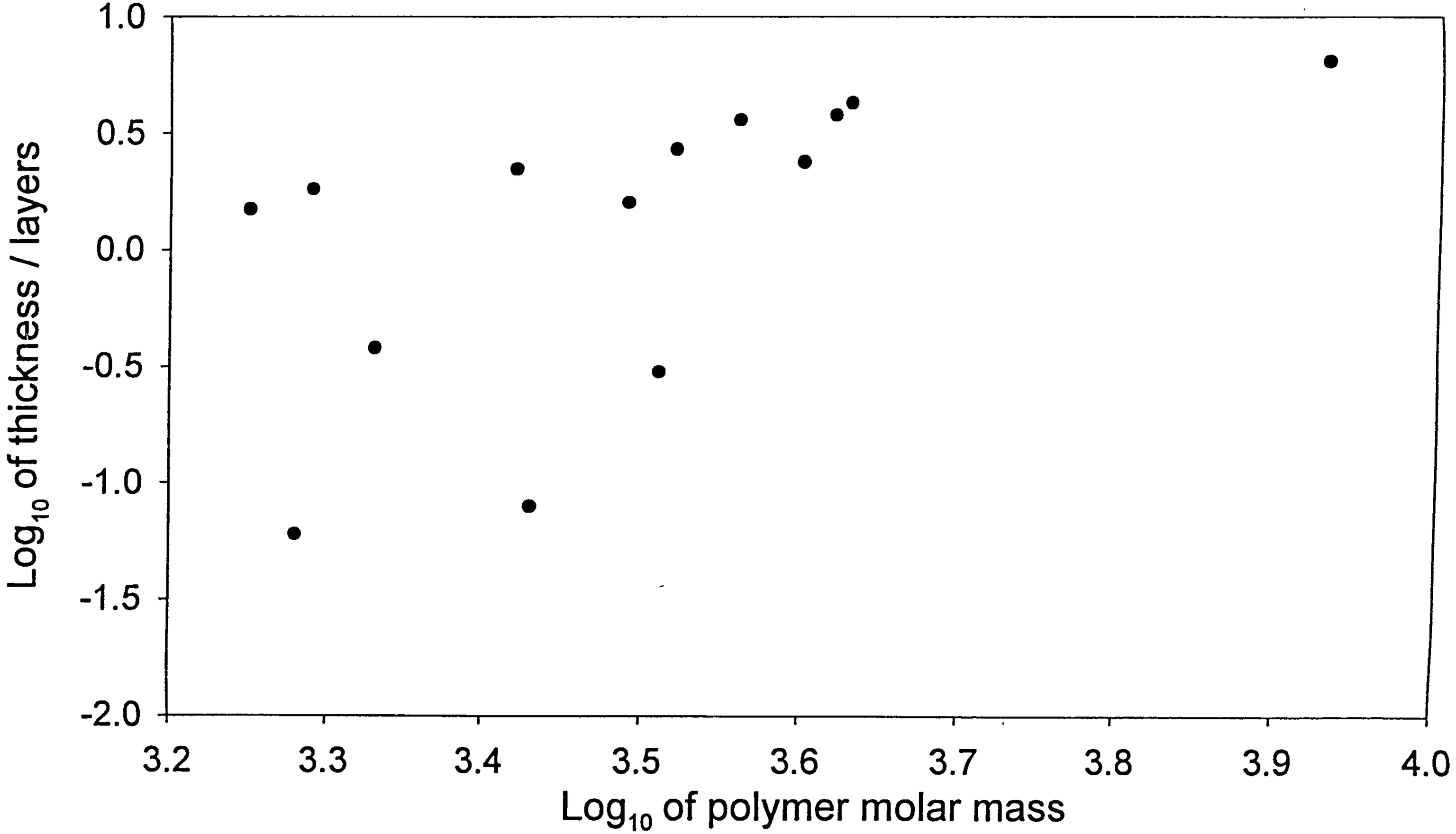


***Figure 6.10 presents the dependence of $log_{10}$ of the calculated adsorbed layer thickness on $log_{10}$ of the total polymer molar mass for the same set of polymers used in this study.***

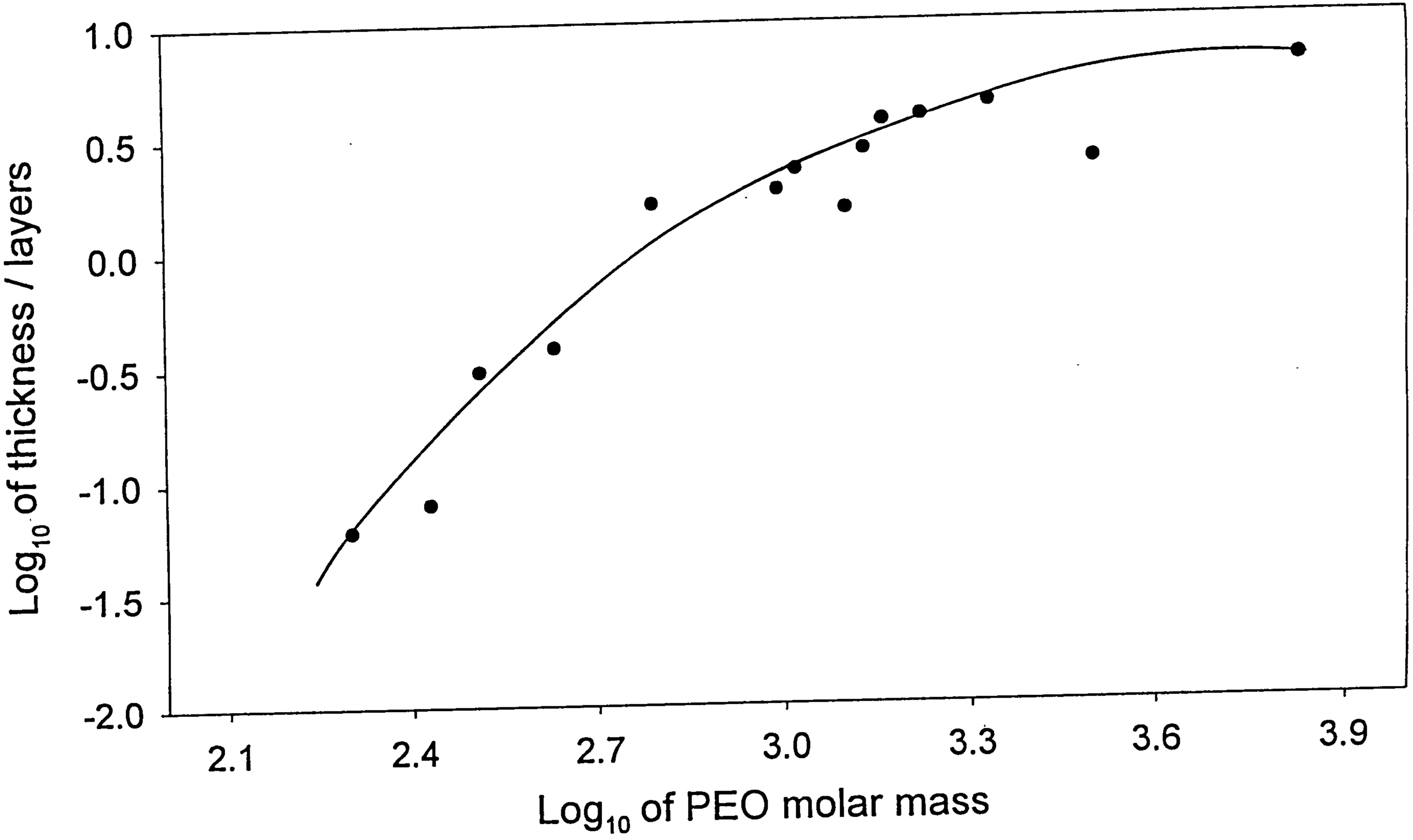


***Figure 6.11 shows the dependence of $log_{10}$ of the calculated adsorbed layer thickness on $log_{10}$ of the PEO block molar mass.***

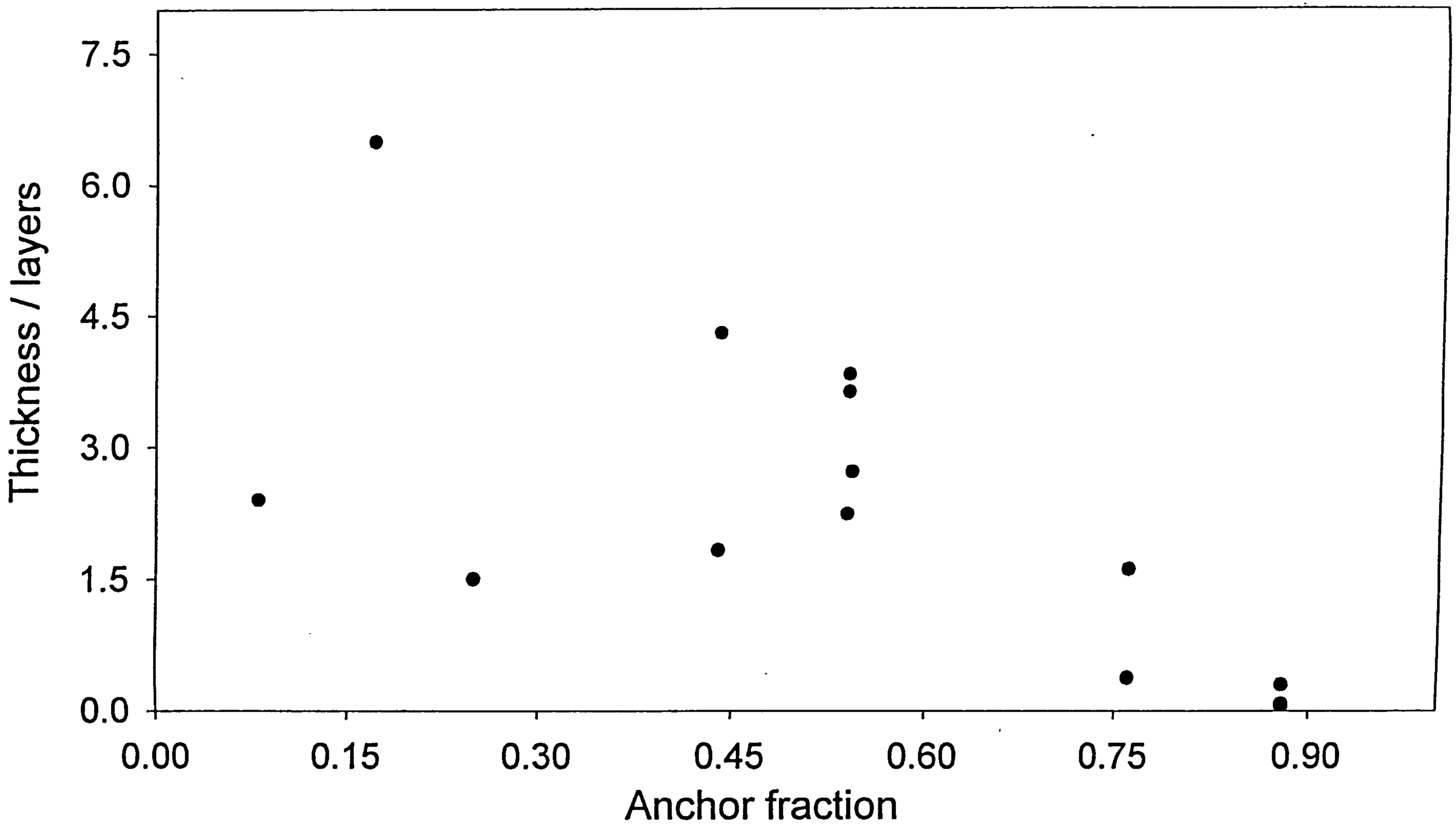


***Figure 6.12 shows the influence of anchor-fraction on the calculated adsorbed layer thickness of the PPO-PEO-PPO triblock copolymers.***

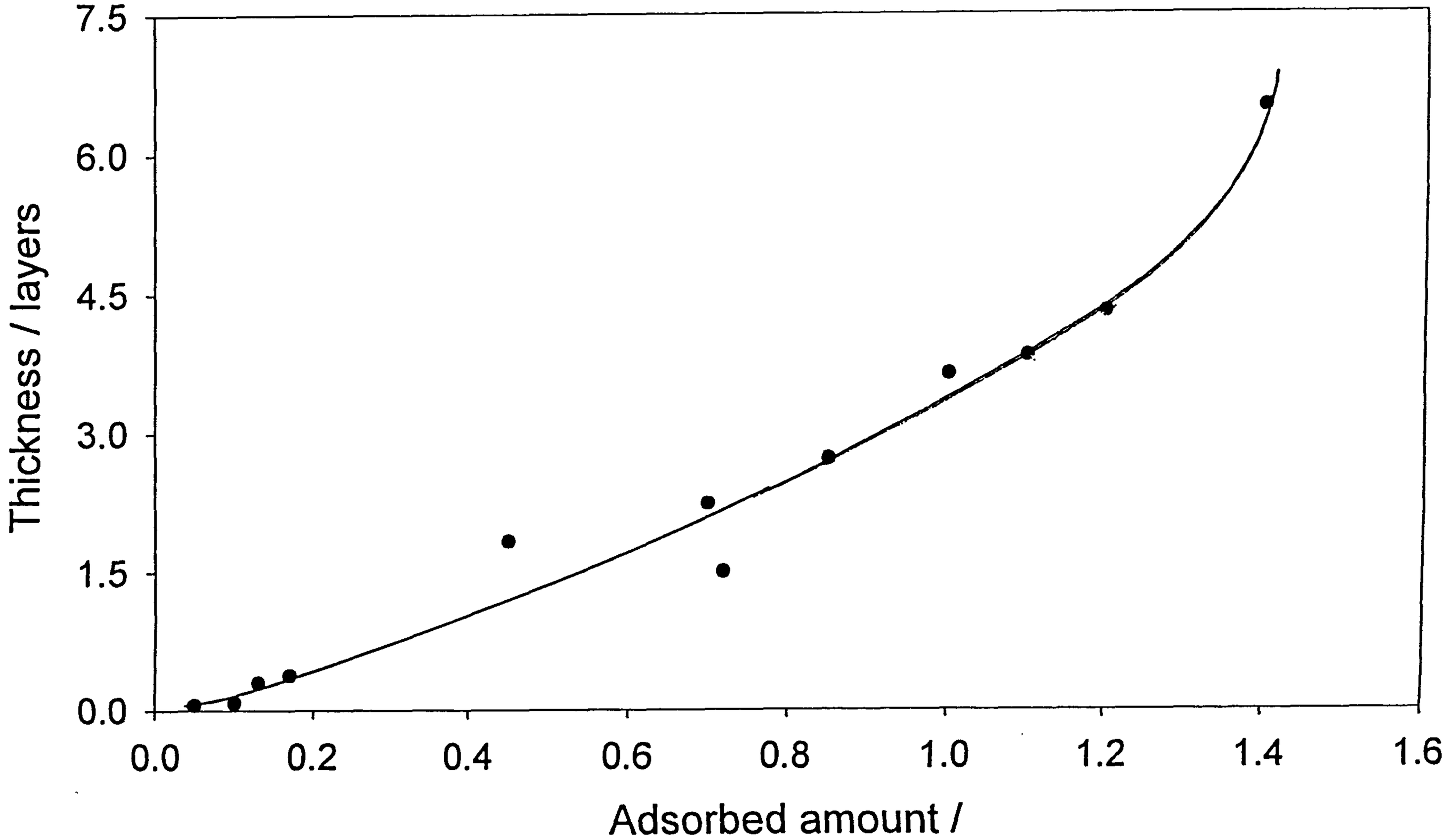


***Figure 6.13 shows the dependence of the adsorbed layer thickness on the adsorbed amount calculated using the SCF model.***

adsorbed on silica do not form any significant bilayers. This effect rules out the possibility of any end-to-end interaction between the two anchor blocks of the neighbouring molecules and indicates the importance of the effect of the particle surface on the polymer adsorption.

3) A strong influence of PPO:PEO block ratio is emphasised from the data which shows that the polymers with similar total polymer molar masses but higher anchor fractions adsorb at higher levels than those of lower anchor fraction. For example, the polymer 25R2 and 25R4.

4) Comparison of the data show that overall, the trends observed in the patterns of the adsorption behaviour of the reverse polymers are similar to those found for the normal Pluronics adsorbed on the polystyrene latex and silica except that very thin adsorbed polymer layers are observed.

5) PCS measurements show that the reverse Pluronics in a similar manner to normal Pluronics adsorb at lower levels on silica than on PSL.

6) The data show that the polymer composition and the polymer architecture play a very important role in the level of polymer adsorption. As for the case of latex surface, relatively, higher adsorbed amounts (derived from the pseudo-plateau levels) are observed for the R. Pluronics than the normal Pluronics when adsorbed on the same surface.

7) As observed theoretically for the reverse Pluronics adsorbed on polystyrene latex a shallow increase (which slows down in the region of high molar mass polymers) in the polymer adsorbed layer thickness with increasing the total polymer molar mass is observed.

8) Theoretical calculations show a strong interdependence of the adsorbed layer thickness on the adsorbed amount determined using the SCF model is observed.

9) It is concluded that the dilute solutions of relatively short polymers may provide the best agents for stabilisation, emulsification, etc. Under such conditions the chain would adsorb in loop conformations, with both anchor blocks bound to the surface. The presence of two anchor blocks ensures that the chains are more securely bound to the surface.

# References


[1] Orwoll, R. A., *Rubber Chemistry and Technology*, 1977, 50, 451.

[2] Blazas, A. C., and Lewandowski, S., *Macromolecules*, 1990, **23**, 839.

[3] Mallagh, L. M., Ph.D. Thesis, Bristol, 1989.

[4] Schroen, C. G. H, Cohen-Stuart, M. A., van der voort Maarschalk, K., van der Padt, A., and van't Riet, K., *Langmuir*, 1995, **11**, 3068.

[5] Killmann, E., Fulka, C., and Reiner, M., *Chem. Soc. Faraday Trans.* 1990, **86**, 1389.

[6] Altinok, H., Yu, G.E., Nixon, S.K., Gorry, P. A., Attwood, D., and Booth, C., *Langmuir*, 1997, **13**, 5837.

[7] Mortensen, K., Brown, W., and Jorgensen, E., *Macromolecules*, 1994, **27**, 5654.

[8] Zhou, Z.., and Chu, B., *Macromolecules,* 1994, **27**, 2025.

[9] Baker, J. A.,and Berg, J. C., *Langmuir* 1988, **4**, 1055.

[10] Malmsten, M., Linse, P., and Cosgrove, T., *Macromolecules*, 1992, **25**, 2474.

[11] Alexandridis, P., and Halton, T. A., *Colloids and Surfaces A: Physicochemical and Engineering Aspects* 1995, **96**, 1.

[12] Marques, C. M., Joanny, J. F., and Leibler, L., *Macromolecules*, 1988, **21**, 1051

[13] Guzonas, D., Hair, M. L., and Cosgrove, T., *American Chem. Soc.*, 1992, **20** 2777.

[14] Evers, O. A., Scheutjens, J. M. H. M. and Fleer, G. J., *J. Chem. Soc. Faraday Trans.I*, 1990, **86** (9), 1333.

[15] Cohen-Staurt, M. A., Waajen, F. W. H., Cosgrove, T., Vincent, B., and Crowley, T. L., *Macromolecules*, 1984, **17**, 1825.

[16] Fleer, G. J., Cohen-Stuart, M. A., Scheutjens, J. M. H. M, Cosgrove, T., and Vincent, B. "Polymers at Interfaces" London: Chapman and Hall, 1993, p 302.

[17] Jochen, M. Sc. Thesis, School of Chemistry, University of Bristol, Bristol, 1995.

# Chapter 7

# *ADSORPTION OF POLYMERS ONTO POLYSTYRENE LATICES*

## 7.1. Introduction

The adsorption results determined for PEO homopolymers, PEO-PBO block copolymers, and the PEO-PPO-PEO block copolymers (Pluronics) of a wide varying range of polymer molar mass and composition adsorbed at the aqueous/polystyrene latex interface are presented in this chapter. The adsorption isotherms and the adsorbed layer thickness were measured as described earlier in the Sections 4.3.1 and 4.3.2. The initial adsorption isotherm and the polymer adsorbed layer thickness data give a basis for the further analysis and interpretation of the results and for evaluating the factors influencing polymer adsorption *i.e.* adsorbed amount, hydrodynamic thickness and the conformation of the polymer adsorbed layers. The results have been analysed in part by using the adsorbed amount and the hydrodynamic thickness values measured at the polymer concentrations corresponding to the plateau levels of the adsorption isotherms. To get a further and better understanding of these systems, a comparison of the adsorption data determined for Pluronic copolymers with those determined for PEO homopolymers and PEO-PBO block copolymers measured in this work and with those found in the literature will also be discussed in this chapter.

## 7.2. Adsorbed Amount

### 7.2.1. Adsorption Isotherms.

Figures 7.1 to 7.6 show adsorption isotherms for the PEO homopolymers, PEO-PBO and the PEO-PPO block copolymers listed in Tables 4.1-4.3 as a function of copolymer equilibrium concentration. Figure 7.1 presents the adsorption isotherms for

the PEO homopolymer, the Figures 7.2 - 7.3 for the PEO-PBO block copolymers whilst, the Figures 7.4 to 7.6 present the adsorption isotherms for the Pluronic copolymers.

Figure 7.1 shows the adsorption isotherms for the set of PEO homopolymers (10K, 114K and 930K,) adsorbed on polystyrene latex as a function of polymer equilibrium concentration. The figure shows an increase in the overall level of adsorption with increasing the PEO molar mass. The low molar mass polymers are observed to give relatively lower affinity adsorption isotherms. The adsorbed amount (*see* Table 7. 1) derived from the pseudo-plateau level of the adsorption isotherms is observed to depend strongly on the polymer molar mass.

Table 7. 1: experimental adsorption data; adsorbed amount and hydrodynamic adsorbed layer thickness for the PEO homopolymers adsorbed onto polystyrene latex.

| PEO | Mw | $\Gamma/\pm 1.03\%/$ $(mg\ m^{-2})$ | $\delta_H/\pm 1.03\%$ /nm |
|---|---|---|---|
| 10K | 10,300 | 0.24 | 3 |
| 114K | 114,000 | 0.48 | 7 |
| 930K | 930.000 | 0.66 | 12 |

Figures 7.2 and 7.3 respectively show the adsorption isotherms for $E_{100}B_{15}$, $E_{200}B_{15}$, R-$E_{200}B_{15}$ and $E_{100}B_{15}E_{100}$, and R-$E_{144}B_{27}$ and $E_{72}B_{27}E_{72}$ copolymers adsorbed at aqueous/polystyrene latex interface determined by the depletion method. These figures show a strong dependence of the level of adsorption isotherms on both the total polymer molar mass as well as the polymer architecture. The largest diblock copolymer $E_{200}B_{15}$ is observed to adsorb at a higher level than those having the same polymer composition but differing only in polymer architecture i.e. R-$E_{200}B_{15}$ and $E_{100}B_{15}E_{100}$. This shows the paramount influence of the polymer architecture on the adsorption of copolymers at the solid-liquid interface. The adsorption data obtained for

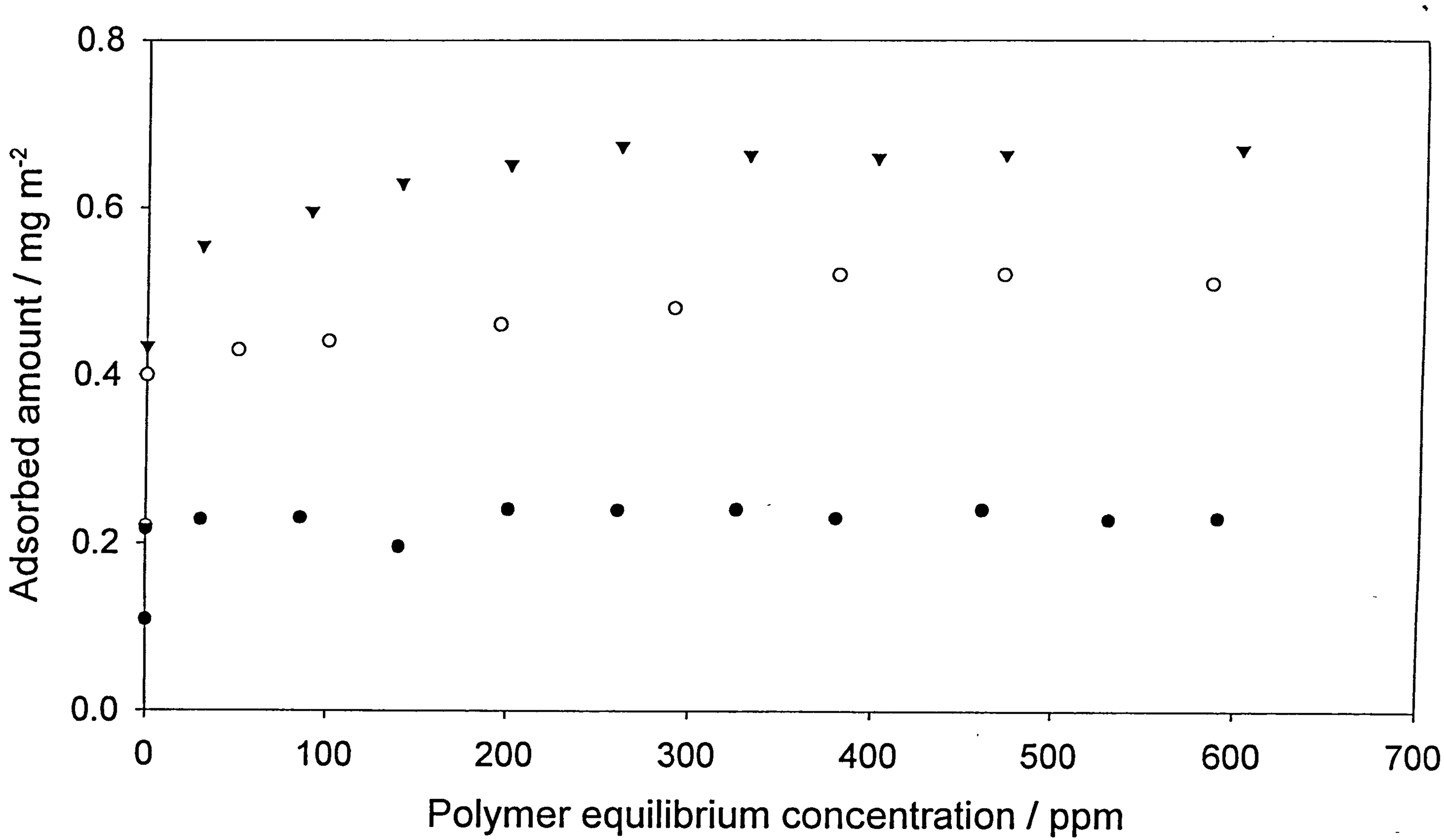


***Figure 7.1 presents the measured adsorption isotherms for PEO homopolymers, adsorbed onto model polystyrene latex particles as a function of polymer equilibrium concentration: ● 10K, o 114K and ▼ 930K.***

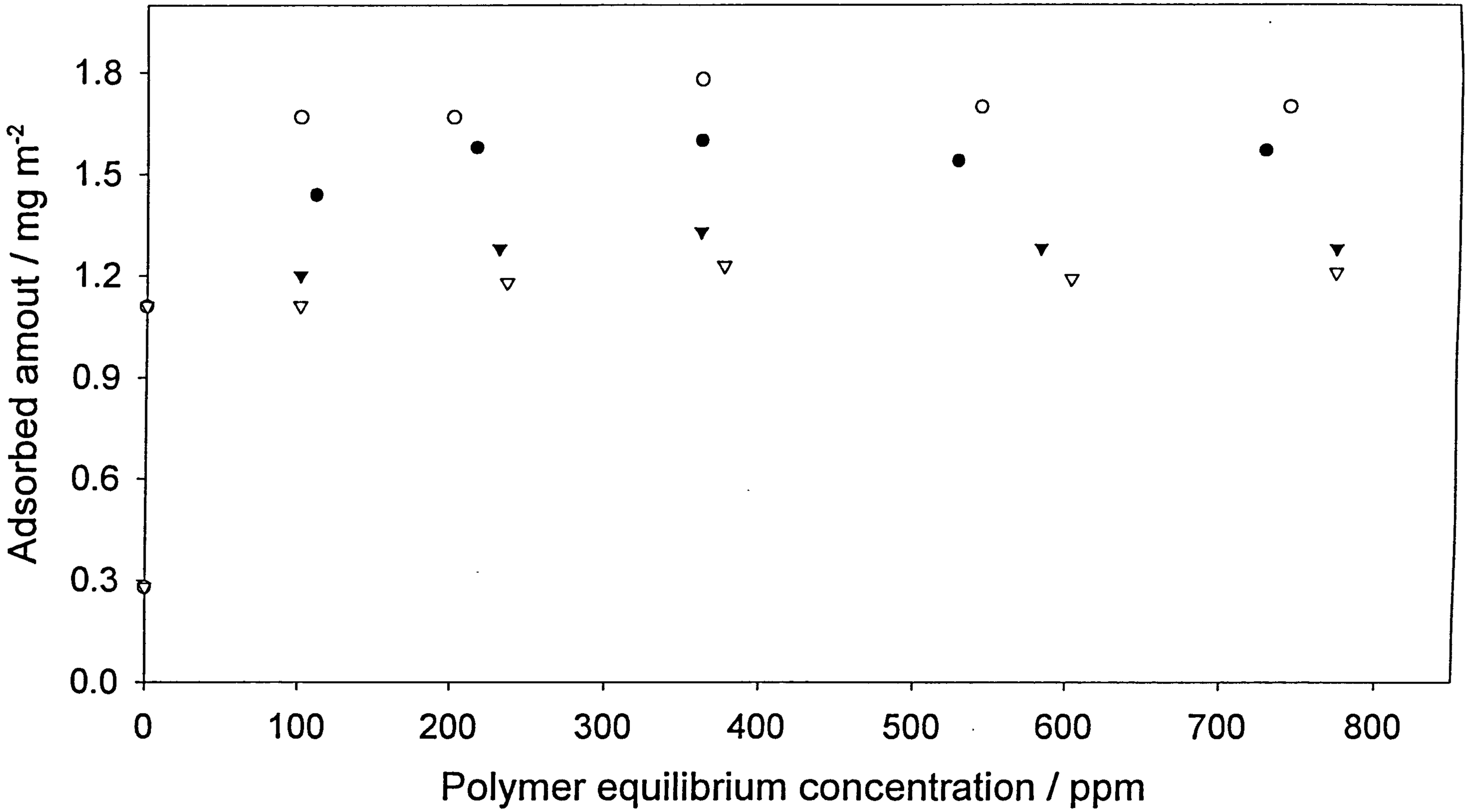


***Figure 7.2 presents the adsorption isotherms for PEO-PBO copolymers adsorbed at aqueous/polystyrene latex interface as a function of polymer equilibrium concentration:*** o $E_{200}B_{15}$, ● $E_{100}B_{15}$, , ▼*R-*$E_{200}B_{15}$ *and* ∇ $E_{100}B_{15}E_{100}$.

these copolymers are presented in Table 7. 2.

Figure 7.3 presents similar behaviour to that observed for the copolymers cited in Figure 11.6 *i.e.* showing maximum adsorption for the diblock copolymer than the triblock copolymer and is in accordance with the theoretical predictions and with that

Table 7. 2: experimental and theoretical data; adsorbed amounts, $\delta_{rms.}$, and adsorbed layer thicknesses for the PEO-PBO block copolymers adsorbed onto polystyrene latex.

| Polymer | $M_w$ | $\Gamma/\pm 1.1\%/$ (mg $m^{-2}$) | $\delta_H/\pm 1.1\%$ /nm | Adsorbed Amount/θ | $\delta_{rms}$/ layers | δ/layers |
|---|---|---|---|---|---|---|
| $E_{144}B_{27}$ | 8,280 | 1.15 | 16 | 4.9 | N/A | 10.7 |
| $E_{72}B_{27}E_{72}$ | 8,280 | 0.8 | 9 | 3.1 | N/A | 6.6 |
| $E_{100}B_{15}$ | 5,480 | 1.55 | 15.7 | 2.6 | 7.1 | 9.0 |
| $E_{200}B_{15}$ | 9,880 | 1.7 | 29 | 2.2 | 6.4 | 11 |
| c-$E_{200}B_{15}$ | 9,880 | 1.3 | 22.5 | N/A | N/A | N/A |
| $E_{100}B_{15}E_{100}$ | 9,880 | 1.2 | 21 | 1.7 | 4.7 | 7 |

observed in this work experimentally. An exception is the continuous increase in the level of adsorption observed for the triblock copolymer $E_{72}B_{27}E_{72}$ having a relatively higher anchor fraction.

The results also show (*see* Table 7.2) that the linear diblock copolymers ($E_{200}B_{15}$, $E_{100}B_{15}$) adsorb at a higher level than the cyclic-diblock and the triblock copolymers of the corresponding molar masses. A detailed discussion for the study of the influence of the polymer architecture of PEO-PBO block copolymers on the adsorption will be given in the SANS section.

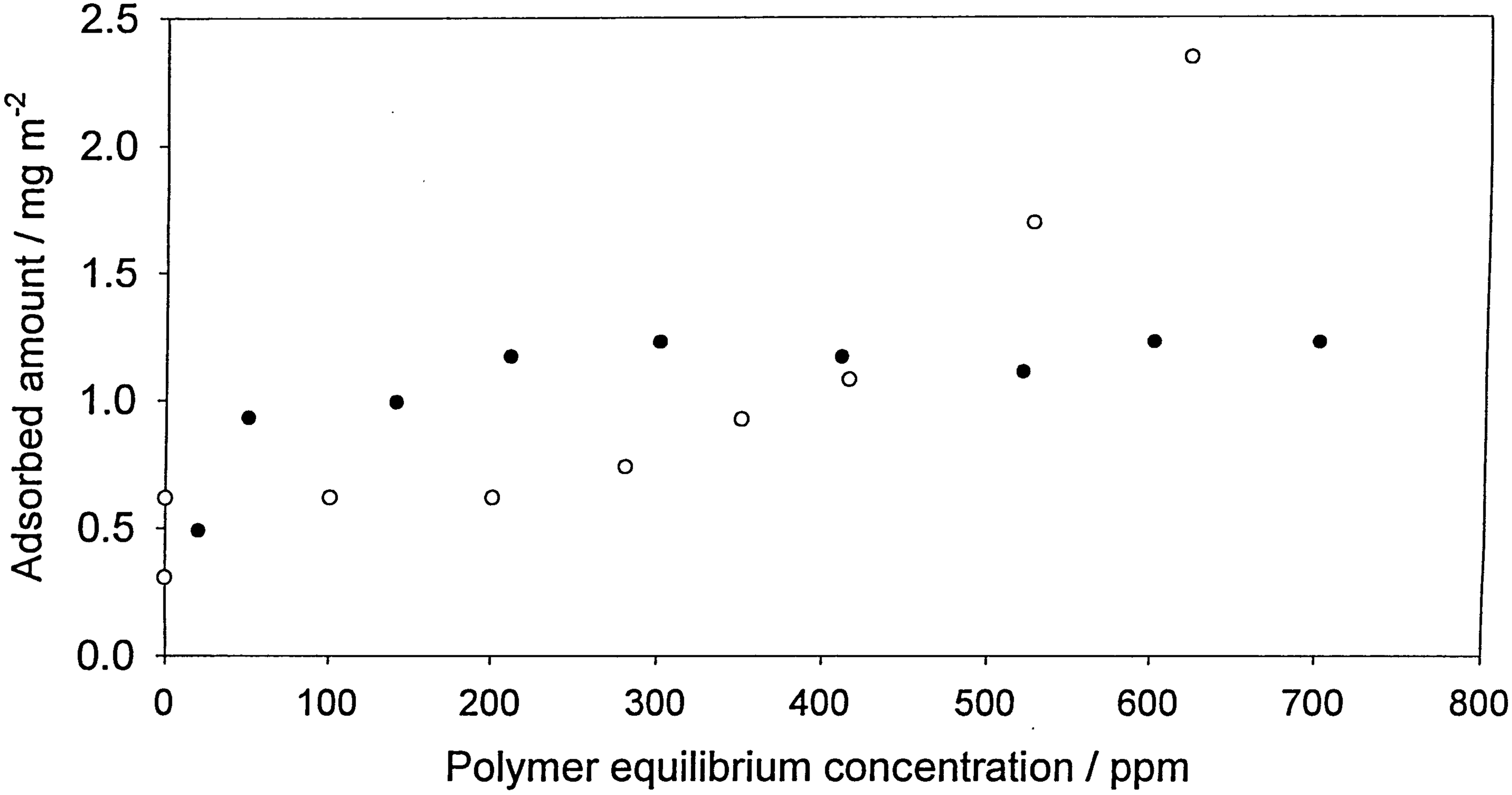


***Figure 7.3 presents the adsorption isotherms for (●) $E_{144}B_{27}$ and (o) $E_{72}B_{27}E_{72}$ copolymers adsorbed at aqueous/polystyrene latex interface as a function of polymer equilibrium concentration.***

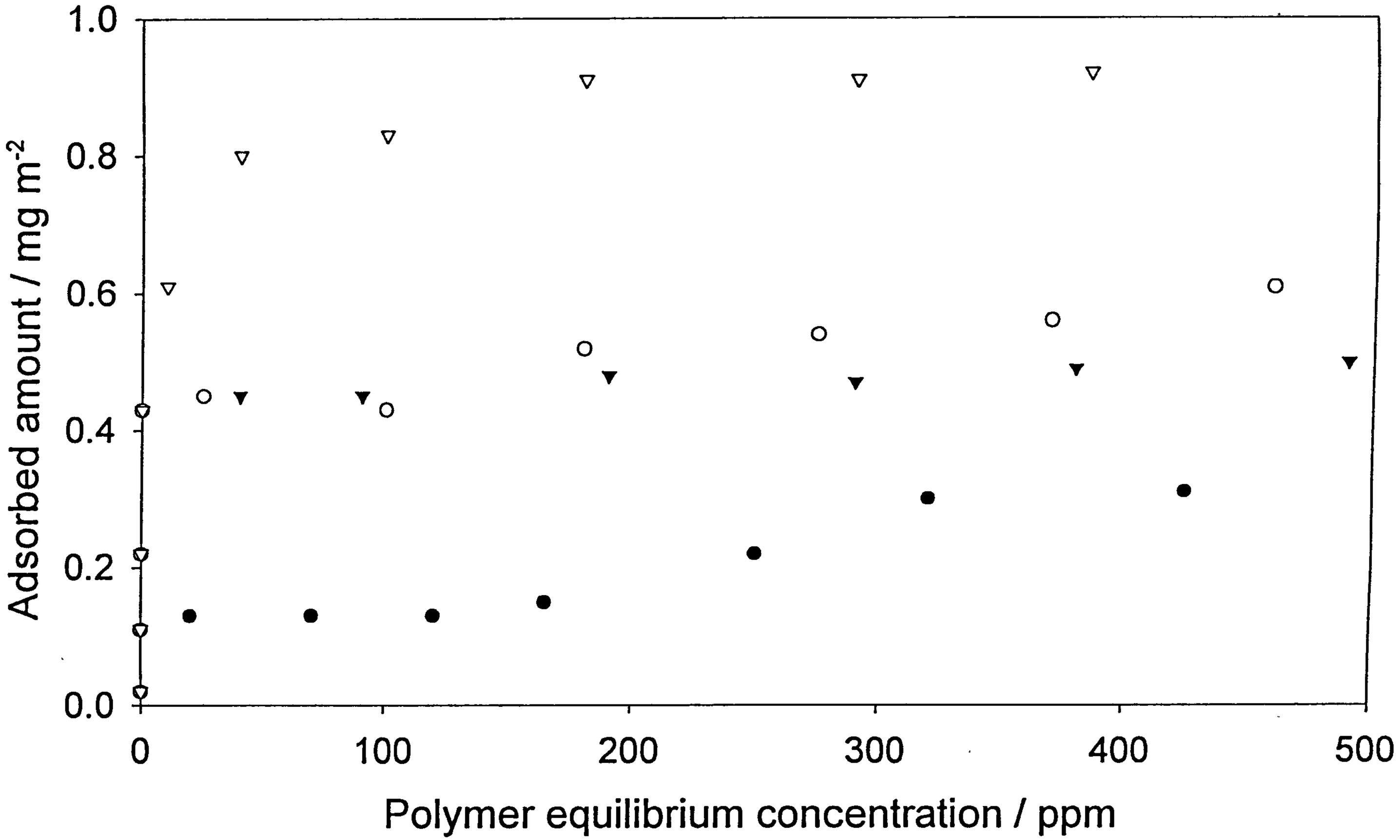


***Figure 7.4 presents the measured adsorption isotherms for $E_m$-$P_n$-$E_m$ Pluronic copolymers adsorbed onto model polystyrene latex particles as a function of polymer equilibrium concentration: ● L62 ($E_7$ $P_{30}$ $E_7$), ▼ F38 ($E_{44}$ $P_{16}$ $E_{44}$), ○ L64 ($E_{13}$ $P_{30}$ $E_{13}$) and ▽ F68 ($E_{75}$ $P_{30}$ $E_{75}$).***

Figure 7.4 shows the adsorption isotherms for four polymers, L62, L64 and F68 with constant central block of 30 PPO monomers (except F38, which has a low central PPO block monomers (16)), and increasing PEO molecular weight. Figure 7.5 shows the isotherms for Pluronics P75, P85 and F87. Typically, Pluronic P85 matches with both P75, having same number of end block PEO monomers (27), but different PPO monomer numbers, and with F87 having the same number of central block PPO monomers (39), but different PEO monomer number. Pluronic P85 adsorbs at a slightly higher a level (due to having a slightly higher PPO, anchor block content) than the P75 and at lower level than the very "hydrophilic" F87 (due to a higher monomer number of buoy, PEO blocks (62), present). Figure 7.6 shows the adsorption isotherms for three high molar mass F88, F98 and F108 Pluronics. In this figure the data are arranged in such a manner that all these three copolymers contain approximately the same PEO block monomer number (~ 120) but differ in the number of PPO block monomers present.

All the adsorption isotherms show a rapid increase (high affinity) in the level of adsorption at very low copolymer concentrations followed by a gradual levelling off until the so-called pseudo-plateau level is reached at an equilibrium concentration of approximately 100 mg/l. The monodispersity, low total polymer molar mass (as compared to PEO homopolymers studied in this work) and polymer composition are considered to play a very important role in the shape (affinity) of the adsorption isotherms. The pattern of the adsorption isotherms presented for the Pluronic copolymers was observed to be similar to those observed for the PEO homopolymers and the PEO-PBO block copolymers, however, thicker polymer adsorbed layers and hence higher adsorbed amounts (derived from the pseudo-plateau levels) were determined for the copolymers than the homopolymers of the corresponding polymer molar mass. Baker *et al*[1] have determined the adsorption of PEO homopolymers, PEO-PPO random and triblock copolymers (Pluronics P75, P85, F68 and F98) at the aqueous/polystyrene latex interface using a turbidity method involving complexation of polymers with tannic acid. They used latex of relatively higher diameter (900 nm) than that used in this work. The comparison of data between our experimentally determined data for PEO homopolymers and the Pluronic copolymers adsorbed at aqueous/hydrophobic (polystyrene latex) interface and those determined by Baker *et al.*[1] shows excellent agreement. Similar to our findings low affinity adsorption

isotherms for the high molar mass copolymers (F98 and F108) (*c.f. Figure 7.6*) were found by Baker *et al.*[1] The (possible) greater polydispersity of the higher molecular weight samples may be responsible.

For each adsorption isotherm we estimate that most of our results were obtained below the CMC of that copolymer. An exception may occur in Figure 7.4 where an unexpected step in the adsorption isotherm for the relatively more hydrophobic Pluronic L62 at approximately 100 ppm equilibrium concentration. This polymer has the highest PPO fraction (among the range of copolymers studied) and a very low HLB value, was shown. In this case the copolymer concentration range studied may be at or close to the CMC values as shown in the Table 4.2. Alexandridis *et al.*[2,3] and Wanka *et al.*[4] have determined the critical micellization concentration and temperature, (CMC) and (CMT) respectively, for a range of triblock copolymer Pluronics as a function of the polymer composition, concentration and the system temperature. It was shown that the CMC decreases with the total polymer molar mass, PPO/PEO block ratio (*i.e.* polymer composition) and the system temperature. Also for L62 the GPC data show a rather high polydispersity (*see* Table 4.2) and hence lower polymer adsorption with lower affinity isotherms were expected. Mallagh[5] has shown by SCF calculations that the polydispersity in the polymer molar mass or in the polymer composition makes the bulk concentration required for plateau adsorption much higher. Koopal[6] has shown that, for polyvinyl alcohol adsorbed at the water/silver iodide and oxidized carbon black interfaces, the polydispersity in the polymer molecular weight distribution or in the composition strongly effects the shape of the adsorption isotherms. Furthermore, bilayer formation and/or some other surface complexation and hence a conformation change may account for the "step" in the isotherm for L62, however, we have no direct evidence to support this hypothesis at the moment.

It can also be seen from the figure that for the more monodisperse systems, the copolymers with the higher fraction of adsorbing segments adsorb at higher levels. For example Pluronics P75 and P85 have the same overall total molar mass but P85 has a larger PPO block hence, adsorbs at a relatively higher level than the Pluronic P75. Similar trends were observed for F68 and F87 copolymers.

The adsorbed amount of the PEO-PPO block copolymers increases in the order of increasing total polymer molar mass (which is due to an increase in the number of PPO

and/or PEO block monomers). This confirms that in each case the adsorbed amount increases with increasing total polymer molar mass and with the variable block molar mass. The influence of molar masses of both, PPO and PEO blocks on the adsorbed amount of polymers will be discussed latter.

### 7.2.1.1. Molar Mass Dependence of Polymer Adsorption

Figure 7.7 shows the dependence of Γ (derived from the pseudo plateau regions from Figures 7.4 - 7.6) on the Logarithm of the total copolymer molar mass of the Pluronic copolymers. A very rapid increase in the adsorbed amount with increasing

Table 7.3: experimental and theoretical data; adsorbed amounts, $\delta_{rms.}$, and adsorbed layer thicknesses for the PEO-PPO triblock copolymers adsorbed onto polystyrene latex.

| Pluronics | Mw | $\nu_A$ | Γ/±1%/ (mg $m^{-2}$) | $\delta_H$/±1%/ nm | Adsorbed Amount/θ | δ/layers |
|---|---|---|---|---|---|---|
| F38 | 4800 | 0.158 | 0.45 | 5.0 | 0.5 | 5.0 |
| L62 | 2400 | 0.671 | 0.25 | 1.5 | 0.61 | 0.85 |
| L64 | 2900 | 0.536 | 0.5 | 3.6 | 0.85 | 2.6 |
| F68 | 8350 | 0.167 | 0.9 | 5.7 | 1.44 | 9.2 |
| P75 | 4450 | 0.393 | 0.7 | 5.0 | 1.18 | 4.6 |
| P85 | 4650 | 0.416 | 0.9 | 6.0 | 1.25 | 4.7 |
| F87 | 7700 | 0.238 | 1.1 | 6.5 | 1.71 | 8.6 |
| F88 | 11800 | 0.152 | 1.1 | 8.0 | 2.02 | 12.4 |
| F98 | 13000 | 0.169 | 1.3 | 9.5 | 2.26 | 12.6 |
| F108 | 14000 | 0.186 | 1.4 | 10.6 | 2.54 | 13.6 |

total polymer molar mass of the samples is observed. It is evident from the data (*see* Table 7. 3) that the adsorbed amount is strongly influenced by both the total copolymer molar mass and the block composition and increases linearly with $Log_{10}$ of total polymer molar mass. Several investigations have also reported this trend for Pluronics, Synperonics and random copolymers of PEO and PPO blocks adsorbed onto hydrophobic polystyrene latex.[1,7,8] Cohen-Stuart *et al.*[8] have shown a very strong dependence of the adsorbed amount on polymer molar mass (slope ~ 0.6 mg $m^{-2}$) for PEO homopolymers/polystyrene latex systems and compared them with the data calculated using Scheutjens-Fleer theory.

Figure 7.7 also compares the adsorbed amount of the block copolymers (•,o) from this work with that of the random copolymers (▲) found in the literature.[1] Baker *et al.*[1] have determined the adsorbed amount for random copolymers of PEO and PPO blocks of relatively higher total polymer molar masses and these have been compared with the present data by extrapolation. The random copolymers used had the two blocks in a 50:50 ratio.[1] All data gave a linear increase in the adsorbed amount with total polymer molar mass. However, a higher rate of increase in the adsorbed amounts is observed for the Pluronic copolymers than that for PEO homopolymer (*see* Figure 7.8) and for the random copolymers. This emphasises the relatively stronger dependence of adsorbed amount on total polymer molar mass for the block copolymers. The influence of the PPO:PEO block composition of the copolymers on the adsorbed amount was also shown from the two sets of data observed for the Pluronic triblock copolymers. Also, higher $\Gamma$ values were observed for the high anchor fraction materials (PPO rich random, ▲, and block copolymers, •). This emphasises a strong influence of the hydrophobic PPO blocks on the adsorbed amount. This figure indicates that copolymers with PEO block sizes smaller than or equal to the PPO block size (random, ▲, and triblock, •, copolymers with higher PPO contents) adsorb more strongly than the copolymers of the corresponding molar masses predominantly consisting of PEO blocks (o).

Figure 7.8 presents the dependence of adsorbed amount of the PEO homopolymers and the PEO-PPO copolymers on PEO block molar mass. Also, this figure compares the adsorbed amounts of PEO homopolymers (o) and the Pluronics (•)

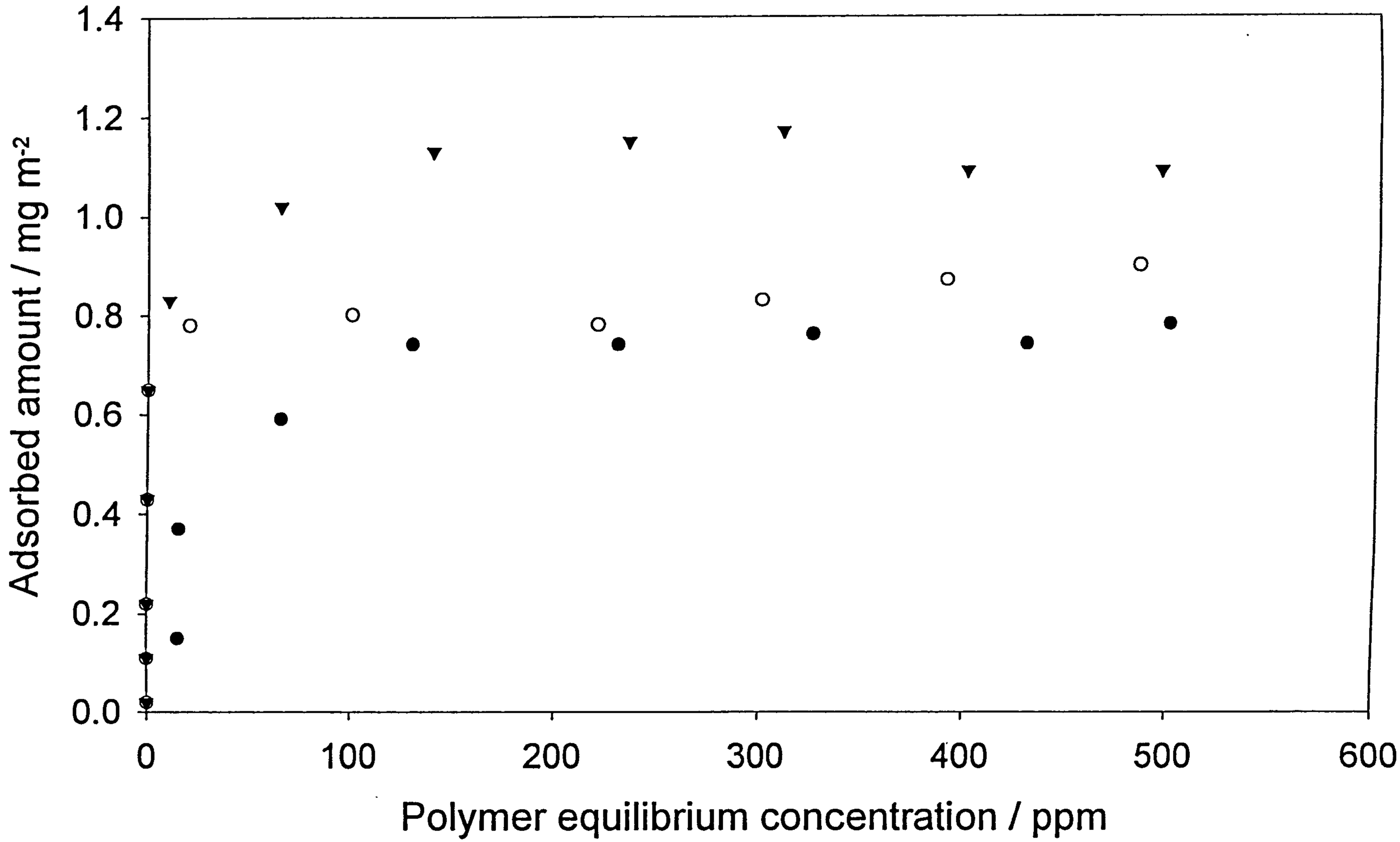


***Figure 7.5 presents the measured adsorption isotherms for Pluronic copolymers adsorbed onto model polystyrene latex particles as a function of polymer equilibrium concentration: ● P75 ($E_{27}$ $P_{35}$ $E_{27}$), o P85 ($E_{27}$ $P_{39}$ $E_{27}$) and ▼F87 ($E_{62}$ $P_{39}$ $E_{62}$).***

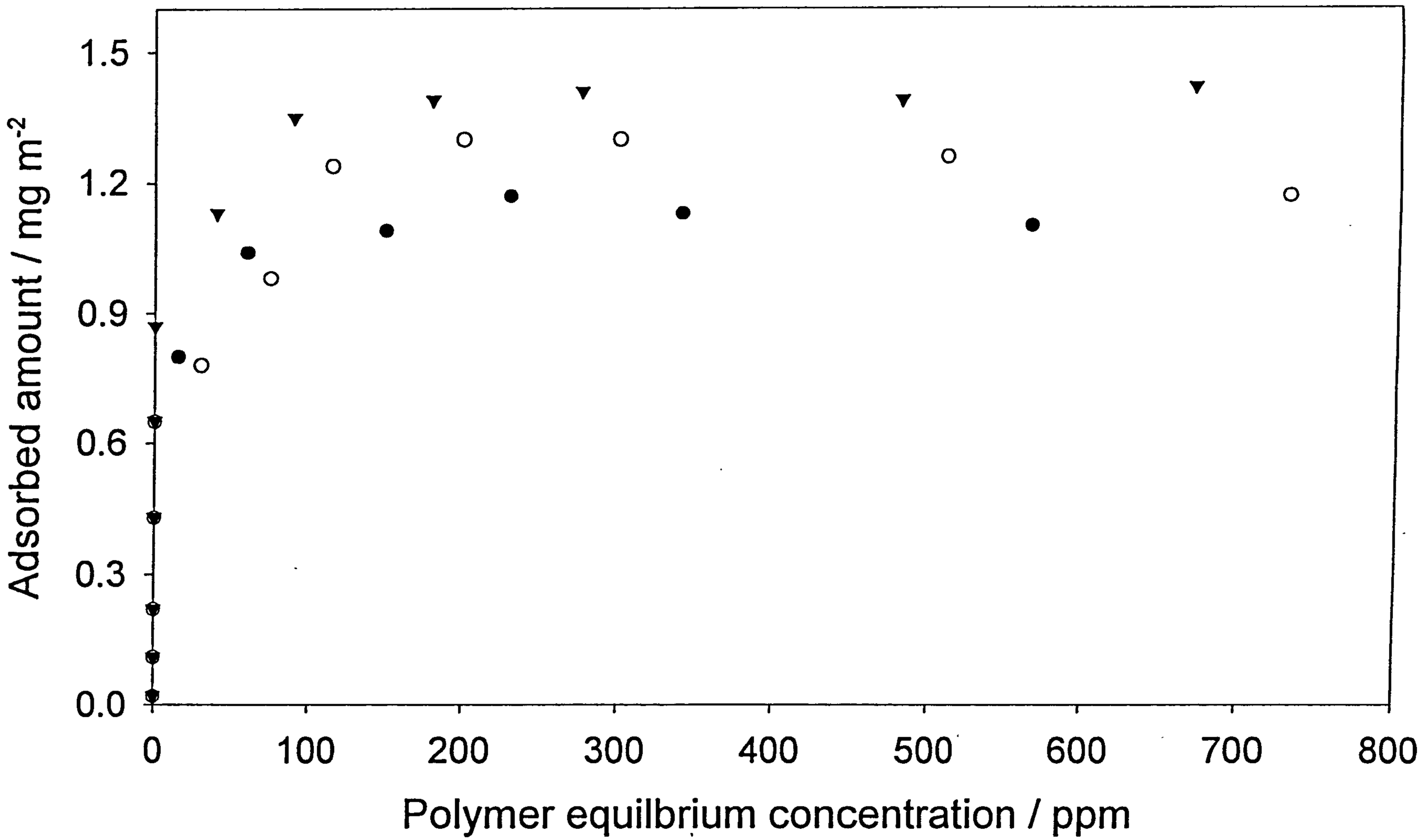


***Figure 7.6 presents the measured adsorption isotherms for Pluronic copolymers adsorbed onto model polystyrene latex particles as a function of polymer equilibrium concentration:*** ● ***F88 ($E_{108}$ $P_{39}$ $E_{108}$),*** o ***F98 ($E_{116}$ $P_{47}$ $E_{116}$),*** ▼***F108 ($E_{122}$ $P_{56}$ $E_{122}$).***

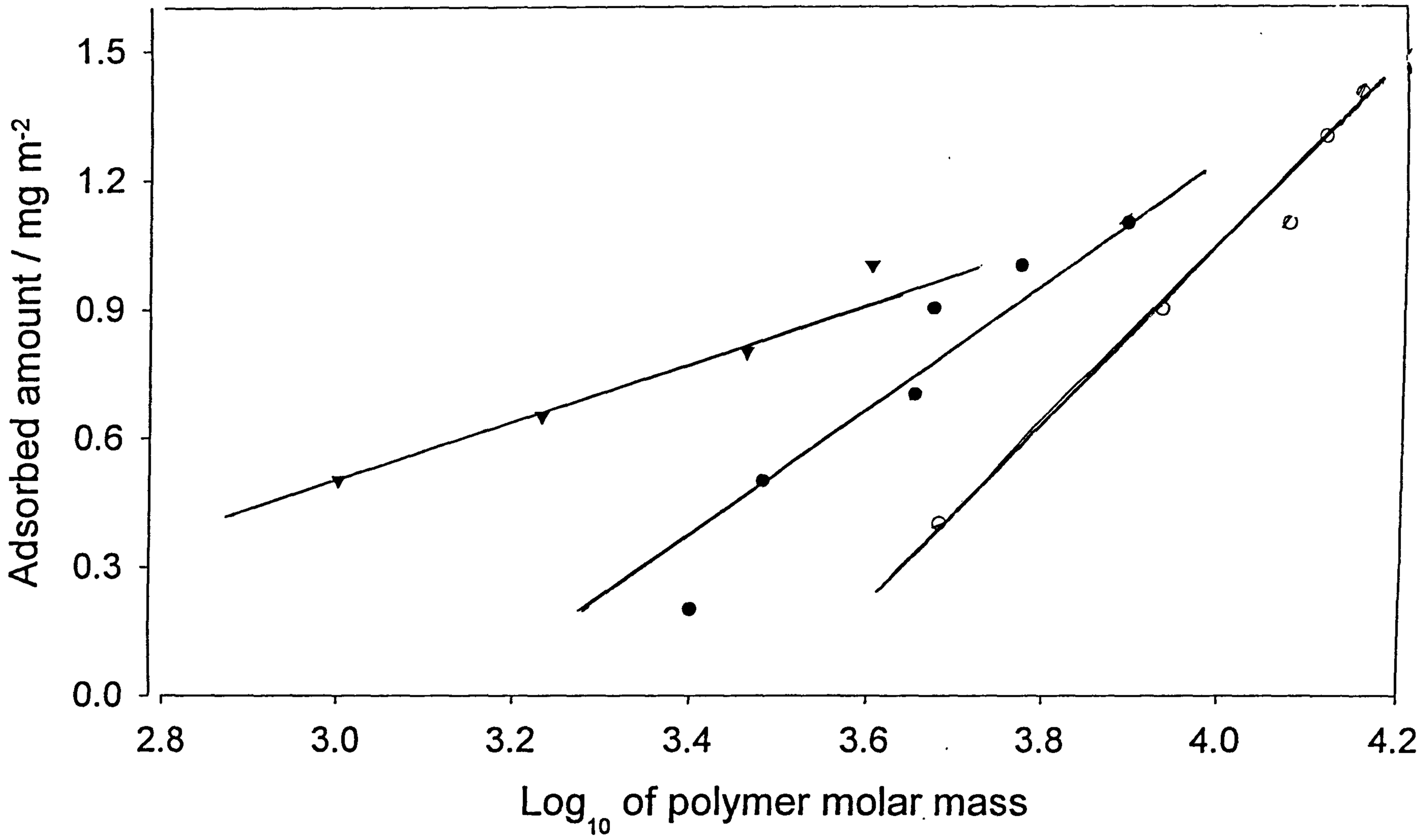


***Figure 7.7 presents the measured adsorbed amount for PEO-PPO block copolymers adsorbed on polystyrene latex as a function of $log_{10}$ of copolymer molar mass: ▲ random copolymers, and our data for Pluronic copolymers: ● PEO≤PPO, o PEO>>PPO.***

determined in this work with those presented by Baker *et al.*[1] for random copolymers (Δ) adsorbed on polystyrene latex substrate. An approximately linear increase in Γ of these random and block copolymers observed as a function of $Log_{10}$ of PEO block molar mass (*c.f.* Figure 7.7) has been observed. Again, the adsorbed amount for the copolymers increased more rapidly than for PEO homopolymers. The high anchor-fraction random and block copolymers adsorb at approximately similar levels but are substantially higher than those observed for the PEO homopolymers. This may be due to the low affinity of PEO homopolymers for the hydrophobic surface. The high molar mass Pluronic copolymers with a high PEO content (hence low anchor fraction) *i.e.* highly hydrophilic in nature, adsorb at levels lower than the random copolymers but higher than those observed for the PEO homopolymers. This difference in the behaviour of these copolymers was not surprising but is due to the presence of very long soluble PEO arms. This again emphasises the strong influence of the hydrophobic PPO blocks on the adsorbed amount on a hydrophobic surface.

Figure 7.9 shows the influence of the hydrophilic (PEO) buoy molar mass on the adsorbed amount at a fixed hydrophobic (PPO) anchor mass. Two sets of data at different fixed PPO block molar masses are shown. The data show that increase in the adsorbed amount for these copolymers is not linear with the PEO block molar mass, but at first $\Gamma_{max}$ increases very rapidly for the low molar mass copolymers (L62, L64 and P85) and then more slowly for the high molar mass samples. This change in the behaviour corresponds to the PEO becoming longer than the PPO and indicates a transition in the system from the anchor to the buoy regime.[9,10,11] This data again emphasises the importance of the hydrophobic PPO anchor in determining the overall level of adsorption. Guzonas *et al.*[11] and Evers *et al.*[12] have already predicted the strong dependence of block copolymer adsorption on the polymer composition.

## 7.2.2. Theoretical Predictions for the Adsorbed Amount

### *7.2.2.1. Pluronic Copolymers*

Figure 7.10 shows the influence of anchor-fraction, $\nu_A$ on the measured adsorbed amount of the Pluronic copolymers. Inset into this figure is the data for the same series

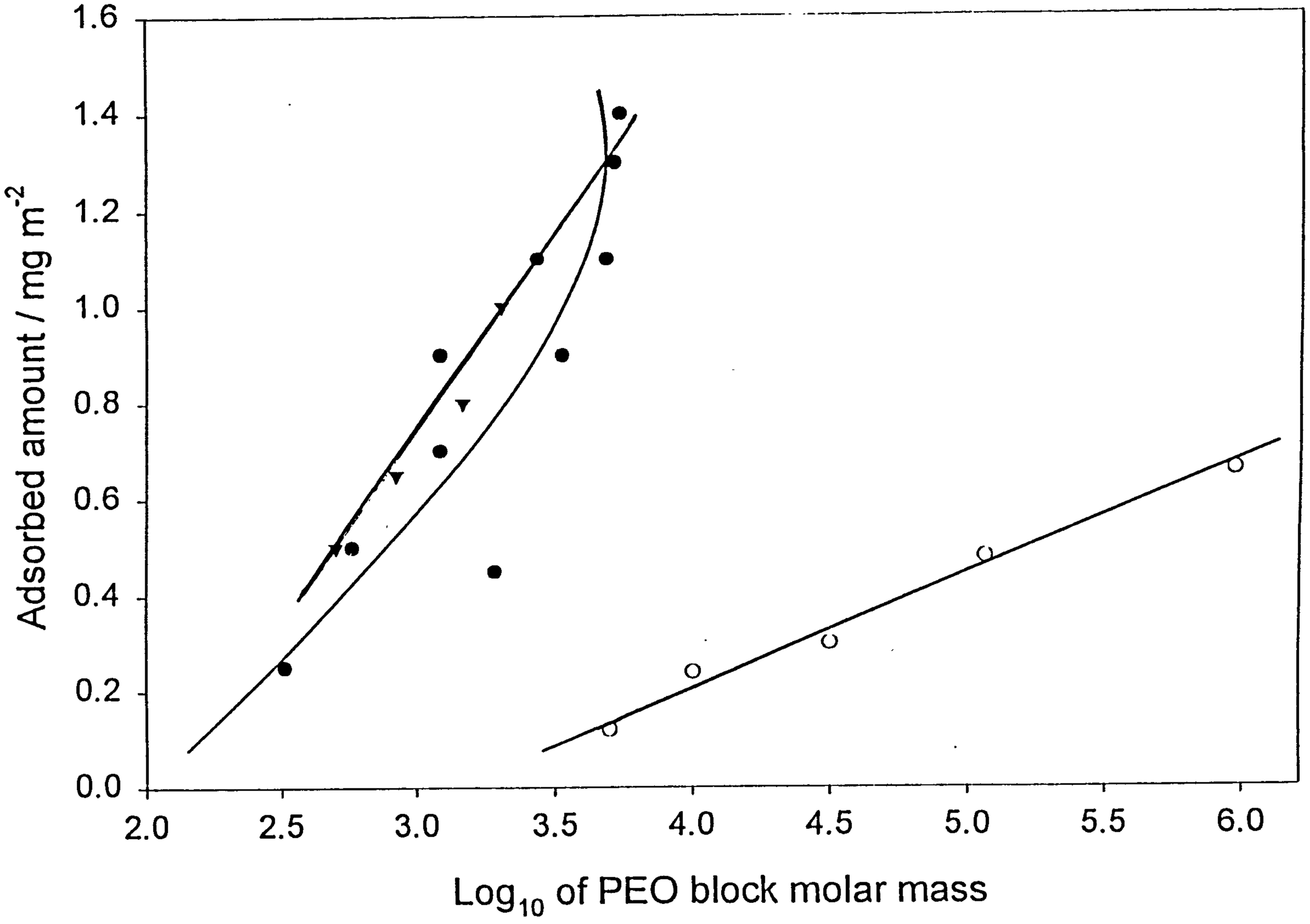


***Figure 7.8 presents the measured adsorbed amounts for polymers as a function of the $Log_{10}$ of PEO block molar mass content: ● Pluronics, ▼random copolymers and o PEO homopolymers.***

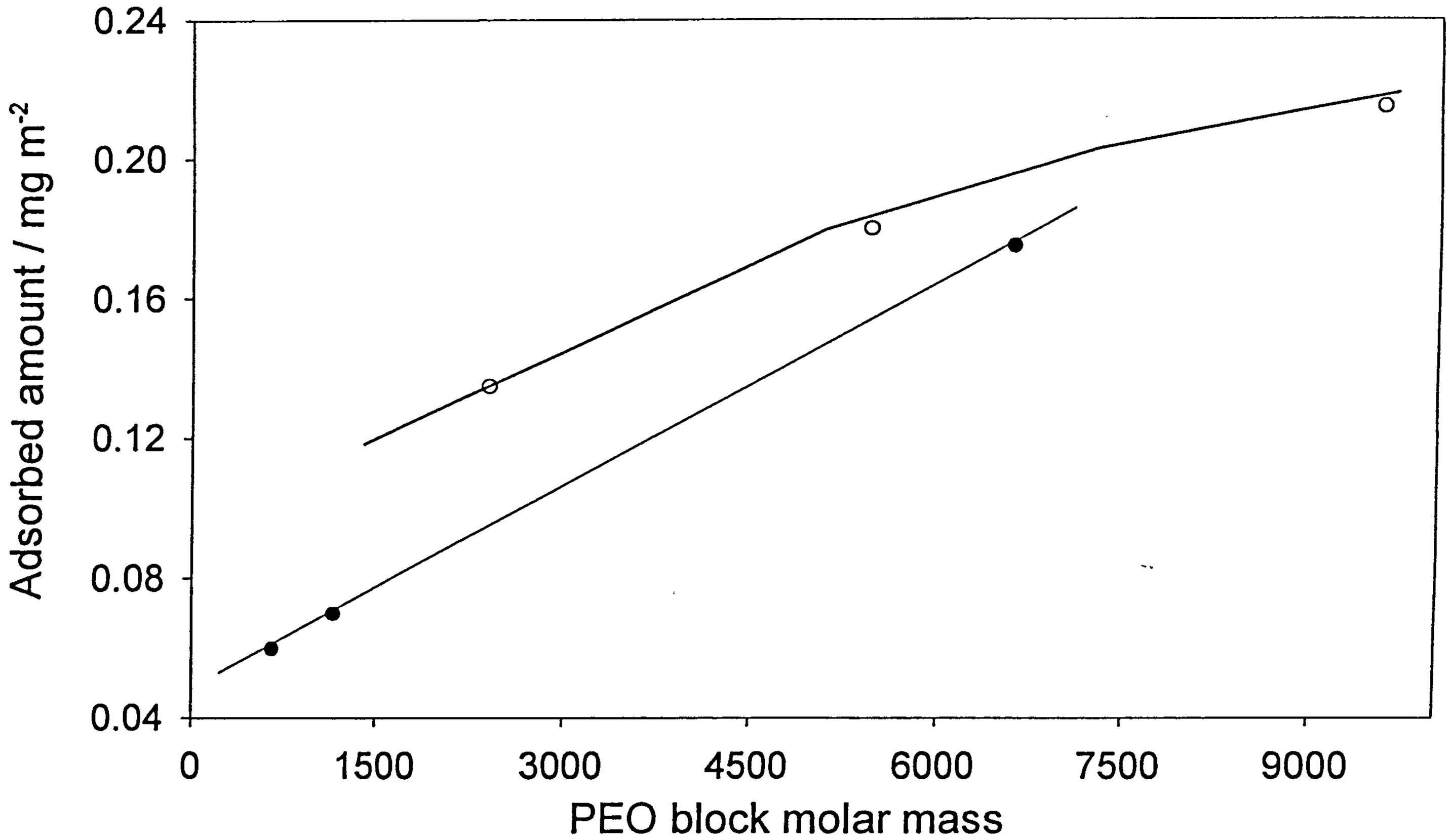


***Figure 7.9 presents the measured adsorbed amount of Pluronic copolymers as a function of PEO block molar mass at a constant PPO block mass: ● PPO≅1750, o PPO≅2250.***

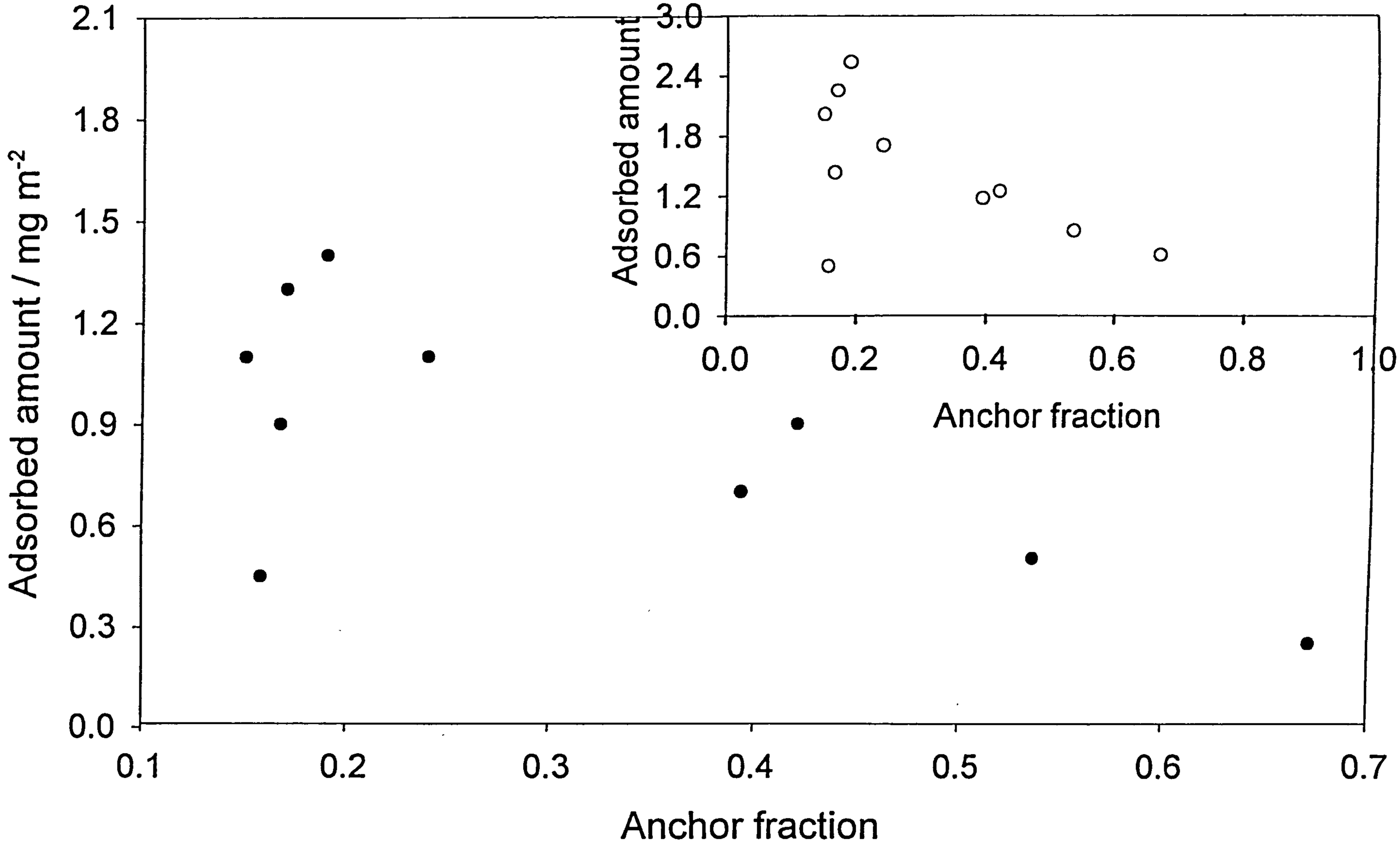


***Figure 7.10 presents the adsorbed amount of Pluronics as a function of the anchor fraction, $\nu_A$: ● our experimental data and o inset data for these copolymers calculated using the SCF model.***

of Pluronic copolymers under study (*see* Table 4.2) calculated using the mean-field lattice model (SCF model) given by Scheutjen-Fleer and Evers.[9,12] Cohen-Stuart *et al*[8] Fleer *et al.*[9] Marques *et al.*[10], and Evers *et al.*[12] describe the adsorption of polymers from nonselective solvents on the solid surface as a swollen anchor block and a more dilute buoy block extending out in the bulk solution. They have also discussed that the level of adsorption depends strongly upon the polymer composition. Our data is in excellent agreement with other experimental data for the diblock copolymers.[11] Guzonas *et al.* [11] have used the MJL model for the adsorption of diblock copolymers to discuss the data for PEO/poly styrene and the adsorption of dimethyl-aminoethyl-methacrylate and butyl-methacrylate adsorbed at silica/2-propanol interface.[13] Good agreement of their measured data was found with the trends in the pattern predicted by Fleer *et al.*, Marques *et al.*, and Evers *et al.* The data give a strong dependence of the adsorbed amount and the hydrodynamic thickness on the copolymer composition, and a maximum in both $\Gamma_{max}$ and $\delta_H$ was observed around $\nu_A \sim 0.2$, if adsorbed amount/adsorbed layer thickness were plotted as a function of the anchor fraction.

The block monomer number ($N_i$) is the molar mass of each individual block divided by the corresponding molecular mass of that block. The number of adsorbed layers was taken as the square root of the number of PEO monomers ($N_B$) present in each sample. In each case, the adsorbed amount was calculated between solution equilibrium concentrations of 1 and 2000 ppm.for a series of normal Pluronic copolymers adsorbed at aqueous/polystyrene latex interface. The same set of Flory parameters[14] as used for the R. Pluronic/polystyrene latex systems (see Section 5.2) were selected for all of the calculations noted in this chapter. Qualitatively, these two data sets, determined experimentally and calculated theoretically, show an excellent agreement in trends: both pass through a maximum as a function of $\nu_A$. The data emphasises the transition between the buoy dominated regime ($\nu_A < 0.2$) and the anchor regime ($\nu_A > 0.2$). Overall, the trends of our data were similar to those measured by Wu *et al.*[13] and to those predicted theoretically for the other diblock copolymers. [8-12]

This indicates that essentially the same mechanism operates i.e. it is the projected relative surface areas of the two blocks which dominate the adsorption behaviour. In addition, a qualitative agreement between our experimental data and the SCF model was a further justification for the presumed preferential adsorption of the PPO blocks.

Figure 7.11(a) presents the theoretical adsorbed amount (θ) calculated using the SCF model[8,9,12] for the same series of Pluronic copolymers used in this study as a function of the measured adsorbed amount. The same set of χ parameters as explained in the earlier part of this section were used. The data present a linear increase in θ with increasing the polymer adsorbed amount and is in accordance with the predictions. This again emphasises a good qualitative agreement between the predicted and experimentally determined data.

### 7.2.2.2. PEO-PBO Block Copolymers

The calculations were performed using the mean-field lattice model for polymer adsorption developed by Scheutjens, Fleer and Evers[9,12] using the 10 to 2000 ppm range of polymer solution concentrations. In each case the adsorption isotherms were presumed to reach the pseudo-plateau levels at 500 ppm polymer equilibrium concentrations. The Flory parameters were taken as follow: $\chi_{BS} = -4$; $\chi_{ES} = -2$; $\chi_{EB} = 2$; , $\chi_{EW} = 0.45$; $\chi_{BW} = 2$; and $\chi_{WS} = 0$, where E is ethylene oxide, B butylene oxide, W water and S is the surface (polystyrene latex). The surface parameters were chosen bearing in mind that the PBO block due to its more hydrophobic nature adsorb preferentially on polystyrene latex. Furthermore, both monomers and water were taken to occupy one lattice site. This latter approximation is not ideal but scaling the monomer sizes based on their molar volume with respect to water leads to very small absolute numbers of monomers which for small polymers such as these becomes unrealistic. The data calculated for the PEO-PBO block copolymers using SCF model is given in Table 7.2 and will be discussed in conjunction with that determined for the same set of copolymers using SANS.

Figure 7.11(b) presents the adsorbed amount calculated using the SCF model for the same set of PEO-PBO block copolymers used in this study as a function of the measured adsorbed amount. The same χ parameters as explained above for these copolymers were used. The two sets of data each representing the polymers with constant anchor fraction are observed. Limited data have been presented in this figure, due to unavailability of the samples. The data indicate that the polymers with higher anchor fraction adsorb at relatively higher levels than those with the lower anchor

fraction and hence indicating a strong influence of the hydrophobic : hydrophilic block ratio on the adsorption of these polymers. The results are in good agreement with the trends in the behaviour to those observed for the PEO-PPO block copolymers adsorbed on polystyrene latices (*c.f.* Figure 7.7). Overall, the data show an approximately linear dependence of the calculated adsorbed amount on experimentally measured adsorbed amount for these polymers. However, the rate of increase in the calculated adsorbed amount is observed to be dependent on the PBO-PEO block ratio *i.e.* it is higher for the high anchor fraction polymers.

## 7.3. Hydrodynamic layer thickness

The hydrodynamic layer thickness for PEO homopolymers and the block copolymers adsorbed at the aqueous/polystyrene latex interface was determined as a function of the copolymer molar mass at a fixed bulk copolymer concentration corresponding to the plateau region of the adsorption isotherms. All the measurements were performed using photon correlation spectroscopy (PCS) in a similar manner to those described in Section 4.3.2. The results present an increase in the layer thickness as a function of polymer composition. The results were compared with the hydrodynamic thickness determined by different methods and in other systems.

### 7.3.1. Molar Mass Dependence of Hydrodynamic Layer Thickness

Figure 7.12 shows a double logarithmic plot of $\delta_H$ versus total polymer molar mass for Pluronic copolymers. This figure shows that except for very low molar mass copolymer, L62 an approximately linear increase in $\delta_H$ was observed for these block copolymers (*i.e.* $\delta_H \sim M^{\alpha}$). However, L62 shows a similar behaviour to that shown in the adsorption isotherms (*c.f. Figure 7.2*) giving very low $\delta_H$ values. This can be attributed to the polydispersity (*i.e.* $M_w/M_n \sim 1.25$) of the sample and/or to its low total polymer molar mass and very low PEO content, which, gives rise to the low adsorbed amount and hence an extremely thin adsorbed layer.

As compared to the copolymers (*see* Tables 7.1-7.3) the homopolymers adsorb at relatively lower levels hence giving thin adsorbed polymer layers. The data show that

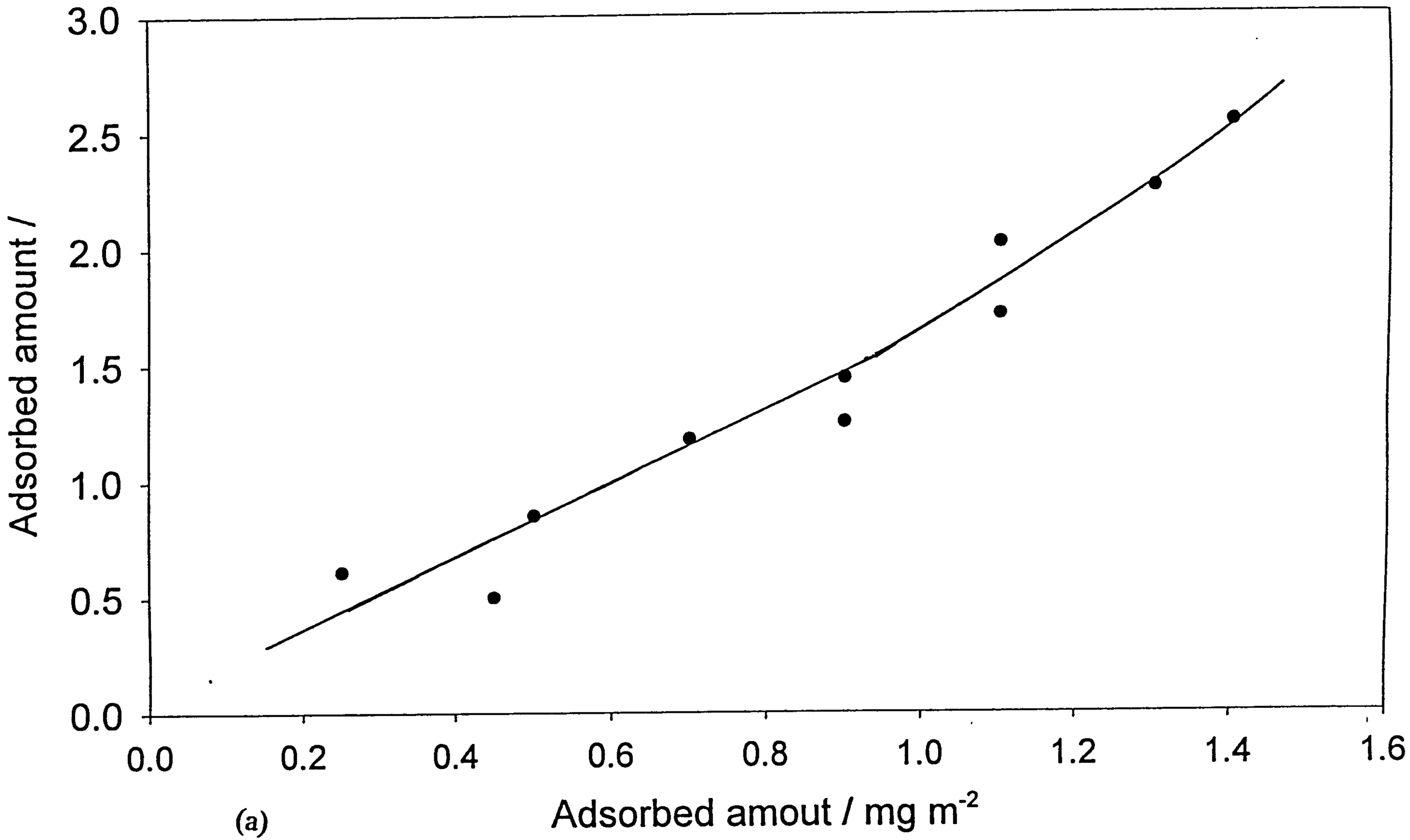


(a)

***Figure 7.11 presents the adsorbed amount calculated for the block copolymers adsorbed on polystyrene latex determined using SCF model as a function of the measured adsorbed amount; Pluronic copolymers.***

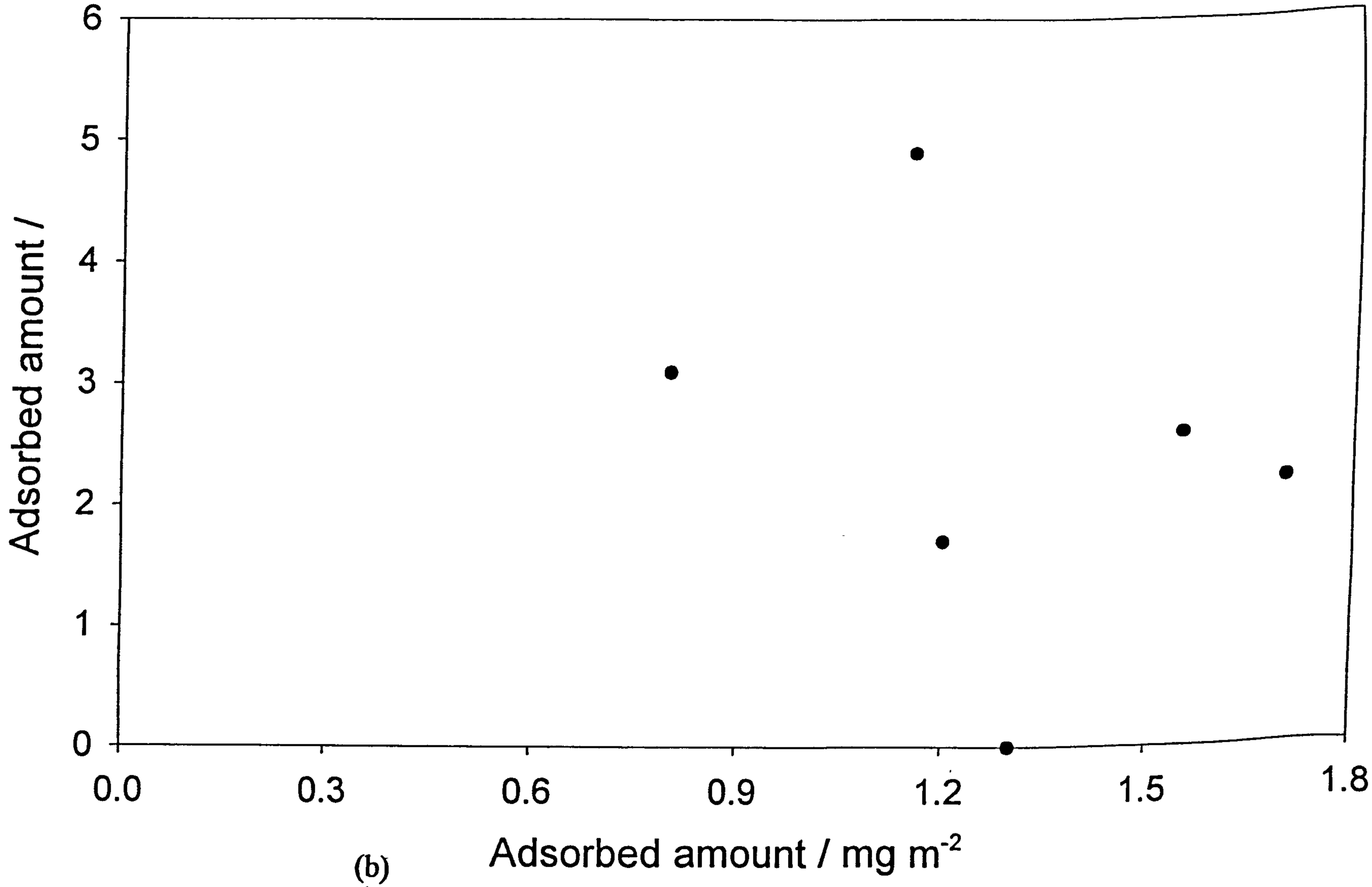


(b)

Figure 7.11 presents the adsorbed amount calculated for the block copolymers adsorbed on polystyrene latex determined using SCF model as a function of the measured adsorbed amount; PEO-PBO block copolymers.

when the polymers are studied in the same systems and under similar conditions the PEO-PBO block copolymers are observed to adsorb at higher levels than the PEO-PPO block copolymers of corresponding molar masses and hence giving relatively thicker adsorbed layers. The linear diblock copolymers, $E_{144}B_{27}$ and $E_{200}B_{15}$, show thicker adsorbed layers in the range studied than the respective cyclic-diblock and the linear triblock copolymers with the same polymer composition but having different polymer conformations. This indicates a strong influence of polymer structure on the polymer adsorption. Baker *et al.*[1] and Killmann *et al.*[15] have also presented a strong dependence of the adsorbed layer thickness on the total polymer molar mass of PEO homopolymers and the PEO-PPO block copolymers. Cosgrove *et al*[16] and Kato *et al.*[17] have also presented a strong dependence of hydrodynamic layer thickness for PEO homopolymers adsorbed on polystyrene latex. They suggested the dependence of the thickness on the total polymer molar mass was of the order $\delta_H \sim M_w^{\alpha}$, where Cosgrove *et al.*[16] suggested $\alpha = 0.8$ and Kato *et al.*[17] found $\alpha = 0.56$. For present data we have found that $\alpha = 0.4$ and 0.8 respectively, for PEO homopolymers and Pluronic copolymers adsorbed on polystyrene latex.

Figure 7.13 shows the influence of the PEO block molar mass on $\delta_H$ as a function of PEO block content of the polymer. Two sets of data measured at two different fixed PPO block molar masses are presented. Similar trends to those found for the adsorbed amounts are observed (*c.f.* Figure 7.9). However, the dependence of $\delta_H$ on block molar mass was found to be stronger than that observed for the adsorbed amount and shows the dominating influence of the hydrophilic PEO block. This may result as any increase made in PEO block size ultimately increases the number of segments in loops and/or tails which, in turn increases the hydrodynamic thickness. It has been predicted that the tails and/or loops contribute more towards the hydrodynamic thickness of the adsorbed layer than they do to the adsorbed amount.[1,8] In addition, this figure also presents the dependence of $\delta_H$ on the PPO block molar mass whilst the PEO block was maintained constant. It was observed that any increase in the PPO block size also increases the net affinity between the hydrophobic polystyrene latex surface and the polymer. This interaction gives rise to an increase in the adsorbed amount and consequently, the hydrodynamic thickness of the adsorbed layer becomes larger. Killmann *et al*[15] have also found a strong influence of the surface-polymer interactions; hydrophobic attractive interactions on the apolar surface, on the conformation of the

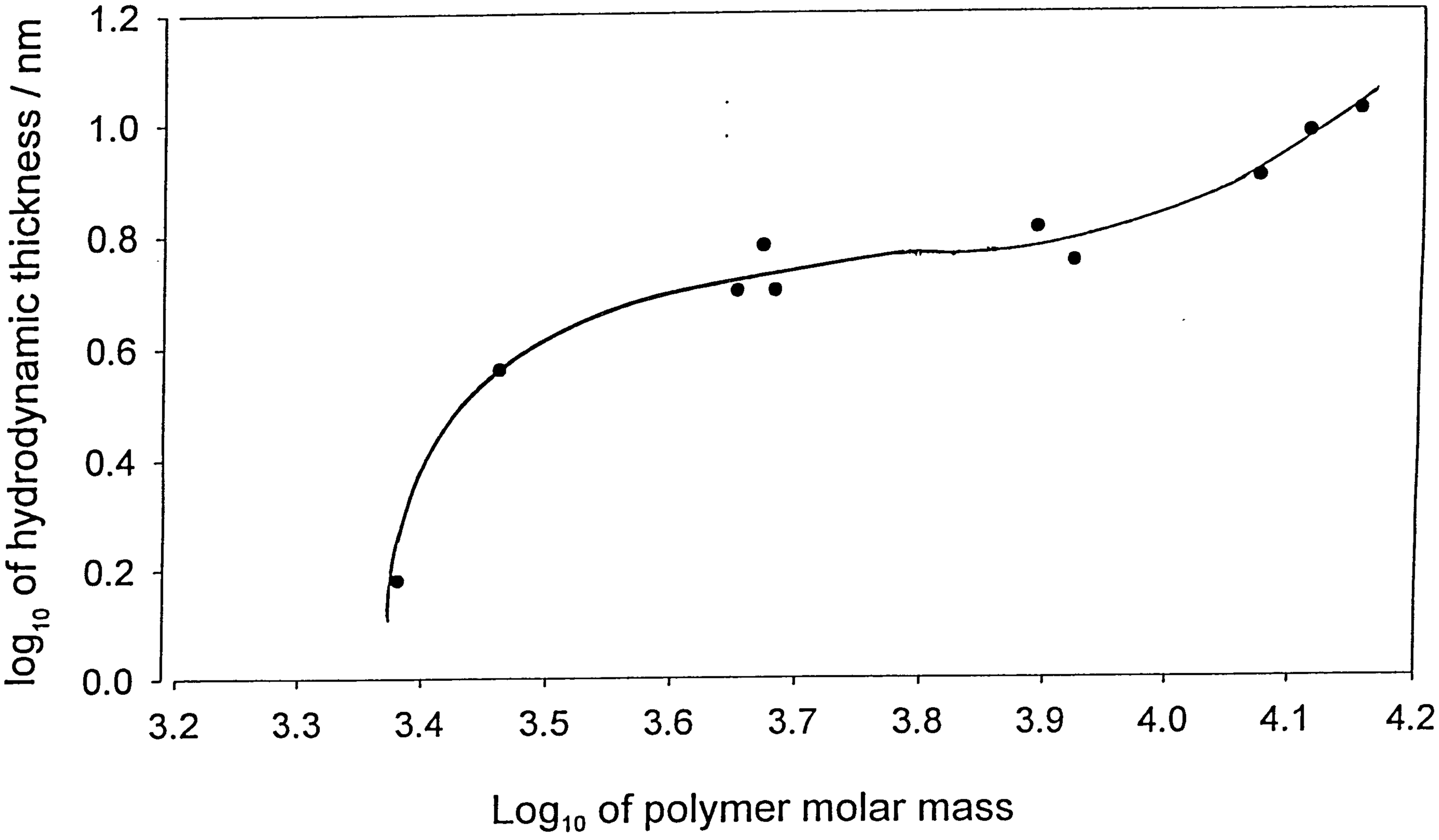


***Figure 7.12 presents the $Log_{10}$ of the measured hydrodynamic thickness of the Pluronic copolymers adsorbed on polystyrene latex as a function of the $Log_{10}$ of the total polymer molar mass.***

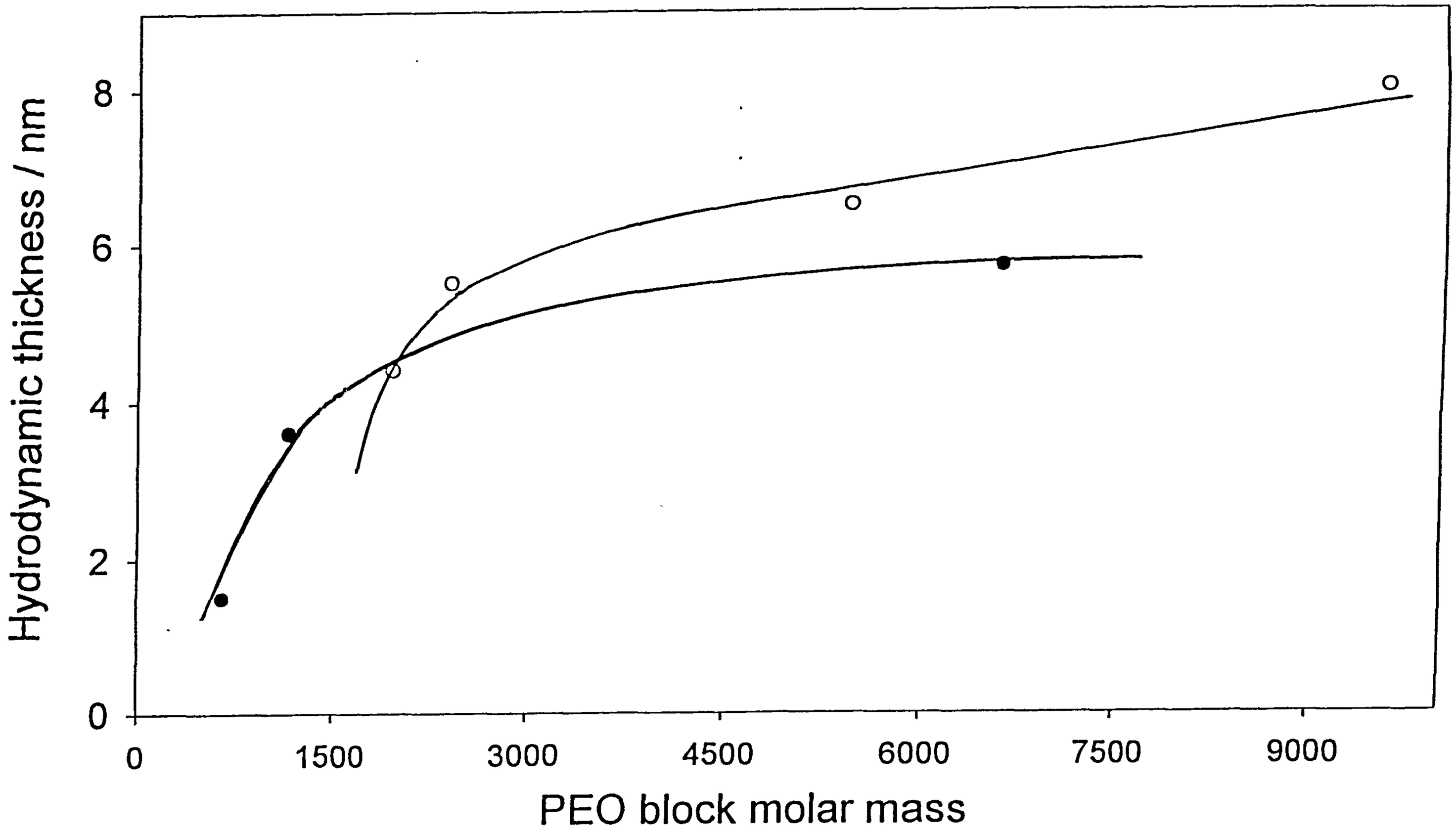


***Figure7.13 presents the measured hydrodynamic thickness of the adsorbed polymer layer of the Pluronic copolymers adsorbed on polystyrene latex as a function of PEO block molar mass at constant PPO block molar mass: ●, PPO≅1750 and o, PPO≅2250.***

adsorbed layer. Overall, it was observed that the influence of the copolymer composition was stronger for the thickness than the adsorbed amount.

Figure 7.14 compares $\delta_H$ of PEO homopolymers and PEO-PPO triblock copolymers with that of PEO-PPO random copolymers (extrapolated data) found elsewhere in the literature[1] as a function of PEO block molar mass. Initially, there is a rapid increase in the hydrodynamic layer thickness for the Pluronic copolymers having low total molar mass which slows down for the samples of intermediate molar mass further followed by a rise for the high molar mass samples. This behaviour may be attributed to the saturation of the polymer segments on the particle surface. The data show much higher hydrodynamic layer thickness values for the random and block copolymers than those determined for the homopolymers. A comparison between the hydrodynamic thickness data for the Pluronics presented in this work and those found in the literature show a good qualitative agreement.[1] The data of Baker *et al.* show similar trends to the pattern as observed in this work. Killmann *et al.*[15] and Kays *et al.*[20] have also determined the hydrodynamic thickness of the adsorbed layer for the Pluronic copolymers adsorbed at the aqueous/polystyrene latex interface. Their data presented show an approximately linear relationship of the hydrodynamic layer thickness with PEO block content of the polymer. A linear increase in $Log_{10}\ \delta_H$ with $Log_{10}$ PEO block molar mass for the homopolymers and random copolymers suggests a scaling relationship of the form $\delta_H \sim M^{\alpha}$. In addition, for the block copolymers of high PPO:PEO ratio the layer thickness was greater for the triblock copolymers than the homopolymers and the random copolymers. An overlap in the hydrodynamic thickness values between the random and the triblock copolymers at very high PEO content of the triblock copolymers suggests a transition from the anchor dominating to the buoy-dominating regime. This indicates the saturation of the long hydrophilic PEO segments on the particle surface: any further increase in the total polymer molar mass and/or PEO block molar mass can not bring any significant change in the adsorbed amount and, hence, in the adsorbed layer thickness.

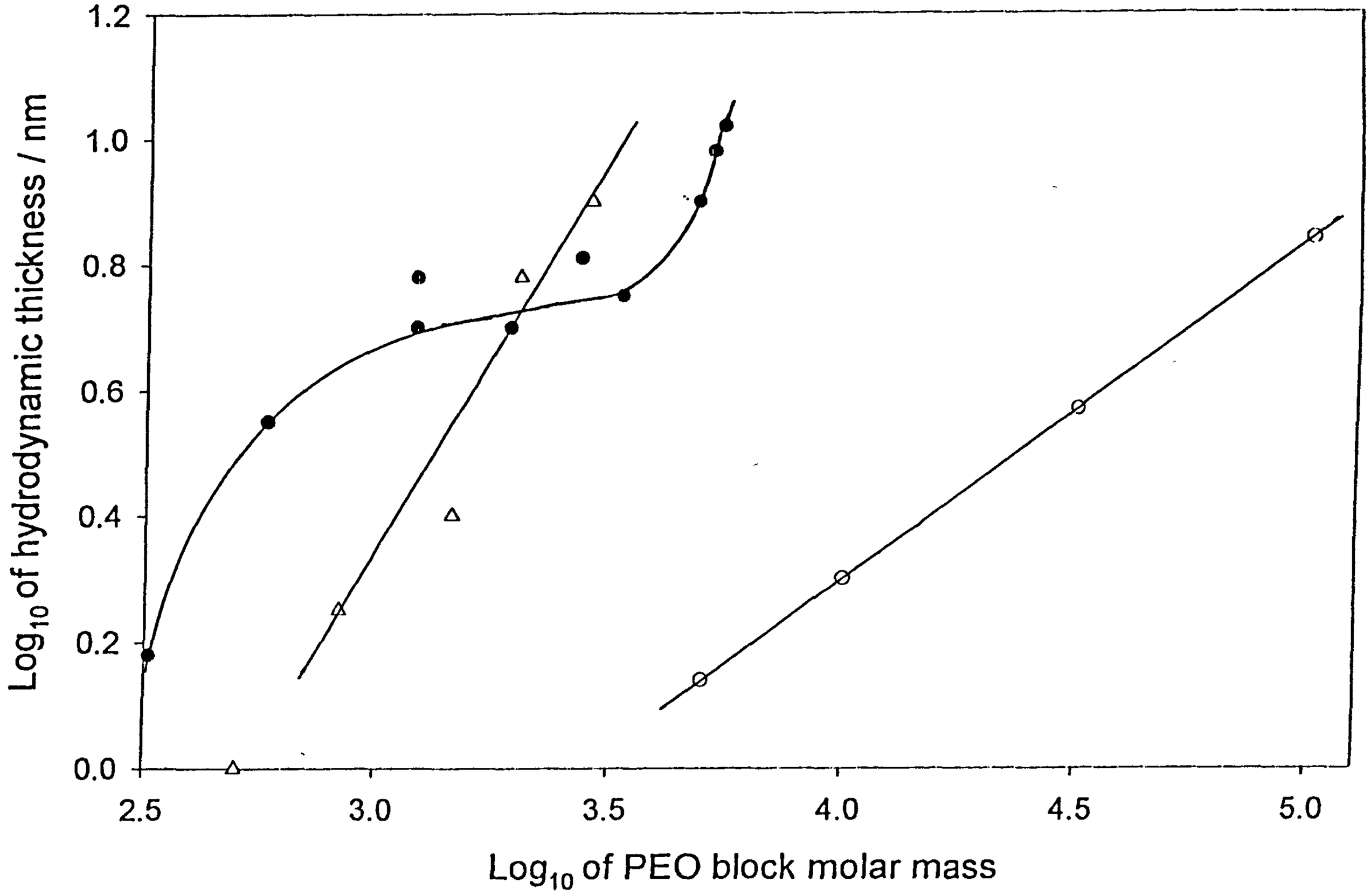


***Figure 7.14 presents the $Log_{10}$ of the hydrodynamic layer thickness of the PEO homopolymers and the PEO-PPO block copolymers adsorbed on polystyrene latex as a function of the $Log_{10}$ of PEO block content of the polymers: ▲, random copolymers, our experimental results for ●, Pluronic copolymers and o, PEO homopolymers.***

## 7.3.2. Theoretical Predictions for Hydrodynamic Layer Thickness

### 7.3.2.1. Pluronic Copolymers:

Figure 7.15 presents the dependence of calculated thickness on $Log_{10}$ of the total polymer molar mass for the same set of copolymers used for adsorption on polystyrene latex. The data were calculated using the SCF model[9,12] in a similar manner as described in the Section 5.2, using the same set of $\chi$ parameters. An approximately linear increase in the thickness with increasing the total polymer molar mass is observed in a similar manner as observed experimentally for these copolymers with an exception that the low molar mass L62 shows a small deviation from the linearity i.e. forms a very thin adsorbed layer (c.f. Figure 7.12). Overall, the trends in the pattern of theoretical and measured adsorbed layer thickness data presented for these copolymers for the polystyrene latex system are in a good qualitative agreement.

Figure 7.16 shows the influence of the anchor-fraction on the adsorbed layer `thickness for the PEO-PPO block copolymers. Inset into this figure is data calculated for the same set of PEO-PPO triblock copolymers under study (*see* Table 7.3) using the SCF model, same $\chi$ parameters were used as described in Section 5.2. Since, the PEO-PBO block copolymers have almost the similar $\nu_A$ values, hence, the dependence of the adsorbed layer thickness on the anchor fraction will not be presented. Again, a good qualitative agreement with the experimental and theoretical results was evident from these two plots. It can clearly be seen from the figure that the effect of the anchor fraction on the adsorbed layer thickness is similar to that observed for the adsorbed amount (*c.f.* Figure 7.10). A similar behaviour has also been observed with diblock copolymers (*see* Section 7.2) but this is the first time that this behaviour has been observed with a wide range of triblock copolymers with varying composition (*c.f.* Figure 7.10).

Figure 7.17(a) presents the adsorbed layer thickness for the same set of PEO-PPO triblock copolymers calculated using the SCF model[9,12] in similar manner as described in the Section 5.2, as a function of the measured hydrodynamic thickness of the polymer adsorbed layer. An approximately linear increase in the calculated thickness

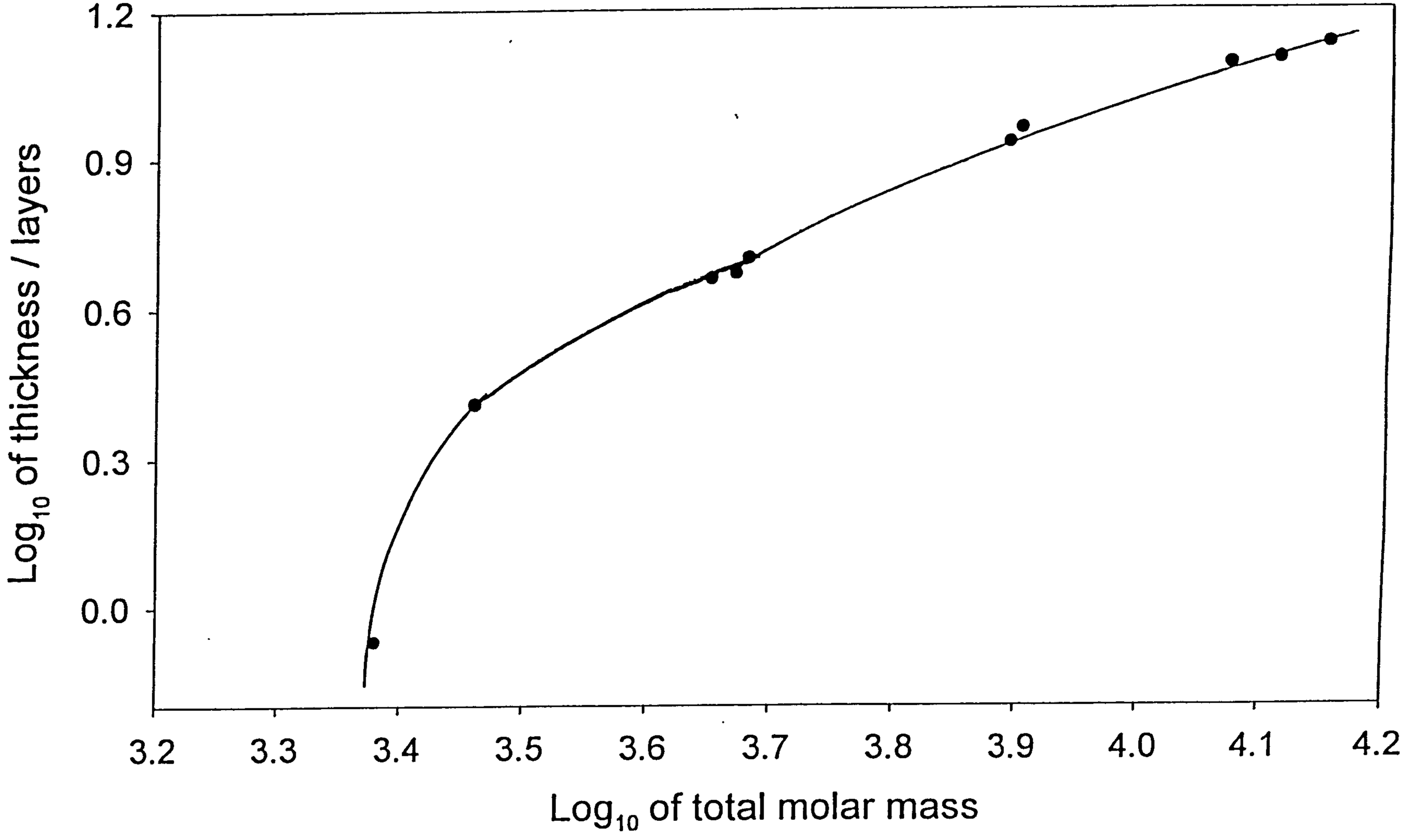


*Figure 7.15 presents the calculated thickness data determined using SCF model, for the same series of Pluronic copolymers used in this study, as a function $Log_{10}$ of the total polymer molar mass.*

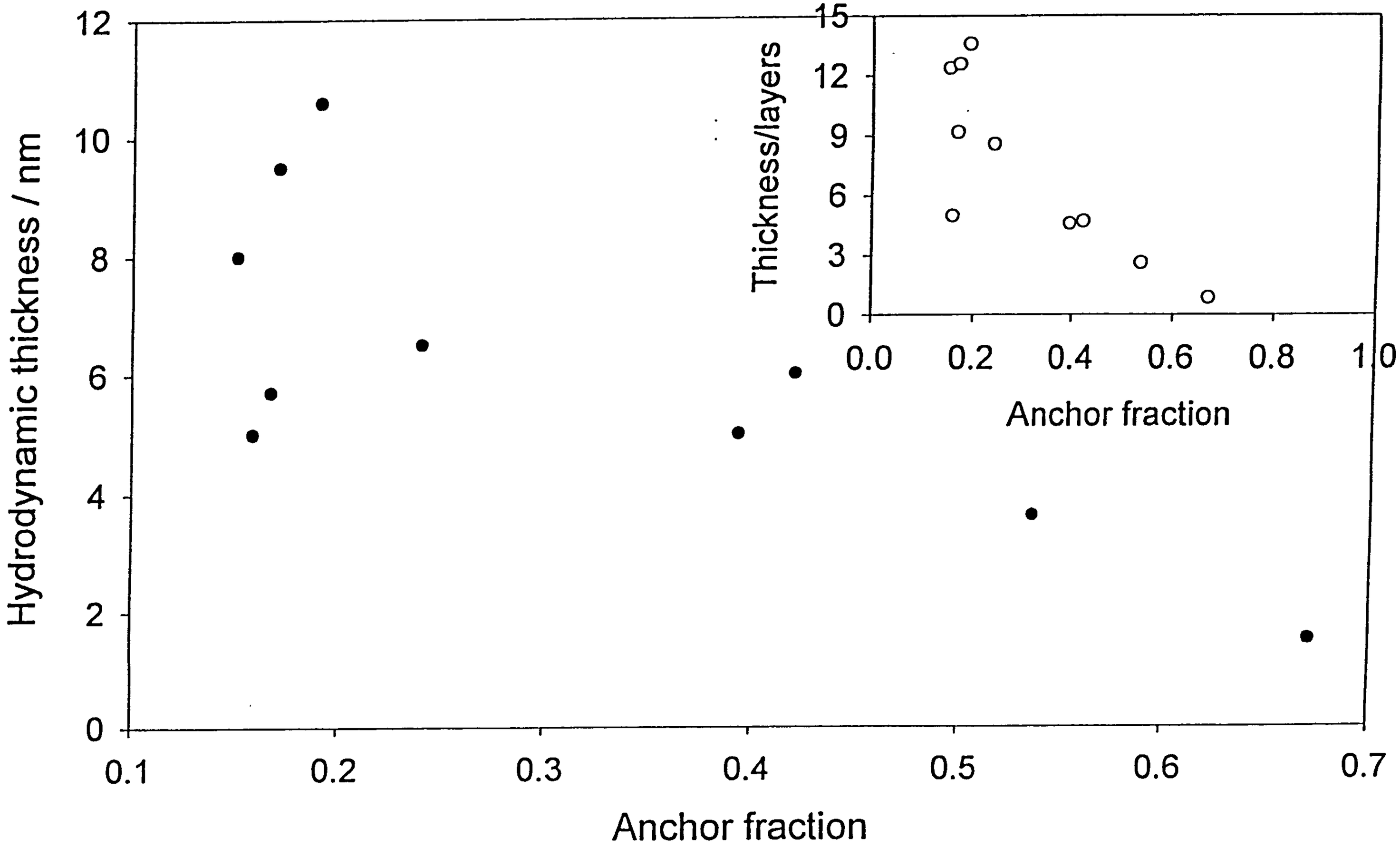


***Figure 7.16 presents the hydrodynamic layer thickness of the Pluronics adsorbed on polystyrene latex as a function of the anchor fraction, $\nu_A$: ●, our experimental data and* o*, calculated data determined using SCF model.***

with increasing the measured thickness was observed and shows a good agreement between the measured data and the theoretical predictions.

#### 7.3.2.2. PEO-PBO Block Copolymers:

Figure 7.17(b) presents the adsorbed layer thickness for the same set of PEO-PBO block copolymers used in this study calculated using the SCF model[9,12] as a function of the measured hydrodynamic thickness of the polymer adsorbed layer. With the exception of polymers $E_{144}B_{27}$ and $E_{100}B_{15}E_{100}$ (where these two polymers show a standard deviation of ± 2.0) an approximately linear dependence of these two adsorption parameters is observed. The data are found to be in a good agreement with those observed for the PEO-PPO block copolymers adsorbed on polystyrene latices (*c.f.* Figure 7.17(a)).

### 7.3.3. Dependence of Hydrodynamic Thickness on the Adsorbed Amount

Figure 7.18(a) compares the measured hydrodynamic thickness of the polymer adsorbed layer, as a function of the measured adsorbed amount, for the Pluronic copolymers (•) with those determined for PEO homopolymers. An approximate linear increase in the hydrodynamic layer thickness with adsorbed amount has been observed for both, PEO homopolymers and the copolymers. This shows a strong interdependence of the two adsorption parameters i.e. $\delta_H$ and $\Gamma_{max}$. Cohen-Stuart *et al.*[8] have determined for the PEO homopolymers adsorbed on polystyrene latex, that initially, a very low adsorbed layer thickness was observed up to a certain level (so-called threshold level) of the adsorbed amount, afterwards, a deep increase in $\delta_H$ with a very high rate was shown in the layer thickness. Our experimental data determined for the triblock copolymers was assumed to be investigated at levels higher than the threshold point, hence, an approximate linearity between $\delta_H$ and $\Gamma_{max}$ was observed. Irrespective of the adsorbed amount, the measured hydrodynamic thickness was always observed to be significantly higher (with a rapid increase) for the homopolymers than the copolymers of corresponding adsorbed amounts. This behaviour clearly shows that for the same set of $\Gamma_{max.}$ values, higher $\delta_H$ was obtained for the PEO homopolymers

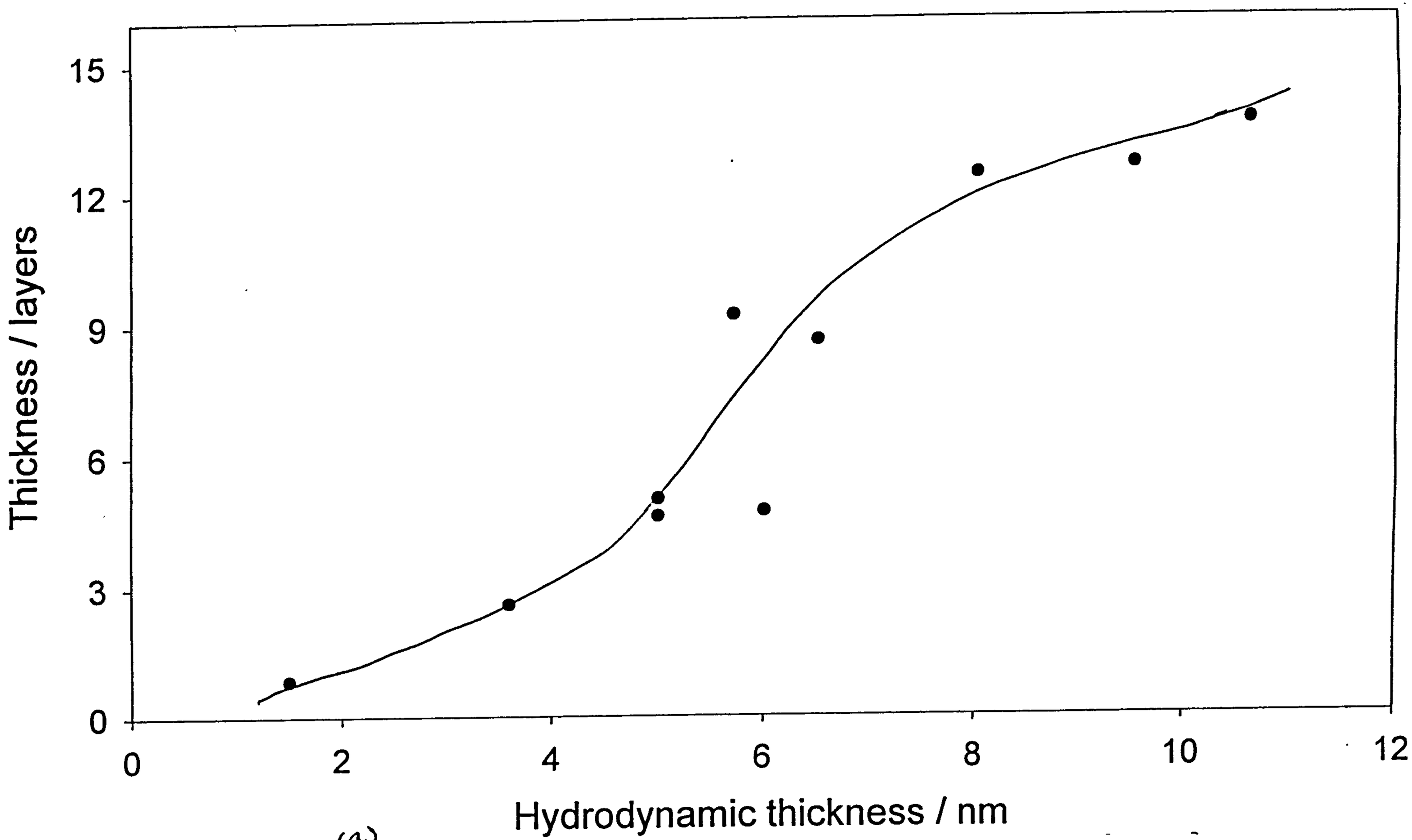


*Figure 7.17 (a) presents the adsorbed layer thickness data for the block copolymers adsorbed on polystyrene latex determined using SCF model as a function of the measured hydrodynamic layer thickness: (a) PEO-PPO block copolymers.*

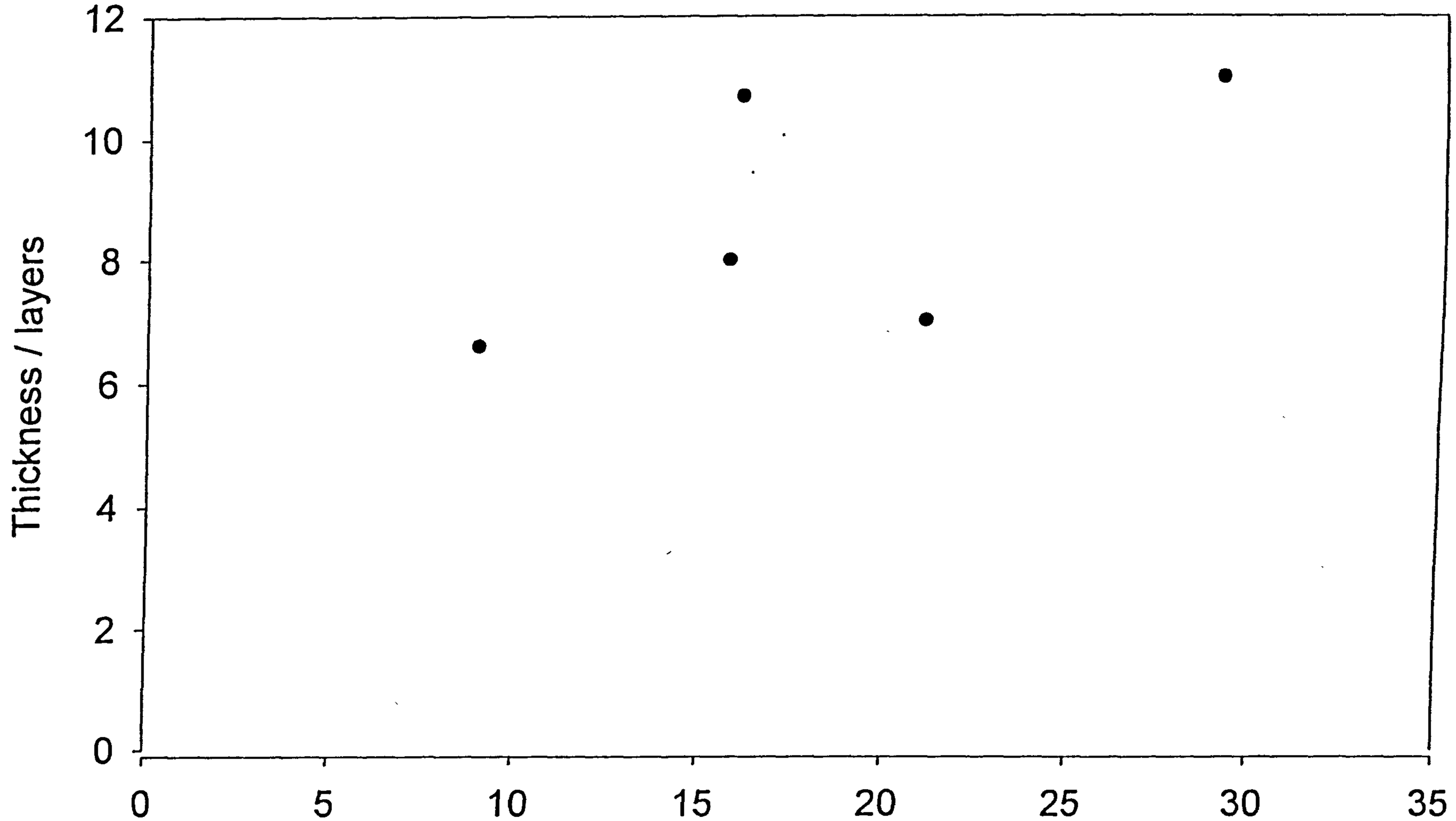


Figure 7.17 (b) presents the adsorbed layer thickness data for the block copolymers adsorbed on polystyrene latex determined using SCF model as a function of the measured hydrodynamic layer thickness: PEO-PBO block copolymers.

than that observed for the copolymers. This behaviour again emphasises that the polymer architecture has a strong influence over the adsorbed layer structure. A given adsorbed amount may be achieved using a Pluronic of much lower molar mass than that needed when using PEO homopolymer. However, for the case of PEO-PBO block copolymers studied the interdependence of these adsorption parameters ($\delta_{II}$ and $\Gamma_{max}$) is observed to be relatively complicated and can be attributed to the different polymer architectures.

The dependence of measured hydrodynamic thickness of the adsorbed polymer layer of the PEO-PBO block copolymers on the adsorbed amount is shown in Figure 7.18(b). An approximately linear increase in the $\delta_{II}$ with an increase in the $\Gamma_{max}$ (at relatively higher rate for these copolymers than that observed for the PEO-PPO copolymers adsorbed on polystyrene latices (*c.f.* Figure 7.18(a))) has been observed. An exception has been observed for the smallest diblock copolymer, $E_{100}B_{15}$, which forms reasonably thin polymer adsorbed layer, hence lower hydrodynamic layer thickness, which may be attributed to the formation of relatively smaller loops and tails by this polymer. Overall, the trends in the pattern of the data determined for the PEO-PBO block copolymers are in a good agreement with those observed for the PEO-PPO copolymers (*c.f.* Figure 7.18(a)).

## 7.4. Conclusion

Under good solvency conditions ABA type triblock copolymers are expected to adsorb onto hydrophobic polystyrene latex surfaces via hydrophobic-hydrophobic interactions of the PPO/PBO anchor block and the substrate surface. The hydrophobic blocks are expected to be preferentially attached to the hydrophobic surface in trains and small loops. The Block copolymers are observed to adsorb at the higher levels than the PEO homopolymers of the corresponding molar masses.

In general, a comparison of the adsorption plateau level values and the layer thickness data shows that the adsorbed amounts of polymers strongly depend on: (I) total polymer molar mass, (II) the hydrophobic (PPO, PBO) block molar mass and/or the relative *hydrophobic to hydrophilic* blocks sizes, (III) the polymer architecture and (IV) the polymer-surface interactions (this is discussed later in the silica section). The

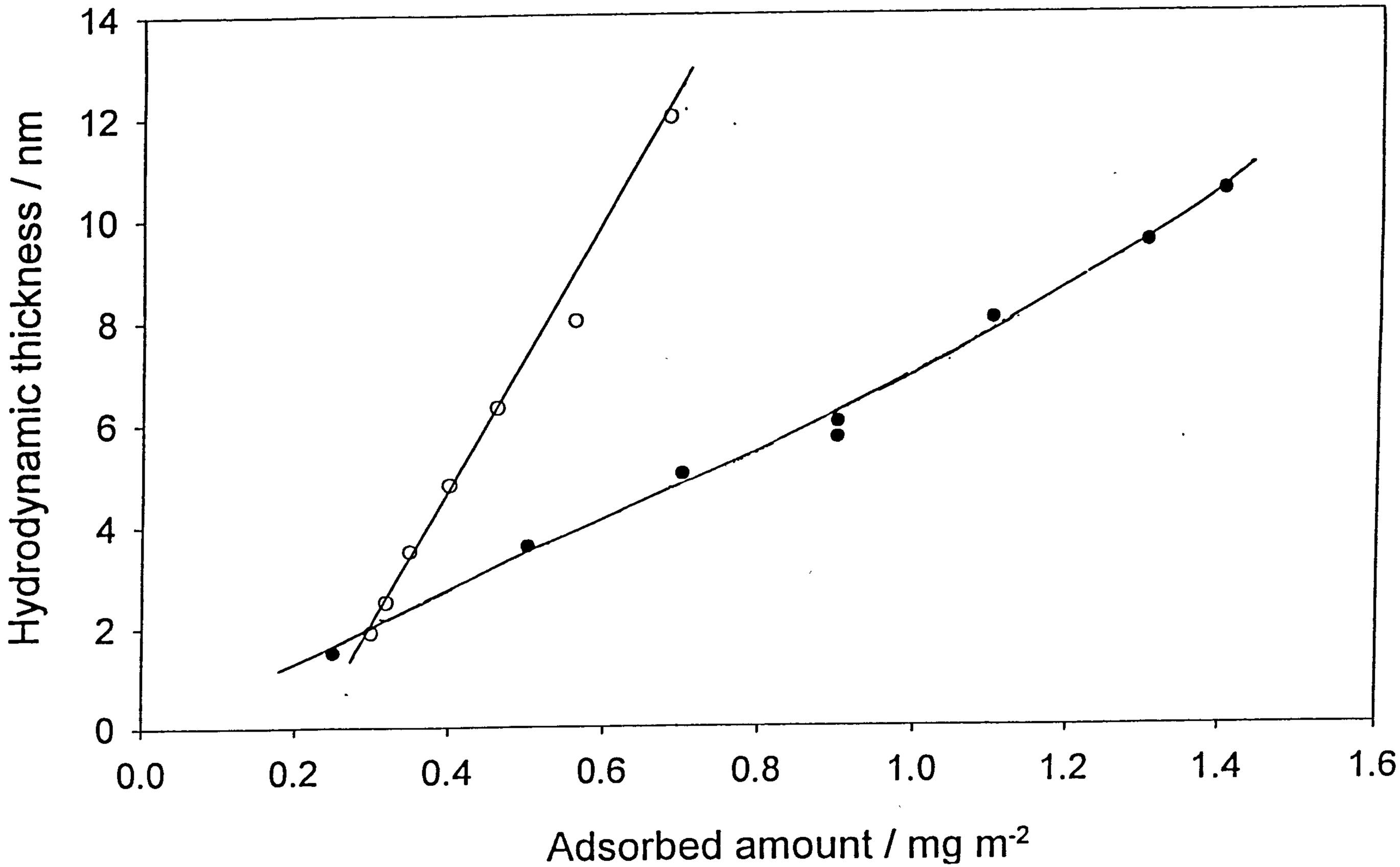


***Figure 7.18*** *(a) presents the measured hydrodynamic thickness of the polymer adsorbed layer for the polymers adsorbed on polystyrene latex as a function of the measured adsorbed amount,* $\Gamma$*;* o, *PEO homopolymers and* ●, *Pluronic copolymers.*

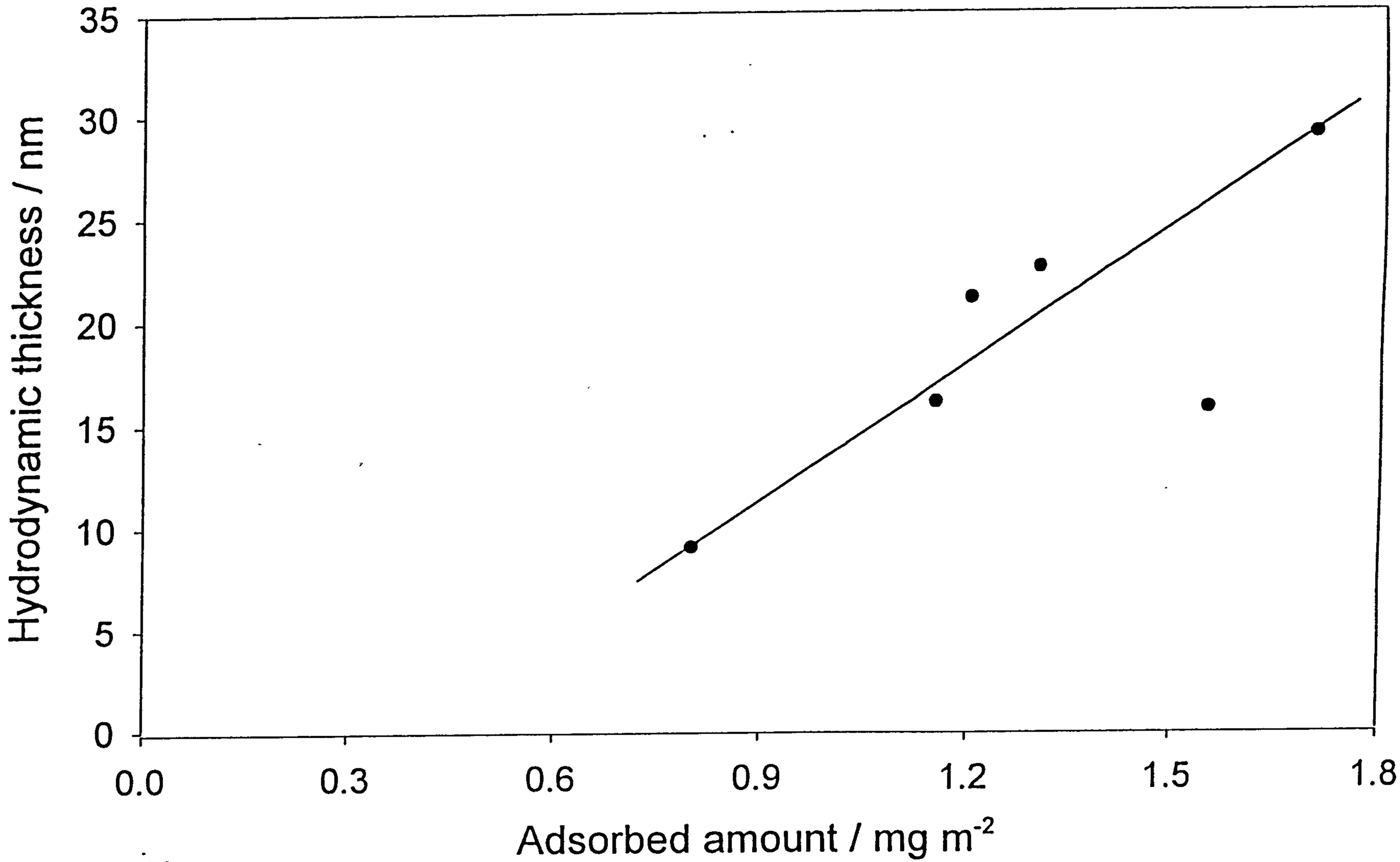


Figure 7.18 (b) presents the measured hydrodynamic thickness of the polymer adsorbed layer for the polymers adsorbed on polystyrene latex as a function of the measured adsorbed amount, Γ; ⁞PEO-PBO block copolymers.

dependence of adsorbed amount on the total polymer molar mass is stronger for low molar mass highly hydrophobic triblock copolymers which, becomes weaker on increasing the total polymer molar mass and/or increasing the hydrophilic nature (decreasing hydrophobicity, by addding more and more PEO blocks to the chain) of the samples.

Baker *et al.*[1] and Schroen *et al.*[18] have also determined the influence of polymer composition on the adsorbed amount and the adsorption conformation for the triblock copolymers on the polystyrene latex substrate. They assumed that the PPO block adsorb onto the hydrophobic latex surface predominantly as trains and small loops, whilst, the hydrophilic PEO blocks stretch out into the solvent in loops and/or tails.

The hydrodynamic thickness of the adsorbed layer was also observed to be strongly influenced by (I) total polymer molar mass (II) PEO block size (and weakly by the PPO block size) (III) the polymer-surface interactions. The size of PEO blocks (or Rg) is roughly a measure of the adsorbed layer thickness and this may be due to the existence of PEO blocks in long loops and/or tails extending out into the bulk solution.

The adsorption parameters observed for the PEO-PPO block copolymers were found to be strongly dependent on the anchor fraction following the trends suggested by SCF theory passing through the maximum at $\nu_A \sim 0.2$ At a very low anchor fraction the system will behave like that of the PEO homopolymer, whilst, at high $\nu_A$ values the surface seems to be saturated with the polymer segments hence a very low adsorbed amount is obtained at the two extreme values of the anchor fraction.[19,20]

Overall, our data presented were in a good agreement (within the limits of experimental errors) with both the theoretically predicted and the limited experimentally determined data available in the literature.[15,21]

# References


[1] Baker, J. A., and Berg, J. C., *Langmuir* 1988, 4, 1055.

[2] Alexandridis, P., Holzwarth, J. F., and Hatton, T. A., *Macromolecules,* 1994, 27, 2414.

[3] Alexandridis, P., and Halton, T. A., *Colloids and Surfaces A: Physicochemical and Engineering Aspects* 1995, 96, 1

[4] Wanka, G., Hoffmann, H., and Ulbricht, W., *Macromolecules*, 1994, 27, 4145.

[5] Mallagh, L. M., Ph.D. Thesis, Bristol, 1989.

[6] Koopal, L. K., *J. Colloid Surf. Sci.* 1981, 83, 116.

[7] Tadros, Th. F.and Vincent, B. *J. Phys. Chem.* 1980, 84, 1575

[8] Cohen-Staurt, M. A., Waajen, F. W. H., Cosgrove, T., Vincent, B. and Crowley, T. L., *Macromolecules*, 1984, 17, 1825.

[9] Fleer, G. J., Cohen-Stuart, M. A., Scheutjens, J. M. H. M, Cosgrove, T. and Vincent, B. "Polymers at Interfaces" 1st Ed., London: Chapman and Hall, 1993, p 302.

[10] Marques, C. M., Joanny, J. F., and Leibler, L., *Macromolecules*, 1988, 21, 1051.

[11] Guzonas, D., Hair, M. L., and Cosgrove, T., *American Chem. Soc.*, 1992, 20 2777.

[12] Evers, O. A., Scheutjens, J. M. H. M., and Fleer, G.J., *J. Chem. Soc. Faraday Trans.* 1990, 86, 1333.

[13] Wu, D. T., Yokohama, and Setterquist, *Polymer, J.*, 1991, 23, 711.

[14] Orwoll, R. A., *Rubber Chemistry and Technology*, 1977, 50, 451.

[15] Killmann, E., Maier, H., and Baker, J. A., *Colloid Surf.* 1988, 31, 51

[16] Cosgrove, T., Vincent, B., Crowley, T. L., and Cohen-Stuart,M. A., *ACS Symposium Ser.*, 1984, 240, 147.

[17] Kato, T., Nakamura, K., Kawaguchi, M., and Takahashi, A., *Polym. J.*, 1981, 13, 1037

[18] Schroen, C .G. P. H, Cohen-Stuart, M. A., van der voort Maarschalk, K., van der Padt, A., and van't Riet, K., *Langmuir*, 1995, 11, 3068.

[19] Killmann, E., Fulka, C., and Reiner, M., *Chem. Soc. Faraday Trans.* 1990, 86, 1389.

[20] Kayes, J. B., and Rawlins, D. A. *Colloid Polym. Sci.* 1979, 257, 622.

[21] Baker, J. A., Pearson, R. A., and Berg, J. C., *Langmuir* 1989, 5, 339.

# Chapter 8

# *ADSORPTION OF POLYMERS ONTO SILICA*

## 8.1. Introduction

This chapter gives the results and discussion for the adsorption data determined for the PEO homopolymers, the PEO-PPO-PEO (Pluronics) and the PEO-PBO block copolymers (listed in Tables 4.1-4.3) at the silica-water interface. The measurements and analysis of the data were performed in the same manner as described in the Sections 4.3.1 and 4.3.2. The initial data obtained for the adsorption isotherms and that for the layer thickness were utilised for further analysis and understanding of the adsorption behaviour of these copolymers on the hydrophilic silica surface. The adsorbed amount was determined from the plateau levels as a function of polymer equilibrium concentration. The hydrodynamic thickness was measured from the decrease in the diffusion coefficient of the particles using the Stokes-Einstein equation (Equation 4.3). Polymer solution concentrations corresponding to the plateau level of the adsorption isotherms were selected for the PCS measurements. A strong influence of polymer-surface interaction was anticipated.

## 8.2. Adsorbed Amount

### 8.2.1. Adsorption Isotherms

The adsorption isotherms measured for a series of PEO homopolymers, PEO-PBO diblock and triblock copolymers, and the PEO-PPO-PEO triblock copolymers are presented in Figures 8.1-8.6, where the copolymers are arranged in a similar manner as described in Section 7.2.1. A rapid increase in the level of adsorption was observed at very low copolymer concentrations followed by a gradual levelling off until the so-called pseudo-plateau level is reached; similar trends to those described in Section 7.2.1 were observed. In general, for the case of copolymers a strong dependence of adsorbed

amount on the total polymer molar mass and the variable block mass is evident in the data. The adsorbed amounts presented in this study are about 2-3 times and 5-6 times respectively *lower* than those measured for the same sets of homopolymers and the block copolymers adsorbed on the hydrophobic polystyrene latex substrate, as reported in Section 7.2.1. This lower level of adsorption for the same set of copolymers suggests a strong influence of the nature of the adsorption surface *i.e.* surface-polymer interaction parameters.

We estimate that with the exception of sample L62 each adsorption isotherm in this work determined for the Pluronic copolymers was obtained below the CMC of the test copolymer (*see* Table 4.2). In Section 7.2.1 of this thesis we speculated that this step may be due in some way to high polydispersity of the sample (*see* Table 4.2) and/or may be due to exceeding the critical micellization concentration (CMC)[1] of the polymer. Also, we can not rule out bilayer formation and/or some other surface complexation.

Figure 8.1 shows the adsorption isotherms for the 10K, 18.6K, 56K, and the 94K PEO homopolymers (listed in Table 4.1) as a function of polymer equilibrium concentration. The data present an increase in the level of adsorption isotherms followed by levelling off until the so-called plateau level is reached. The adsorption data are presented in Table 8. 1. The amount adsorbed is observed to

Table 8. 1: experimental data; adsorbed amounts and $\delta_{II}$ for the PEO homopolymers adsorbed onto silica.

| Polymer | 10K | 18.6K | 37.4K | 56K | 94K | 114K |
|---|---|---|---|---|---|---|
| $M_{wPEO}$ | 10,000 | 18,600 | 37,400 | 56,000 | 93,750 | 114,000 |
| $\Gamma/\pm 1.1\%/(mg\ m^{-2})$ | 0.10 | 0.11 | N/A | 0.13 | 0.14 | 0.17 |
| $\delta_H/\pm 1.1\%/nm$ | 1.0 | 3.0 | 6.0 | 10.0 | 13.0 | 20.0 |

increase with increasing the total polymer molar mass. However, this effect becomes weaker for the case of higher molar mass polymers which is expected in a good

solvent.[2,3]

Figure 8.2 shows the adsorption isotherms as a function of polymer equilibrium concentration for $E_{100}B_{15}$, $E_{200}B_{15}$, c-$E_{200}B_{15}$ and $E_{100}B_{15}E_{100}$ copolymers adsorbed from aqueous solution onto a silica surface. Unexpectedly, all the copolymers (except c-$E_{200}B_{15}$, which, shows a smooth and a high affinity adsorption isotherm) deviate from the behaviour observed on polystyrene latex (*c.f.* Figure 7.2). A constant increase in the adsorbed amount is found with increasing an equilibrium concentration of the $E_{100}B_{15}$ and $E_{200}B_{15}$ polymers without reaching plateau level. This may be attributed to complex or multilayer formation. It is also observed that the triblock $E_{100}B_{15}E_{100}$ shows a smooth adsorption isotherm in the beginning until a polymer equilibrium concentration of approximately 450 ppm is reached. Afterwards, a rapid increase in the adsorbed followed by levelling off the plateau level is observed. This strongly suggests of bilayer formation of some kind.

The adsorption isotherms for c-$E_{144}B_{27}$ and $E_{72}B_{27}E_{72}$ copolymers adsorbed at the aqueous-silica interface are shown as a function of polymer equilibrium concentration in Figure 8.3. Similar trends in the pattern to those found for the same set of the polymers adsorbed on polystyrene latex (*c.f.* Figure 7.3) have been observed. As expected[4] the diblock copolymer, $E_{144}B_{27}$, shows a relatively higher level of adsorption than that observed for the triblock $E_{72}B_{27}E_{72}$ having the same total polymer molar mass but different copolymer architecture. The data determined for the adsorption of these polymers are presented in Table 8.2. Malmsten *et al.*[7] have presented data obtained for the adsorption of $EO_{99}$-$PO_{65}$-$EO_{99}$ triblock copolymers adsorbed on silica. Their findings for the adsorbed amount (0.3 mg $m^{-2}$ ) and hydrodynamic thickness (determined by dynamic light scattering corresponded to the radius of gyration of the PEO block) were the same for both copolymers, which is contrary to our findings.

The comparison between the data presented in the Figures 8.2 and 8.3 show that the higher anchor fraction polymers ($E_{144}B_{27}$ and $E_{72}B_{27}E_{72}$) adsorb at relatively higher levels than those having lower anchor fraction (*i.e.* $E_{100}B_{15}$, $E_{200}B_{15}$, c-$E_{200}B_{15}$ and $E_{100}B_{15}E_{100}$). Overall, a lower level of adsorption is observed for the same set of copolymers

Table 8. 2: experimental and theoretical data; adsorbed amounts, and adsorbed layer thicknesses for the PEO-PBO block copolymers adsorbed onto silica.

| Polymer | $M_w$ | $\Gamma/\pm 1.1\%$ /(mg $m^{-2}$) | $\delta_H/\pm 1.1\%$/ nm | Adsorbed amount/$\theta$ | $\delta$/layers |
|---|---|---|---|---|---|
| $E_{144}B_{27}$ | 8,280 | 0.55 | 17 | 1.5 | 4.5 |
| $E_{72}B_{27}E_{72}$ | 8,280 | 0.5 | 9.6 | 2.1 | 6.0 |
| $E_{100}B_{15}$ | 5,480 | 0.33 | 17 | 1.27 | 3.0 |
| $E_{200}B_{15}$ | 9,880 | 0.33 | 22 | 1.4 | 5.0 |
| c-$E_{200}B_{15}$ | 9,880 | 0.12 | 10 | N/A | N/A |
| $E_{100}B_{15}E_{100}$ | 9,880 | 0.08 | 10 | 1.4 | 4.0 |

on silica than on polystyrene latex. This is similar to the pattern observed in the adsorption behaviour of the other polymers (PEO homopolymers, Pluronic and R. Pluronic copolymers) when adsorbed on these two different surfaces. This difference in the adsorption behaviour of these polymers can be attributed to stronger polymer-particle interaction.

Figure 8.4 shows that the L62 and L64 polymers having low total polymer and PEO block molar mass (hence highly hydrophobic in nature) give low affinity behaviour at low polymer concentration (*c.f.* Figure 7.4), and overall have a very low $\Gamma_{max}$. Killmann *et al.*[5] have also found similar trends in the adsorption isotherms determined for the Pluronic copolymers adsorbed at the silica/$CCl_4$ and silica/$CHCl_3$ interfaces. This behaviour may be characteristic of low total polymer molar mass and/or due to a flat adsorbed configuration of both the PPO and PEO blocks. However, relatively high molar mass F38 and F68 Pluronics (as anticipated) show high affinity adsorption isotherms and higher plateau levels.

It can clearly be seen in Figure 8.5 and Figure 8.6 that the Pluronics P75 and P85 having approximately 50% PEO-PPO blocks give very high affinity adsorption isotherms, whilst, high PEO content Pluronics (F87, F88, F98 and F108) have low affinity isotherms. This behaviour can be explained by the hydrophilic nature of the high total molar mass polymers with high PEO content which makes the samples more soluble in the bulk solution and hence less attractive to the particle surface. Furthermore, these low affinity adsorption isotherms for the higher molar mass polymers may also be due to the polydispersity of the samples in both the total polymer molar mass and the relative block masses as the affinity changes with molar indices ($M_w/M_n$) of the polymers. In particular, Pluronic F108 has a relatively high $M_w/M_n \sim 1.2$. Schroen *et al.*[6] have shown that for PPO-PEO block copolymers adsorbed on the hydrophilic surface, both the PPO and PEO blocks interact with the surface through hydrogen bonds and are firmly attached to the surface. This gives rise to a flat pancake configuration of the adsorbed layers, hence very low adsorbed amounts and thin adsorbed layers were observed.

### 8.2.2. Molar Mass Dependence of Adsorbed Amount

Figure 8.7 shows the dependence of the adsorbed amount of the Pluronics (derived from the so-called pseudo-plateau regions in Figures 8.4-8.6) on the logarithm of the total polymer molar mass. An increase in the adsorbed amount with increasing total polymer molar mass of the samples was observed from the data. (*see* Table 8.3). Malmsten *et al.*[7] have shown that the triblock copolymers adsorb on silica at a very low level and have further shown that that both the adsorbed amount and the adsorbed layer thickness for these systems are independent of the total polymer molar mass (up to 15000). However, we found a strong dependence of the adsorbed amount on the total polymer molar mass. The comparison between the adsorption behaviour of the same series of triblock copolymers for silica, (●) and for polystyrene latex, (○, ▲), (Section 7.2) show overall lower $\Gamma_{max}$ for the hydrophilic silica than the polystyrene latex substrate. Two sets of data, (○, ▲), on polystyrene latex were distinguished by having different PPO:PEO block ratios. It can be seen from the trends observed for the copolymers with higher PPO content, (○), being more hydrophobic in nature interact more with the hydrophobic latex surface than those having lower PPO:PEO ratio. This

behaviour of the polymers gives rise to the higher adsorbed amounts for the higher PPO

Table 8.3: presents the experimental and theoretical data; adsorbed amounts and adsorbed layer thicknesses for the PEO-PPO block copolymers adsorbed onto silica.

| Pluronics | M | $\nu_A$ | $\Gamma/\pm1.0\%$ /(mg $m^{-2}$) | $\delta_H/\pm1.0\%$ /nm | Adsorbed Amount/θ | δ / layers |
|---|---|---|---|---|---|---|
| F38 | 4800 | 0.16 | 0.115 | 1.5 | 1.16 | 3.7 |
| L62 | 2400 | 0.67 | 0.06 | 0.00 | 0.25 | 0.45 |
| L64 | 2900 | 0.54 | 0.07 | 0.6 | 0.74 | 2.3 |
| F68 | 8350 | 0.17 | 0.175 | 1.5 | 1.35 | 5.7 |
| P75 | 4450 | 0.39 | 0.13 | 1.0 | 1.19 | 4.1 |
| P85 | 4650 | 0.42 | 0.135 | 1.0 | 1.23 | 4.3 |
| F87 | 7700 | 0.24 | 0.18 | 1.5 | 1.38 | 6.3 |
| F88 | 11800 | 0.15 | 0.215 | 2.2 | 1.44 | 7.2 |
| F98 | 13000 | 0.17 | 0.235 | 2.4 | 1.48 | 7.8 |
| F108 | 14000 | 0.19 | 0.23 | 3.0 | 1.53 | 9.0 |

(anchor) content, (O) copolymers than those having lower values (▲). However, this effect of PPO:PEO block ratio was not observed by Malmsten *et al.*[7] for Pluronic copolymers (P75, F98 and F127) adsorbed on precipitated silica by ellipsometry. Killmann *et al.*[8] have also presented relatively lower adsorption of PEO homopolymers for the precipitated silica than that for the polystyrene latex, suggesting a flat configuration on the hydrophilic particles. Lucie *et al.*[9] have studied the adsorption of the copolymers on a substrate with a hydrophilic gradient using ellipsometry. For the same set of triblock copolymers they have presented relatively lower adsorbed amounts for the more hydrophilic and the higher adsorbed amounts for the more hydrophobic

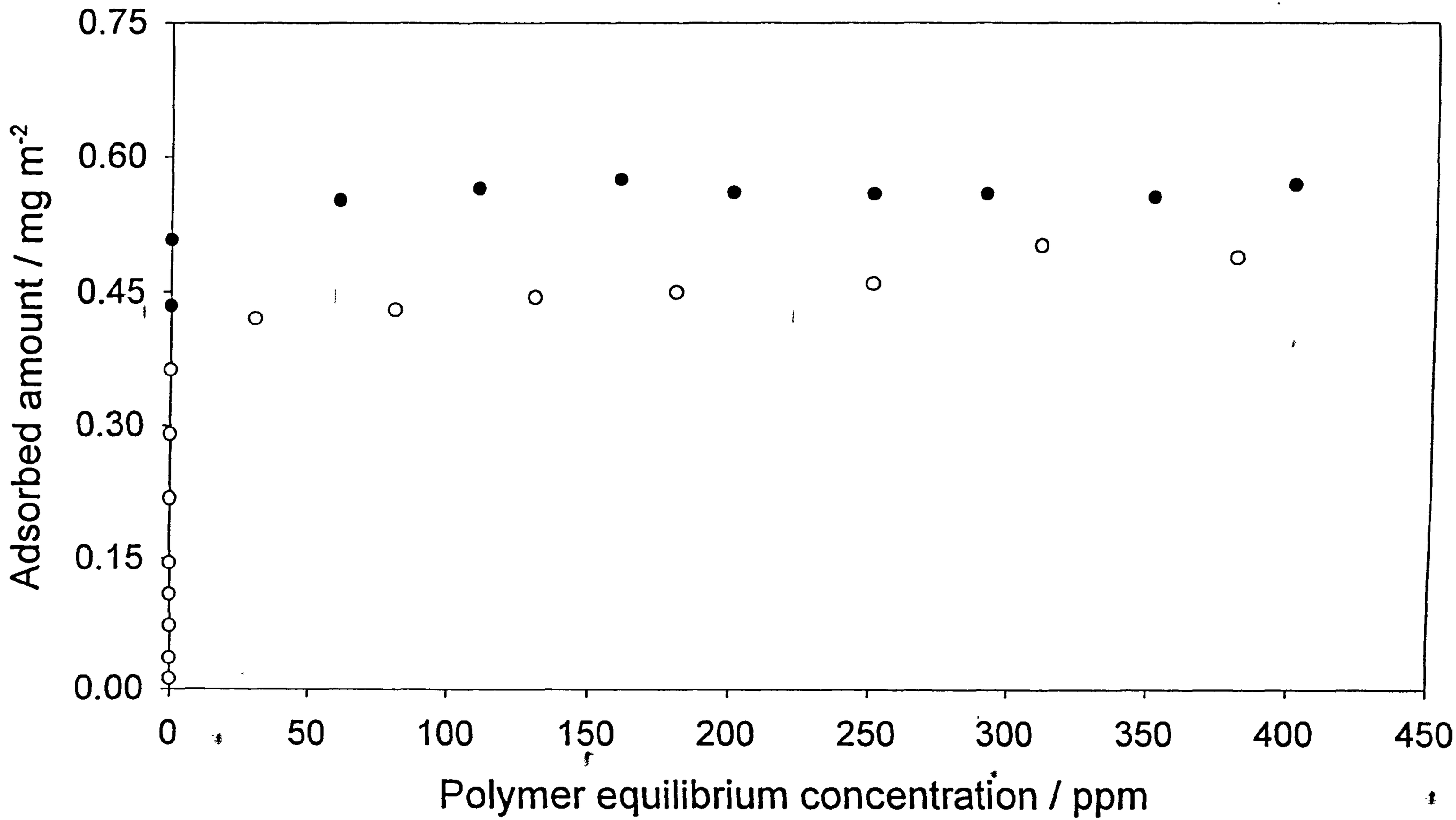


***Figure 8.3 shows the adsorption isotherms for (●) $E_{144}B_{27}$ and (o) $E_{72}B_{27}E_{72}$ copolymers adsorbed from aqueous solution onto silica surface as a function of polymer equilibrium concentration.***

surface. Furthermore, they also observed that this effect becomes weaker for the higher total molar mass copolymers having high PEO content and stronger for low molar mass and high anchor fraction polymers. Interaction energies were anticipated to exist in the order of PEO-silica > PEO-latex and PPO-silica < PPO-latex. The balance of these interactions leads to lower adsorbed amounts for the silica systems than the polystyrene latex systems which has already been discussed in Section 7.2. Also observed are concomitant changes in the layer thickness.

Figure 8.8 compares the adsorbed amount of Pluronic copolymers (●) with that of PEO homopolymers (o), as a function of the logarithm of PEO block molar mass. Much lower adsorbed amounts are found for PEO homopolymers than those for the block copolymers. The trends are in qualitative agreement with the pattern determined experimentally for the hydrophobic latex system (see Section 7.2). Killmann *et al.*[8] and Fleer *et al.*[2] have also presented data for the same systems and have shown that these copolymers adsorb on the silica surface at a lower level than on the polystyrene latex surface but at a higher level than that of the PEO homopolymers. The data indicates a rapid increase in the adsorbed amount, $\Gamma_{max}$ for the copolymers with PEO block molar mass and compares to a slower increase for the PEO homopolymers. This suggests a less extended adsorbed configuration of the PEO homopolymers and emphasises the strong influence of the copolymer composition *i.e.* molar masses of both PPO and PEO blocks, over the adsorbed amount. This increase in the adsorbed amount with PEO block molar mass of the block copolymers is steeper for silica than that for the hydrophobic latex system.

Figure 8.9 shows the dependence of the adsorbed amount of PEO-PPO block copolymers on the PEO block mass (buoy fraction) at a fixed hydrophobic PPO block mass (anchor fraction). Two sets of data at two different PPO block sizes show an approximately linear increase in the adsorbed amount with increasing the variable block molar mass. However, this dependence of adsorbed amount on the polymer composition (PPO:PEO block ratio) was strongest for the low molar mass samples (with high PPO contents) and becomes weaker for the high molar mass samples and is stronger for the silica surface than the polystyrene latex systems. Malmsten *et al.*[7] have shown that at low PPO content (0 - 30%), the dependence of the adsorbed amount of the copolymers on PPO block molar mass is weaker and the copolymers behave as

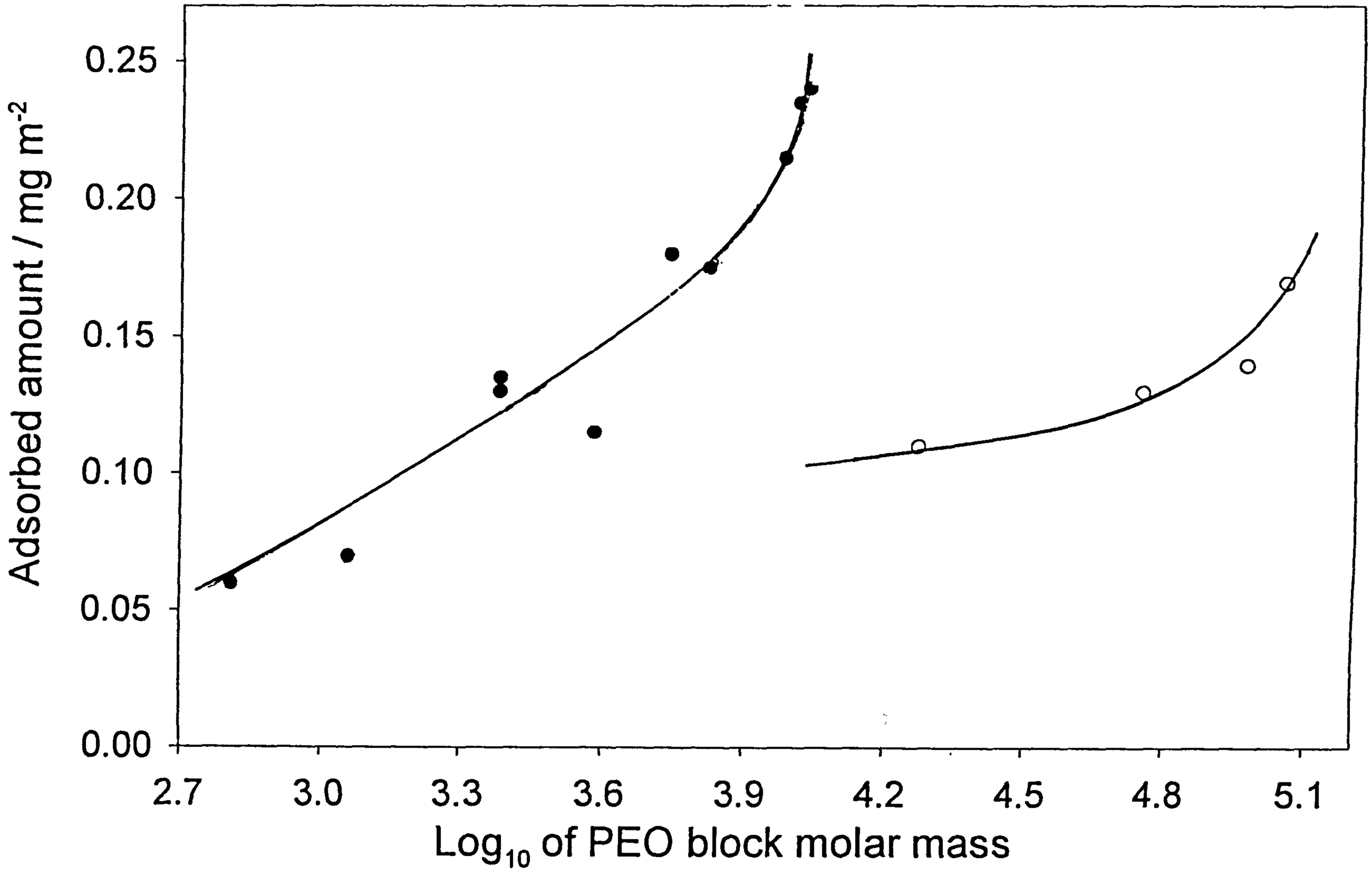


***Figure 8.8 presents the measured adsorbed amount for polymers adsorbed on silica as a function of the $Log_{10}$ of PEO block molar mass:*** o ***PEO homopolymers and*** ● ***PEO-PPO triblock copolymers.***

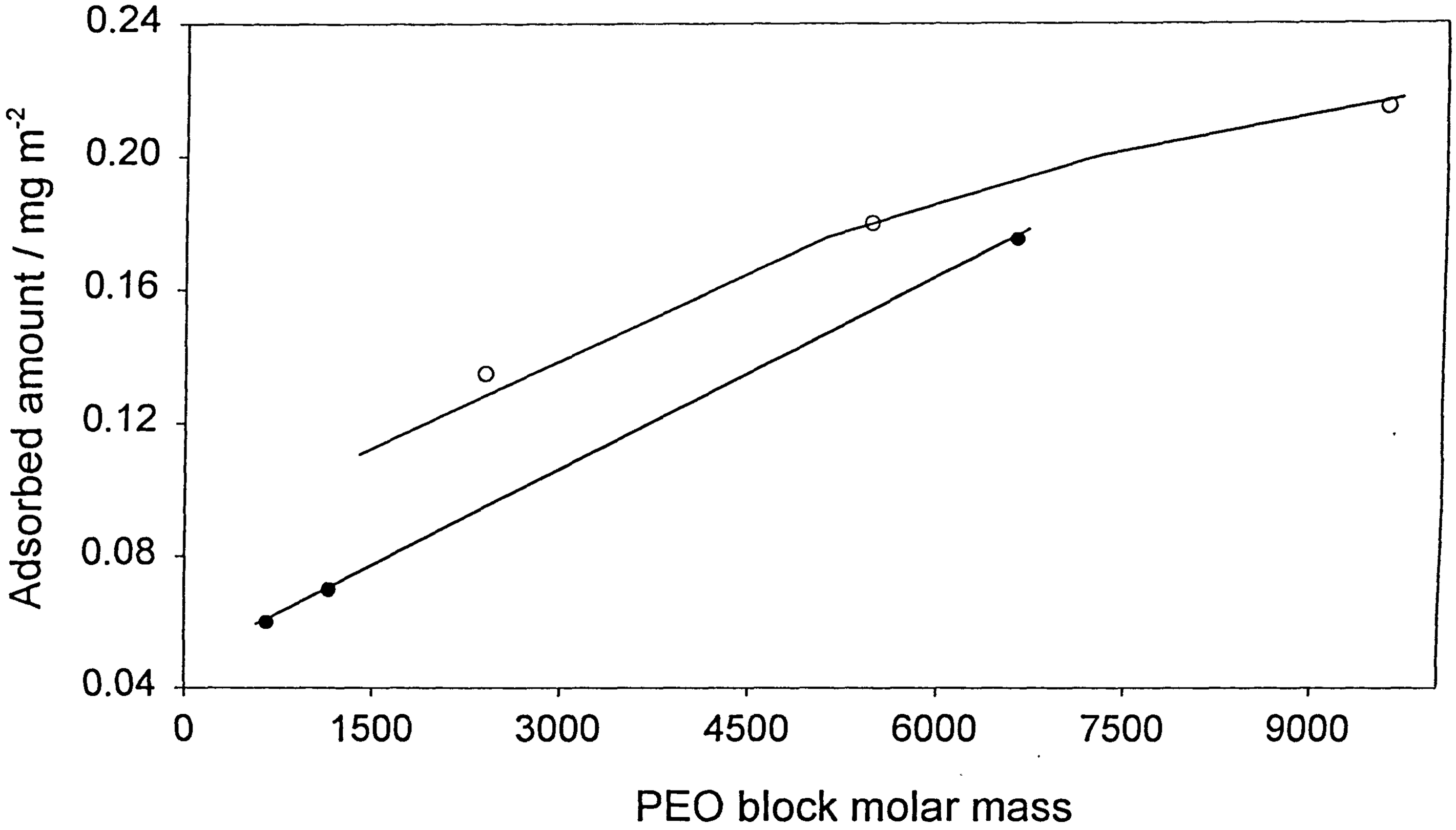


***Figure 8.9 presents the measured adsorbed amount for the PEO-PPO triblock copolymers adsorbed on silica as a function of PEO block molar mass at constant PPO block mass: ● PPO≅1750 and o PPO≅2250.***

homopolymers. Similar trends in the behaviour of the copolymers having high PEO content and high total polymer molar mass have also been observed from this work and are in a good agreement with those predicted theoretically.[2,10,11,12] This indicates that the adsorbed amount depends on both anchor *and* buoy blocks.

## 8.2.3. Theoretical Predictions for Adsorbed Amount

### 8.2.3.1. PEO-PPO-PEO block copolymers

Figure 8.10 shows the dependence of measured adsorbed amount on the anchor fraction, $\nu_A$. The inset figure shows calculated data for the same series of copolymers under study (*see* Table 4.2) using the SCF model described by Fleer, Evers[2] and Cohen-Stuart *et al.*[12] Data clearly show that the adsorption from non-selective solvents leads to a swollen anchor block and more dilute buoy block extending out in the bulk solution. The level of adsorption also depends upon the polymer composition. Our data is in an excellent agreement with those measured experimentally for diblock copolymers investigated in some other systems by Guzonas *et al.*[11] Guzonas *et al.*[11] have used the MJL model described by Marques *et al.*[10] for diblock copolymers and discussed its validity by interpreting data for PEO/polystyrene systems.[13] Wu *et al.*[13] have determined the adsorption of a copolymer of dimethyl-aminoethyl-methacrylate and butyl-methacrylate adsorbed at silica/2-propanol interface. The adsorption of these copolymers was observed to depend strongly on the copolymer composition. The data show a maximum in the curve at $\nu_A \sim 0.2$ indicating a good qualitative agreement with the trends in the pattern predicted by the SCF and the MJL models.

The SCF calculations in each case were performed for polymer solution equilibrium concentrations of 0 to 2000 ppm chosing same set of Flory parameters as used for the reverse Pluronic/silica systems (*see* Section 6.2). In all of these calculations the block monomer number ($N_i$) is the molar mass of each individual block divided by the corresponding molecular mass of that block. The number of adsorbed layers was taken as the square root of number of PEO monomers ($N_B$) present in each sample. Both, experimental and calculated data presented in this figure suggest the transition between buoy and anchor regimes at anchor fraction, $\nu_A \sim 0.15$ and is in good

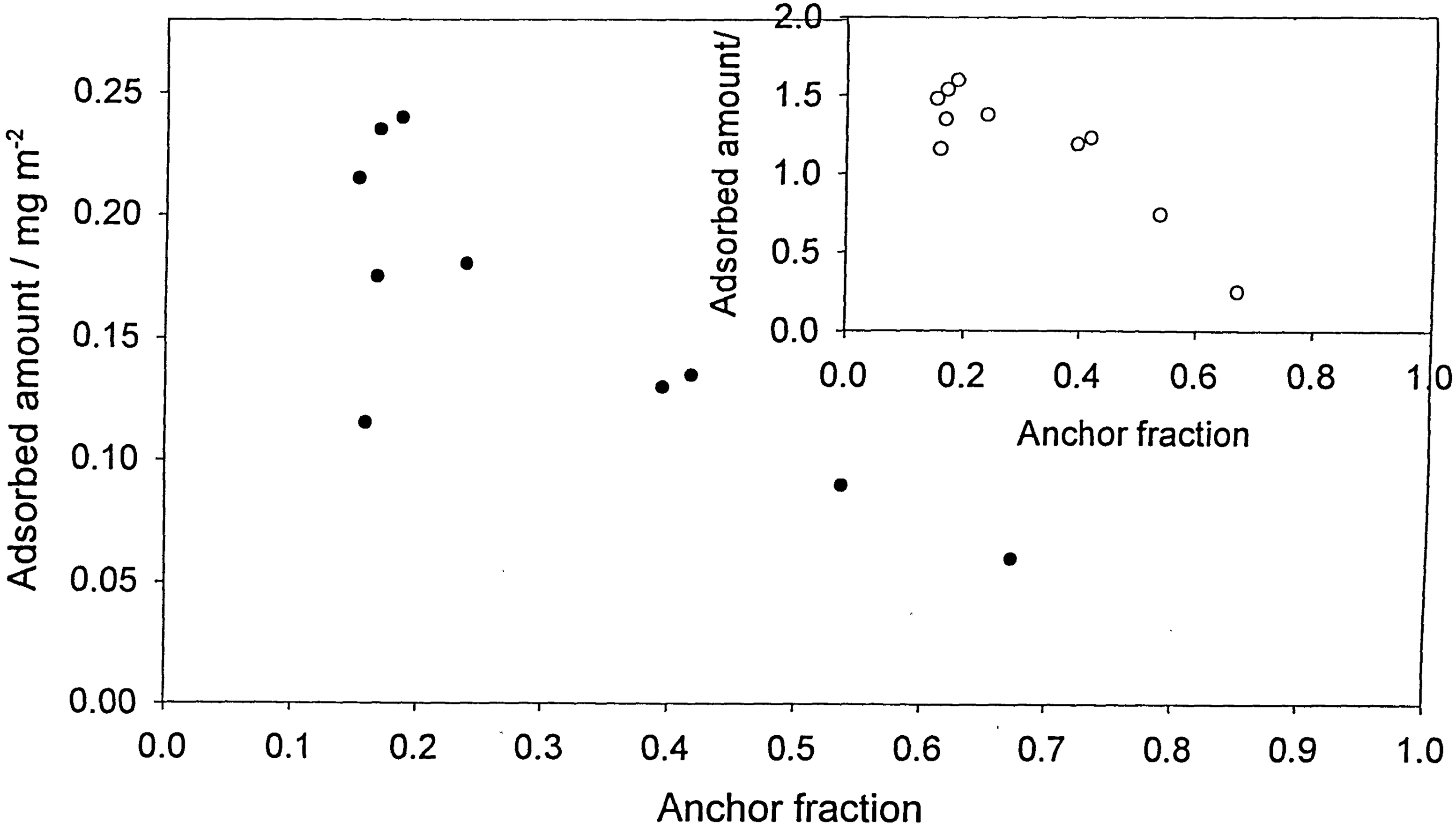


***Figure 8.10 presents the measured adsorbed amount for the PEO-PPO triblock copolymers as a function of the anchor fraction, $\nu_A$: ● our experimental data and o (inset data) calculated using the SCF model.***

agreement with the predictions made by Evers *et al.*[2] As with the data for the polystyrene latex, *see* Figure 7.10, there is an exceptionally good agreement of our experimental data with those calculated. This further justifies the presumed adsorption of both the PPO and PEO blocks on the hydrophilic silica surface.

Figure 8.11 (a) presents the theoretical adsorbed amount, θ, calculated using the SCF model[2,12] for a series of PEO-PPO block copolymers under study, as a function of the measured adsorbed amount. The $\chi$ parameters as explained in (*see* Section 6.2) were used for these calculations. Initially, the data show a rapid increase (for the low molar mass L62 and L64), which afterwards show a low rate linear increase in the calculated adsorbed amount with increasing the experimentally determined adsorbed amount. The data were observed to be in a good qualitative agreement between the theoretically predicted and the experimentally determined data.

### 8.2.3.2. PEO-PBO block copolymers:

The calculations were performed using the mean-field lattice model for polymer adsorption developed by Evers-Scheutjens and Fleer[2,12] using the 0 to 2000 ppm range of polymer solution concentration. In each case the pseudo-plateau level of the adsorption isotherms was presumed to occur at 500 ppm polymer equilibrium concentration. The Flory parameters were taken as follow: $\chi_{BS} = -2$; $\chi_{ES} = -4$; $\chi_{EB} = 2$; $\chi_{EW} = 0.45$; $\chi_{BW} = 2$; and $\chi_{WS} = 0$, where E, B, W and S stand for the ethylene oxide, butylene oxide, water and the surface (silica) respectively. Both monomers and water were taken to occupy one lattice site. Calculated data for the PEO-PBO block copolymers using SCF model is given in Table 8.2.

Figure 8.11 (b) presents the theoretical adsorbed amount, θ, calculated using the SCF model[2,12] as a function of the measured adsorbed amount for a series of PEO-PBO block copolymers listed in Table 4.3 adsorbed at aqueous/silica interface. Overall, an approximately linear increase in θ with the measured adsorbed amount (with the standard error of ± 0.25 for $E_{144}B_{27}$ and $E_{100}B_{15}E_{100}$) has been observed for these polymers.

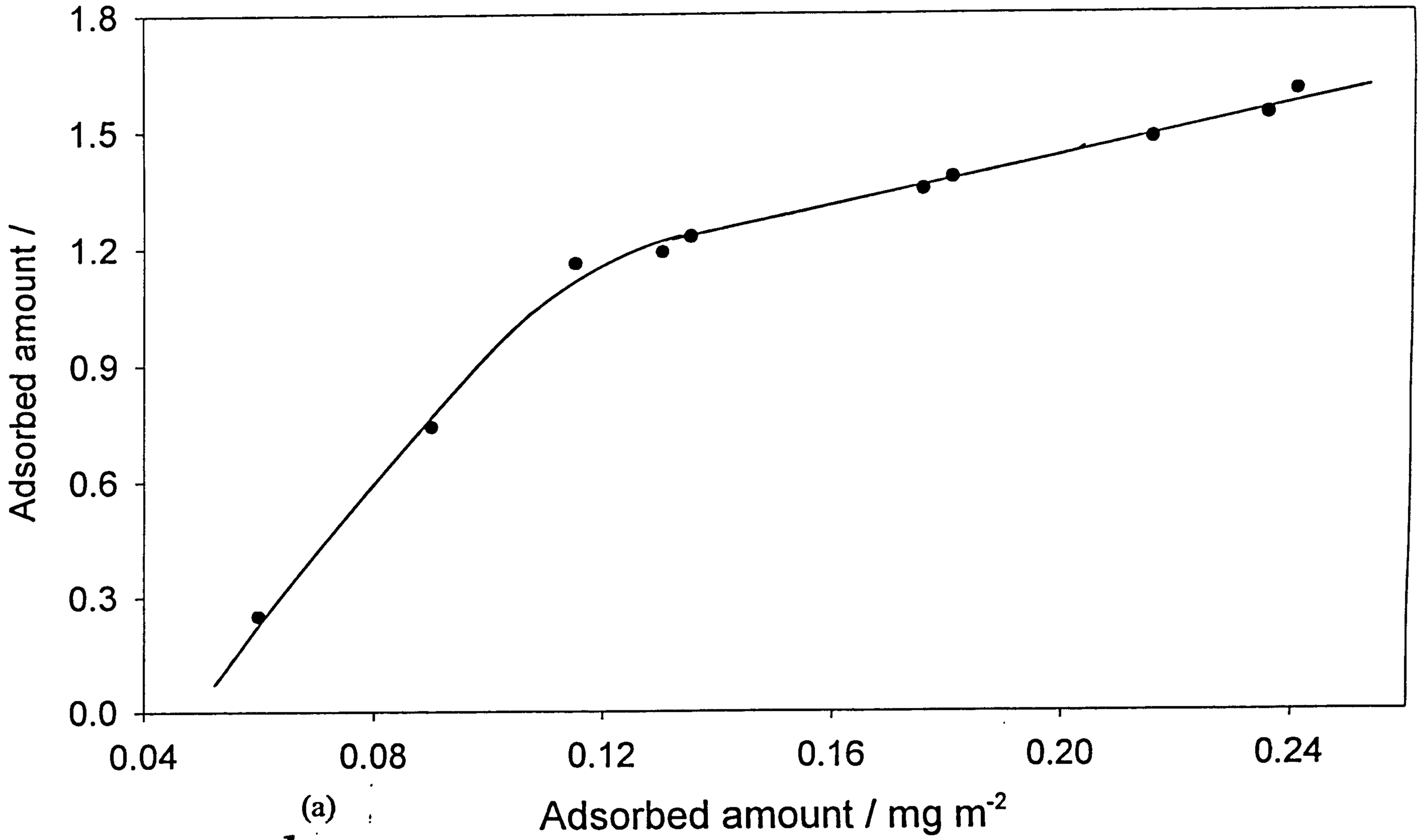


***Figure 8.11 presents the adsorbed amount for the copolymers calculated using the SCF model as a function of the measured adsorbed amount for PEO-PPO copolymers.***

## 8.3. Hydrodynamic Layer Thickness

All the adsorbed layer thickness measurements were performed in a similar manner to those described in Section 4.3.2 using PCS, as a function of the total polymer molar mass at a fixed polymer solution concentration corresponding to the plateau level adsorption of that sample. Very small layer thickness of only few nanometers were observed for PEO-PPO block copolymers on silica. This may be attributed to the low adsorbed amounts, which, reduces the polymer tendency for long loop and long tail formation. However, the PEO homopolymers (may be due to their higher molar masses) and PEO-PBO block copolymers show relatively thicker adsorbed layers ~ 10 nm. Malmsten *et al.*[7] have presented data for two triblock copolymers, $E_{99}P_{65}E_{99}$ and $E_{125}P_{47}E_{125}$ adsorbed onto silica. Their findings show same adsorbed amount (0.36 $mgm^{-2}$) as well as the hydrodynamic layer thickness for the two copolymers. The hydrodynamic thickness determined by dynamic light scattering corresponded to approximately the radius of gyration of the PEO blocks present in the polymer. Table 8.2 presents the measured hydrodynamic thicknesses observed for the PEO-PBO block copolymers in this study. Like the case of adsorption of polymers on polystyrene latex, this study also shows that the $E_{200}B_{15}$ diblock copolymer forms the thickest adsorbed layer in the range, however, the difference in the hydrodynamic layer thicknesses of the heavier and the lighter diblocks is observed to be much smaller for the case of silica than that observed for the polystyrene latices (*c.f.* Chapter 7). The data also show that the triblock $E_{100}B_{15}E_{100}$ forms a layer of comparable adsorbed amount and the hydrodynamic thickness to the cyclic diblock c-$E_{200}B_{15}$ showing lowest adsorption in the range. The data also show the comparable adsorbed layer thicknesses for $E_{144}B_{27}$, $E_{72}B_{27}E_{72}$ and $E_{100}B_{15}$ copolymers. Generally, the adsorbed amounts, rms. and the hydrodynamic thicknesses observed for the triblock $E_{100}B_{15}E_{100}$ and cyclic diblock c-$E_{100}B_{15}$ are all very similar suggesting that the effects of joining the two ends of the triblock polymer to form the diblock only has a small effect on the layer structure.

### 8.3.1. Molar Mass Dependence of Hydrodynamic Layer Thickness

Figure 8.12(a) shows a double logarithmic plot of the hydrodynamic thickness of the polymer adsorbed layer on the total polymer molar mass. The approximately linear behaviour suggests a scaling law of the term $\delta_H \sim M^{\alpha}$ where $\alpha = 1.1 \pm 0.3$ and $0.72 \pm$

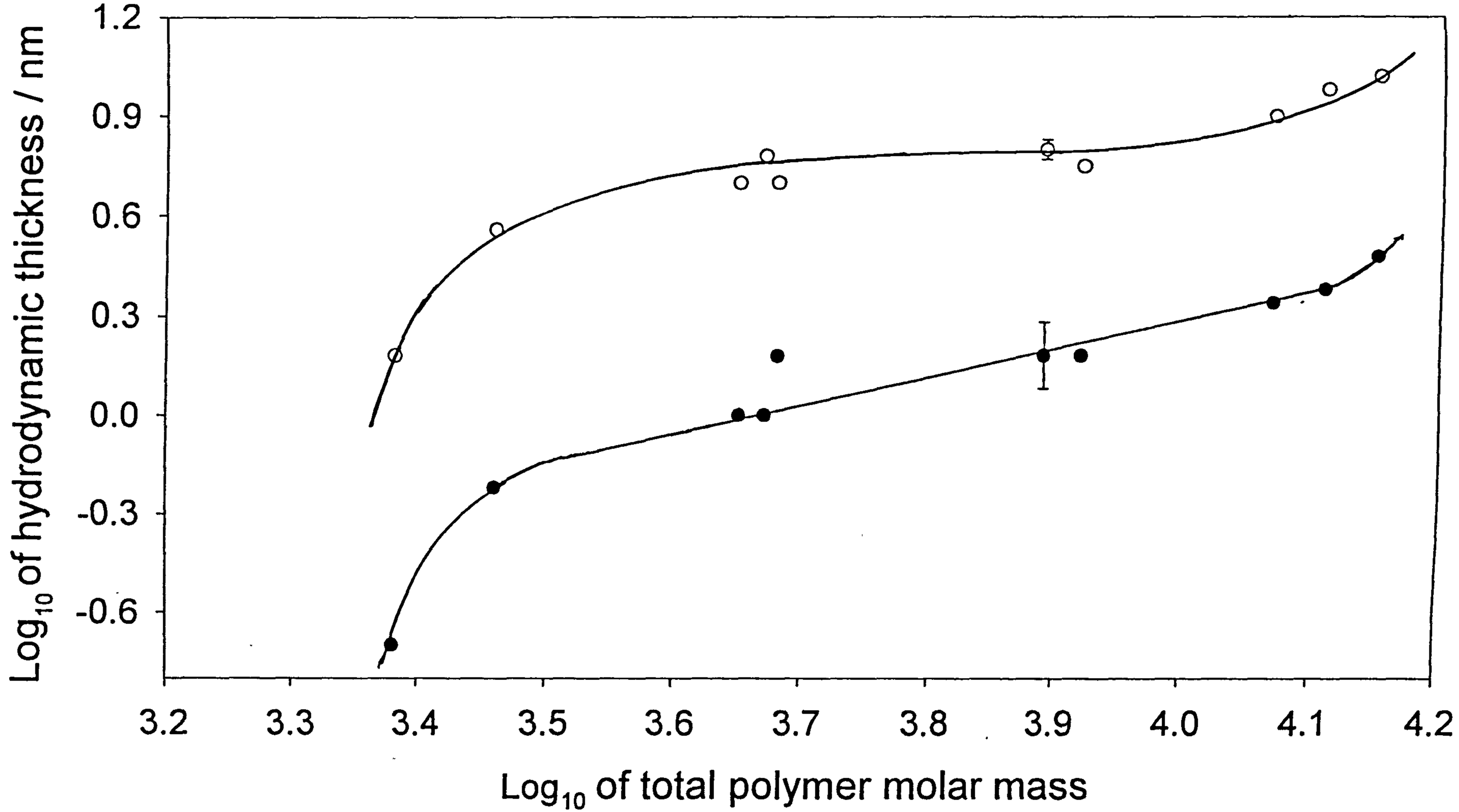


***Figure 8.12 presents the $Log_{10}$ of hydrodynamic thickness of the polymer adsorbed layer as a function of $Log_{10}$ of the total polymer molar mass adsorbed on: ● silica and O polystyrene latex.***

0.2 for PEO homopolymers and Pluronics respectively, adsorbed on silica which are higher (particularly that for PEO homopolymer) than those found in the literature. Kato *et al.*[14] and Cosgrove *et al.*[15] found $\alpha$ to be 0.56 and 0.8 respectively, for PEO homopolymers adsorbed on polystyrene latex. Fleer *et al.*[2] report values of $\alpha$ for PEO homopolymers for polystyrene latex and for silica to be 0.7 and 0.44 respectively. In Chapter 7. (adsorption of Pluronic copolymers on polystyrene latex) we found $\alpha$ to be 0.4 and 0.8 respectively, for PEO homopolymers and block copolymers (Pluronics) adsorbed onto polystyrene latex. For comparison purposes the data for these copolymers adsorbed on polystyrene latex as already discussed in Section 7.3 are also shown and a similar dependence is observed for both systems. Evers *et al.*[2] predicted a strong dependence of $\delta_H$ on the total polymer molar mass and polymer composition of diblock copolymers. However, the situation is more complicated for the triblock copolymers, as in addition to copolymer composition, the adsorbed layer thickness is strongly dependent on the polymer-surface and polymer-polymer interactions. As was observed with the polystyrene latex system (*c.f.* Chapter 7), the dependence of $\delta_H$ on the total copolymer molar mass is very strong but its magnitude is found to be approximately 4 times lower than that observed for the polystyrene latex surface. The estimated error in the data is $\pm$ 0.5 nm. Our much lower $\delta_H$ values again emphasise a less extended configuration is adopted by these copolymers at the silica surface and are indicative of the influence of strong surface-segment interactions.

As in the adsorption data presented in this work L62 shows an analogous behaviour to that shown in the adsorption isotherms (*c.f.* Figure 8.4) giving very low/negligible $\delta_H$ values. This may be attributable to its low molar mass, which gives rise to the low adsorbed amount and hence an extremely thin adsorbed layer.

Figure 8.13 shows a double logarithmic plot of the influence of PEO block molar mass on $\delta_H$ as a function of PEO block content of the PEO-PPO-PEO copolymer. Also shown are the $\delta_H$ values for PEO homopolymers investigated during this study. An approximately linear increase in $\delta_H$ of Pluronic copolymers with PEO block molar mass was observed up to a certain level whereafter a very rapid increase in the $\delta_H$ was observed. Whilst, a very sharp increase in the layer thickness gave a very high slope (1.1 $\pm$ 0.3) was observed for the PEO homopolymers throughout the set of samples

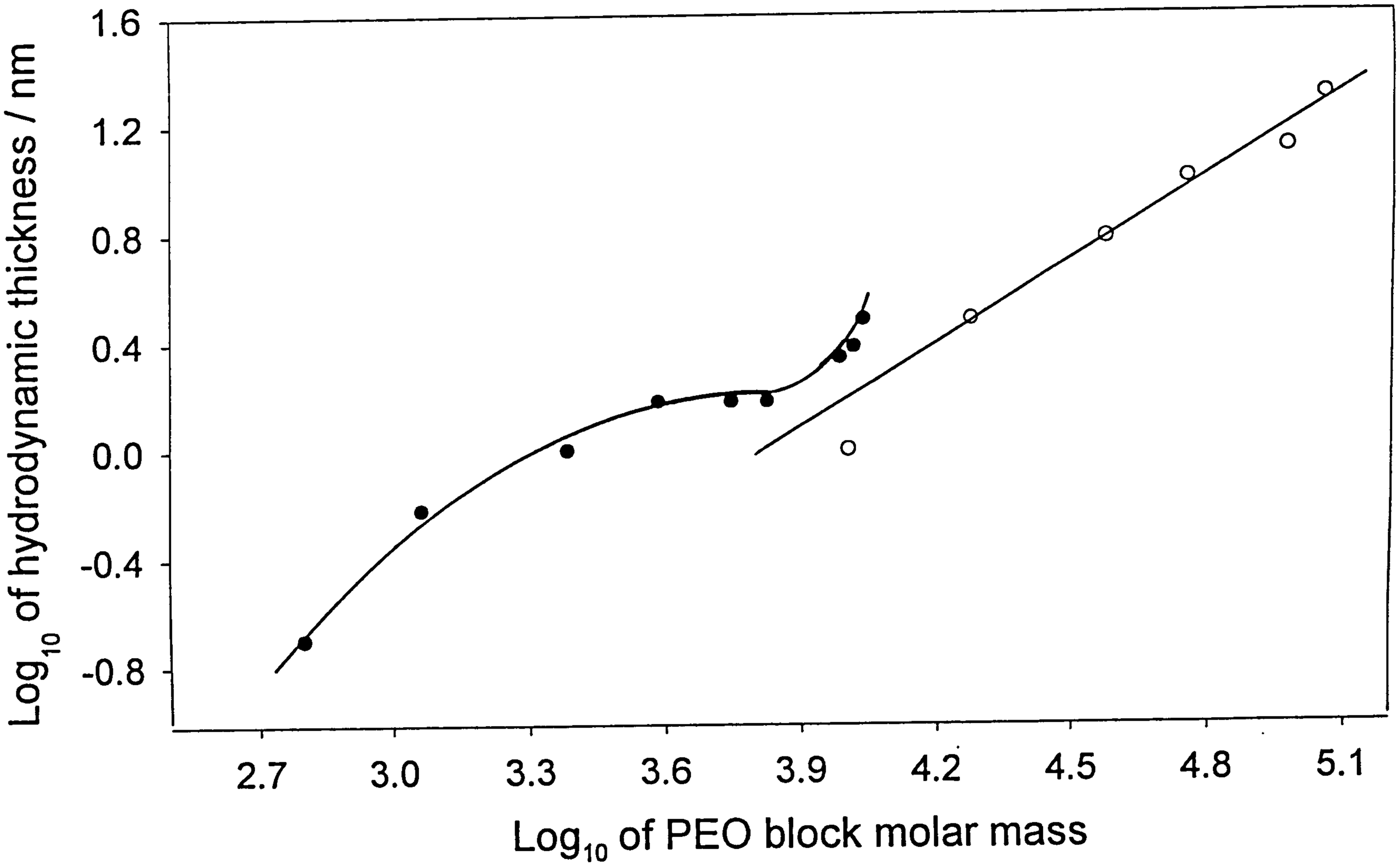


***Figure 8.13 presents the $Log_{10}$ of hydrodynamic layer thickness of the polymers adsorbed on silica as a function of the $Log_{10}$ of PEO block molar mass:*** o ***PEO homopolymers and*** ● ***PEO-PPO triblock copolymers.***

studied. These two sets of data show higher $\delta_H$ values for the block copolymers than those for the PEO homopolymers of the corresponding total molar masses. The difference in the trends of $\delta_H$ and the adsorbed amounts for these polymers suggests that the contribution of PPO blocks to the layer thickness is less important than their contribution to the adsorbed amount (*see* Figure 8.8). Overall, we find higher $\delta_H$ values for the homopolymers adsorbed on silica than those reported by Killmann *et al.*[16], however, they report higher adsorbed amounts for PEO homopolymers but a detailed comparison will depend on the surface characteristics of the particular silica.

Figure 8.14 shows the dependence of $\delta_H$ of the polymer adsorbed layer of the Pluronic copolymers on the PEO block molar mass at *constant* PPO block molar mass. Two sets of data obtained for fixed PPO blocks indicate a relatively weak influence of the PPO/PEO ratio on the adsorbed layer thickness. The trends are similar to those found for the adsorbed amount (*c.f.* Figure 8.9) and to those discussed in Section 7.2 and Section 7.3 for the polystyrene latex substrate. These data show the importance of the PEO block size in determining the hydrodynamic layer thickness. A strong increase in the hydrodynamic layer thickness is predominantly observed by increasing the PEO block whilst the PPO block is maintained constant. This figure also shows a dramatic increase in $\delta_H$ for the low total molar mass polymers in a similar manner to the Pluronic/polystyrene latex system *(see* Section 7.3). However, this increase in $\delta_H$ is linear with PEO block molar mass for the relatively high molar mass samples (o) presented in the upper plot of this figure. This figure also shows that there is an increase in the hydrodynamic thickness of the adsorbed layer with increasing PPO block size for constant PEO block size, indicating that the PPO block also contributes to $\delta_H$ but to a lesser extent. This effect is, however, smaller than that observed for the polystyrene latex system indicating weaker PPO-silica interactions. The data presented by Killmann *et al.*[16] also indicate a weaker PPO - silica interaction than that of PEO - silica.

## 8.3.2. Theoretical Predictions for Hydrodynamic Layer Thickness

Figure 8.15 presents the dependence of the logarithm of the calculated layer thickness for the same set of copolymers adsorbed on silica as a function of the $\log_{10}$ of

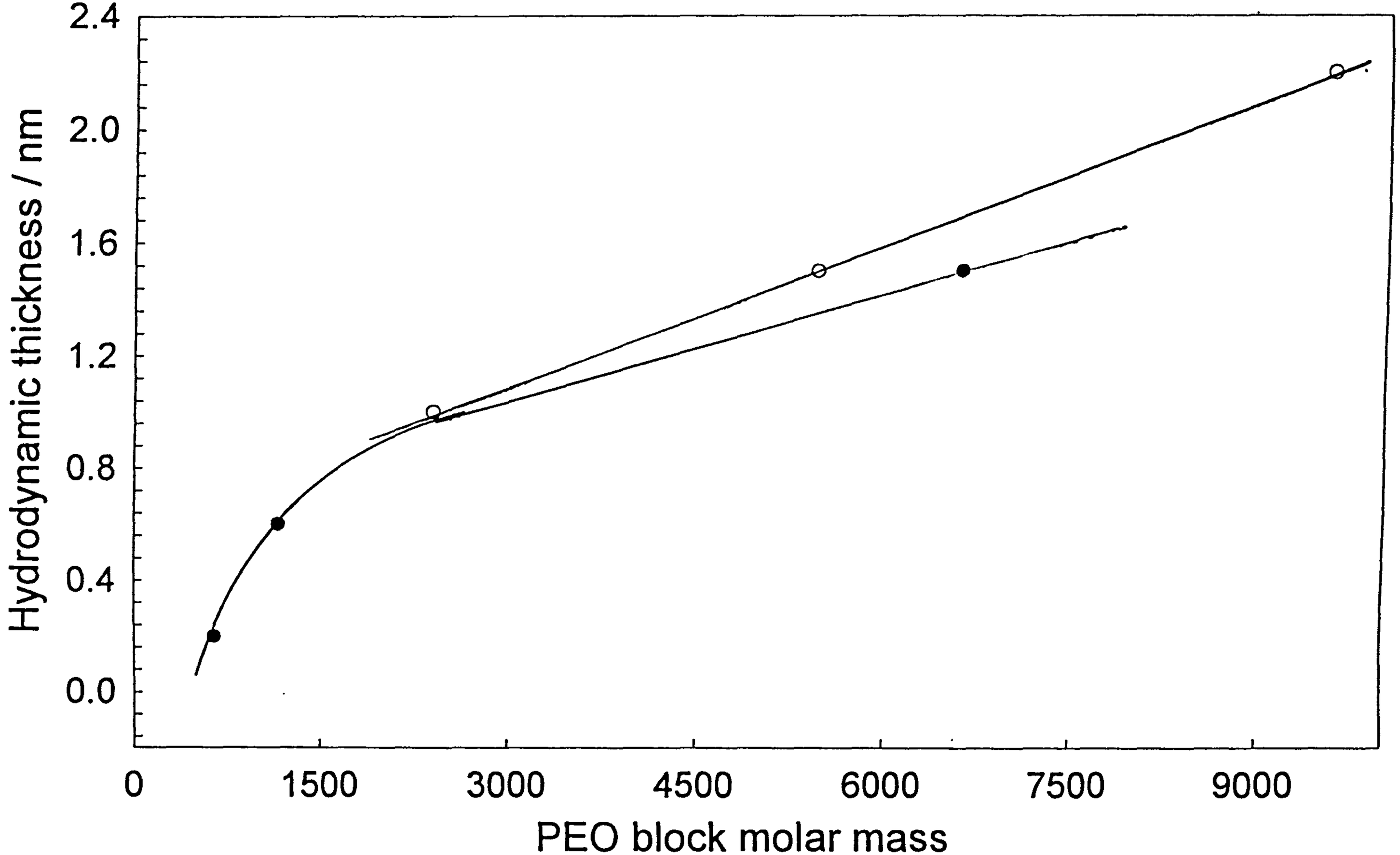


*Figure 8.14 presents the hydrodynamic layer thickness of the Pluronic copolymers adsorbed on silica as a function of PEO block molar mass at constant PPO block mass: ● PPO≅1750 and O PPO≅2250.*

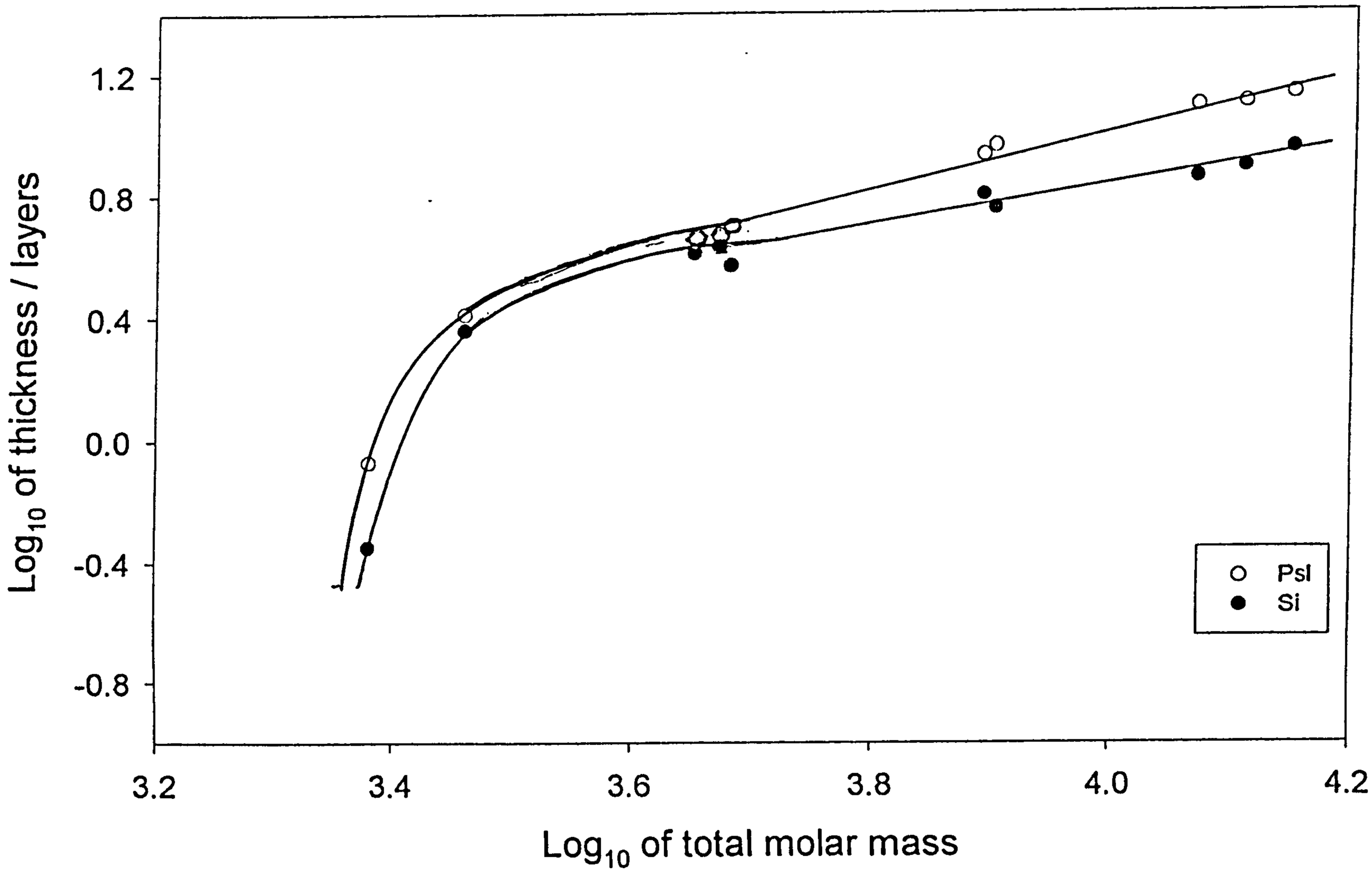


***Figure 8.15 presents the $Log_{10}$ of layer thickness of the Pluronic copolymers calculated using the SCF model as a function of the $Log_{10}$ of total polymer molar mass for: ● silica and O polystyrene latex substrates.***

the total polymer molar mass. The data were calculated using the SCF model[2,12] in the similar manner as described in the Section 6.2, using the same set of $\chi$ parameters. Also, for comparison purposes the calculated thickness data (*see* Section 7.2) for these copolymers adsorbed on polystyrene are presented. Both of these plots show a linear relationship between the logarithmic scales of calculated thickness and the total polymer molar mass in a similar manner as observed experimentally (*c.f.* Figure 8.12), with an exception, that the low molar mass L62 show a very thin polymer adsorbed layer. Overall, a good agreement is observed in the trends in the patterns of the theoretical to that of the experimental data has been observed for the polymers adsorbed on silica and polystyrene latices.

Figure 8.16(a,b) present the adsorbed layer thickness data for the PEO-PPO and PEO-PBO block copolymers adsorbed on silica calculated using SCF model[2,12] in the similar manner as described in the Section 6.2, as a function of the measured hydrodynamic thickness of the polymer adsorbed layer. For all the cases an approximately linear increase in the layer thickness with the measured hydrodynamic layer thickness has been observed which confirms the ability of the model to predict the experimental data. However, the rate of increase in thickness is observed to be higher for the PEO-PPO copolymers than that observed for the PEO-PBO (with an estimated error of $\pm$ 1.5).

Figure 8.17 shows the dependence of measured $\delta_H$ on the anchor fraction for the Pluronic copolymers. The behaviour is similar to that observed for the adsorbed amount (*c.f.* Figure 8.10), except, that a somewhat steeper decay in the curve is observed for the thickness than that for the adsorbed amount. Inset into this figure is the calculated data for the copolymers under study (*see* Table 4.2) using the SCF model[2,12] The same $\chi$ parameters as were used in Section 6.2 were selected. Again a good qualitative agreement between the calculated and experimental results is evident from these two figures. This again confirms that low molar mass, high anchor fraction (PPO block) polymers contribute less to the adsorbed layer thickness (*i.e.* to the tails), hence, a very sharp decay in the curve was observed (after passing through the maximum) with increasing the PPO:PEO ratio (*i.e.* increasing hydrophobicity of the copolymers) which is not unexpected. Any increase in the PPO block can cause: an overall decrease (I) in the net surface-polymer interaction and (II) in the extent of tails /

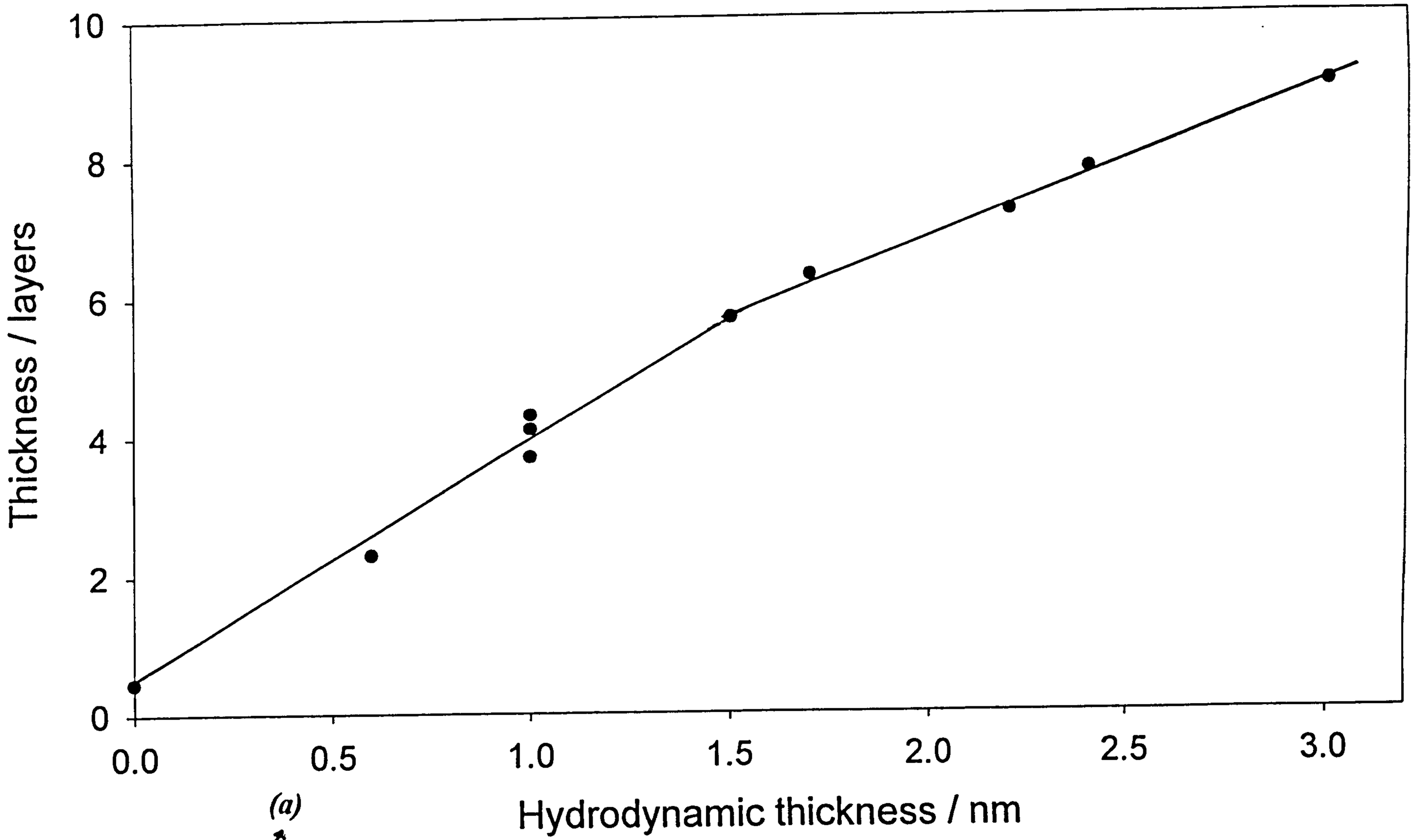


***Figure 8.16 presents the layer thickness for the copolymers adsorbed on silica calculated using SCF model as a function of the measured hydrodynamic thickness;  PEO-PPO triblock copolymers.***

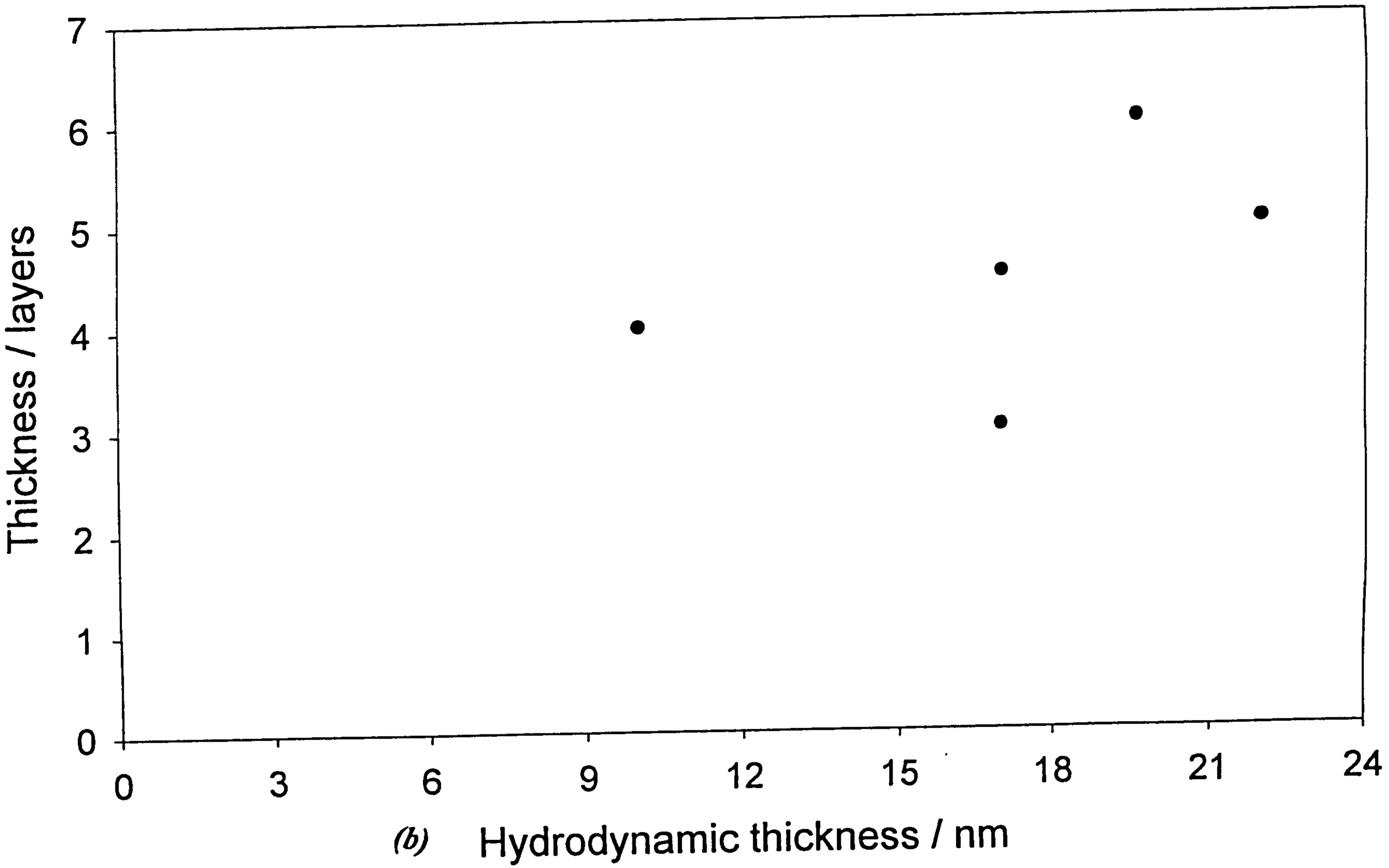


Figure 8.16 presents the layer thickness for the copolymers adsorbed on silica calculated using SCF model as a function of the measured hydrodynamic thickness; ***PEO-PBO copolymers.***

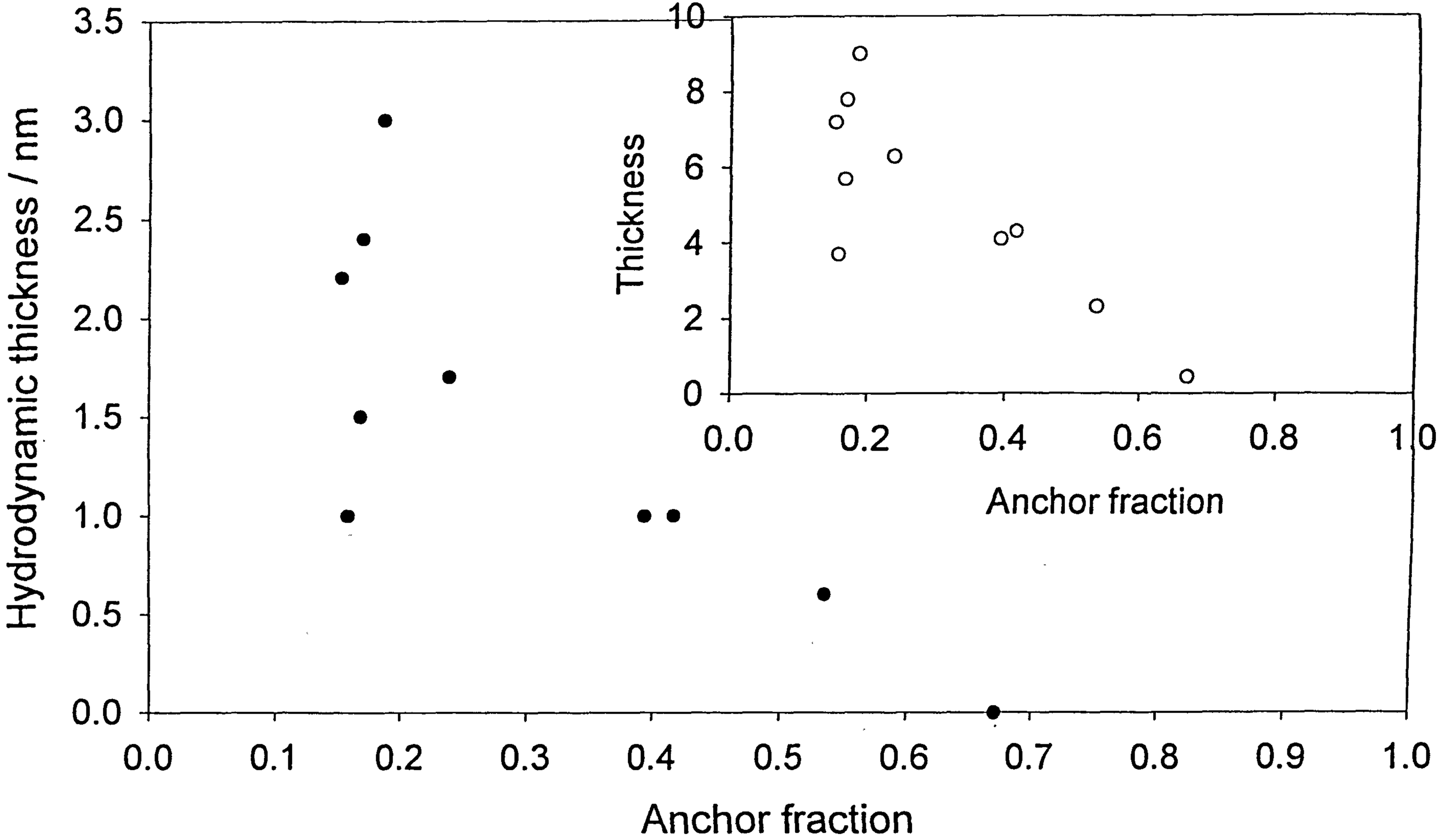


***Figure 8.17 presents the hydrodynamic layer thickness for the PEO-PPO triblock copolymers adsorbed on silica as a function of the anchor fraction, $\nu_A$: ● our experimental data and o (inset data) SCF calculations.***

loops in the bulk solution.

### 8.3.3. Dependence of Hydrodynamic Thickness on Adsorbed Amount

Figure 8.18(a) compares the hydrodynamic thicknesses of the Pluronic copolymers for silica and polystyrene latex systems (data are discussed in Chapter 7.0), as a function of the adsorbed amount. This figure shows that for silica a very thin adsorbed layer thickness is evident at low adsorbed amounts, which, becomes thicker with increasing the adsorbed amount. This curve later joins (within the experimental errors shown for F108 and L62 copolymers for the silica and polystyrene systems, respectively) the falling curve of these copolymers observed for the polystyrene latex system and gives rise to a universal curve. The Scheutjens-Fleer theory[2] has already predicted such a steep increase in the layer thickness at a certain threshold level of adsorbed amount and Cohen-Stuart *et al.*[12] have also experimentally observed the similar trends for the PEO homopolymer/polystyrene latex systems. However, the polymers on the silica surface become saturated at $\Gamma_{max} \sim 0.25$ mg $m^{-2}$ which limits the maximum value of $\delta_H$. On the polystyrene latex however much large values of both $\Gamma_{max}$ and $\delta_H$ can be realised. The major differences between the two sets of data are the stronger affinity of the PEO blocks for silica and that of PPO blocks for polystyrene latex systems, respectively.

Figure 8.18(b) presents the dependence of thickness of the PEO-PPO copolymers on the theta calculated using SCF model, same $\chi$ parameters as given above were used. Also, for comparison the data for the same set of copolymers adsorbed on polystyrene latex are shown. A good qualitative agreement between the trends in the pattern of that determined experimentally and those calculated theoretically is evident from the Figures 8.18 (a) and (b). It is not surprising that the more hydrophilic F38 copolymer contributes more towards the adsorbed layer thickness than to the adsorbed amount, which is evident from both experimental as well as theoretical data.

The dependence of the measured hydrodynamic layer thickness of the PEO-PBO block copolymers on the adsorbed amount determined for the silica system is presented in Figure 8.19. Also, for the comparison purposes, the adsorption data measured for the same set of PEO-PBO polymers adsorbed on polystyrene latices are shown in this

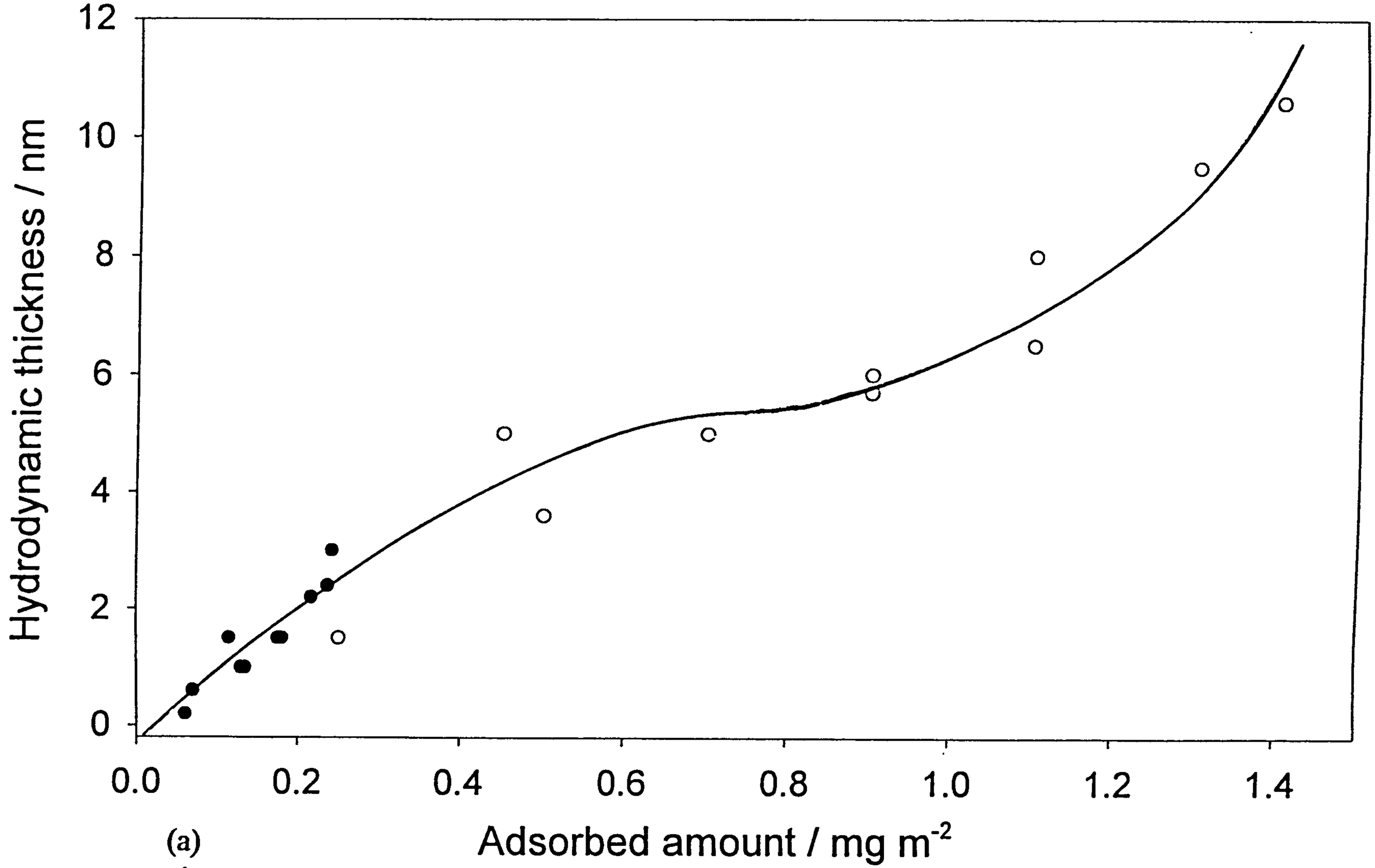


(a)

***Figure 8.18 presents the hydrodynamic layer thickness for the Pluronic copolymers as a function of the adsorbed amount, $\Gamma_{max}$ determined experimentally for • silica and o polystyrene latex systems.***

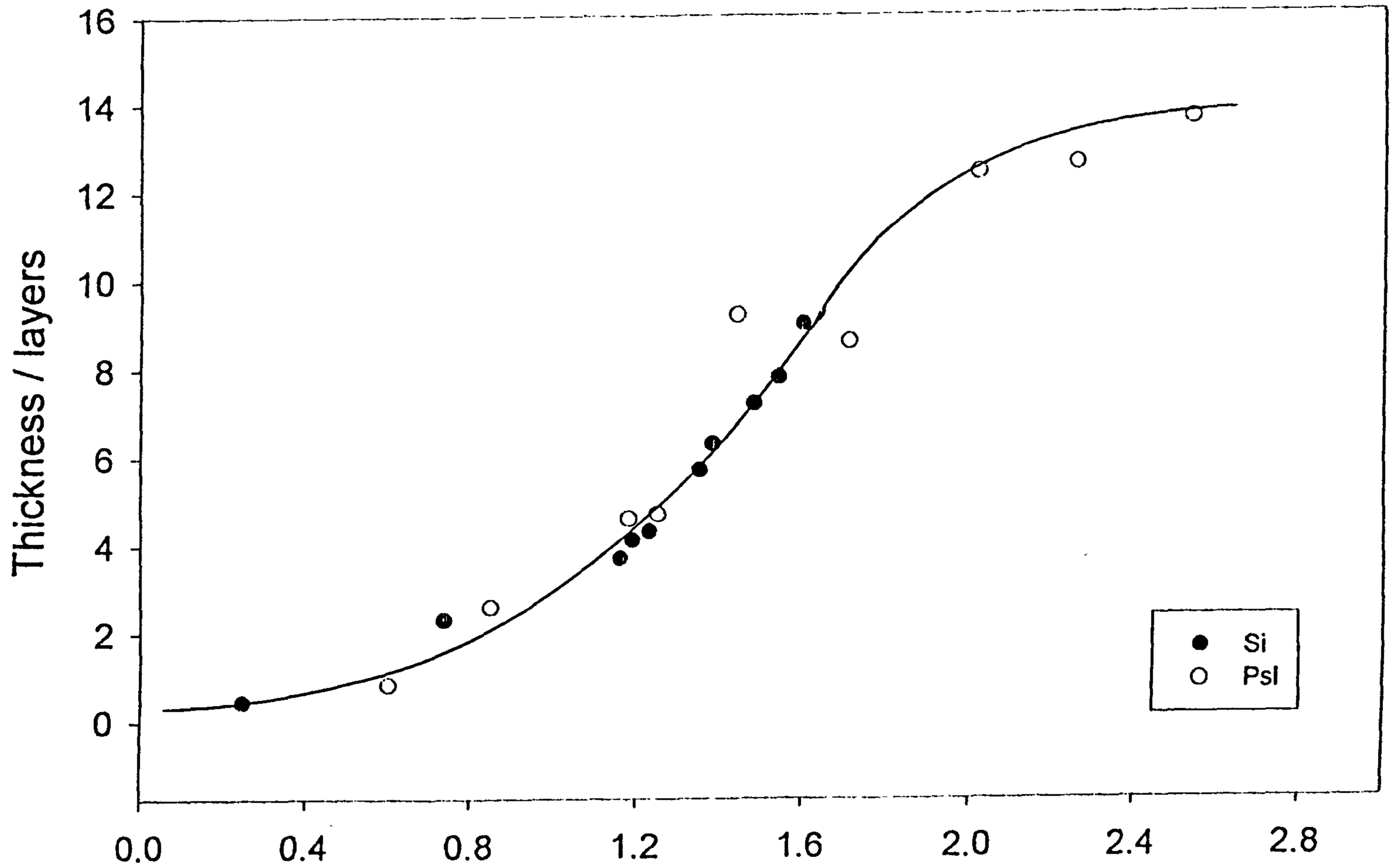


(b)

Figure 8.18 presents the hydrodynamic layer thickness for the Pluronic copolymers as a function of the adsorbed amount, $\Gamma_{max}$ calculated for ● *silica* and o *polystyrene latex systems.*

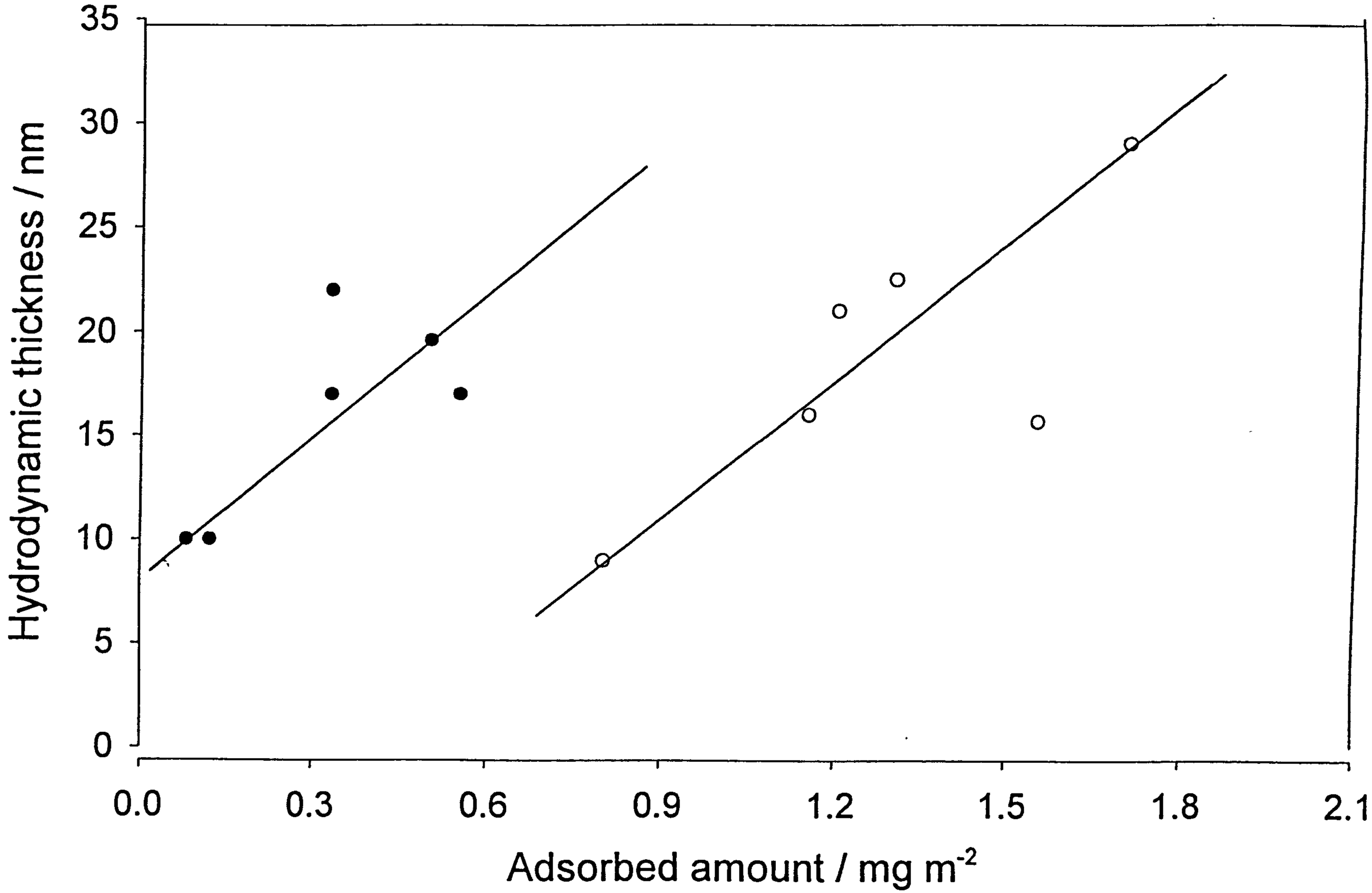


***Figure 8.19 presents the hydrodynamic layer thickness for the PEO-PBO block copolymers as a function of the adsorbed amount, $\Gamma_{max}$ for: ● silica and o polystyrene latex systems.***

figure. In contrary to the adsorption of PEO-PPO copolymers (*c.f.* Figure 8.18(a)), the PEO-PBO copolymers show relatively thicker adsorbed layer for the same adsorbed amounts for the silica than that observed for the polystyrene latex. The PBO is much more hydrophobic than the PPO and this may enhance the net surface interactions with silica.

## 8.4. Conclusion

The data presented for PEO homopolymers adsorbed on silica show a pronounced dependence of the adsorbed amount and the hydrodynamic thickness on the total polymer molar mass.

In the case of PEO-PBO block copolymers a continuous increase in the adsorbed amount of linear diblock copolymers has been observed. A great influence of the copolymer architecture on the adsorption of these polymers has been observed and is in agreement with the trends in the pattern of the adsorption observed for these polymers in some other systems and/or methods (*see* Chapters 7 and 10). Overall, relatively higher values of adsorbed amount and the hydrodynamic thickness presented indicate stronger adsorption of these copolymers on silica than that observed for the polystyrene latices and can be attributed to the insolubility of the PBO block which aids to the adsorption and in some cases may lead to bilayer formation.

It has been shown that total polymer molar mass and the PPO:PEO ratio have a paramount importance in explaining the adsorption of Pluronic copolymers. The data show a weak influence of the PPO blocks on the overall level of adsorption, in a similar manner to that observed for these copolymers adsorbed on polystyrene latex (*see* Figure 7.9).

The increase in the hydrodynamic thickness was observed to be strongly dependent on both total polymer molar and the PEO block mass. Overall, the data suggest that when these copolymers adsorb on the hydrophilic silica surface the hydrophilic PEO segments contribute overwhelmingly towards the hydrodynamic layer thickness (*i.e.* as tails).

The dependence of adsorbed amount and the hydrodynamic thickness on the

anchor fraction is presented. It is shown that the low molar mass copolymers with a large anchor fraction, $\upsilon_A$, adopt a less extended conformation at the silica surface because:

(I) The hydrophilic PEO blocks have a strong interaction for the silica surface.

(II) PPO blocks being hydrophobic in nature are either insoluble or "partially soluble" (the solubility depends upon the PPO molecular weight) in the bulk solution, and hence are forced onto the surface.

Hence, in such cases both the PEO and PPO blocks are expected to bind themselves to the surface, which is confirmed by the low adsorbed amount and hydrodynamic thickness determined. Whilst, for higher molecular weight samples with lower $\nu_A$, the PEO buoy blocks are pushed away from the surface into the bulk solution in long loops and/or tails, and hence showing adsorption at a higher level.

The influence of the chemical nature of the substrate on the adsorption parameters (and therefore on the conformation) of the adsorbed polymers has been presented. This interaction is a consequence of the net interactions between the polymer blocks (PPO-Silica, PEO-Silica and PPO-PEO) and the solvent molecules with the particle surface (water-silica). Hydrogen bonds are expected to form on polar silica surfaces between the SiOH surface donor group and the acceptor (PEO) block of the polymer in a similar manner as hydrophobic interactions were primarily responsible for the polymer-surface interaction on the non-polar polystyrene latex surface (*see* Chapter 7). Due to the existence of such different interactions, the same set of polymers under the same experimental conditions was observed to adsorb very differently on silica and polystyrene latex. These block copolymers adsorb onto silica in a similar manner to PEO homopolymers *i.e.* giving relatively low adsorbed amount and hydrodynamic thickness values.

The comparison between the adsorption of polymers on silica and polystyrene latex systems also show that relatively lower adsorption and hence lower plateau levels and thin adsorbed layers are observed for silica than for the polystyrene latex. For the case of both the systems (hydrophobic and hydrophilic) the PEO homopolymers are found to adsorb at lower levels than the block copolymers hence showing low adsorbed

amount as well as hydrodynamic thickness values. A universal dependence of hydrodynamic thickness on the adsorbed amount (*c.f.* Figure 8.18) of copolymers for the polystyrene latex and silica systems is shown in the plot of $\delta_H$ versus $\Gamma_{max}$. Overall, the trends observed in the pattern of both theoretical and measured data presented for both silica and polystyrene latex systems are in a good qualitative agreement.

# References


[1] Alexandridis, P., Holzwarth, J. F., and Hatton, T. A., *Macromolecules* 1994, 27, 2414.

[2] Evers, O. A., Scheutjens, J. M. H. M., and Fleer, G. J., *J. Chem. Soc. Faraday Trans.I*, 1990, 86 (9), 1333.

[3] Fleer, G. J., Cohen-Stuart, M. A., Scheutjens, J. M. H. M, Cosgrove, T., and Vincent, B. "Polymers at Interfaces" London: Chapman and Hall, 1993, p 302.

[4] Schillen,K., Claeson, P. M, Malmsten, M, Linse, P., and Booth, C., *J. Phys. Chem. B* 1997,*101*, 4238.

[5] Killmann, E., Fulka, C., and Reiner, M., *Chem. Soc. Faraday Trans.I* 1990, 86, 1389.

[6] Schroen, C. G. P. H, Cohen-Stuart, M. A., van der voort Maarschalk, K., van der Padt, A., and van't Riet, K., *Langmuir*, 1995, 11, 3068.

[7] Malmsten, M., Linse, P., and Cosgrove, T., *Macromolecules*, 1992, 25, 2474.

[8] Killmann, E., Maier, H., and Baker, J. A., *Colloids Surf.* 1988, 31, 51.

[9] Lucie, M. A., Van de Steeg and Carl-Gustaf Golander, *Colloid & Surf.* 1991, 55, 105.

[10] Marques, C.M., Joanny, J.F. and Leibler, L. *Macromolecules*, 1988, 21, 1051.

[11] Guzonas, D., Hair, M.L. and Cosgrove, T., *American Chem. Soc.*, 1992, 20 2777

[12] Cohen-Staurt, M.A., Waajen, F.W.H., Cosgrove, T., Vincent, B. and Crowley, T.L., *Macromolecules*, 1984, 17, 1825.

[13] Wu, D.T., Yokohama, and Setterquist, *Polymer, J.*, 1991, 23, 711.

[14] Kato, T., Nakamura, K., Kawaguchi, M. and Takahashi, A., *Polym. J.*, 1981, 13, 1037.

[15] Cosgrove, T., Vincent, B., Crowley, T.L. and Cohen-Stuart, *ACS Symposium Ser.*, 1984, 240, 147.

[16] Killmann, E., Maier, H., Kaniut, P. and Gulling, N., *Colloids Surf.*, 1985, 15, 261.

# Chapter 9

# *ADSORPTION OF DIBLOCK COPOLYMERS AT CYCLOHEXANE/CARBON INTERFACE*

## 9.1. Introduction

To optimise steric stabilisation it is of paramount importance to understand the influence of polymer architecture on the conformation of the adsorbed polymer layer.[1,2,3,4,5,6,7,8,9,10,11] This can be achieved by characterising the adsorbed layer in terms of its hydrodynamic thickness and adsorbed amount. In this study we shall confine our discussions to the adsorbed amount, as thickness measurements in carbon dispersion are very difficult with conventional light scattering methods.

In this study we aim to understand the influence of polymer composition and architecture upon adsorption at the solid/liquid interface in non-aqueous dispersions. For this purpose a range of polystyrene-hydrogenated polyisoprene (PS-HPIP) AB-type diblock copolymers with different polymer composition *i.e.* different total polymer molar mass and/or varying PS-HPIP ratio, were selected and their adsorption from cyclohexane onto carbon black determined.

The most likely mechanism for the adsorption of these block copolymer surfactants from cyclohexane onto a carbon surface is thought to be through the polystyrene block whilst the HPIP block remains solvated in the continuous phase.[12] Initially, at low polymer equilibrium concentrations both blocks are presumed to lie close to the particle surface whilst at higher concentrations any increase in the number of adsorbed segments enhances the competition of segments in the train layer. This competitive process forces the HPIP buoy blocks away from the surface and in consequence forms an extended "brush"-like layer with a concomitant increase in the thickness of the adsorbed layer.[13]

## 9.2. Adsorption Data Determined by Molecular Modelling

A planar carbon surface was created with dimensions of 24.59 Å x 24.60 Å. The surface was manipulated such that it lay along the X-Y plane of a periodic box with a Z-axis of 48 Å in length. The carbon surface was then energy minimised until the root mean square force had reduced to a level of 0.01 kcal $mol^{-1}$. The molecular mechanics approach used was the conjugate gradient method implementing parameters and potentials specified in the Dreiding II force field.[14] Intermolecular interactions were cut off between 8.0 Å and 8.5 Å using a spline switching function. To the periodic box an explicit atomistic cyclohexane solvent was added. The solvent was created by taking a single minimised solvent molecule, cloning it and then randomly orientating the solvent molecules within the periodic box at a density of 0.777 g $cm^{-3}$. The solvent system was then minimised using the same specifications as applied to the carbon surface.

A randomly orientated isotactic diblock copolymer was built using ten polystyrene monomers and ten hydrogenated poly(isoprene) monomers. The polymer was end capped with hydrogen (H) atoms. This was also minimised to a level of 0.01 kcal $mol^{-1}$ using the Dreiding II force field. The copolymer was added to the periodic box containing both the carbon and the solvent. The terminal polystyrene monomer was tethered centrally on the surface. Fixing the polymer to a point at the surface assures that polymer-surface interactions are observed by preventing the possibility of the polymer following an energy pathway into the bulk solvent.

Molecular mechanics calculations were then performed and the block copolymer was allowed to explore the potential energy surface of the carbon. The same minimisation conditions and potentials, which have been applied throughout this work, were applied to the complete system calculations. The molecular system described was exposed to 100 ps of NPT molecular dynamics calculations at 300 °K and fixed pressure. Atomic co-ordinate data as a function of time allowed volume fraction profiles to be derived for the polymer. These were created by calculating the distance, from the surface of every atom within the polymer backbone, for every time step during energetic equilibrium. This data was then normalised and presented as a running average.

Figure 9.1(a) is a snap shot of the PS/HPIP copolymer adsorbed on the carbon surface at thermodynamic equilibrium. The solvent molecules have been removed for clarity of the image. It is clear that the polystyrene block (black balls) prefers to orient itself at the surface in a pancake like structure. The HPIP fragment (white balls) shows no tendency to move towards the surface and stretches out into the solution. This is reflected in Figure 9.1(b), which is the probability distribution for polymer segments at the carbon surface. The PS segments are distributed within 12 Å of the surface inferring preferential adsorption onto the particle surface from cyclohexane. Peaks at 2 Å and 4 Å represent atoms tethered to the surface. HPIP segments are evenly distributed throughout the bulk solvent but none were found within 10 Å from the surface and hence a preference to not adsorb on carbon is assumed. With this insight suitable $\chi$ values were chosen for the SCF modelling.

## 9.2.1. Theoretical Calculations

The SCF model of Evers[15] and Fleer[16] has been used to estimate the relative adsorption affinities of the anchor and buoy components of the copolymers at the carbon/cyclohexane interface. The block monomer number ($N_i$) is the molar mass of each individual block divided by the corresponding molecular mass of that block. Each block monomer number obtained was again divided by 6 to account for chain flexibility. The number of adsorbed layers was taken as the square root of number of hydrogenated-polyisoprene monomers ($N_B$) present in each sample. In each case, the adsorbed amount was calculated between solution equilibrium concentrations of 1 and 2000 ppm. The adsorbed amount ($\theta$) was derived from the pseudo-plateau level of the adsorption isotherm (*see* for instance Figure 9.2(a,b)) at polymer equilibrium concentrations of 1000 ppm. Figure 9.2(a,b) shows the adsorption isotherms determined for the diblock copolymers as a function of polymer concentration in the bulk ($\varphi_b$) calculated using the SCF model.[15,16] For this purpose polymers with a fixed polymer molar mass, Mw of 30,000, but varying PS-HPIP ratio (hence varying anchor fraction) were selected. The level of adsorption was observed to vary with $\nu_A$ and this will be discussed in detail latter. For the cyclohexane/carbon system, the polystyrene blocks were presumed to adsorb preferentially to the carbon surface. The poor solvency of the polystyrene block also aids adsorption. The dependence of the polymer

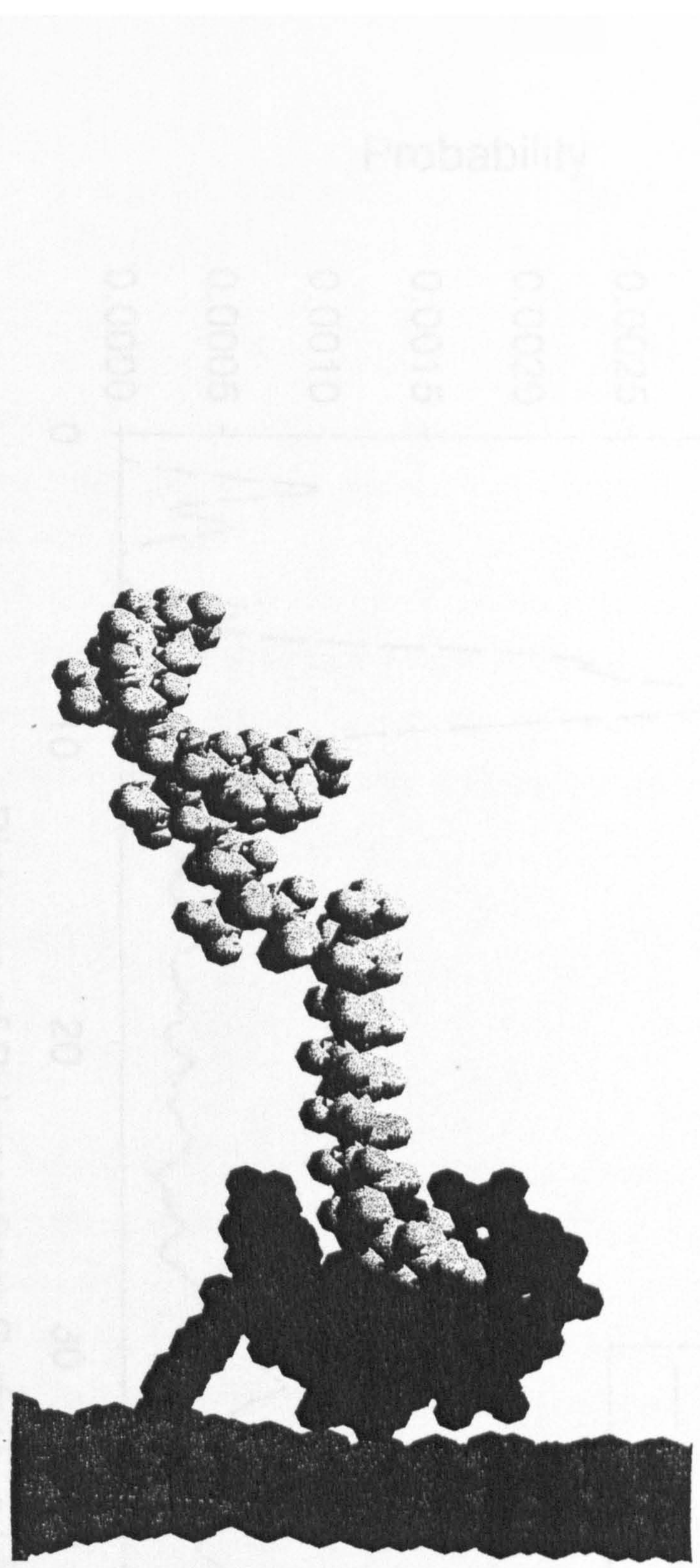

*Figure 9. 1(a) presents the snap shot of the PS-HPIP diblock copolymer adsorbed on the carbon surface at thermodynamic equilibrium.*

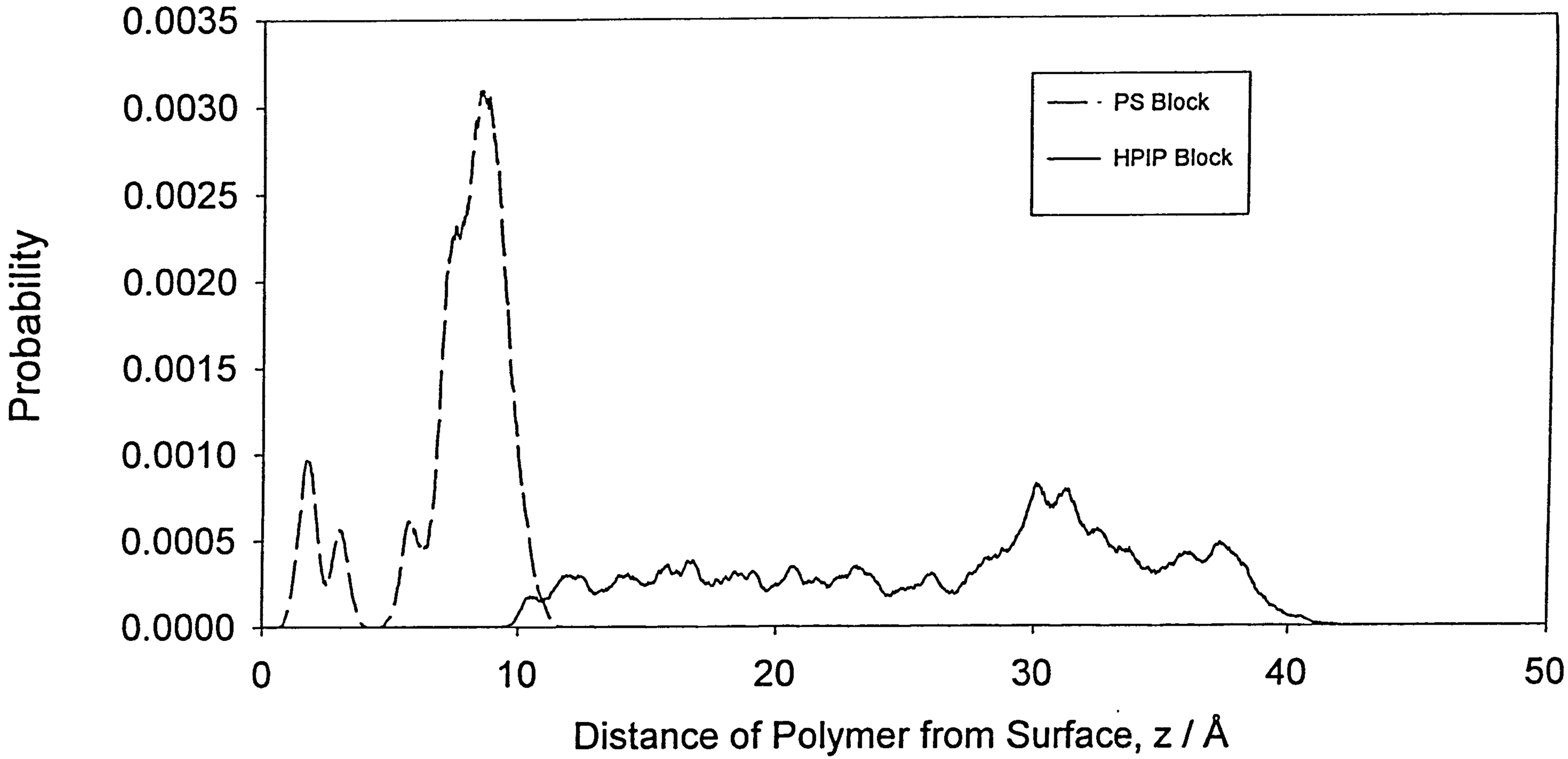


*Figure 9. 1(b) presents the probability distribution for polymer segments at the carbon surface.*

adsorption on the $\chi_{solvent\text{-}styrene}$ parameter was also determined. For this purpose copolymers with constant polymer molar mass, Mw ~ 50,000 (50 K), but of varying polymer block composition were selected (*see* Figure 9.2(b)). The adsorbed amount for each polymer was derived from the plateau levels of its calculated adsorption isotherm over a range of $\chi_{solvent\text{-}styrene}$ values *i.e.* between 0.4 and 0.6. An increase in the magnitude of the calculated adsorbed amount with increasing the $\chi_{solvent\text{-}styrene}$ parameters is also observed because of a decrease in the solubility of the polymer segments, which in turn increases the number of polymer segments adsorbing on the surface. Also, the dependence of polymer adsorption on $\chi_{solvent\text{-}HPIP}$ parameter was determined by varying $\chi_{solvent\text{-}HPIP}$ ($\chi_{HP}$) using values of 0.45, 0.5 and 0.55. Finally $\chi_{HP}$ = 0.45 was chosen to give the best representation of the experimental data.

## 9.3. Experimental

### 9.3.1. Materials

A range of diblock copolymers of polystyrene and hydrogenated-polyisoprene ($PS_m$-$HPIP_n$) with varying polymer composition (Mw~7 K to 150 K) was selected for this study. The physicochemical properties (total polymer molar mass, PS and HPIP block molar masses and their polydispersity as stated by the manufacturers are given in Table 9.1.[17] These diblock copolymers (supplied by Shell Additives International Ltd.) are of research grade and were used as received without any further treatment. For convenience the copolymers will be given codes which represent their total polymer molar mass and their anchor fraction, for example, the copolymer with total molar mass 9,500 and anchor fraction 0.44 is symbolized as 9.5K0.44. The substrate carbon black (supplied by Shell Additives International Ltd.) was used as the adsorbent for the polymer and was used as received without any further purification. Its physicochemical properties are given in Table 9.2.

The surface area, $S_A$, of the carbon substrate was determined by measuring the nitrogen adsorption isotherm using the B.E.T. method in the similar manner as detailed by Cosgrove *et al.*[18], which, also indicates the meso and micro pore sizes. The particle

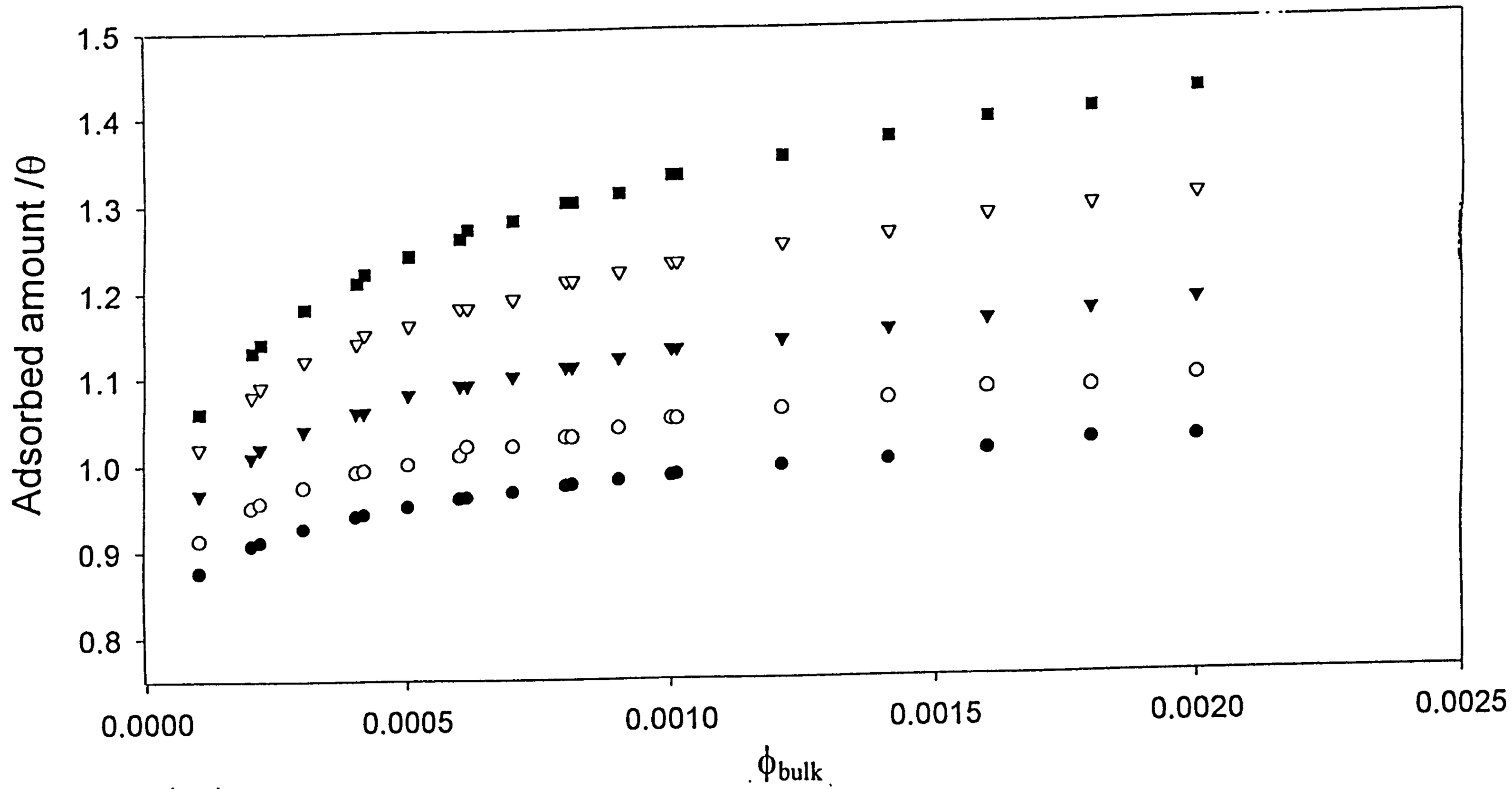


***Figure 9. 2(a) shows the dependence of the adsorption isotherms on $\varphi_b$ calculated using the SCF model for the diblock copolymers of varying anchor-buoy ratio;*** $\nu_A =$ ● ***0.94,*** o ***0.83,*** ▼ ***0.68,*** ▽ ***0.56 and*** ◆ ***0.45.***

Table 9. 1: physicochemical properties of the non-ionic, water-soluble PS-HPIP diblock copolymers as stated by the manufacturers.[17]

| Polymer | $M_w$ | $M_{wPS}$ | Mol% PS | $M_{wHPIP}$ | Mol% HPIP | $\upsilon_A$ | $M_w/M_n$ |
|---|---|---|---|---|---|---|---|
| 10K0.82 | 10,000 | 9,000 | -- | 1,000 | 0.18 | 0.82 | N/A |
| 10K0.06 | 10,000 | 1,000 | -- | 9,000 | 0.94 | 0.06 | N/A |
| 17K1.00 | 17,000 | 17000 | 100.00 | Nil | 0.0 | 1.00 | N/A |
| 14.7K0.85 | 14,740 | 13500 | 85.42 | 1240 | 14.57 | 0.85 | 1.07 |
| 7K0.57 | 7,000 | 4970 | 57.14 | 2030 | 42.86 | 0.57 | 1.65 |
| 11.8K0.56 | 11,810 | 8320 | 56.34 | 3490 | 43.66 | 0.56 | 1.11 |
| 9.5K0.44 | 9,506 | 5620 | 44.26 | 3890 | 55.74 | 0.44 | 1.14 |
| 100K0.22 | 100,000 | 35000 | 24.00 | 65000 | 76 | 0.22 | N/A |
| 7.5K0.21 | 7,470 | 2520 | 21.51 | 4950 | 78.49 | 0.21 | 1.8 |
| 153K0.2 | 153,000 | 48000 | 19.75 | 105000 | 80.25 | 0.20 | N/A |

size and the polydispersity of the particles were estimated using transmission electron microscopy (*see* Table 9.2). The polymer was assumed to adsorb only on the external surface of the adsorbate particles without having access to the meso and/or micro pore areas of the particles. The cyclohexane used in the preparation of the entire polymer solutions *etc.* (BDH "AnalaR" grade) was used without any further treatment.

## 9.3.2. Methods

Adsorption isotherms were determined as a function of bulk equilibrium polymer concentration and copolymer molar mass, using the standard depletion method.[19,20]

The general method was as follows: stock solutions (~ 3000 - 4000 ppm) of each polymer under study, were prepared. A range of solution concentrations (50 – 3000 ppm) was prepared from these stock solutions. 7mg of carbon were added to 3 ml of each polymer solution. The samples were then left tumbling for 24 hours to reach

Table 9.2: characteristics of the carbon used in this study

| | |
|---|---|
| Size /±10.0%/nm | ? |
| Surface Area /±5% /($m^2$ $g^{-1}$) | 230 |
| Meso Pore area /±5% /($m^2$ $g^{-1}$) | 225 |
| Micro Pre area /±5% /($m^2$ $g^{-1}$) | 2.98 |

adsorption equilibrium. Special care was taken to prevent evaporation by sealing with "parafilm". In order to find a suitable calibration peak a full range UV spectrum (190 - 900 nm) was taken for each polymer dissolved in pure cyclohexane. A wavelength of 263 nm, corresponding to the aromatic region of polystyrene, was selected as the best absorption. The free polymer was separated from adsorbed polymer (dispersion) by centrifugation at 1300 rpm for half an hour using an MSE Microcentaur centrifuge. The supernatant was taken without disturbing the residue and analysed at *263 nm* using a Uvikon 940 UV spectrophotometer.[21] The path length of the quartz cell used was 1cm and the temperature of the cell housing in the spectrophotometer was 25.0 ± 1.0 °C. The reference cell contained cyclohexane. The resultant absorption peaks were compared with previously obtained calibration curves for the corresponding copolymers and, hence, the equilibrium polymer concentration of the original system was obtained.

The calibration curves of the UV absorbance peaks obtained at 263 nm, for each polymer solutions, were observed to be linear with polymer concentration. The adsorbed amount, Γ, of polymer was determined by measuring the difference between the polymer initial concentration, $C_i$, and the polymer equilibrium concentration, $C_{eq}$, (parts per million or ppm) upon exposure to a known surface area, $S_A$, ($m^2$ $mg^{-1}$) of the adsorbent (carbon) and volume, V, of the bulk solution (litres). The adsorbed amount, Γ, in mass per unit area (mg $m^{-2}$) is given by:

$$\Gamma = \frac{(C_i - C_e) \times V}{S_A} \qquad \text{Equation 0.1}$$

## 9.4. Results and Discussion

### 9.4.1. Adsorbed Amount

#### 9.4.1.1. Adsorption Isotherms

Figures 9.3(a,b,c) show the adsorption isotherms for a set of PS-HPIP diblock copolymers (as listed in Table 9.1) adsorbed at the cyclohexane/carbon black interface as a function of the polymer equilibrium solution concentration. In general, a rapid increase in the level of adsorption of these diblock copolymers (with the exception of the low anchor fraction 10K0.06 polymer) was observed at very low copolymer concentrations followed by a gradual levelling off until the so-called pseudo-plateau level is reached at an equilibrium concentration of approximately 100 ppm. The data show that except for the 7.5K0.21, 9.5K0.44, 100K0.22 and 153K0.20 polymers (*see* Figure 9.3(c )) all of the polymers studied show an incipient phase separation which gives rise to a rapid increase in the level of the adsorption at polymer equilibrium concentrations in the range ~1200 - 2000 ppm. This behaviour was not unexpected because of the poor solvency of the polystyrene blocks in cyclohexane *i.e.* where multilayer or complex formation at the interface is possible. These figures also show that the magnitude of the pseudo-plateau levels for these copolymers is strongly dependent on the polymer composition.

Figure 9.3(a) shows the adsorption isotherms determined for 17K1.0, 14.7K0.85, 10K0.82[a] and 10K0.06[b] polymers adsorbed at the cyclohexane/carbon black interface. High affinity adsorption isotherms are shown for the high molar mass 17K1.0 and 14.7K0.85 polymers with a higher level of adsorption than that observed for the 10K0.82 and 10K0.06 polymers. It is evident from this figure that the polymers

---

[a] 90%(w/w) PS
[b] 90%(w/w) HPIP

10K0.82 and 10K0.06 with equal total polymer molar masses but different anchor-buoy ratios behave in a very different manner when adsorbed on carbon black. The polymer 10K0.06 with a very low anchor fraction (0.056), is highly soluble in cyclohexane and does not adsorb onto the surface until a high polymer equilibrium solution concentration (2300 ppm) is reached. The low level of adsorption demonstrates that the HPIP dominated polymer has a low affinity for carbon black surface. The rapid rise in the plateau level of 10K0.06 at an equilibrium concentration of 2300 ppm is similar to a Langmuir type III isotherm. In comparison, the copolymer 10K0.82 (with the same molar mass as 10K0.06 with a large polystyrene block fraction) adsorbs at a much higher level over the whole range of equilibrium concentrations. The rapid rise in the level of adsorption with a continuous increase in the adsorbed amount without reaching any adsorption plateau level was also found for 17K1.0 and 14.7K0.85 polymers between equilibrium solution concentrations of 1200 ~1700 ppm. The pattern in the rise of the plateau level is observed to depend strongly on the polymer molecular weight and anchor fraction.

Figure 9.3(b) shows adsorption isotherms for copolymers 7K0.57 and 11.8K0.56 adsorbed on carbon black as a function of polymer equilibrium concentration. These two polymers have a similar anchor fraction but different total polymer molar masses. The adsorption of these polymers at slightly different levels indicates the influence of the overall polymer molar mass. Like other samples used in this study (*see* Table 9.1), the polymers 7K0.57 and 11.8K0.56 also show a rapid rise in the pseudo-plateau level at equilibrium concentration ~ 1500 ppm which may again be attributed to multilayer formation and/or precipitation of the polymer at the particle surface.

Figure 9.3(c) shows classic plateau level adsorption isotherms for two pairs of more soluble copolymers, 7.5K0.21 and 9.5K0.44, 100K0.22 and 153K0.20. These two pairs of polymers differ from each other in their total polymer molar masses (one pair with lower molar masses and the other pair with very high molar masses) but are similar in having equally low anchor-buoy ratios, with the exception of 9.5K0.44, which has intermediate anchor fraction value. The two copolymers (100K0.22 and 153K0.20) with higher overall polymer molar mass show high affinity adsorption isotherms. Polymer 153K0.20 has the highest molar mass in the range studied and adsorbs to the highest extent.

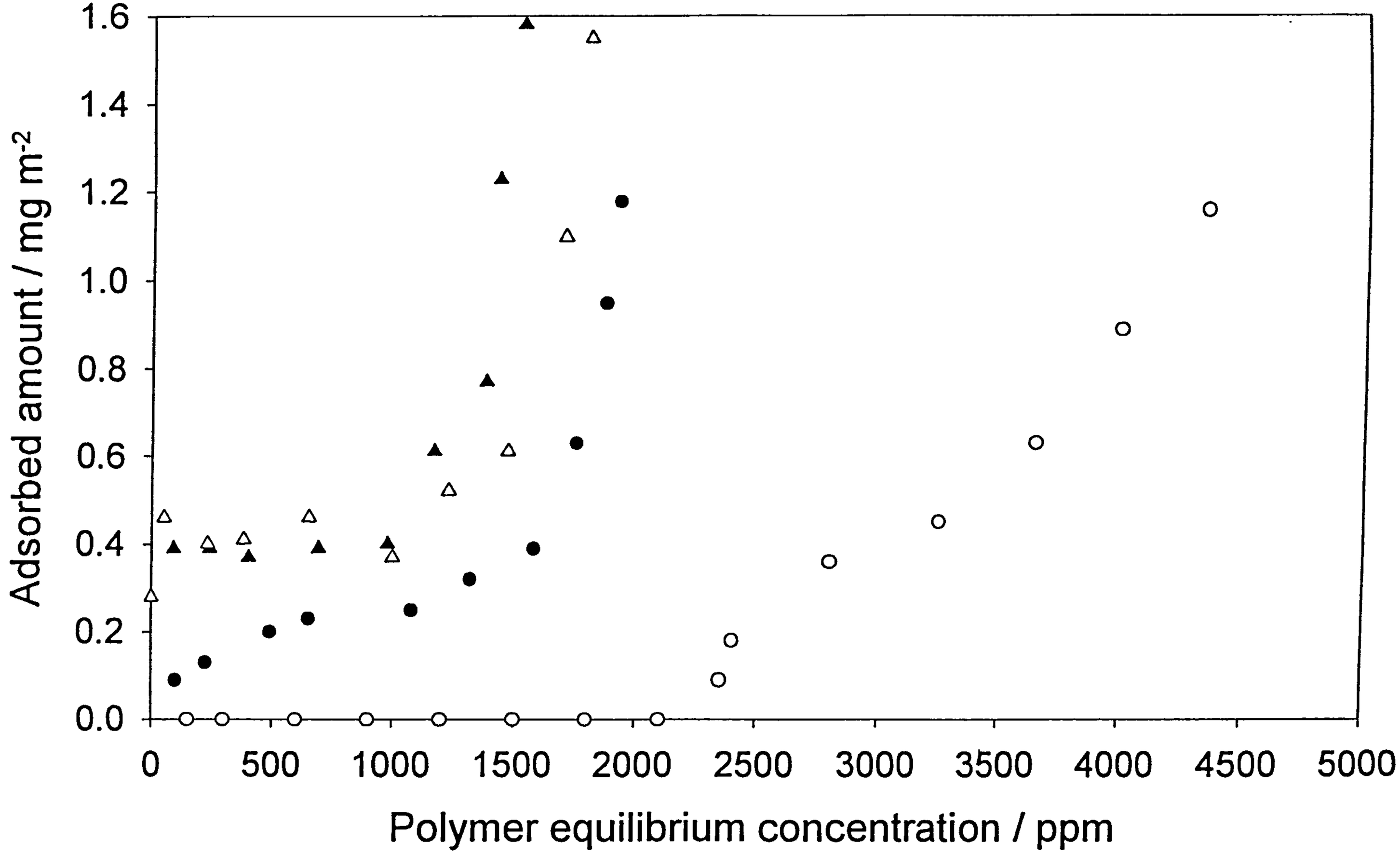


***Figure 9.3(a) shows the adsorption isotherms determined for polymers adsorbed at the cyclohexane/carbon black interface: ▲ 17K1.0, Δ 14.7K0.85, ● 10K0.82 and o 10K0.06.***

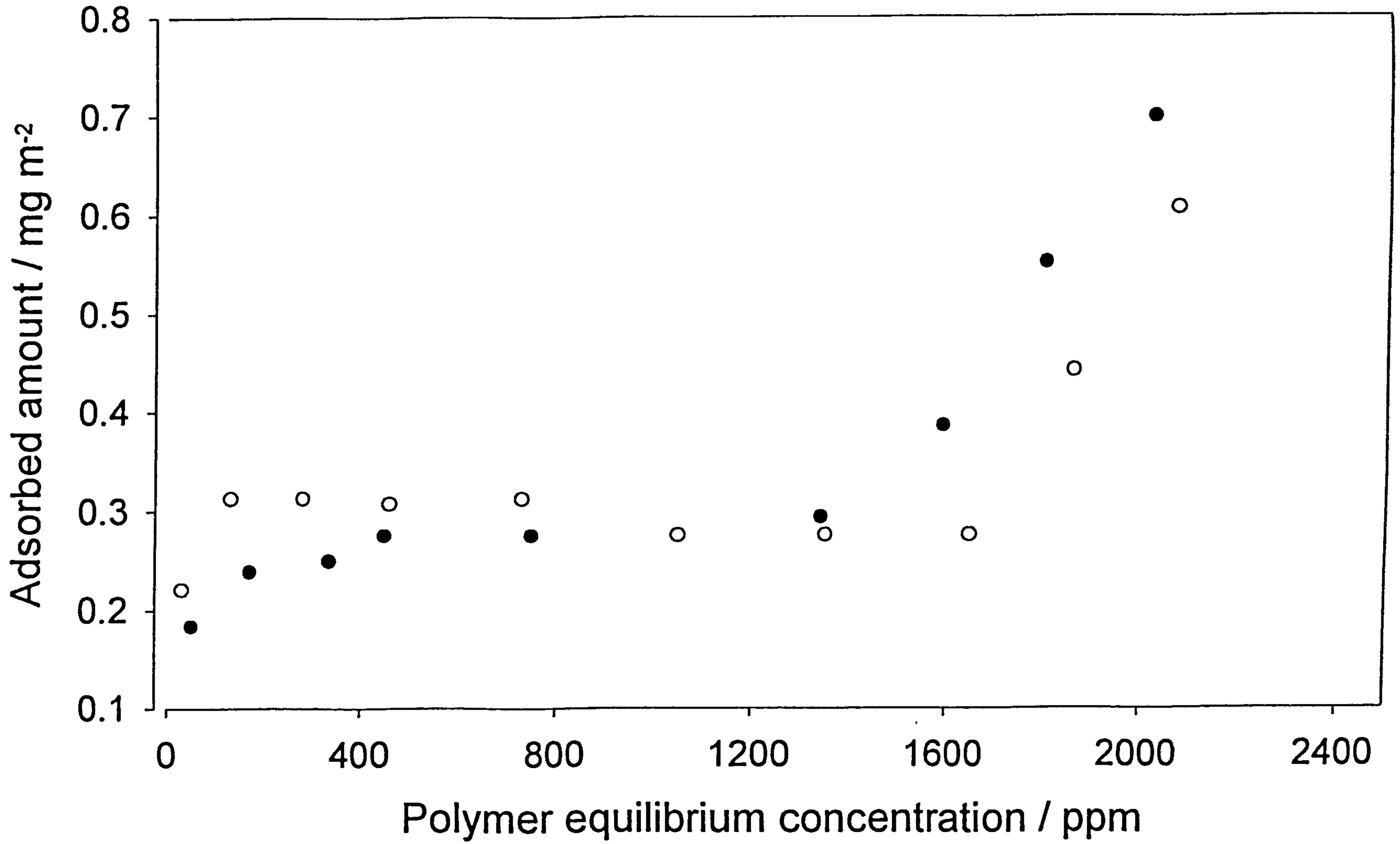


***Figure 9. 3(b) shows the adsorption isotherms for copolymers ● 7K0.57 and o 11.8K0.56 adsorbed on carbon black as a function of polymer equilibrium concentration.***

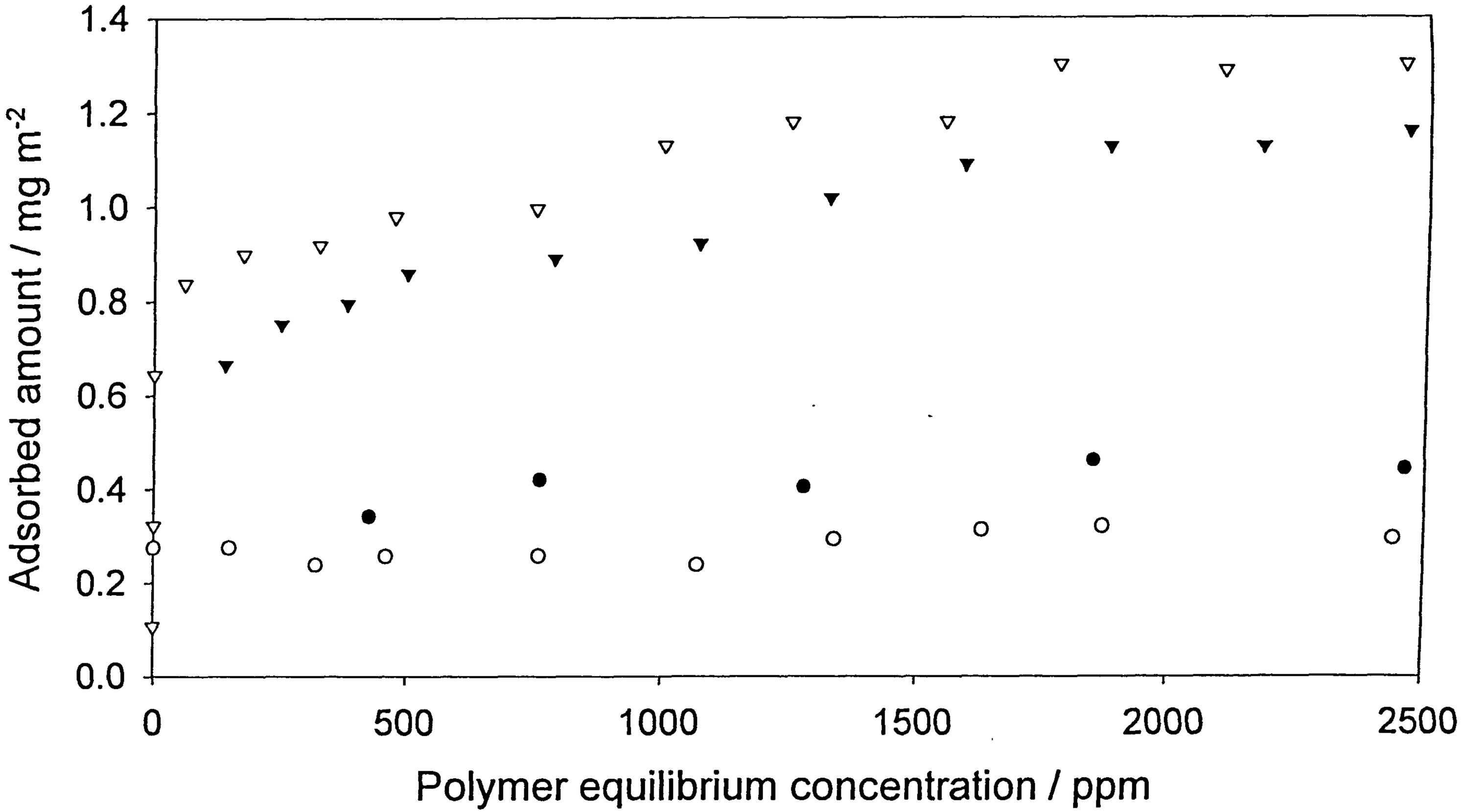


*Figure 9.3 (c) shows the classic plateau level adsorption isotherms for two pairs of more soluble copolymers,* o *7.5K0.21 and* ● *9.5K0.44,* ▼*100K0.22 and* ▽ *153K0.20.*

### 9.4.1.2. Molar Mass Dependence of the Adsorbed Amount

Figure 9.4 presents the adsorbed amount for the diblock copolymers as a function of $Log_{10}$ of total polymer molar mass. With the exception of polymer 10K0.06, which has the lowest anchor fraction in the range studied, all the polymers studied show an increase in the adsorbed amount with increasing total polymer molar mass, *see* Table 9.3. Interestingly, the low molar mass and the medium anchor fraction 7K0.57, 9.5K0.44 and 7.5K0.21 polymers show a slightly higher level of adsorption than those polymers with similar molar mass but with higher anchor fractions. The adsorbed amount rises linearly with the logarithm of molecular weight for the lower anchor fraction polymers in a similar way to homopolymers in a poor solvent. The insignificant adsorption was observed for the 10K0.06, the polymer with the lowest anchor fraction in the range studied, which confirms the strong influence of polystyrene block on the adsorption process.

### 9.4.1.3. Theoretical Predictions for the Adsorbed Amount

The SCF model of Evers[15] and Fleer[16] was used for the theoretical calculations for estimating the polymer adsorption at the carbon/cyclohexane interface. The Flory parameters ($\chi$) used for these calculations were taken as $\chi_{CH} = 0.00$, $\chi_{CS} = -4.00$, $\chi_{CP} = -1.00$, $\chi_{PS} = 2.00$, $\chi_{HP} = 0.45$ and $\chi_{HS} = 0.5$. Where H stands for cyclohexane (solvent), C for the carbon surface, P for hydrogenated-polyisoprene monomers and S for polystyrene monomers. The solvent-polymer interaction parameters were chosen from the literature[22] in the light of results derived from the molecular modelling and the known properties of the polymers.

Figure 9.5 presents the dependence of the experimentally measured adsorbed amount for the PS-HPIP diblock copolymers as a function of the anchor fraction (polystyrene block fraction) for polymers; the molecular weight range 7 to 17 K (•) and 100 to 150K (o). Inset into this figure is the adsorbed amount ($\theta$) calculated for the same set of copolymers using the SCF model.[15,16] A slow continuous rise in the adsorbed amount is observed for the small molar mass polymers for both the experimental as well as theoretical curves. Whilst, the data (both measured and calculated) shown for a limited number of high molar mass polymers (100K and 153K)

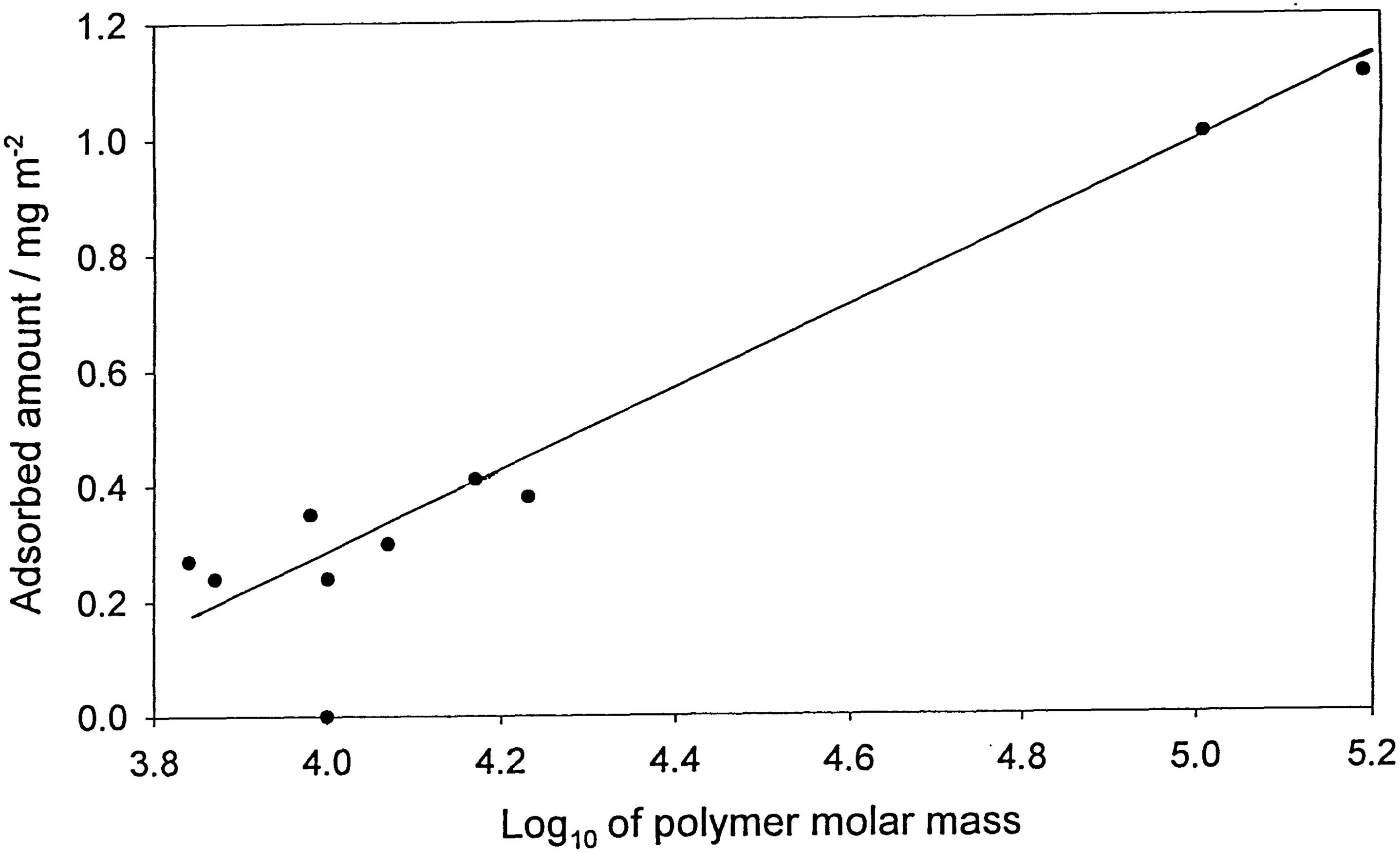


***Figure 9. 4 presents the adsorbed amount for the diblock copolymers as a function of the $log_{10}$ of total polymer molar mass adsorbed at cyclohexane/carbon interface.***

give high adsorbed amounts.

Table 9. 3: experimental and theoretical amount adsorbed for the PS-HPIP diblock copolymers adsorbed at cyclohexane/carbon interface

| Polymer | $\upsilon_A$ | Γ/±1.2% (mg $m^{-2}$) | Adsorbed amount/θ | Polymer | $\upsilon_A$ | Γ/±1.2% (mg $m^{-2}$) | Adsorbed amount/θ |
|---|---|---|---|---|---|---|---|
| 10K0.82 | 0.82 | 0.24 | 0.35 | 11.8K0.56 | 0.56 | 0.30 | 0.28 |
| 10K0.06 | 0.06 | 0.00 | 0.02 | 9.5K0.44 | 0.44 | 0.35 | 0.15 |
| 17K1.00 | 1.00 | 0.38 | 0.85 | 100K0.22 | 0.22 | 1.00 | 2.80 |
| 14.7K0.85 | 0.85 | 0.41 | 0.60 | 7.5K0.21 | 0.21 | 0.24 | 0.03 |
| 7K0.57 | 0.57 | 0.27 | 0.10 | 153K0.2 | 0.20 | 1.10 | 3.70 |

Figure 9.6 shows the dependence of the adsorbed amount on the mole fraction of the polystyrene block (anchor fraction) for a series of diblock copolymers of varying total polymer molar mass (Mw~10 K to 100 K) determined using the SCF model.[15,16] Each curve in this figure represents a copolymer of constant total polymer molar mass but varying PS-HPIP composition. For low total molar mass samples (up to Mw~20 K) a constant increase in the adsorbed amount is observed with increasing polystyrene block content and is in coincident with the experimental measurements. For very short chain samples the maximum in the curve is absent as in such cases the total adsorption energy per chain becomes too low to support the formation of a brush. However, for the case of high molar mass samples a maximum in the adsorbed amount is observed, since, the adsorption energy per chain is enough to support the formation of thick adsorbed layers. Due to the unavailability of samples, our measurements were confined to two high molar mass samples, 100K and 153K, (*see* 'o' in Figure 9.5) and show a good qualitative agreement with the calculated data. The maximum in the curve is observed to shift from high to lower anchor fraction region and to become sharper with increasing total polymer molar mass.[15] For instance, the PS-HPIP

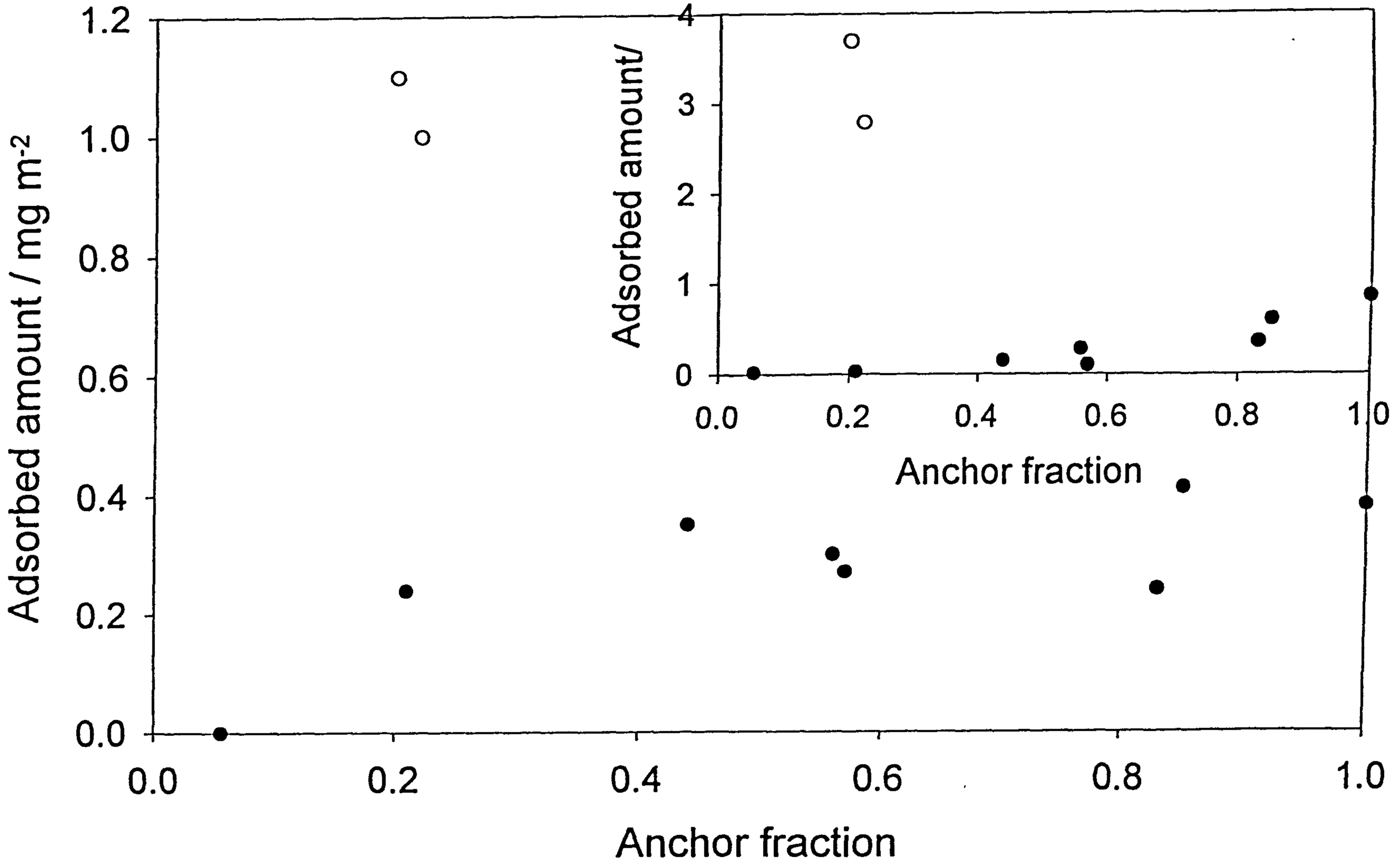


***Figure 9. 5 presents the dependence of the experimentally measured adsorbed amount on the anchor fraction determined for a series of polymers of molecular weight range 7 to 17 K (●) and 100 to 150K (○). Inset into this figure is the adsorbed amount calculated for the same set of polymers using the SCF model.***

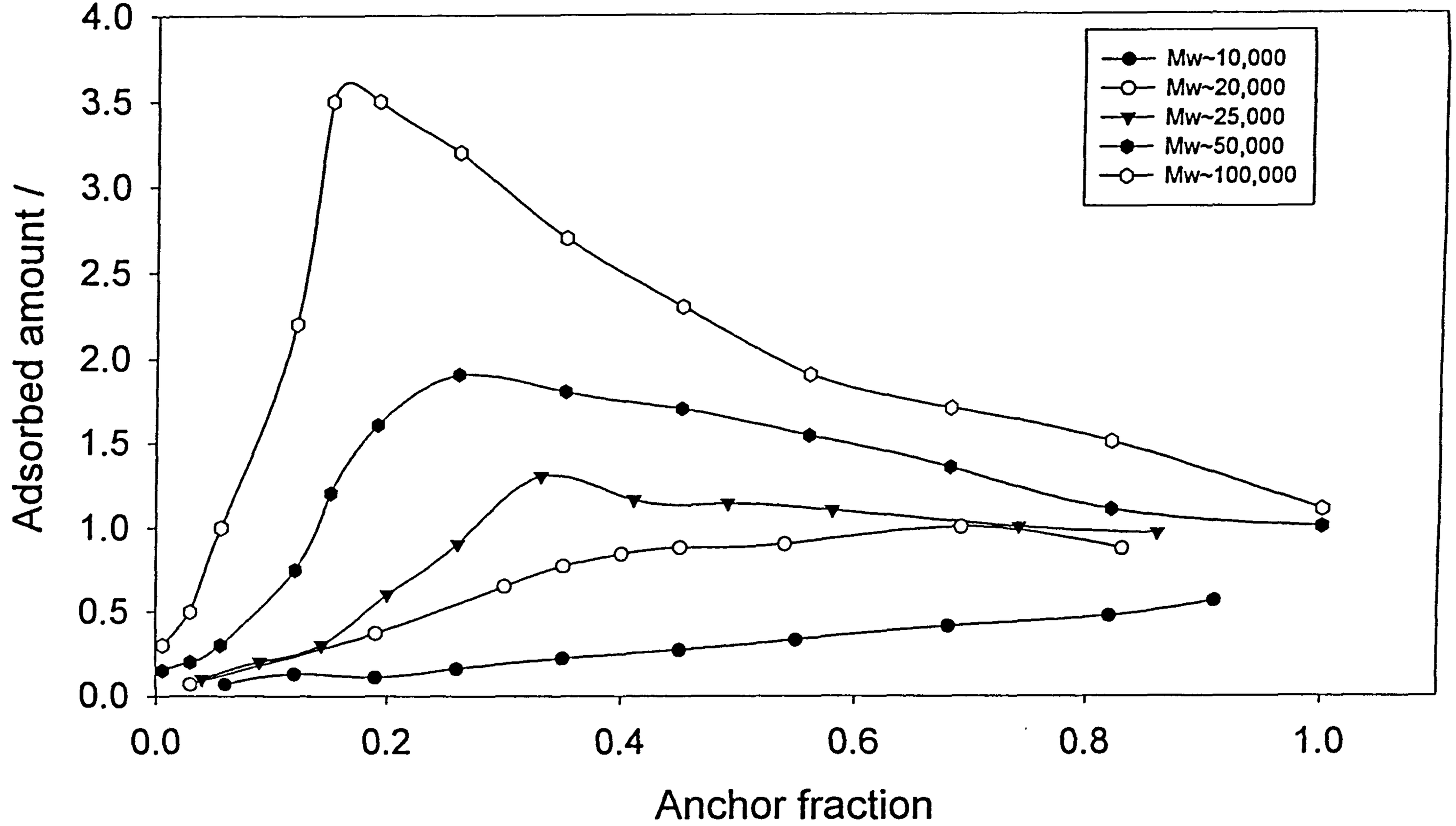


***Figure 9. 6 presents the dependence of the adsorbed amount on anchor fraction for a series of diblock copolymers of varying total polymer molar mass determined using the SCF model: Mw ~ ● 10 K, ○ 20 K, ▼25 K, ● 50 K and ● 100 K.***

copolymer with a total polymer molar mass ~20K (N ~ 225), $\nu_A^{max}$ (the point showing the maximum adsorbed amount) is found to be 0.69; for the case of a copolymer of Mw ~ 100K (N ~ 1550) $\nu_A^{max}$ this shifts to ~ 0.19. These data highlight the transition between the buoy dominated regime ($\nu_A < 0.2$) and the anchor regime ($\nu_A > 0.2$).[23]

Figure 9.7 presents the dependence of the adsorbed amount (calculated using the SCF model)[15,16] on the anchor fraction for a series of diblock copolymers of varying total polymer molar mass but constant polymer monomer number (N ~100, 300 and 500). Each curve in this figure represents copolymers of constant chain length (N) but varying polymer composition (varying polymer molar mass and/or *anchor-buoy* ratio). The data show a strong influence of the polymer composition on the adsorbed amount. The trends observed in the pattern of the data are similar to those measured previously, for instance see Figures 5.7, 6.6, 7.10 and 8.11.

Figure 9.8 shows the dependence of maximum adsorbed amount, $\theta_{max}$, on total polymer molar mass determined for a set of high molar mass polymers calculated using the SCF model.[15,16] The data show an approximately linear relation between the two parameters and are in a good agreement with those measured, *see* Figure 9.4.

## 9.5. Conclusion

The adsorption isotherms for a series of diblock copolymers (polystyrene-block-hydrogenated polyisoprene) with different polymer composition have been determined at the cyclohexane/carbon black interface both experimentally and theoretically. The conformation of the adsorbed polymer layer is largely determined by the surface-copolymer interaction, especially by the carbon-polystyrene block interactions. An estimation of the relative adsorption affinities of the two polymers (PS and HPIP blocks) was determined using the self-consistent mean field (SCF) model of Scheutjens and Fleer. For the cyclohexane/carbon system the polystyrene blocks are presumed to adsorb preferentially to the hydrogenated-polyisoprene blocks though the poor solvency of the polystyrene block also aids adsorption. It is evident that the polymers 10K0.82 and 10K0.06 with the same total molar mass but very different anchor-buoy ratios behave in a very different manner when adsorbed on carbon black. The 10K0.06 with

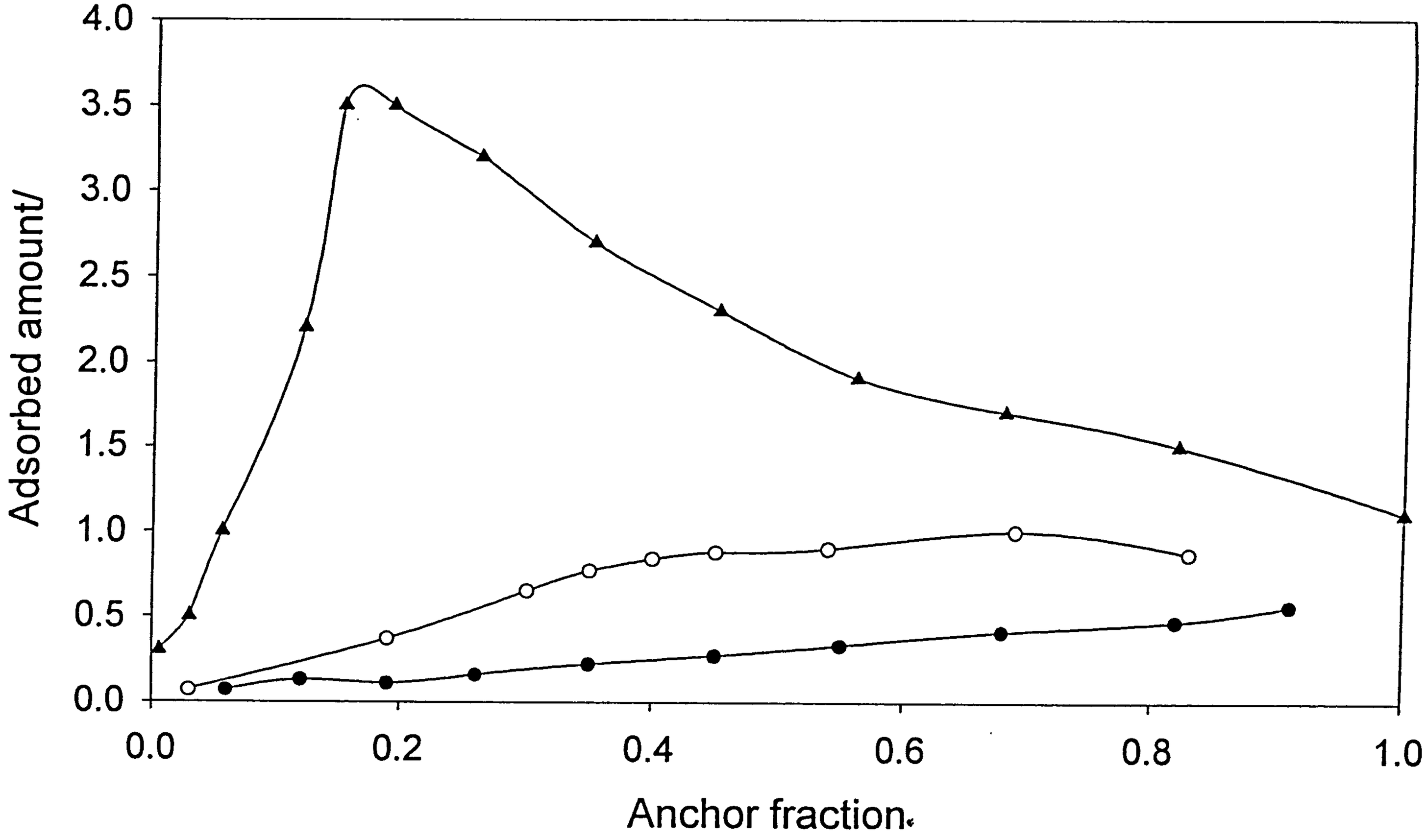


***Figure 9. 7 presents the dependence of the adsorbed amount (calculated using the SCF model) on the anchor fraction for diblock copolymers of varying total monomer number, N: N ~ ● 100, ○ 300 and ▼ 500.***

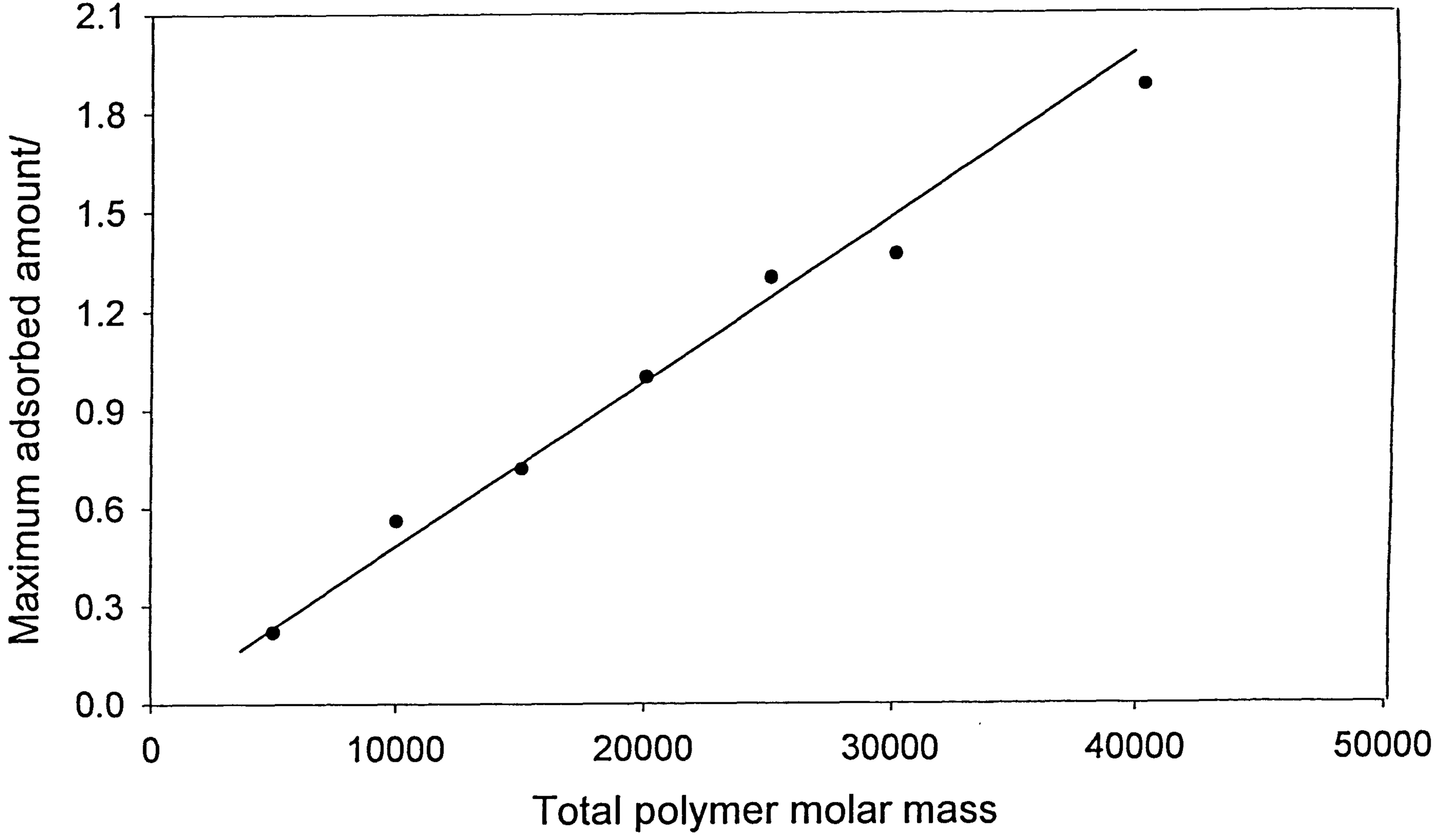


*Figure 9. 8 shows the dependence of maximum adsorbed amount, $\theta_{max}$, on total polymer molar mass determined for a set of high molar mass polymers calculated using the SCF model.*

a very low anchor fraction (0.056) behaves very much like a hydrogenated-polyisoprene homopolymer and shows a lower affinity for the carbon black surface. It was also observed that polymers with similar anchor fractions but different total polymer molar masses (*i.e.* copolymers 100K0.22 and 153K0.20) adsorb at different levels indicating the dependence of the adsorbed amount on the overall molar mass.

The dependence of the adsorbed amount on the anchor fraction has been calculated for a range of copolymers of varying composition (Mw ~ 5 K to 150 K) using the SCF model.[15,16] A constant increase in the adsorbed amount with increasing polystyrene block fraction in the samples is observed for the low total molar mass samples (up to Mw ~ 20 K). However, for the case of the high molar mass samples a maximum in the adsorbed amount is observed, which shifts from high to low anchor fraction and becomes sharper as the total polymer molar mass increases. In general, it can be said that the adsorbed amount of these diblock copolymers depends strongly on the total polymer molar mass and the block composition. Overall, a good qualitative agreement is observed between the measured as well as the theoretical data.

[1] Killmann, E., Maier, H., and Baker, J. A., *Colloids Surf.* 1988, **31**, 51.

[2] Baker, J. A., Pearson, R. A., and Berg, J. C., *Langmuir* 1989, **5**, 339.

[3] Baker, J. A., and Berg, J. C., *Langmuir* 1988, **4**, 1055.

[4] Kayes, J. B., and Rawlins, D. A., *Colloid Polym. Sci.* 1979, **257**, 622.

[5] Tadros, Th. F., and Vincent, B., *J. Phys. Chem.* 1980, **84**, 1575.

[6] Alexandridis, P., Holzwarth, J. F., and Hatton, T. A., *Macromolecules* 1994, **27**, 2414.

[7] Cosgrove, T., Mallagh, L. M., Ryan, K., and Scheutjens, J. M. H. M., *J. Surface Sci. Technol.* 1988, **4**, 81.

[8] Tiberg, F., Malmsten, M., Linse, P., and Lindman, B. *Langmuir*, 1991, **7**, 2723.

[9] Cosgrove, T., *J. Chem. Soc., Faraday Trans-1* 1990, **86**,1323

[10] Van de Steeg, L. M. A., Golander, C. G., *Colloids and Surface* 1991, **55**, 105.

[11] Napper, D. H., "Polymeric Stabilization of Colloidal Dispersions", Academic, London, 1983.

[12] Schroen, C. G. P. H., Cohen-Stuart, M. A., van der voort Maarschalk, K., van der Padt, A., and van't Riet, K., *Langmuir*, 1995, **11**, 3068.

[13] Van der Beek, G. P., and Cohen-Stuart, M. A., *Langmuir*, 1991, **7**, 327.

[14] Mayo, S. L., Olafson, B. D., and Goddard, W. A., *J. Phys. Chem.*, 1990, **94** 8897.

[15] Evers, O. A., Scheutjens, J. M. H. M., and Fleer, G. J., *J. Chem. Soc. Faraday Trans.* 1990, **86**, 1333.

[16] Cohen-Staurt, M. A., Waajen, F. W. H., Cosgrove, T., Vincent, B., and Crowley, T. L., *Macromolecules*, 1984, **17**, 1825.

[17] Manufacturer's "Shell" statement for the physicochemical properties of the copolymers.

[18] Cosgrove, T., and Salt, M, Shell Report 2 1996.

[19] Garvey, M. J., Tadros, Th. F., and Vincent, B., *J. Colloid and Interface Sci.*,1974, **49**, 57.

[20] Boomgaard, V., Th. King, T. A., J. *Colloid and Interface Sci.* 1978, **66**, 68.

[21] Nuysink, J., and Koopal, L. K., *Talanta*, 1982, **29**, 495.

[22] Orwoll, R. A., *Rubber Chemistry and Technology*, 1977, 50, 451.

[23] Wu, D. T., Yokohama, and Setterquist, *Polymer, J.*, 1991, **23**, 711.

# Chapter 10

# *SMALL-ANGLE NEUTRON SCATTERING*

## 10.1. Introduction

Many different forms of radiation have been used to probe the structure and properties of bulk and solvated macromolecules in the colloidal systems. The many advantages include:

(1) The scattered radiation can be collected instantaneously from about $10^7$ particles and hence the technique is suitable for dilute or a small quantity of sample.

(2) Since these techniques generally involve very small energy transfer, samples are illuminated with minimal possible risk of chemical change or damage.

(3) The investigations are performed by direct methods without disturbing the sample.

(4) Scattering techniques are very versatile due to the availability of a wide variety of detectors, radiation wavelengths and detection angles.

Visible light is the most widely used form of radiation and may be used for the determination of molecular weight and particle size of colloidal systems. Since, the resolution of visible light is limited by the wavelength, this type of radiation is not suitable for certain applications such as the determination of molecular architecture.

Due to having many special characteristics neutrons are often used to study polymer adsorption at interfaces in colloidal systems. Small-angle neutron scattering (SANS) and neutron reflectivity have been widely used and are the most powerful techniques available for determining the radius of gyration of a polymer in solution, and polymer adsorption and conformation, in different environments.[1,2] An important facet of SANS is that by varying the hydrogen-deuterium ratio in the system, it becomes

possible to choose (highlight) certain parts of the structure for study and eliminate the others by so-called "contrast matching".[3] This is analogous to refractive index matching in light scattering. One limiting factor in SANS is the time available at a neutron facility. X-rays techniques are similar to neutrons, however, they are largely unsuitable for the probe of polymer systems, since the magnitude of the scattering depends upon the atoms involved and protonated systems have poor contrast. However, X-rays (wavelengths 0.1 to 1.2 nm) are able to probe much smaller distances within the macromolecule than light (wavelengths ~ 400 to 600 nm). Contrast matching requires changing the chemical nature of the system (atomic exchange).

### 10.1.1. Neutron

The nucleus of an atom is comprised of positively charged protons and uncharged particles called neutrons. The neutron has a magnetic moment and a mass (m) virtually equal to that of a proton *i.e.* $1.66 \times 10^{-27}$ kg. The interaction of neutrons with nuclei is governed by nuclear forces and also by magnetic forces, if unpaired electrons are present. Neutrons travel with a de Broglie wavelength, $\lambda$, which is given by the following relation.

$$\lambda = h / mv \qquad \text{Equation 10. 1}$$

where h = Planck's constant and $\nu$ is the neutron velocity. Neutrons used for the scattering experiments are generally produced in a nuclear reactor or spallation source.

The intensity of small-angle X-ray scattering (SAXS) is governed by the interaction of the incident X-rays with the electron cloud of the target atom. As such, a number of limitations are apparent when SAXS is applied to the determination of macromolecular structure and properties. Firstly, the incorporation of atoms, which are strong scatterers, will generally perturb the macromolecule and secondly there is little or no isotopic sensitivity variation of SAXS since the electron cloud remains similar between isotopes.

In contrast, neutrons are scattered predominantly by short-range interactions with nuclei of atoms in the sample material. The scattered intensity varies between

elements and between their isotopes and this isotopic variation is used to achieve contrast variation with little or no perturbation to the system. The commonest isotopic variation is the substitution of deuterium for hydrogen.

SANS may be used to determine the conformation of adsorbed polymer layers normal to the interface without perturbing the structure of that layer. At present the SANS technique is one of the few means of measuring the volume fraction profile of an adsorbed polymer. Recently, a number of studies have been reported for polymers adsorbed at the solid/liquid interface.[4] Higgins *et al.*[5] investigated the distribution of anchor segments of a chemisorbed block copolymer polystyrene (PS) and poly(dimethyl siloxane) (PS/PDMS) and the scattering was observed from the PDMS as well as PS blocks, hence, it was difficult to interpret the data observed.

Barnett *et al.*[6,7,8] first presented studies of the density distribution within the adsorbed layer for both physically adsorbed and terminally attached polymers on a polystyrene latex substrate and observed a good qualitative agreement with the theoretical predictions by Scheutjens and Fleer.[9]

Further work by Cosgrove and co-workers; have studied many different polymers in different systems, PS/silica/$CCl_4$[10], polyelectrolyte/latex/water[11] and ABA block copolymers adsorbed at the liquid/liquid interface.[12] Where possible, comparisons with theoretical predictions were made and good agreement in the shape of the density profiles was observed.

The following sections describe the theory of the SANS technique and its application to the study of colloidal dispersions, particularly the use of coherent and elastic scattering to determine the volume fraction profiles of adsorbed copolymers. Also a new method for calculating the volume fraction profile is described and comparisons made with the Crowley method.[13]

## 10.2. SANS Theory

### 10.2.1. General:

Nuclear interactions are very short range, $10^{-15}$ m, thus, compared to the wavelengths of the low energy neutrons (and to develop scattering theory) the nucleus maybe considered as a point scatterer. The intensity of the scattered neutrons does not follow any simple rule, however, it is dependent on the nucleus and to some extent on its mass.

### 10.2.2. Scattering Lengths of the Atoms

The intensity of the interaction between the neutron and the atom is described by the scattering length density of the atom and is proportional to the square of the scattering length, b. In a real system, many atoms present in the sample may scatter the neutron waves. This may give rise to the following consequences.

(a) Interference between neutron waves scattered by different nuclei of the samples: the analysis of which may give us information about molecular conformation.

(b) Since the atoms may not be rigidly fixed in space, the scattering will be inelastic and may be similar to a Doppler shift in conventional light scattering. This type of scattering will not be considered in this discussion.

The scattering cross section of the nucleus is said to be an alternative measure of the scattering strength of an atom and can be defined as;

$$\sigma = 4\pi b^2 \qquad \text{Equation 10. 2}$$

When the neutrons interact, normally, three types of neutron scattering processes are observed *i.e.* elastic, inelastic and quasi-elastic scattering. Different properties may be investigated by the observation of these different forms of scattering. The elastic scattering gives information regarding the structural and conformational properties of the polymers under study. It becomes relatively complicated to understand for the case when atoms possess a nuclear spin, *e.g.*, a proton, as in such cases the scattering cross-section must be split into two parts called the coherent (phase conserved) and

incoherent (phase randomised) cross-section. The elastic, incoherent scattering is isotropic and contains no direct structural information about the system and so its overall effect is to generate a background scattering irradiation to the coherent scattering.

$$\left|\bar{K}\right| = \frac{2\pi}{\lambda}$$

For the event of an elastic scattering to occur the magnitudes of the incident, $K_i$, and scattered, $K_s$ wave vectors are equal. In a SANS experiment the intensity ($I$) is measured as a function of scattering vector, $Q$, where, $Q$ is given by

$$\bar{Q} = \bar{K}_i - \bar{K}_s = 2\left|\bar{K}\right|\sin\frac{\theta}{2} \qquad \text{Equation 10. 3}$$

By substitution

$$Q = \frac{4\pi}{\lambda}\sin\frac{\theta}{2} \qquad \text{Equation 10. 4}$$

Where $\lambda$ is the wavelength of the incident neutrons and $\theta$ is the scattering angle. The structure of an adsorbed polymer layer can be studied by selecting a suitable $Q$ range.

### 10.2.3. Scattering from Spherical Colloidal Particles

The scattering from spherical colloidal particles with and without adsorbed polymer layers will be discussed in this section. The scattering of radiation by a point, P, on a particle in the direction defined by the vector, $K_s$, is presented by the following relationship (*see* Figure 10. 2).

$$A_p = A_0 f_p e^{-i\bar{Q}.\bar{r}} \qquad \text{Equation 10. 5}$$

Where $A_p$ is the amplitude of the scattered radiation, $A_o$ is the amplitude of incident radiation, r defines the position vector between the point P and the particle centre, 0, and $f_p$ is the scattering factor at point P.

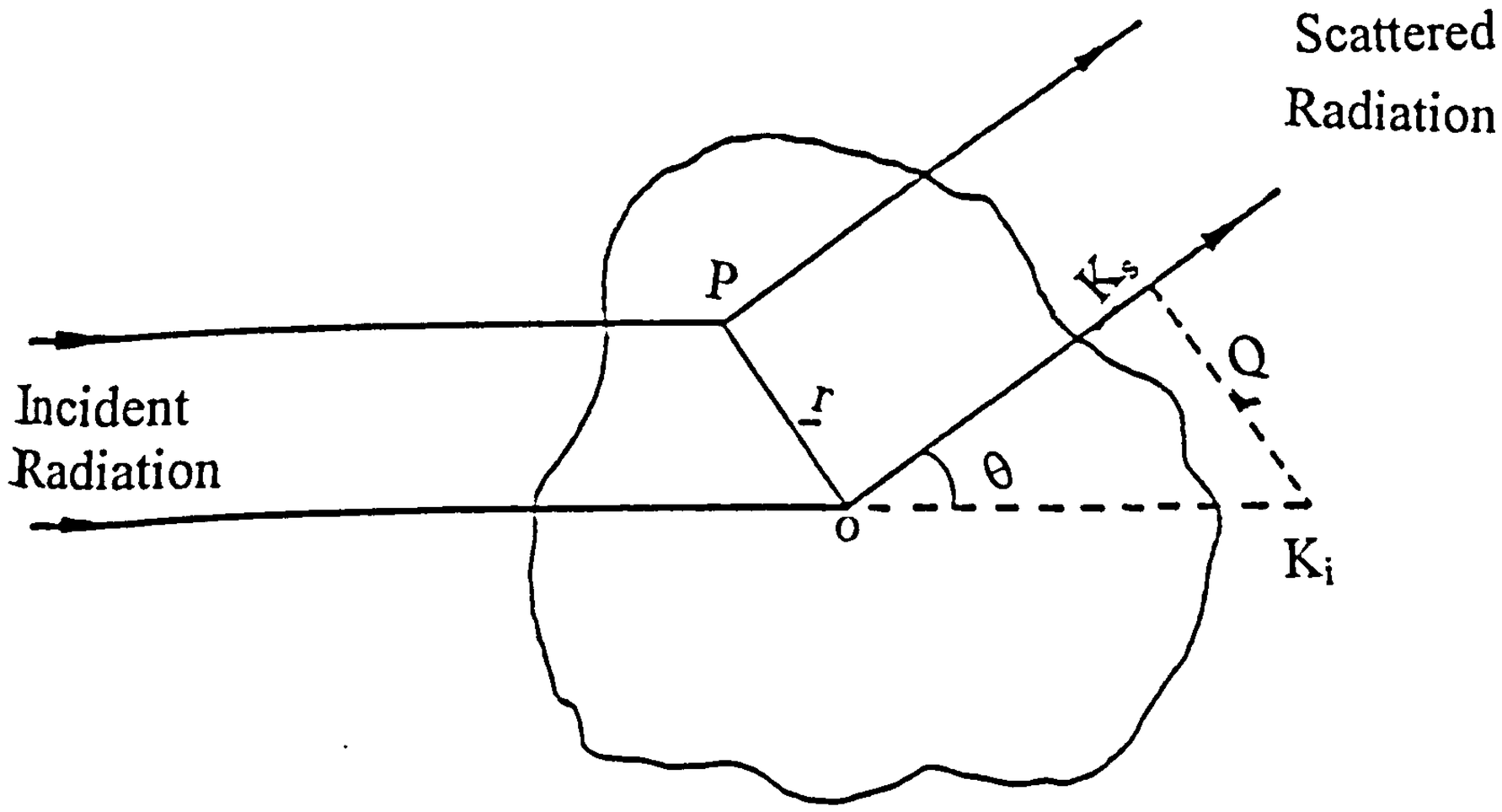


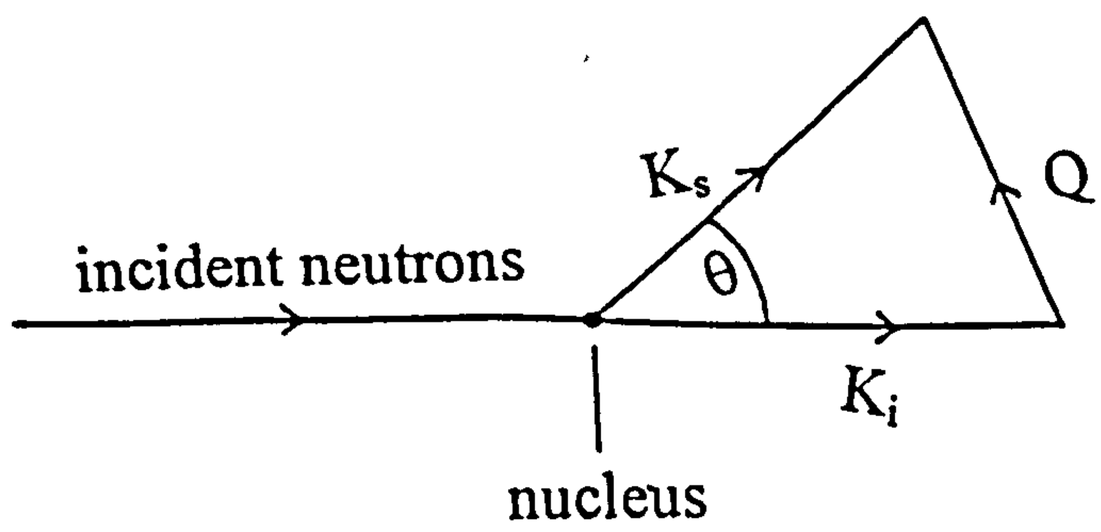


*Figure 10.2: schematic representation of the scattering from a particle.*

The total scattering intensity, $I(Q)$, arising from a whole particle, is given by the square of the sum of amplitudes $A_p$;

$$I(Q) = I_{II}\left|\sum_p f_p e^{-i\bar{Q}.\bar{r}}\right|^2 \qquad \text{Equation 10. 6}$$

Where the summation is made for all of the scattering particles. The scattered intensity of the radiation is the square of the amplitude as $(I_{II} = A_o^2)$

The form factor of the particle, F(Q), is defined as the ratio of the total scattered amplitude, $A_p(Q)$, to the incident radiation, $A_0$

$$F(Q) = \sum_p \frac{A_p(Q)}{A_o} = \sum_p f_p \cos(\bar{Q}.\bar{r}) \qquad \text{Equation 10. 7}$$

For simplicity, consider that an incident flux, $I_{II}=1$ neutron $sec^{-1}$ $cm^{-2}$ then the above equation will reduce to

$$I(Q) = F^2(Q) \qquad \text{Equation 10. 8}$$

It is presumed that since the rotation about the centre of the particle (*see* Figure 10. 2) will not bring about any modification in the distribution of the scattering centres, hence, $F(Q)$ will remain constant over all orientations.

$$F(Q) = \int_0^\infty \rho_{(r)} \sin\frac{(\bar{Q}.\bar{r})}{Q.r} 4\pi r^2 dr \qquad \text{Equation 10. 9}$$

A number of simplifications can be made from the assumption that the scattering particle is centrosymmetric and is dispersed in a continuous medium of scattering density, $\rho_o$. The total scattering must be considered as the superposition of a continuous medium of solvent, with scattering length density $\rho_o$ and isolated particles with scattering length density $\rho_{(r)} - \rho_o$.

hence,

$$I(Q) = F^2(Q) = 16\pi^2 \left| \int_0^\infty \Delta\rho_{(r)} \sin \frac{(\bar{Q}.\bar{r})}{\bar{Q}.\bar{r}} r^2 dr \right|^2 \qquad \text{Equation 10. 10}$$

Where, $\Delta\rho_{(r)}$ is given by the relation;

$$\Delta\rho_{(r)} = \rho_{(r)} - \rho_o \qquad \text{Equation 10. 11}$$

For a given homogeneous particle, $\Delta\rho_{(r)}$ is a constant, $\Delta\rho_{ps}$, within the radius of the particle, $r_o$, and zero for $r > r_o$, hence;

$$I(Q) = 16\pi^2 \left| \int_o^{ro} \Delta\rho_p \sin \frac{(Q.r)}{Q.r} r^2 dr \right|^2 \qquad \text{Equation 10. 12}$$

$$F(Q) = F\ \rho(Q)\Delta\rho_{ps} \qquad \text{Equation 10. 13}$$

Various components can selectively be made 'invisible' to the neutrons by varying the scattering length density of the continuous phase (solvent), to the point where it matches to a particular component (for example by isotopic substitution). This can be arranged by adding $D_2O$ in the case of an aqueous system until observed scattering from the particle becomes zero *i.e.* $\Delta\rho_{(r)} = 0$ and is known as "contrast matched".

### 10.2.4. Scattering from the systems with physically adsorbed polymer layers

According to Crowley,[13] the total scattering from a dispersion of particles with an adsorbed layer is given by;

$$I(Q) = I_{pp}(Q) + I_{p\ell}(Q) + I_{\ell\ell}(Q) + I_{inc}. \qquad \text{Equation 10. 14}$$

Where $I_{pp}(Q)$ is the scattering from the pure particles, $I_{\ell\ell}(Q)$ scattering due to the

average structure of the adsorbed polymer layer which in this case includes a fluctuation contribution arising from spatial variations in the concentration of polymer in the layer, $I_{p\ell}(Q)$ is a particle-layer interference term and $I_{inc}$ is a incoherent background which in this case is a Q independent term, where, the momentum transfer vector, Q, can be defined according to Equation 10. 4, if $\phi_p$ is the total particle volume fraction, r the particle radius and $\rho$ is the neutron scattering length density of the particle (p) and solvent (s) and polymer ($\ell$) respectively.

The scattering from the bare particles is given by a form of Porod's law[14] which has its validity only for the values of $Qr >> 1$) and takes account of the particle polydispersity. The scattering due to the pure particles can be defined as;

$$I_{pp}(Q) = \frac{6\pi\phi_p(\rho_p - \rho_s)^2}{Q^4 r} \qquad \text{Equation 10. 15}$$

The interference term, which has no fluctuation contribution,[13] averaged over instrument resolution and particle polydispersity, is given by;

$$I_{p\ell}(Q) = 2\frac{6\pi\phi_p(\rho_p - \rho_s)(\rho_\ell - \rho_s)}{Q^4 r^2}\left[\int_0^t \phi(z)\cos(Qz)dz - Qr\int_0^t \phi(z)\sin(Qz)dz\right]$$

Equation 10. 16

Where $\phi(z)$ is the volume fraction of polymer at a distance z normal to the interface, t is the thickness of the layer and $\rho_\ell$ is the neutron scattering length density of the layer. The interference term ($I_{p\ell}(Q)$) can be used to obtain a characteristic volume fraction profile for the polymer layer. However, to do so a larger number of measurements are required, and an extra care is required in the preparation of the samples and their respective backgrounds. In practice, it is easier to use the $I_{\ell\ell}(Q)$ term described below.

The isotopic composition of the solvent in which the particles are dispersed is adjusted in order, to selectively suppress the scattering from the particles; a condition commonly referred to as "contrast match". At contrast match conditions both the terms $I_{pp}(Q)$ and $I_{p\ell}(Q)$ become zero (since $\rho_p - \rho_s = 0$), and so the scattering observed is due

to the adsorbed layer only ($I_{tt}(Q)$), and is given by the relation;[13,15,16,17]

$$I_{tt}(Q) = \bar{I}(Q) + \tilde{I}(Q)$$

Equation 10. 17

Where $\bar{I}$ is the scattering from the average structure of the adsorbed layer and $\tilde{I}$ is the scattering from spatial concentration fluctuations and are detailed as below. In Crowley's analysis, the fluctuation contribution is ignored and the scattering is described only in terms of the scattering due to the average concentration in the adsorbed layer *i.e.* $I_{tt}(Q) = \bar{I}$, and is given as follows;

$$\bar{I}(Q) = \frac{6\pi(\rho_t - \rho_s)^2 \phi_p}{Q^2 r} F(Q)$$

Equation 10. 18

Where $\rho_t$ is the scattering length density of the polymer layer. The surface form factor, F(Q), is given by the relation;[13]

$$F(Q) = \left[\sin(Qr)\left(\int_0^t \phi(z)\cos(Qz)\right) + \cos(Qr)\left(\int_0^t \phi(z)\sin(Qz)\right)\right]^2$$

Equation 10. 19

Assuming that the adsorbing particle is monodisperse and that the scattering instrument has infinite Q resolution, the equation describes the scattering from the layer. It has widely been assumed[7,18,19,20] that to simplify the Equation 10. 18 neither of these criteria could be met. If $\Delta(Qr)$ is the spread in Qr arising from the polydispersity in the particle size ($\Delta r$) and finite instrumental Q resolution ($\Delta Q$) such that;

$$\Delta(Qr) = Q\Delta r + r\Delta Q >> 1$$

Equation 10. 20

Then scattering from the layer Equation 10. 18 can be simplified to;[13]

$$\bar{I}(Q) = \frac{6\pi(\rho_t - \rho_s)^2 \phi_p}{Q^2 r}\left|\int_0^t \phi(z)\exp(iQz)dz\right|^2$$

Equation 10. 21

The substrate used in this study was reasonably low polydisperse latex (± 11.1%) and the camera used was high Q resolution D22 camera. Such an experimental set-up precluded the use of the simplification introduced in Equation 10. 20, which, means that Equation 10. 21 can no longer be used to describe the scattering from the adsorbed polymer layer. Hence, Equation 10. 18 must be modified to account for both of these features.

The particle polydispersity has been accounted for using the standard zeroth order logarithmic distribution, which is known to describe latex particle size distributions. If p(r) is the probability of the occurrence of a particle with radius r, $r_m$ is the modal particle radius, σ describes the width and skewsness of the distribution and C is a normalisation constant such that the sum of the probabilities is unity, then the distribution is given by;

$$p(r) = \frac{\exp\left[-\frac{\left(\ln r - \ln r_m\right)^2}{2\sigma^2}\right]}{(2\pi)^{1/2}\sigma\, r_m \exp\left(\frac{\sigma^2}{2}\right)} \Big/ C$$

Equation 10. 22

Hence, Equation 10. 18 becomes as;

$$\bar{I}(Q,r) = \sum_r p(r)\frac{6\pi\left(\rho_\ell - \rho_s\right)^2\phi_p}{Q^2 r}F(Q,r)$$

Equation 10. 23

In order to overcome the finite Q resolution of the detector, the fit has been convoluted with a simple triangular resolution function with a variable width. This can be achieved by averaging the calculated intensity at a given Q point and is given by;

$$\bar{I}_{res}(Q) = \frac{\sum_{i=-n}^{i=+n} I(Q+i\alpha)}{2n+1}$$

Equation 10. 24

Where, α is the step which specifies the amount of smearing and 'n' is the number of steps.

The local variations (non-uniformity) in the average concentration of the

adsorbed layer gives rise to the $\tilde{I}$ term, the scattering due to fluctuations in the adsorbed layer. Cosgrove *et al.*[21] have indicated that the fluctuation term becomes insignificant if the radius of gyration ($R_g$) of the adsorbed polymer is smaller than that of the particle. However, a significant background can be observed for the systems having either a very high polymer density at the interface or large polymers adsorbed on smaller particles.[17,22] Auroy and Auvray *et al.*[15,16] consider that, in addition, to the incoherent background scattering effects, there was a significant contribution from the fluctuations in the adsorbed layer, however, the magnitude of these fluctuations strongly depends upon the structure of an adsorbed layer.

Auvray and Auroy describe the fluctuations in a grafted polymer brush as showing Lorentzian dependence in the following manner;

$$\tilde{I} = \frac{1}{1+\xi^2 Q^2}$$

Equation 10. 25

Where $\xi$ is a characteristic correlation length. The total scattering is given by;

$$I = \frac{C}{Q^2} + A\tilde{I} + B_{inc}$$

Equation 10. 26

Where, A and C are constants. C is considered to be associated with the average volume fraction and is independent of the profile shape at $\theta = 0$. According to Auvray *et al.*[23] the fluctuations in an adsorbed layer will be of the order $Q^{-4/3}$. By substitution the above equation becomes as follow;

$$I = \frac{C}{Q^2} + \frac{A}{Q^{\frac{4}{3}}} + B_{inc}$$

Equation 10. 27

By simplifying the above expression;

$$IQ^{\frac{4}{3}} = \frac{C}{Q^{\frac{2}{3}}} + A + Q^{\frac{4}{3}} B_{inc}$$

Equation 10. 28

This indicates that a flat incoherent background is obtained from the slope of a plot of $Q^{\frac{4}{3}}I vs Q^{\frac{4}{3}}$ whilst the intercept on the y-axis yields the magnitude of the fluctuation term.

The fluctuation term is a contribution to the scattering from the adsorbed layer as a result of spatial fluctuations in the polymer concentration within the layer. The work of Crowley[13] addressed the problem of scattering from adsorbed layers both at and away from particle contrast match. At contrast match the fluctuation term has been ignored because we argued that, in the limit of low Q, the fluctuation contribution is small. Whilst, in the limit of high Q, the scattering from fluctuations is of the order of the incoherent background and so deconvolution of the two terms is difficult. However, Auvray and de Gennes[15] have criticised this approach saying that the contribution due to fluctuations cannot be neglected. Using a scaling argument de Gennes[24] has demonstrated that for a volume fraction profile decaying as $z^{-4/3}$ (where z is the distance normal to the interface), the fluctuation term scales as $(Qa)^{-4/3}$, where a is the length of a segment. As a result, the measured scattering has been fitted to a combination of Crowley's original equation and a fluctuation term varying as $Q^{-4/3}$, thus;

$$I_{ll}(Q,r) = \sum_r p(r)\frac{6\pi(\rho_l-\rho_s)^2\phi_p}{Q^2 r}P(Q)+\frac{6\pi(\rho_l-\rho_s)^2\phi_p a^4}{(Qa)^{4/3} r}$$

Equation 10. 29

The data is fitted by mathematically creating a volume fraction profile, which can be selected from a variety of shapes such as exponential, gaussian, parabolic, *etc.* This profile is inserted into Equation 10. 29 and the result is smoothed with Equation 10. 24 in order to calculate the scattering from the polymer adsorbed layer. This calculated curve is compared with the measured scattering and the parameters describing the profile are varied using a non-linear regression until a best fit to the measured data is found. The most likely profile can then be selected on the basis of other available physical parameters such as adsorbed amount.

## 10.2.5. Contrast Match Condition

The scattering length density, ρ, for each molecule in a system may be calculated by the relationship given as under;

$$\rho = \frac{dN_A \sum b_i}{M} \qquad \text{Equation 10. 30}$$

Where d stands for the density of the material, $N_A$ for Avogadro's number, $\Sigma b_i$ stands for the sum of the scattering lengths of the atoms present in a molecule or polymer segment, whereas M stands for the polymer molar mass. The coherent aspect of the scattering length density may be given by $\rho = \frac{\Sigma b_i}{V}$, where $\Sigma b_i$ is sum of the both coherent and incoherent scattering length terms and V stands for the polymer molar volume. As polystyrene latex used may not be homogenous in its contents, hence, for this case "d" is taken as an average density. If $\Sigma b_i$, ρ and d for the various components of the system under study are known then it is possible to calculate the scattering length density (for polymer, solvent and particle), and also $\Delta\rho_{Ps}$ and $\Delta\rho_{lS}$ by using the above given equation. The contrast match is considered as the simplest form of analysis for the particles. Normally, the particle and the solvent used are chosen in such a manner so to achieve a very small $\Delta\rho_{Ps}$ and further by the addition of small amounts of another solvent or preferably by isotopic substitution (commonly proton/deuteron), ρ-solvent may also be adjusted to ρ-particle, ($\rho_p=\rho_s$) and hence, $\Delta\rho_{ps}$ may be brought to zero ($\Delta\rho_{ps}=0$). Isotopic substitution is preferred as addition of a different solvent can alter the configuration of the adsorbed polymer or even desorb it. Under these conditions the scattering from the layer, the incoherent scattering and the fluctuation term are observed. The aim of using contrast match is to use the correct combination of deuterated and protonated components to give the same scattering length density in both the phases in the system with the adsorbed polymer at two different scattering length densities.

### 10.2.6. Volume Fraction Profile of the Polymer Adsorbed Layer

The conformation of the polymer adsorbed layer can be determined from the two terms, $I_{ll}(Q)$ and $I_{pl}(Q)$ which, in turn, can be useful to determine the segment density distribution, $\rho(z)$, within that layer.

If the terms $I(Q)$, $I_{ll}(Q)$ and $I_{pp}(Q)$ are known then the term $I_{pl}(Q)$ (away from the contrast match) may be used to calculate $\rho(z)$ by the relationship;

$$I_{pl}(Q) = I(Q) - I_{ll}(Q) - I_{pp}(Q) \qquad \text{Equation 10. 31}$$

Using the trigonometric expansions for sine and cosine (Equation 10. 16) may be simplified to give; $(Q.r_0 >> 1)$

$$I_{pl}(Q) = \frac{16\pi^2 r_0^2}{Q^3}\int_0^t \rho(z)\sin(Qz)dz \qquad \text{Equation 10. 32}$$

$\rho(z)$ may be determined from the above equation by using the complex Fourier transform of intensity data as $Q^3 I_{pl}(Q)$. Barnett *et al.*[6] used this method to obtain the first reported segment density distribution for an adsorbed polymer, PVA/PS latex/water. The $I_{ll}(Q)$ term is effectively measured only at the contrast match condition between particle and the solvent *i.e.* when:

$$I_{pl}(Q) = I_{pp}(Q) = 0$$

Crowley[14] determined $\rho(z)$ at contrast match condition by obtaining $I(Q)$ data over a limited $Q$ range and the data was extrapolated using theoretical model and the resulting set, as $Q^2 I_{ll}(Q)$. An alternate method of determining $\rho(z)$ is first calculating the corresponding $I_{ll}(Q)$ using Equation 10. 17 and then the guessed $\rho(z)$ is iterated by a non-linear least squares.

### 10.2.7. Parameters Measurable from $I(Q)$ and $\rho(z)$

In addition to calculating term $\rho(z)$, the $I_{ll}(Q)$ term maybe used for calculating the following parameters.

(a) Second moment of the density distribution: $\sigma$ is the second moment of the layer and is given by the relation;

$$\sigma^2 = \langle z^2 \rangle - \langle z \rangle^2 \qquad \text{Equation 10. 33}$$

Where, z is the distance from the surface. The second moment is independent of any model of the volume fraction profile of the adsorbed polymer layer (*see* Figure 10. 1).

$$\langle z \rangle = \frac{\int (\phi(z) z) dz}{\int \phi(z) dz} \qquad \text{Equation 10. 34}$$

Where $\phi(z)$ is the probability for a segment *i.e.* the volume fraction being in layer z, and $\sqrt{\langle z^2 \rangle}$ is the rms. value of z. Further using the Guinier approximation $\left(i.e. \sigma^2 Q^2 < 1\right)$, Equation 10. 12 can be modified in such a manner to obtain a linear dependence of $\ln Q^2 I \, vs \, Q^2$ giving slope of $\sigma^2$ and is given as under;

$$I_{ll}(Q) = \frac{K_0}{Q^2} \exp(-\sigma^2 Q^2) \qquad \text{Equation 10. 35}$$

where $K_o$ is a normalisation constant and depends on $\Gamma$ (see over). Usually, a non-linear least square iteration procedure is applied for calculating $\sigma^2$ from the first 4 or 5 values of $I(Q)$ at low $Q$ and it ($\sigma^2$) is roughly a measure of the thickness of the adsorbed layer. Once the incoherent background and the fluctuations have been subtracted the scattered intensity of the layer becomes solely visible and can then be fitted.

(b) Adsorbed amount: It is represented by $\theta$, and is given by;

$$\theta = \int \phi(z) dz \qquad \text{Equation 10. 36}$$

where $\phi$ is the volume fraction profile. In order to calculate the absolute adsorbed amount, $\Gamma$, $\theta$ in the above mentioned equation is multiplied by the density, d, of the polymer.

$$\Gamma = d \int \phi(z) dz \qquad \text{Equation 10. 37}$$

After calculation of $\rho(z)$ the profile is normally converted to a volume fraction profile, $\phi(z)$.

The volume fraction profile gives both the layer thickness, $\delta$, and the bound fraction, p. The layer thickness is calculated in the similar manner as suggested elsewhere in the literature,[1] whilst, the volume fraction profile, $\rho$, is calculated by integration of $\rho(z)$ to a value of z corresponding to the thickness of an adsorbed polymer segment.

## 10.3. SANS Experimental

### 10.3.1. The Experimental System

The overall aim in designing a system is to contrast match the particle and the solvent so that the $I_{II}(Q)$ term alone is effectively measured. Additionally, it is desirable, though not always possible, to minimise the number of incoherent scatterers in the system, e.g. protons, as this type of scattering must be subtracted prior to analysis. As the adsorbed polymer is present in relatively low concentrations, the greater the proton content of the solvents, the larger the signal-to-noise ratio. Polymer in solution, at equilibrium with adsorbed polymer, must also be minimised, as this constitutes another background, which must be subtracted if significant. The density profiles were to be determined for polymer samples adsorbed onto polystyrene particles.

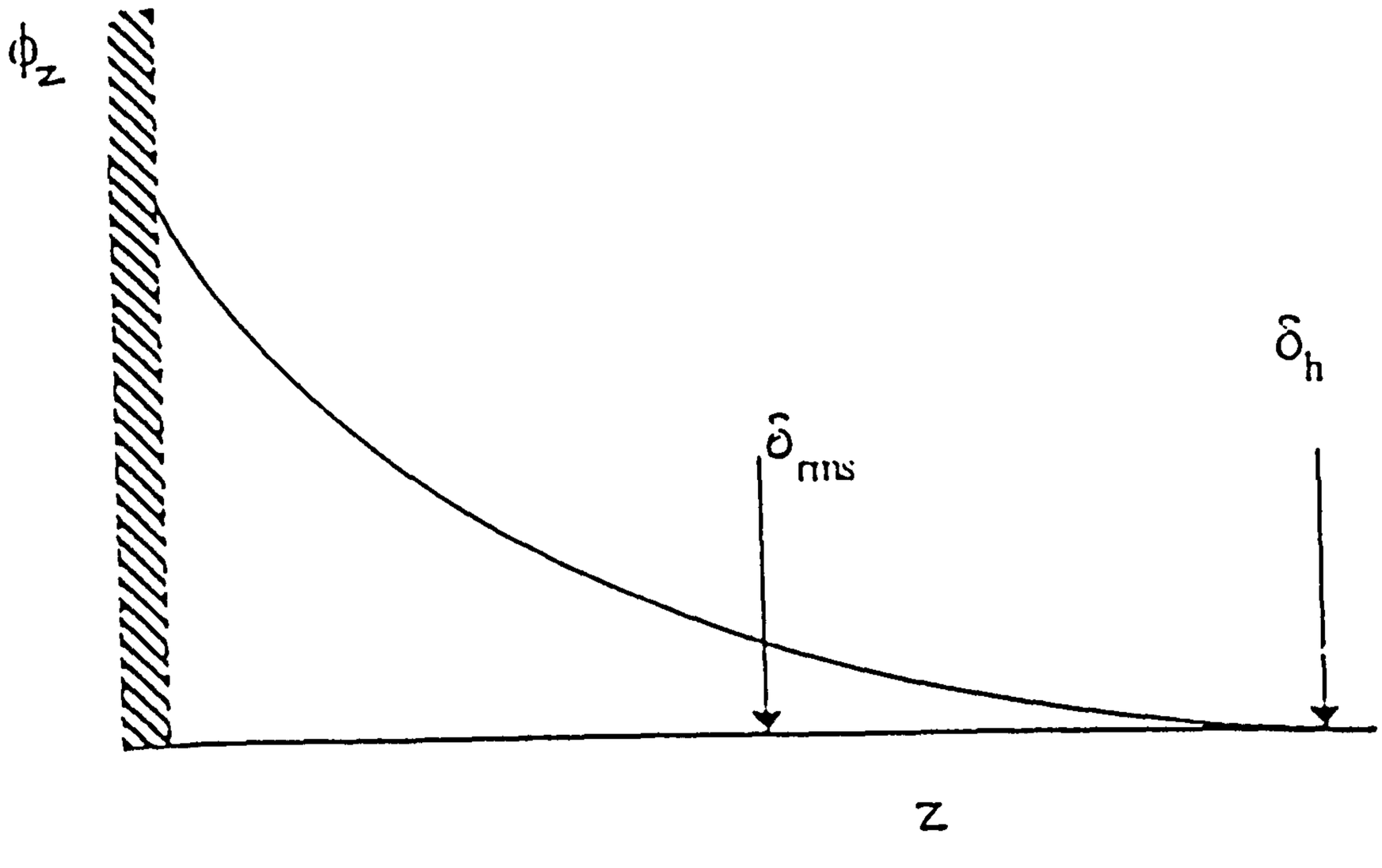


*Figure 10.3: Schematic diagram of a typical volume fraction profile.*

$\Delta\rho_{ps}$ and $\Delta\rho_{ls}$ can be determined by the following relation, whilst, the scattering length density of the solvent is considered as the reference state

$$\Delta\rho_{ps} = (\rho_{particle} - \rho_{solvent})$$

$$\Delta\rho_{ls} = (\rho_{polymer} - \rho_{solvent})$$

The equilibrium concentration of the samples was fixed at 100 ppm, *i.e.* full coverage for the samples, and to subtract the scattering from a 100 ppm polymer solution as this concentration may yield some background scattering.

## 10.3.2. Preparation and Characterisation of Samples

### 10.3.2.1. Particle Preparation

A partially deuterated polystyrene latex (D-PSL) was prepared using a surfactant-free emulsion polymerisation.[25] The following procedure was adopted for the preparation of the partially deuterated polystyrene latex (D-PSL). All the glassware used for the polymerisation reaction was cleaned in a concentrated base bath (ethanol saturated with NaOH) overnight, followed by a couple of hours in an acid bath (aqueous $HNO_3$). Excess acid was removed with copious amounts of water and the glass finally rinsed with distilled water and dried. A thermostatically controlled oil-bath was heated to 70 °C and a three-necked round bottomed flask, containing an appropriate amount of $D_2O$ (Fluorochem 99.9 atom % D) was clamped in the bath. A nitrogen line, glass stirrer and reflux condenser respectively were connected to the flask through its three necks. The $D_2O$ was degassed under nitrogen for ~30 minutes before some of the $D_2O$ was removed and used to dissolve the appropriate amount of initiator (ammonium persulphate, Aldrich 98+%) and comonomer (4 - styrenesulphonic acid sodium salt, Aldrich). H-styrene (BDH 99%), and D-styrene (Aldrich 98 + atom % D including ~ 0.5% 4-*tert*-butylcatechol) were added and degassed for a further 10 minutes. Finally the dissolved co-monomer and initiator were added and the reaction was left to proceed overnight under a nitrogen atmosphere. The system was allowed to cool before the latex was poured through glass wool into dialysis tubing, which had been previously boiled in distilled water and was purified by dialysis against $D_2O$ and characterised in the similar manner as described in the Chapter 4.

All small-angle neutron scattering samples were made up in an identical manner to those used for adsorption isotherm measurements and allowed to equilibrate for four days prior to SANS experiments. The SANS samples were made up in 95% $D_2O$ and 5% $H_2O$ - the contrast match point for the deuterated polystyrene latex (nominally 90% d-styrene 10% h-styrene, radius 520 ± 50 nm and volume fraction ~ 0.03). Great care was taken to ensure that particle concentrations were equivalent to volume fractions below 5% to minimise inter-particle interactions and multiple scattering by particles. Aliquots of a copolymer solution of sufficient concentration were added to a $\phi = 0.05$ stock particle dispersion to ensure that the plateau of the adsorption isotherm had been reached in all cases, with approximately 100 ppm copolymer in solution.

### 10.3.3. Small-Angle Neutron Scattering Instrumentation

The small-angle neutron scattering measurements of PEO-PBO copolymers were performed on the LOQ diffractometer instrument at the ISIS Spallation Neutron Source, Rutherford Appleton Laboratory, Oxfordshire, UK. The LOQ is a fixed-geometry, time-of-flight (TOF), instrument equipped with a 64 × 64 cm position-sensitive gas detector and uses neutron wavelengths between 2 and 10Å to give a $Q$-range of approximately 0.008 to 0.22 $Å^{-1}$. The momentum transfer $Q$ is defined in Equation 10. 4. The principal advantage of using a TOF instrument like *LOQ*, compared to a reactor-based (fixed wavelength) instrument, is that all of the instrument's $Q$-range is accessible in a single measurement. *LOQ* therefore is ideally suited to the study of systems where a range of length scales are involved or where model-fitting of the data is required.

The samples were contained in 2mm path length, UV-spectrophotometer grade, quartz cuvettes (Hellma Ltd.) and mounted in aluminium holders on top of an enclosed, computer-controlled, sample changer. The cells used for these experiments were quartz of optical quality, which, give rise to a small amount of scattering which has to be subtracted as a background. Sample volumes were approximately 0.4 $cm^3$. Temperature control was achieved through the use of a thermostatted circulating bath pumping fluid through the base of the sample changer. Under these conditions a temperature stability of ± 0.5 °C can be achieved. Experimental measuring times were

between 60 and 180 minutes.

The scattering data were (I) normalised for the sample transmission and incident wavelength distribution, (II) background corrected using an empty quartz cell (this also removes the inherent instrumental background arising from vacuum windows, *etc.*) and (III) corrected for the linearity and efficiency of the detector using the instrument-specific software. The data were put onto an absolute scale by reference to the scattering from a well-characterised partially-deuterated polystyrene-blend standard sample. In order to reduce the background scattering, the amount of free polymer in bulk solution was minimised whilst the amount of adsorbed polymer was maximised. For these reasons the polymers were adsorbed at an initial concentration of 100 ppm, as determined from the adsorption isotherms measured by the depletion method.

### 10.3.4. Background Subtraction and Data Normalisation

Prior to analysis of the data to give segment density profiles it was necessary to subtract the background spectra and correct for non-linear detector response by dividing by the theoretically flat water spectrum.

Provided the contrast match condition has been met, the final spectrum, $I(Q)$, is the scattering intensity resulting from the adsorbed layer alone. However, as protons are present a significant part of the scattering is incoherent, containing no structural information. The incoherent background, which is independent of $Q$, is of the order of the intensity of the data point at the highest measured for these systems. So a flat baseline is subtracted from each $I(Q)$ until the intensity at high $Q$ is small. This subtraction maybe defined by subtracting a small baseline from I(Q) and then plotting $Q^2I(Q)$ against Q. Relatively smaller $Q^2I(Q)$ values (~ $10^{-5}$) at larger Q values indicate that the incoherent background has been subtracted, if not then the procedure is repeated in the similar manner until a small value of $Q^2I(Q)$ is obtained.

## 10.4. Results and discussion

Results obtained by SANS experiments for PEO-PBO diblock and triblock copolymers adsorbed on polystyrene latices will be presented and discussed in this section. Also, the comparisons between the data determined by SANS with those measured by depletion and PCS and with those calculated theoretically using the SCF model[9,26.] will be presented.

### 10.4.1. Data Analysis

The total scattering from a dispersion of polymer-coated particles arises from a number of contributions which are very close to- or on-contrast for the particles ($\rho_{ps}=\rho_{ls}$).

A difficult task is the correct interpretation of SANS data for the adsorbed polymer layers, the treatment of the so-called "fluctuation term". This term represents an attempt to account for spatial inhomogenieties in the average structure of the polymer layers and is insignificant for (relatively) small polymers adsorbed onto large particles.[27] However, for higher density polymer layers (block copolymers, grafted layers or large polymers adsorbed onto small particles), this is not necessarily so. In these cases, a large contribution to the scattering at high $Q$ is evident.[28]

The traditional analysis, valid for situations where the fluctuation term is insignificant or absent, is to (I) subtract the *measured* residual particle scattering, (II) subtract the scattering from a suitable concentration polymer solution to account for any non-adsorbed polymer in solution and (III) subtract a constant $B_{inc}$ term so the measured $I(Q)$ decays to zero. This "corrected" data is then model fitted or inverted after suitable interpolation and extrapolation to obtain the volume fraction profile. In this analysis, in order to treat the baseline accurately, a slightly different approach was adopted. The incoherent background was carried through the various data reduction steps and treated in the final analysis. There is no a priori reason for this, merely that it reduces the error introduced by subtracting data sets with poor signal-to-noise (such as the nominally on-contrast particle and the scattering from a dilute polymer solution). To further reduce these errors, the particle scattering has been fitted to

$I(Q) = kQ^{-4} + B_{inc}$. These corrections have little effect on the final result, merely reducing the error at the intermediate stages.

For volume fraction profiles that follow the scaling prediction $\phi(z) \sim z^{-4/3}$, the fluctuation term, $\tilde{I}$ is predicted to have various dependencies on $Q$; $\tilde{I}(Q) \alpha Q^{-4/3}$ where, the particle radius ($r_o$) is much larger than the radius of gyration of the polymer ($R_g$), $\tilde{I}(Q) \alpha Q^{-5/3}$, where, $r_o < R_g$.[29,30,31] It is therefore preferable to first determine whether fluctuations are present and estimate their intensity before attempting to model-fit the data.

The adsorption of a series of poly(ethylene oxide)-poly(butylene oxide) copolymers; $E_{100}B_{15}$ (diblock), $E_{100}B_{15}E_{100}$ (triblock), $E_{200}B_{15}$ (diblock) and a cyclic copolymer, c-$E_{200}B_{15}$, at aqueous/polystyrene latex interface was determined using SANS. In particular, the influence of copolymer architecture on the adsorption parameters (adsorbed amount, rms. and adsorbed layer thickness) was investigated. The experimental data obtained by SANS are compared with those determined for the same set of copolymers using the depletion method, photon correlation spectroscopy and with those simulated theoretically using SCF model.[9,26] Since, three of the four polymers studied in this work have the same composition but different architectures, our data is fundamentally different to many copolymer adsorption studies, which give a more of an insight into the influence of polymer architecture on the adsorption. Further, since the copolymers used in this study were relatively of smaller size ($R_g \approx 30$ - 40 Å) as compared to the substrate particles ($r_o \approx 520$ Å), hence fluctuations expected in the intensity of the scattered radiation could be of the order $\tilde{I}(Q) \alpha Q^{-4/3}$.

Figure 10. 4 presents a plot of $Q^{4/3}I(Q)$ as a function of $Q^{4/3}$ (*see* Equation 10.28) and shows a characteristic limiting linear behaviour. The slope of the curve yields $B_{inc}$ whilst the intercept gives the fluctuation intensity, $\tilde{I}$. The first, non-linear portion of the curve shown in the figure presents the information regarding the average structure of the adsorbed layer.

Figure 10. 5 shows the experimental scattering data for the adsorbed copolymer $E_{100}B_{15}$ and also presents the layer scattering data fitted to the experimental data for the

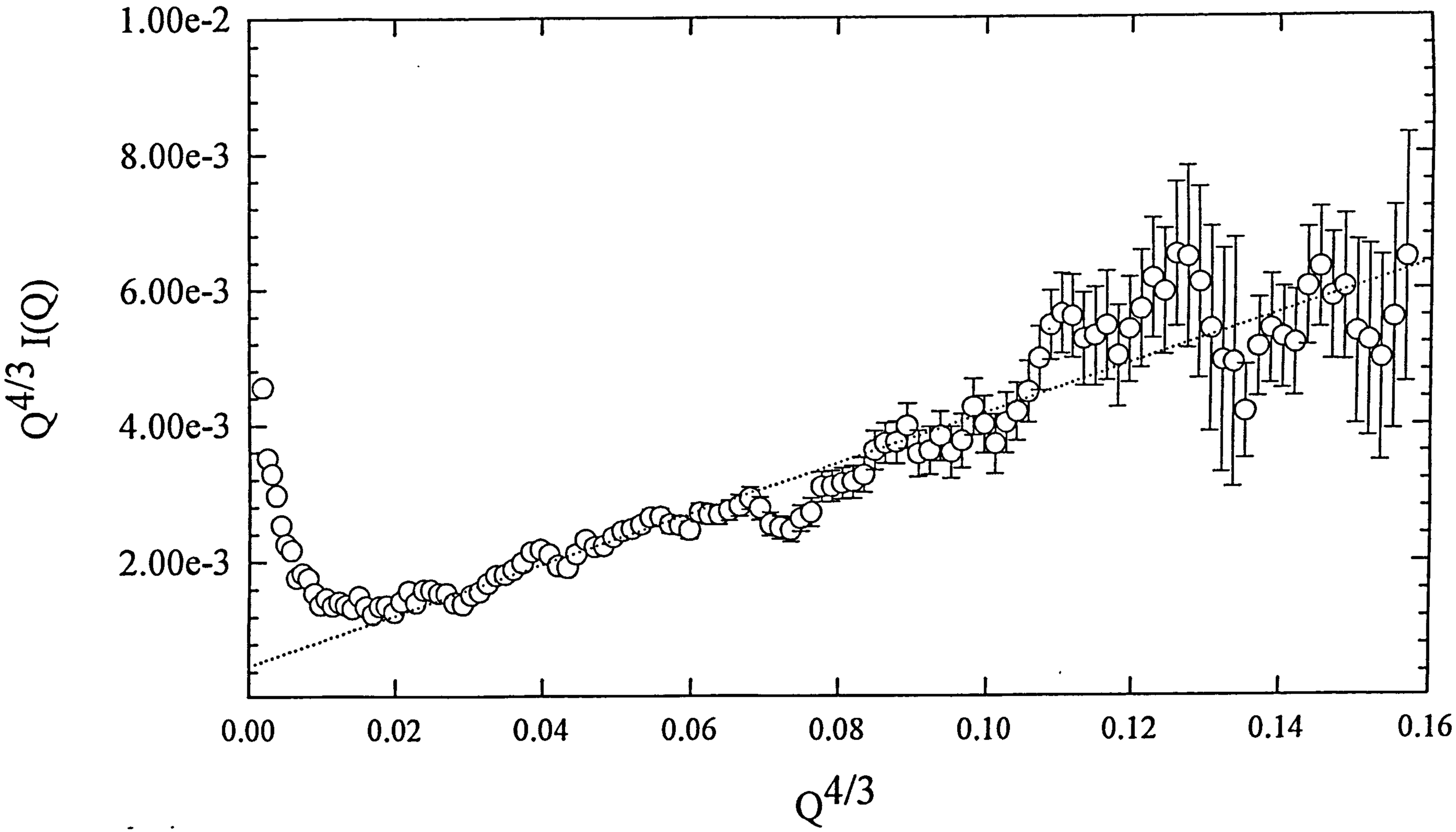


***Figure 10. 4: $Q^{4/3}$ I(Q) versus $Q^{4/3}$ representation of the small-angle neutron scattering from block copolymer $E_{100}B_{15}$ adsorbed onto deuterated polystyrene latex from aqueous solution at contrast match. The dotted line corresponds to the limiting slope used to fit the fluctuation contribution to the scattering.***

same copolymer for an exponentially shaped volume fraction profile. The most likely shape of the volume fraction profile can be obtained by model fitting the data using those parameters obtained from the fluctuation analysis as initial guesses. The simple exponential was selected from a range of shapes based on a $\chi^2$ analysis. It is usually a difficult task to select an appropriate data from the complex shapes, since most of them looked to fit equally well. The parameters describing the more complex profiles were often "non-physical" (*e.g.* very large adsorbed amounts), (effectively "single exponential" profiles) or required a fluctuation term significantly different from that extracted from the $Q^{4/3}$ analysis and indicated an incorrect shape for the volume fraction profile. Previously Cosgrove *et al.*[32] and Griffiths *et al.*[33] have studied the adsorption of block copolymers using SANS and have shown that the neutron scattering could be detected from both blocks due to a combination of very different concentrations and/or scattering length densities. Griffiths *et al.*[33] have determined the adsorption of polystyrene - poly(ethylene oxide) diblock copolymers adsorbed at the aqueous/porous silica interface and were best described by a rectangle plus exponential. In such cases the model volume fraction profiles were considered to be of two shape components, one for each block. In contrast matched conditions the neutron scattering can be detected only from the protonated PBO block, hence the copolymers with analogous composition containing a deuterated PEO block under contrast matched conditions were studied, but this study did not show any measurable intensity from the PBO block. This variation in the behaviour of these copolymers may be due to the small size as well as the similarity in the scattering length densities of the PEO and PBO blocks ($\Delta\rho_{EO\text{-}BO} = 0.37 \times 10^{-6}$ $A^{-2}$).

Figure 10. 6 presents the best-fit (exponential) profiles for these block copolymers studied in the SANS experiments. The adsorbed amount derived from the SANS data was obtained by integrating under the volume fraction profile and using the average bulk mass density of the polymers. Fleer *et al.*[26] have studied the adsorption of a poly(ethylene oxide) homopolymer, $M_n$ 10,000, at aqueous/polystyrene latex interface. The comparisons between the data presented for PEO hompolymer (adsorbed amount ~ 0.3 ± 0.1 $mgm^{-2}$ and $\delta_{rms}$ ~ 8 Å) and those for block copolymers show that even though no scattering could be detected from the PBO block but still there is a significant effect of the PBO block on the adsorbed layer conformation *i.e.*

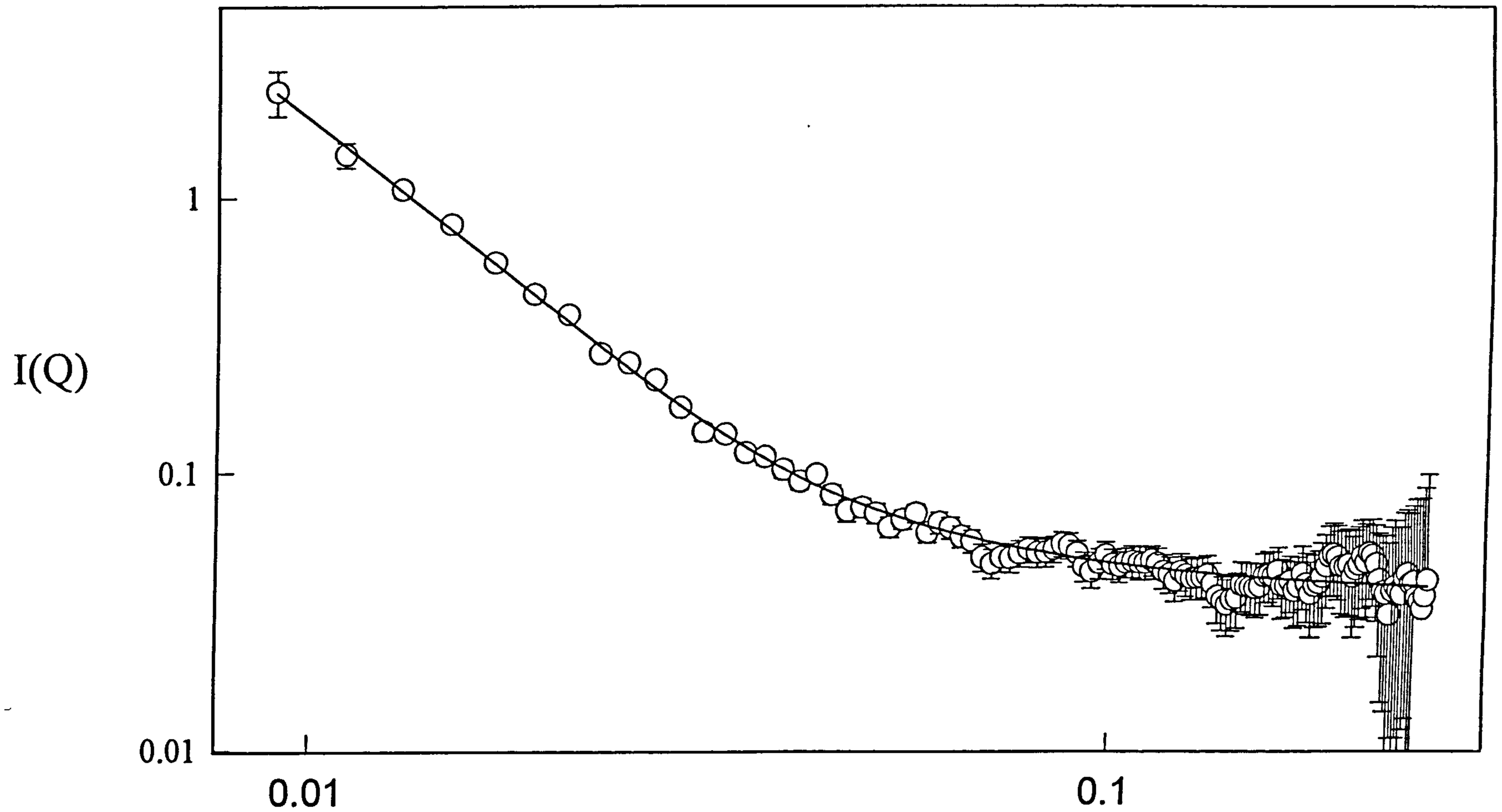


**Figure 10. 5:** I(Q) *versus* Q representation of the small-angle neutron scattering from block copolymer $E_{100}B_{15}$ adsorbed onto deuterated polystyrene latex from aqueous solution with fit to an exponentially shaped volume fraction profile.

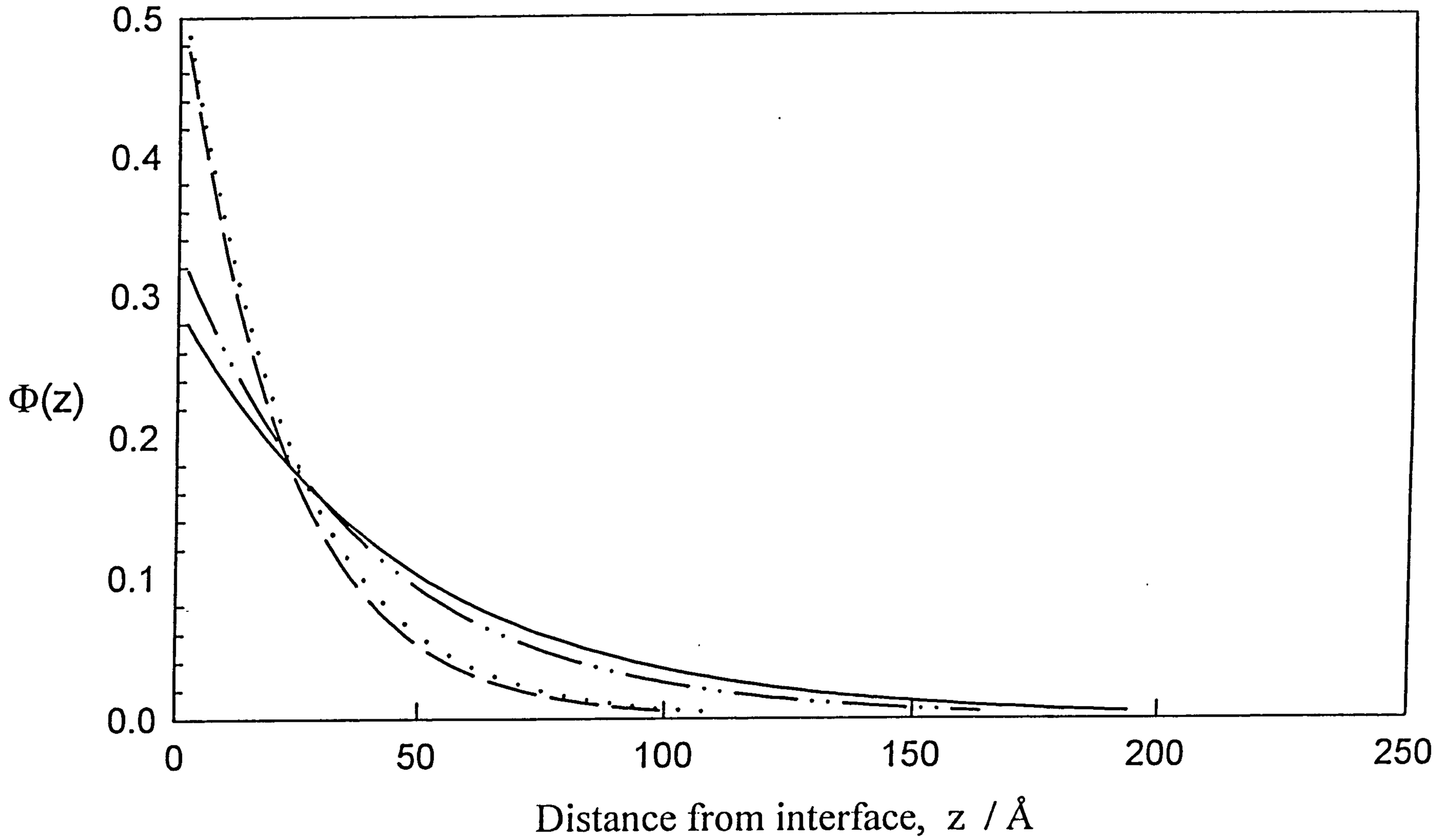


***Figure 10. 6: Best fit volume fraction profiles for the four polymers used in this study: solid line - small diblock $E_{100}B_{15}$, long dashed line - triblock $E_{100}B_{15}E_{100}$, dotted line - cyclic diblock c-$E_{200}B_{15}$, dash-dotted line - large diblock $E_{200}B_{15}$.***

increasing the adsorbed amount of block copolymers of corresponding molar mass by a factor of five.

An extensive work for the adsorption of the triblock copolymers of poly(ethylene oxide) and poly(propylene oxide) has been presented in the literature.[34,35,36,37] Baker and Berg[35,36] have observed in their work that the PPO block has a smaller effect on the hydrodynamic layer thickness ($\delta \propto N_{EO}^{0.55}$). Mallagh[12] in his work presented the rms layer thicknesses for two copolymers, $E_{32}P_{56}E_{32}$ and $E_{140}P_{56}E_{140}$ ~ 22 and 42 Å respectively. A good agreement between the interpolated value (30 Å) for $E_{100}$ obtained from these two polymers and that measured for the triblock copolymer $E_{100}B_{15}E_{100}$ (31 Å) have been observed. Malmsten *et al.*[37] have studied the adsorption of two block copolymers $E_{99}P_{65}E_{99}$ and $E_{125}P_{47}E_{125}$, differing from each other in anchor-buoy ratio, at the aqueous/silica interface using dynamic light scattering. They concluded that in contrast to the findings presented in the literature these two polymers inspite of having different composition show similar adsorbed amounts (0.36 $mgm^{-2}$) as well as the hydrodynamic thickness. The layer thickness measured corresponded to approximately the radius of gyration of the PEO block.

The data presented in Table 10. 1 show that the large diblock copolymer, $E_{200}B_{15}$, forms a relatively thicker adsorbed layer, with hydrodynamic thickness approximately twice that of the smaller diblock $E_{100}B_{15}$. However, the triblock ($E_{100}B_{15}E_{100}$) and the cyclic diblock (c-$E_{100}B_{15}$) both form a layer of comparable size and that their thickness values are intermediate to those measured for two diblocks, $E_{200}B_{15}$ and $E_{100}B_{15}$. Further more, the triblock $E_{100}B_{15}E_{100}$ and cyclic diblock c-$E_{100}B_{15}$ show similar adsorbed amounts, rms and hydrodynamic thicknesses. This suggests that the effects of joining the two ends of the triblock polymer to form the diblock have little effect on the polymer adsorption.

The volume fraction profiles determined experimentally (using SANS) for these block copolymers are depicted in Figure 10. 6. This figure shows that the diblock copolymer ($E_{100}B_{15}$) smallest in the series studied extends itself away into the solution to the greatest extent and is observed to be in contrast with its hydrodynamic thickness measured by PCS. The diblock copolymer $E_{100}B_{15}$ is observed to extend up to 180 ± 25 Å which is about 6 - 7x $R_g$, comparable to its $\delta_H$ and is in a good agreement to the

behaviour predicted by Schillen *et al.*[38] (for diblock copolymer $E_{41}B_8$) *i.e.* "brush" formation of adsorbed polymer layer. This may be due to the relatively higher anchor-buoy ratio for $E_{100}B_{15}$ than the $E_{200}B_{15}$, which provides a sufficient energy from adsorption to enable the polymer chains to extend further and simultaneously accommodate a greater number of molecules at the surface. By contrast, $E_{200}B_{15}$ is less stretched and extends to only 4 - 5x $R_g$. The hydrodynamic thickness, 290 ± 10 Å, observed for this copolymer is greater than the extent of the volume fraction profile, 175 ± 25 Å. This indicates that there must be some dilute, highly extended "tails" which are undetectable in the SANS experiment. Overall, the triblock and cyclic diblock copolymers form thinner adsorbed layers than the diblock copolymers. Also, similar volume fraction profiles are observed for the triblock and cyclic diblock copolymers. The layer thicknesses of the triblock and cyclic diblock (2x $R_g$) are more reminiscent of the extent that would be expected for an adsorbed homopolymer with approximately equivalent monomer units (100). This similarity is also observed in the hydrodynamic thickness of these copolymer determined by PCS.

#### 10.4.1.1. Self–Consistent Mean Field Theory Calculations:

The volume fraction profiles for the same set of PEO PBO block copolymers used in this study ( *see* Table 10.1) were calculated using the SCF model.[9,26] Same Flory parameters were used as shown for these polymers in Chapter 5. Under contrast match conditions, since, no scattering could be detected from the PBO block when using copolymers with deuterated PEO blocks, hence it was not possible experimentally to separate the contributions to the total volume fraction profile arising from the individual PEO and PBO blocks. However, this is possible by calculating the data using the SCF model.[9,26]

Figures 10. 7 and 10. 8, respectively, show the volume fraction profiles for these polymers as a function of layer numbers for PEO and PBO blocks present in the block copolymers calculated using the SCF model. These figures show that for all three linear copolymers (with the exception of ring copolymer as it could not be fitted with this program), the PBO segments are only found in the first two layers with majority of those are located in the layer next to the particle surface, whilst, as expected some of PEO segments were present at the surface. This reflects the relative surface affinities

of the two blocks. An approximately exponential shape to the calculated volume fraction profiles supporting the use of such a shape in the SANS data fitting is observed. A good qualitative agreement has been observed between the data calculated theoretically and those determined experimentally.

Table 10. 1: Experimental and theoretical data; adsorbed amounts, $\delta_{rms}$, $\delta$ and hydrodynamics thicknesses for the PEO-PBO block copolymers adsorbed onto deuterated polystyrene latex.

| Polymer | Γ /1.2%/ ($mgm^{-2}$) (SANS) | Γ /1.2%/ ($mgm^{-2}$) (Depletion) | $\delta_H$/1.2 %/nm (PCS) | $\delta_{rms}$/ nm | Adsorbed Amount/ϑ | $\delta_{rms}$./ layers | δ/ layers |
|---|---|---|---|---|---|---|---|
| $E_{100}B_{15}$ | 1.5 (± 0.1) | 1.6 (± 0.1) | 16 ± 1 | 6.7 ± 0.5 | 1.42 | 7.1 | 9 |
| $E_{200}B_{15}$ | 1.4 (± 0.1) | 1.7 (± 0.1) | 29 ± 1 | 5.6 ± 0.5 | 1.16 | 6.4 | 11 |
| $E_{100}B_{15}E_{100}$ | 1.2 (± 0.1) | 1.2 (± 0.1) | 21 ± 1 | 3.1 ± 0.5 | 1.07 | 4.7 | 7 |
| c-$E_{200}B_{15}$ | 1.3 (± 0.1) | 1.3 (± 0.1) | 22.5± 1 | 3.3 ± 0.5 | N/A | N/A | N/A |

A decrease in rms layer thickness (δ) with increasing PEO block has been observed in both theoretical as well as experimental data and are in accordance with the predictions made by Cosgrove *et al.*[39] Also, a decrease in the adsorbed amount determined by depletion method as well as by SANS has been observed though it is much less pronounced. This may primarily be due to the experimental error associated with determination of adsorbed amounts coupled with the rather small absolute values of the adsorbed amounts due to the low polymer molar mass.

The comparison of the data for the two diblock copolymers determined by SCF model also show that higher adsorbed amount (θ) is obtained for the low molar mass diblock copolymer, $E_{100}B_{15}$, and is due to the high surface occupancy of the preferentially adsorbed PBO blocks and the closer packing of the PEO blocks. For the smaller copolymer, the lateral interactions between the buoy blocks can be compensated

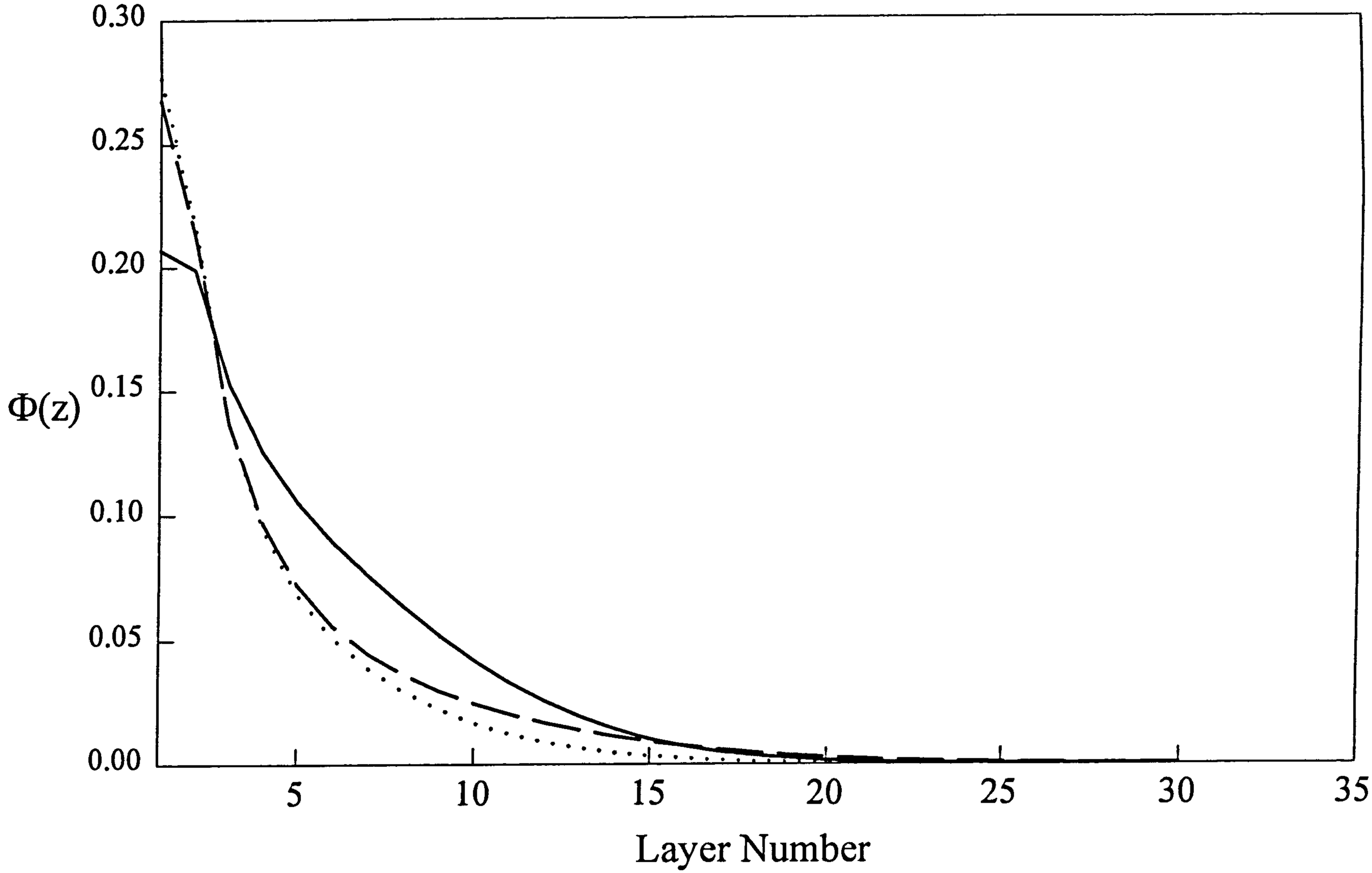


***Figure 10. 7 shows simulated PEO volume fraction profiles for three polymers used in this study: solid line - small diblock $E_{100}B_{15}$, dotted line - triblock $E_{100}B_{15}E_{100}$, dashed line - large diblock $E_{200}B_{15}$.***

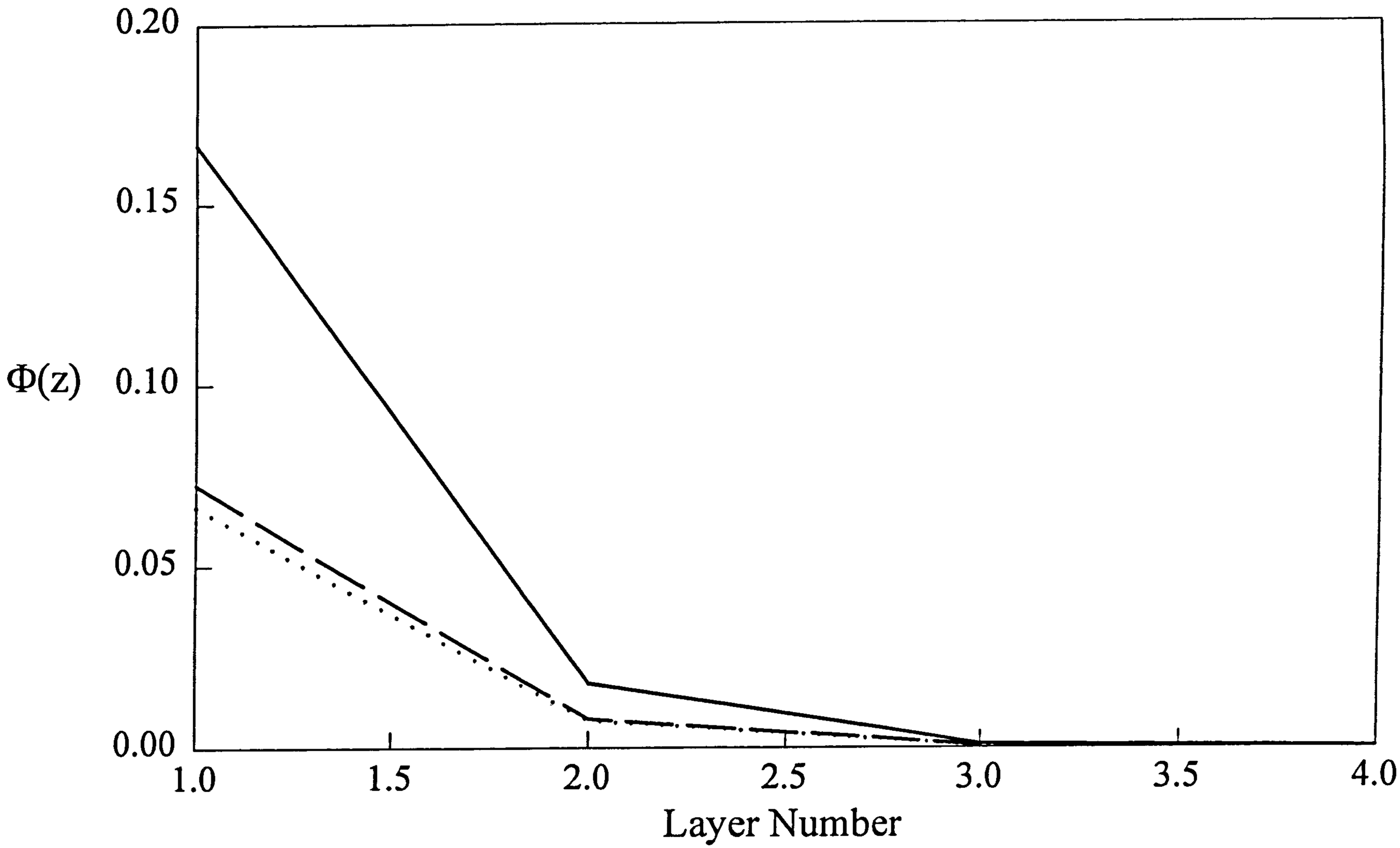


***Figure 10. 8 shows simulated PBO volume fraction profiles for three polymers used in this study: solid line - small diblock $E_{100}B_{15}$, dotted line - triblock $E_{100}B_{15}E_{100}$, dashed line - large diblock $E_{200}B_{15}$.***

by the energy gained by relatively larger number of anchor segments. The theoretical profiles however, are observed to cross over at ≈ 16 layers and thus, the larger copolymer $E_{200}B_{15}$ has a few highly extended tails giving a slightly larger hydrodynamic thickness. The smaller copolymer also has rather less PEO blocks in the first layer. These general features are also seen in the experimental volume fraction profiles, where, the $E_{200}B_{15}$ has a smaller rms thickness than the $E_{100}B_{15}$ (and the triblock). The more subtle features however cannot be resolved in the experimental neutron data.

## 10.5. Conclusion

The adsorption of a series of poly(ethylene oxide)-poly(butylene oxide) copolymers; $E_{100}B_{15}$ (diblock), $E_{100}B_{15}E_{100}$ (triblock), $E_{200}B_{15}$ (diblock) and a cyclic copolymer, c-$E_{200}B_{15}$, at aqueous/polystyrene latex interface was determined using SANS. In particular, the influence of copolymer architecture on the adsorption parameters (adsorbed amount, rms. and adsorbed layer thickness) was investigated.

In theory and experiment, both diblock copolymers are observed to adsorb at higher level than the triblock copolymers (of the corresponding total polymer molar mass). Overall, the triblock and cyclic diblock copolymers form thinner adsorbed layers than the diblock copolymers. This complication in the behaviour of the copolymers can be seen more significantly in the volume fraction calculated theoretically. For instance, both the $E_{200}B_{15}$ and $E_{100}B_{15}E_{100}$ have almost exactly the same number of anchor segments ($N_A$) in the first and second layers, almost similar volume fraction profiles are observed for these copolymers. The comparison of the data for the two diblock copolymers determined by SCF model also show that higher adsorbed amount ($\theta$) is obtained for the low molar mass diblock copolymer, $E_{100}B_{15}$, and is due to the high surface occupancy of the preferentially adsorbed PBO blocks and the closer packing of the PEO blocks.

The final significant observation is that the cyclic and the triblock copolymers, whilst, having identical compositions but somewhat different architectures, have very similar adsorbed amounts and layer thicknesses. Cyclic polymers generally exhibit a much smaller radius of gyration than the linear samples with similar polymer

composition[40]. This difference in solution molecular size is not reflected in the surface structure presumably due in part to the fact that the effective higher loop density in the cyclic polymer is balanced by its smaller size compared to the triblock copolymers.

# References


[1] Cohen-Staurt, M. A., Waajen, F. H. W. H., Cosgrove, T., Vincent, B., and Crowley, T. L., *Macromolecules*, 1984, **17**, 1825.

[2] Richards, R. W. R., Maconnachle, and Allen, G., *Polymer* 1981, **22**, 158.

[3] Stuhrmann, H. B., *Acta. Cryst.*, 1970, **A26**, 297.

[4] Mears, S. J., Ph.D. Thesis, University of Bristol, 1996.

[5] Higgins, J. S., Dawkins, J. V., and Taylor, G., *Polymer*, 1980, **21**, 627.

[6] Barnett, K. G., Cosgrove, T., Crowley, T., Tadros, Th. F., and Vincent, B., in "The Effects of Polymers on Dispersion Stability", Ed. Tadros, Th. F., Academic Press, 1982, 183.

[7] Cosgrove, T., Crowley, T. L., Vincent, B., Barnett, K. G., and Tadros, Th. F., *Faraday, Symp. Chem. Soc.*, 1982, **16**, 101.

[8] Barnett, K. G., Cosgrove, T., Vincent, B., Burgess, A. N., Crowley, T. L., King, T., Turner, J. D., and Tadros, Th. F., *Polymer*, 1981, **22**, 283.

[9] Evers, O. A., Scheutjens, J. M. H. M., and Fleer, G. J., *J. Chem. Soc. Faraday Trans.* 1990, **86**, 1333.

[10] Cosgrove, T., Heath, T. G., Ryan, K., and van Lent, B., Private communications.

[11] Obey, T. M., Ph.D. Thesis, University of Bristol, 1987.

[12] Mallagh, L., Ph. D. Thesis, University of Bristol, 1989.

[13] Crowley, T. L., *D. Phil. Thesis*, University of Oxford, 1984.

[14] Porod, G., *Kolloid Z.*, 1951, **124**, 83.

[15] Auvray, L., and de Gennes, P. G., *Europhys. Lett.* 1986, **2**, 647.

[16] Auvray, L., Auroy, P., eds Linder, P., and Zemb, Th., "Neutron, X-Ray and Light Scattering Elsevier Science Publishers": Holland 1991

[17] Auroy, P., Auvray, L., and Leger, L., *Phys. Rev. Lett.* 1991, **66**, 719.

[18] Cosgrove, T., Obey, T. M., and Vincent, B., *J. Colld. and Interf. Sci.* 1986, **111**, 409.

[19] Cosgrove, T., abd Ryan K., *Langmuir* 1990, **6**, 136.

[20] Cosgrove, T., Heath, T. G., and Ryan K., *Langmuir*, 1994 **10** 3500.

[21] Cosgrove, T.- Private communications.

[22] Auroy, P., Mir, Y., and Auvray, L., Phys. *Phys. Rev. Lett.* 1993, **69**, 93.

[23] Auvray, L., and Cotton, J. P., *Macromolecules*, 1987 **20** 202.

[24] de Genes, P.G., *Macromolecules* 1986, **14**, 1637.

[25] Juang, M. S. D., and Krieger, I. M., *J. polymer Sci.* 1976, **14**, 2089.

[26] Cohen-Staurt, M. A., Waajen, F. W. H., Cosgrove, T., Vincent, B., and Crowley, T. L., *Macromolecules*, 1984, **17**, 1825.

[27] Cosgrove, T., Griffiths, P.C., and Obey, T,M., *Macromolecules,* submitted 1998.

[28] Auroy, P., and Auvray, L., *J Phys II* 1993, **3**, 227.

[29] Auroy, P., and Auvray, L., *Macromolecules* 1996, **29**, 337.

[30] Auroy, P.; Auvray, L., and Leger, L., *Macromolecules* 1991, **24**, 2523.

[31] Auroy, P.; Auvray, L., and Leger, L., *Physica A* 1991, **172**, 269.

[32] Cosgrove, T., *J. Chem. Soc., Faraday Trans* 1990, **86**, 1323.

[33] Griffiths, P. C., Cosgrove, T., and Hair, M. L., *Macromolecules* 1996, *submitted.*

[34] Kayes, J. B., and Rawlins, D. A., *Coll. and Polym. Sci.* 1979, **6**, 22.

[35] Baker, J. A., Pearson, R. A., and Berg, J. C., *Langmuir* 1989, **5**, 339.

[36] Baker, J. A., and Berg, J. C., *Langmuir* 1988, **4**, 1055.

[37] Malmsten, M., Linse, P., and Cosgrove, T., *Macromolecules* 1992, **5**, 2474.

[38] Schillen, K., Claeson, P. M., Malmsten, M., Linse, P., and Booth, C., *J. Phys. Chem. B* 1997, **101**, 4238.

[39] Cosgrove, T., Hair, M. L., and Guzonas, D. A., *Macromolecules* 1992, ***25***, 2777.

[40] Griffiths, P. C., Stilbs, P., Yu, G. E., and Booth, C., *J. Phys. Chem.* 1995, ***99***, 16752.

# APPENDIX I

# GPC Summary Report

Run No: D809
Sample: 1 (9023)

**Calculation:** Standard Calc

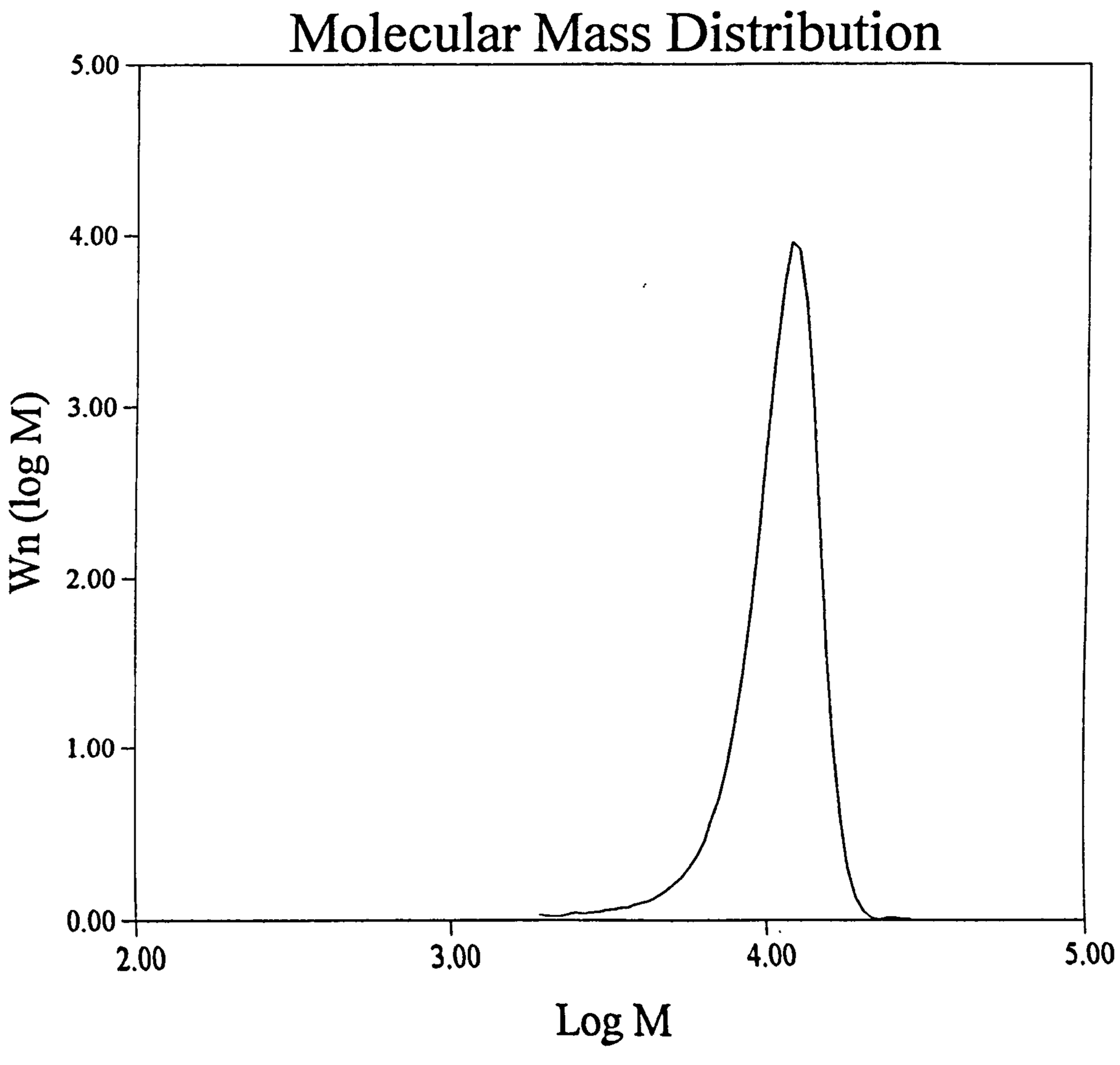


## Molecular Mass Values

| | |
|---|---|
| **Mw:** | 11100. |
| **Mn:** | 10200. |
| **Mp:** | 11700. |
| **Mw/Mn** | 1.09 |

## Parameters

| | |
|---|---|
| CONCENTRATION (mg/ml) | 2.240 |
| FLOW RATE (ml/min) | 1.002 |
| INJECTION VOLUME (ul) | 200.0 |
| SOLVENT | DMF |
| COLUMNS | B |
| DETECTOR | RI |
| PEAK AREA: | 14.274 |

| | |
|---|---|
| Calibration file: | thfb528.nar |
| Run date: | 07/10/9516:42 |
| Peak Parameters: | dmf528.pkp |
| Tau | 0.135 |
| Sigma | 0.133 |

**Baseline Sets:**

| | | |
|---|---|---|
| Int. limits: | 12.20 | 14.19 |
| baseline: | 12.08 | 20.76 |

**Operator:** JC

# GPC Summary Report

Run No: D807
Sample: 2 (9024)

**Calculation:** Standard Calc

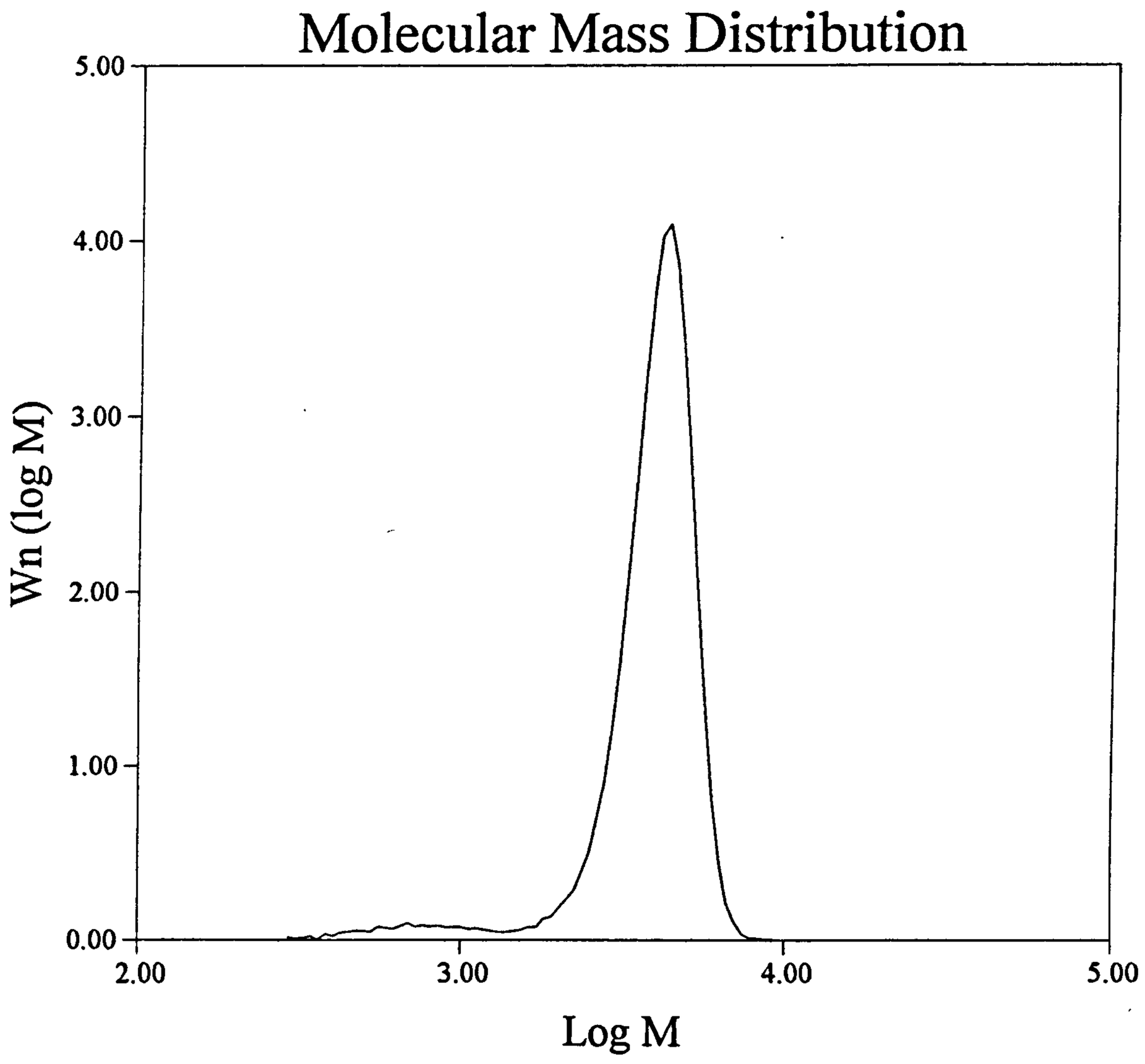


## Molecular Mass Values

| | |
|---|---|
| **Mw:** | 3990. |
| **Mn:** | 3340. |
| **Mp:** | 4330. |
| **Mw/Mn** | 1.19 |

## Parameters

| | |
|---|---|
| CONCENTRATION (mg/ml) | 2.120 |
| FLOW RATE (ml/min) | 1.000 |
| INJECTION VOLUME (ul) | 200.0 |
| SOLVENT | DMF |
| COLUMNS | B |
| DETECTOR | RI |
| PEAK AREA: | 11.807 |

| | |
|---|---|
| Calibration file: | DMF528.nar |
| Run date: | 07/10/9515:54 |
| Peak Parameters: | dmf528.pkp |
| Tau | 0.135 |
| Sigma | 0.133 |

**Baseline Sets:**

| | | |
|---|---|---|
| Int. limits: | 13.01 | 15.61 |
| baseline: | 12.85 | 20.74 |

**Operator:** JC

# GPC Summary Report

Run No: D808
Sample: 3 (9025)

**Calculation:** Standard Calc

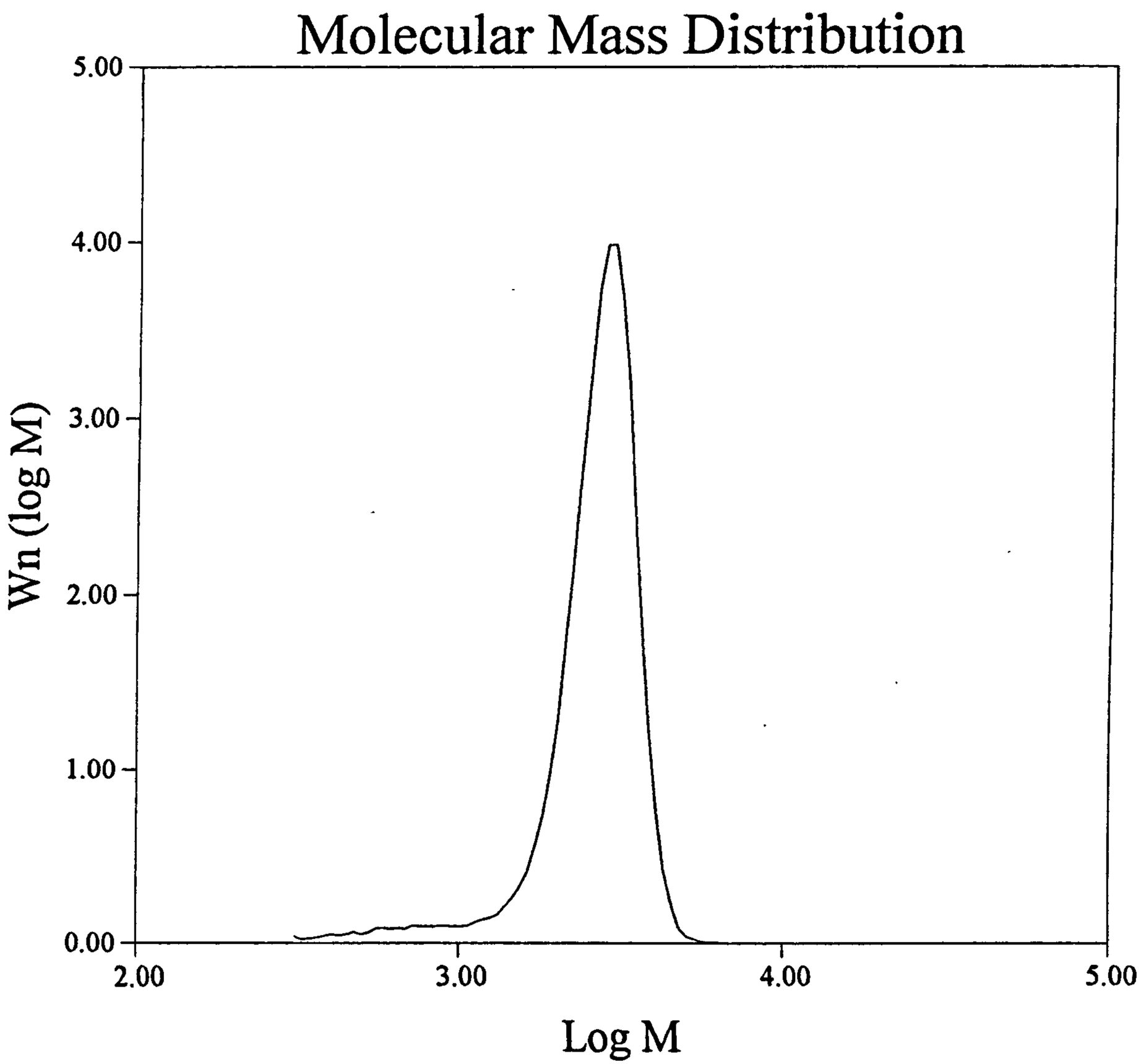


## Molecular Mass Values

| | |
|---|---|
| **Mw:** | 2710. |
| **Mn:** | 2360. |
| **Mp:** | 2970. |
| **Mw/Mn** | 1.15 |

## Parameters

| | |
|---|---|
| CONCENTRATION (mg/ml) | 2.350 |
| FLOW RATE (ml/min) | 1.000 |
| INJECTION VOLUME (ul) | 200.0 |
| SOLVENT | DMF |
| COLUMNS | B |
| DETECTOR | RI |
| PEAK AREA: | 12.162 |

| | |
|---|---|
| Calibration file: | DMF528.nar |
| Run date: | 07/10/9516:18 |
| Peak Parameters: | dmf528.pkp |
| Tau | 0.135 |
| Sigma | 0.133 |

**Baseline Sets:**

| | | |
|---|---|---|
| Int. limits: | 13.28 | 15.59 |
| baseline: | 12.93 | 22.62 |

**Operator:** JC

# GPC Summary Report

Run No: D810
Sample: 4 (9026)

**Calculation:** Standard Calc

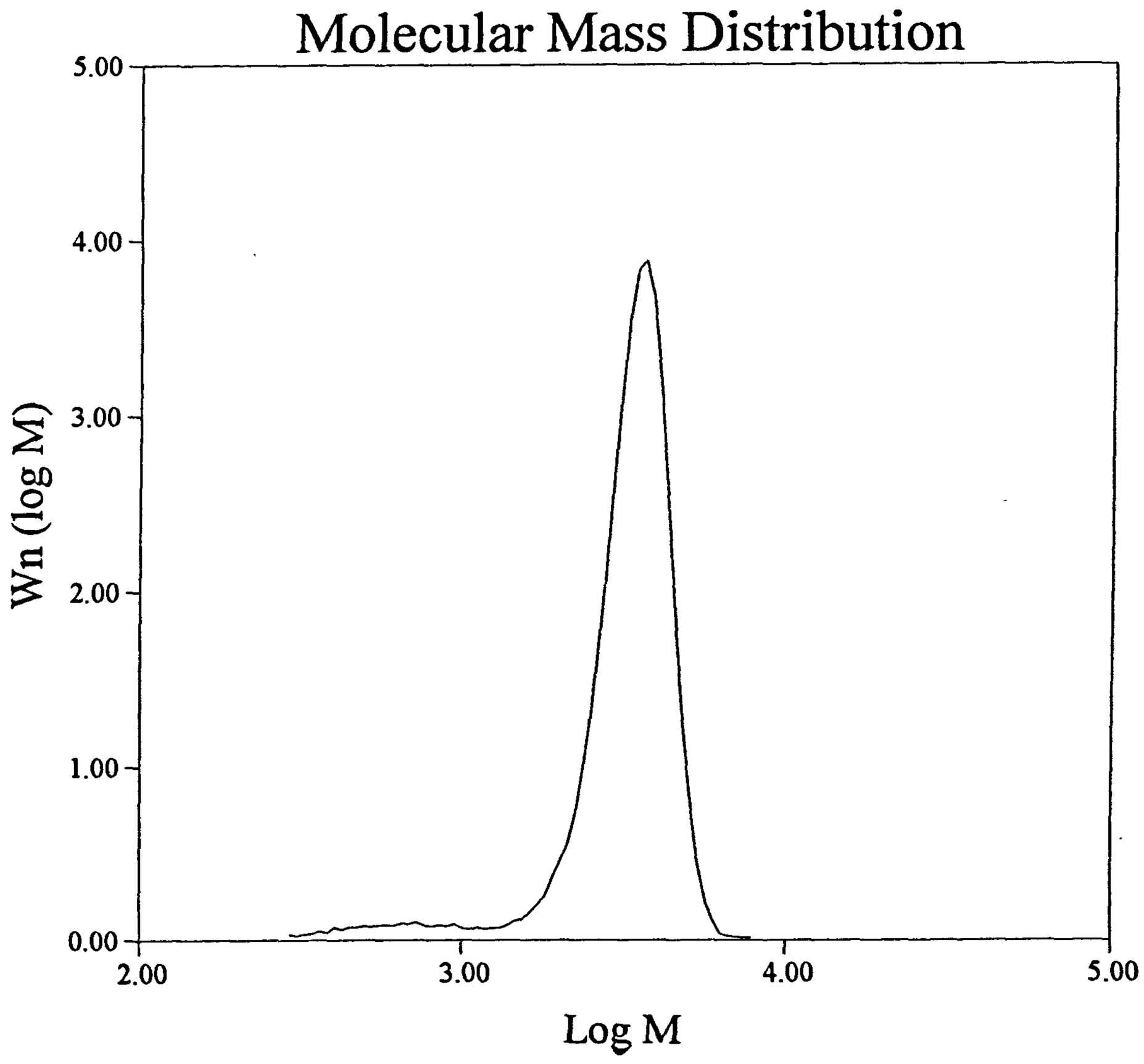


## Molecular Mass Values

| | |
|---|---|
| **Mw:** | 3360. |
| **Mn:** | 2750. |
| **Mp:** | 3680. |
| **Mw/Mn** | 1.22 |

## Parameters

| | |
|---|---|
| CONCENTRATION (mg/ml) | 1.900 |
| FLOW RATE (ml/min) | 1.000 |
| INJECTION VOLUME (ul) | 200.0 |
| SOLVENT | DMF |
| COLUMNS | B |
| DETECTOR | RI |
| PEAK AREA: | 10.644 |

| | |
|---|---|
| Calibration file: | thfb528.nar |
| Run date: | 07/10/9517:06 |
| Peak Parameters: | dmf528.pkp |
| Tau | 0.135 |
| Sigma | 0.133 |

**Baseline Sets:**

| | | |
|---|---|---|
| Int. limits: | 13.13 | 15.60 |
| baseline: | 13.02 | 21.45 |

**Operator:** JC

# GPC Summary Report

Run No: D811
Sample: 5 (9027)

**Calculation:** Standard Calc

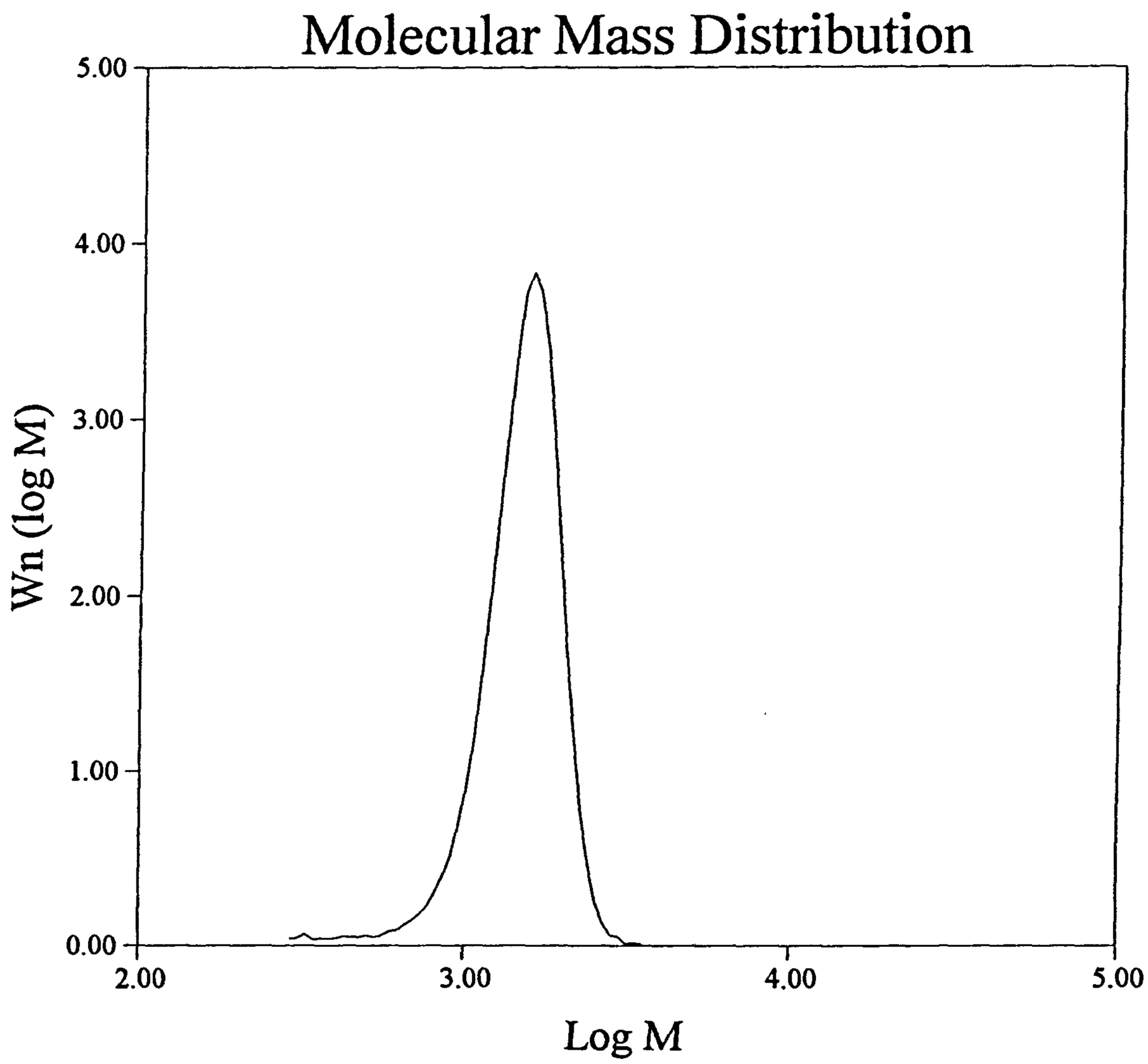


## Molecular Mass Values

| | |
|---|---|
| **Mw:** | 1520. |
| **Mn:** | 1400. |
| **Mp:** | 1570. |
| **Mw/Mn** | 1.09 |

## Parameters

| | |
|---|---|
| CONCENTRATION (mg/ml) | 2.370 |
| FLOW RATE (ml/min) | 1.002 |
| INJECTION VOLUME (ul) | 200.0 |
| SOLVENT | DMF |
| COLUMNS | B |
| DETECTOR | RI |
| PEAK AREA: | 12.334 |

| | |
|---|---|
| Calibration file: | DMF528.nar |
| Run date: | 07/10/9517:32 |
| Peak Parameters: | dmf528.pkp |
| Tau | 0.135 |
| Sigma | 0.133 |

**Baseline Sets:**

| | | |
|---|---|---|
| Int. limits: | 13.71 | 15.62 |
| baseline: | 12.91 | 21.88 |

**Operator:** JC

# GPC Summary Report

Run No: D823
Sample: 6 (9028)

**Calculation:** Standard Calc

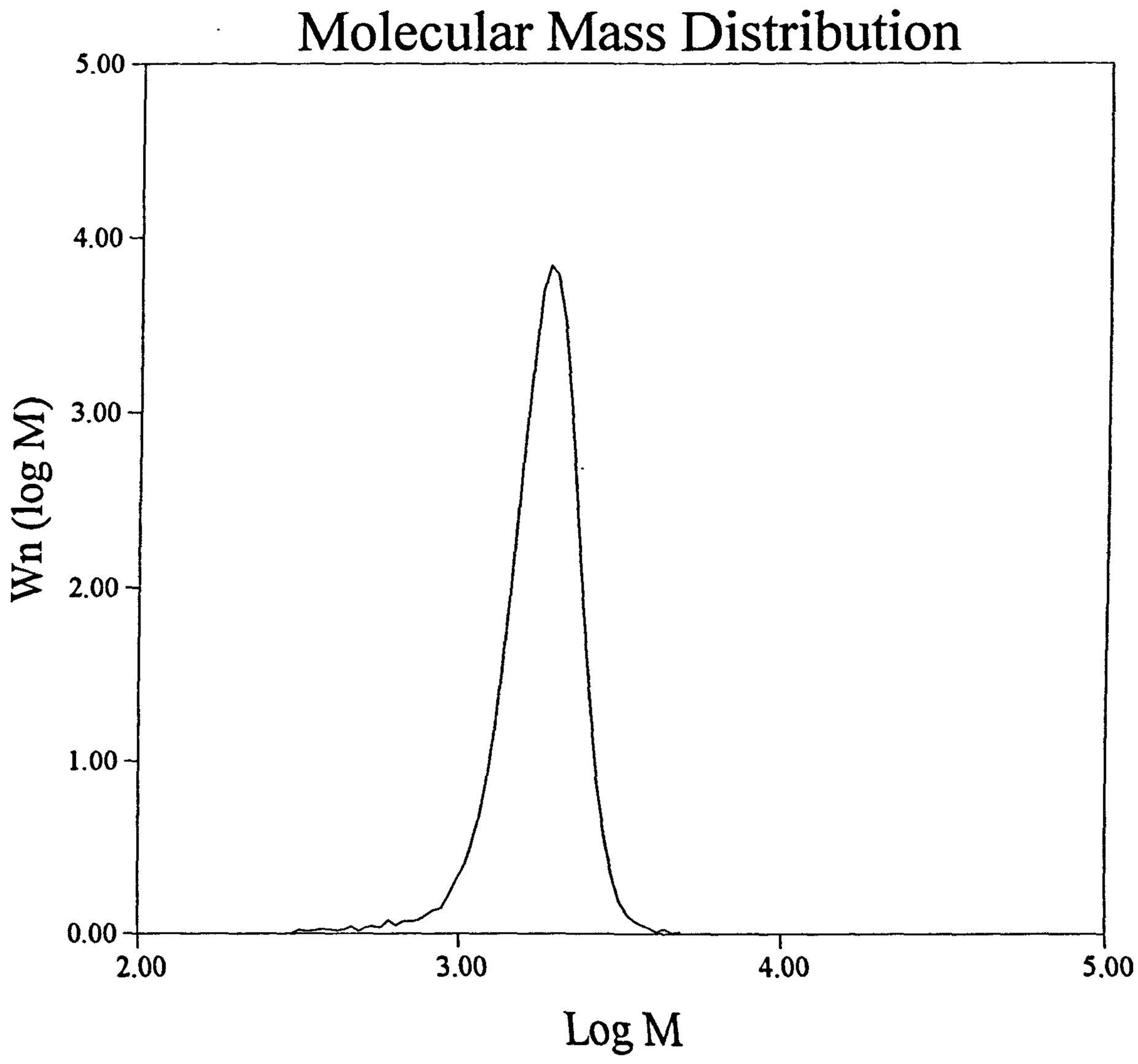


## Molecular Mass Values

| | |
|---|---|
| **Mw:** | 1840. |
| **Mn:** | 1710. |
| **Mp:** | 1870. |
| **Mw/Mn** | 1.08 |

## Parameters

| | |
|---|---|
| CONCENTRATION (mg/ml) | 1.860 |
| FLOW RATE (ml/min) | 0.993 |
| INJECTION VOLUME (ul) | 200.0 |
| SOLVENT | DMF |
| COLUMNS | B |
| DETECTOR | RI |
| PEAK AREA: | 9.582 |

| | |
|---|---|
| Calibration file: | DMF528.nar |
| Run date: | 07/11/9514:12 |
| Peak Parameters: | dmf528.pkp |
| Tau | 0.135 |
| Sigma | 0.133 |

**Baseline Sets:**

| | | |
|---|---|---|
| Int. limits: | 13.50 | 15.60 |
| baseline: | 13.04 | 22.42 |

**Operator:** JC

# GPC Summary Report

Run No: D825
Sample: 7 (9029)

**Calculation:** Standard Calc

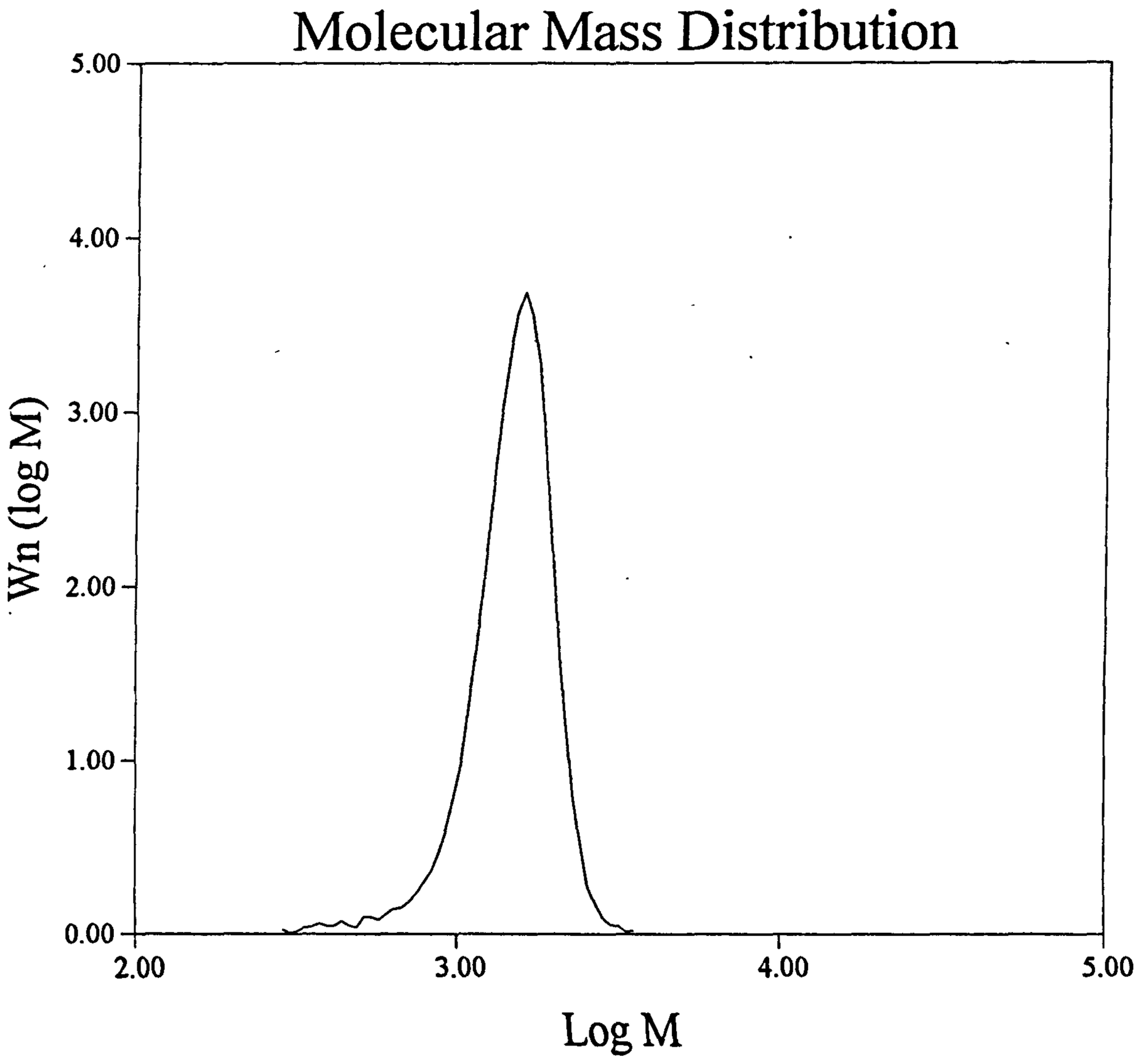


## Molecular Mass Values

| | |
|---|---|
| **Mw:** | 1520. |
| **Mn:** | 1400. |
| **Mp:** | 1590. |
| **Mw/Mn** | 1.09 |

## Parameters

| | |
|---|---|
| CONCENTRATION (mg/ml) | 2.220 |
| FLOW RATE (ml/min) | 0.993 |
| INJECTION VOLUME (ul) | 200.0 |
| SOLVENT | DMF |
| COLUMNS | B |
| DETECTOR | RI |
| PEAK AREA: | 10.210 |

| | |
|---|---|
| Calibration file: | DMF528.nar |
| Run date: | 07/11/9515:08 |
| Peak Parameters: | dmf528.pkp |
| Tau | 0.135 |
| Sigma | 0.133 |

**Baseline Sets:**

| | | |
|---|---|---|
| Int. limits: | 13.71 | 15.63 |
| baseline: | 13.55 | 23.26 |

**Operator:** JC

# GPC Summary Report

Run No: D818
Sample: 8 (9030)

**Calculation:** Standard Calc

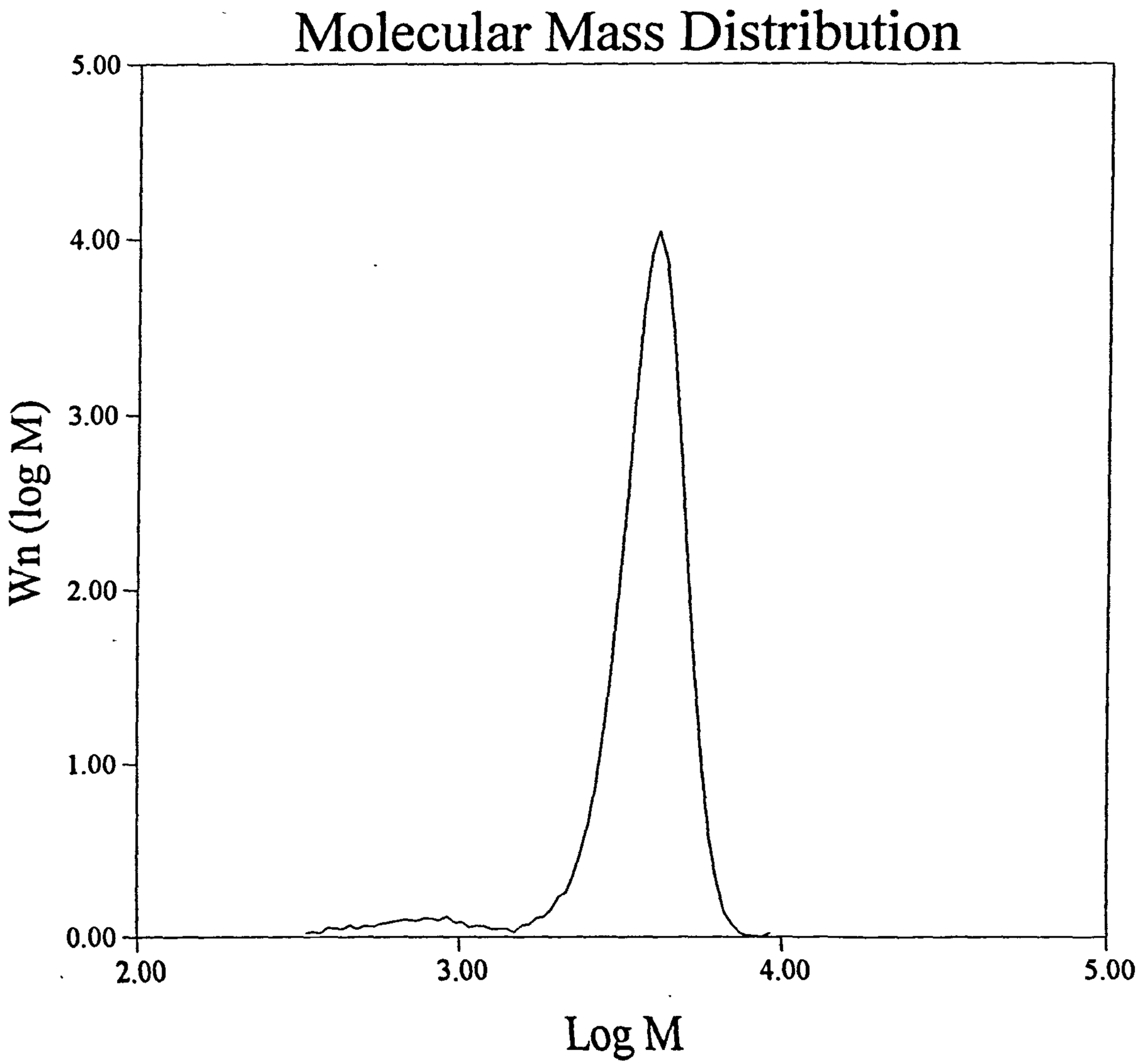


## Molecular Mass Values

| | |
|---|---|
| **Mw:** | 3840. |
| **Mn:** | 3180. |
| **Mp:** | 4120. |
| **Mw/Mn** | 1.21 |

## Parameters

| | |
|---|---|
| CONCENTRATION (mg/ml) | 2.000 |
| FLOW RATE (ml/min) | 0.991 |
| INJECTION VOLUME (ul) | 200.0 |
| SOLVENT | DMF |
| COLUMNS | B |
| DETECTOR | RI |
| PEAK AREA: | 11.101 |

| | |
|---|---|
| Calibration file: | DMF528.nar |
| Run date: | 07/11/9511:58 |
| Peak Parameters: | DMF528.pkp |
| Tau | 0.135 |
| Sigma | 0.133 |

**Baseline Sets:**

| | | |
|---|---|---|
| Int. limits: | 13.04 | 15.53 |
| baseline: | 12.53 | 21.76 |

**Operator:** JC

# GPC Summary Report

Run No: D821
Sample: 9 (9031)

**Calculation:** Standard Calc

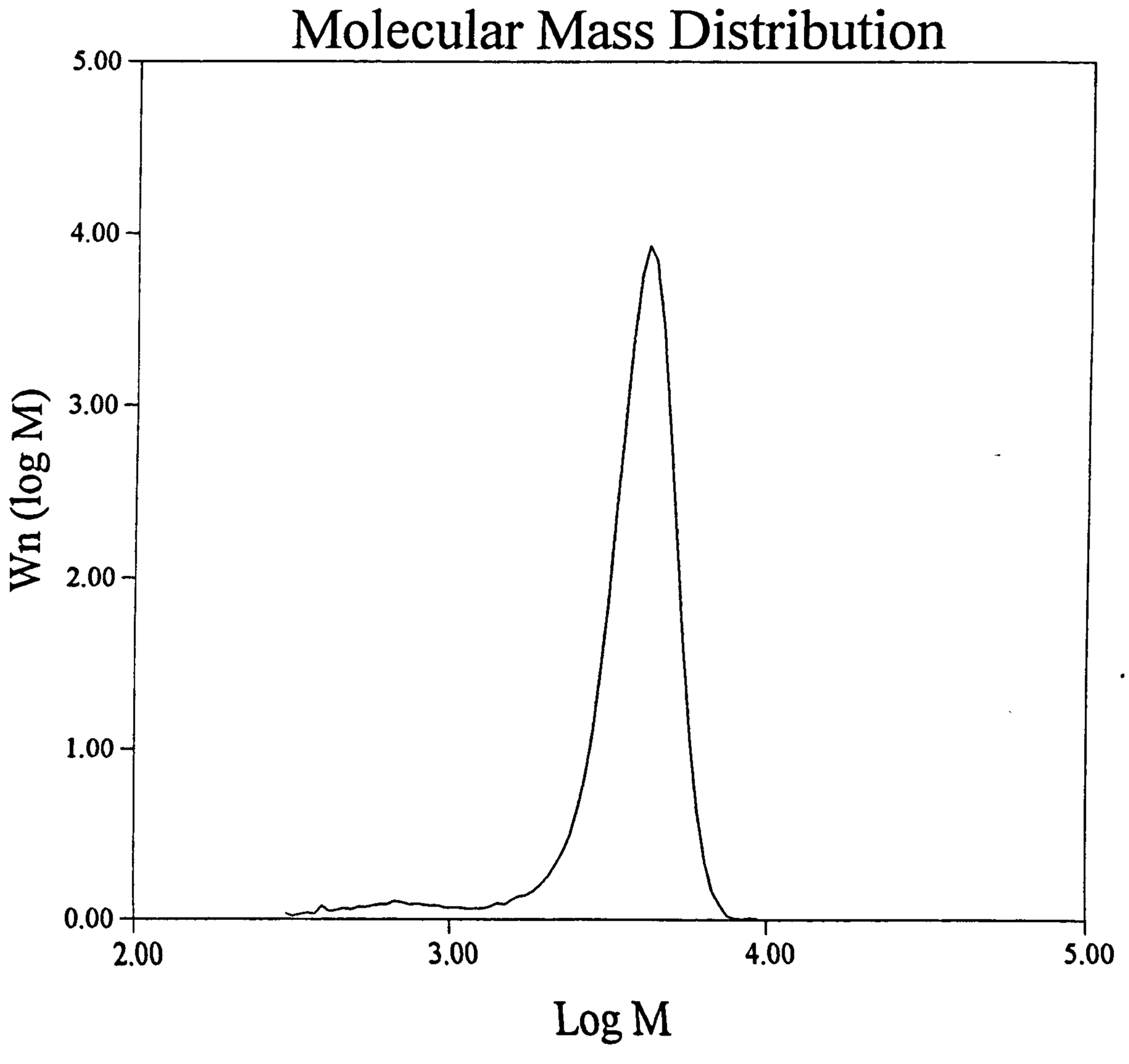


## Molecular Mass Values

| | |
|---|---|
| **Mw:** | 3890. |
| **Mn:** | 3140. |
| **Mp:** | 4170. |
| **Mw/Mn** | 1.24 |

## Parameters

| | |
|---|---|
| CONCENTRATION (mg/ml) | 2.280 |
| FLOW RATE (ml/min) | 0.993 |
| INJECTION VOLUME (ul) | 200.0 |
| SOLVENT | DMF |
| COLUMNS | B |
| DETECTOR | RI |
| PEAK AREA: | 13.503 |

| | |
|---|---|
| Calibration file: | dmf528.nar |
| Run date: | 07/11/9513:21 |
| Peak Parameters: | dmf528.pkp |
| Tau | 0.135 |
| Sigma | 0.133 |

**Baseline Sets:**

| | | |
|---|---|---|
| Int. limits: | 13.03 | 15.61 |
| baseline: | 12.68 | 22.89 |

**Operator:** JC

# GPC Summary Report

Run No: D822
Sample: 10 (9032)

**Calculation:** Standard Calc

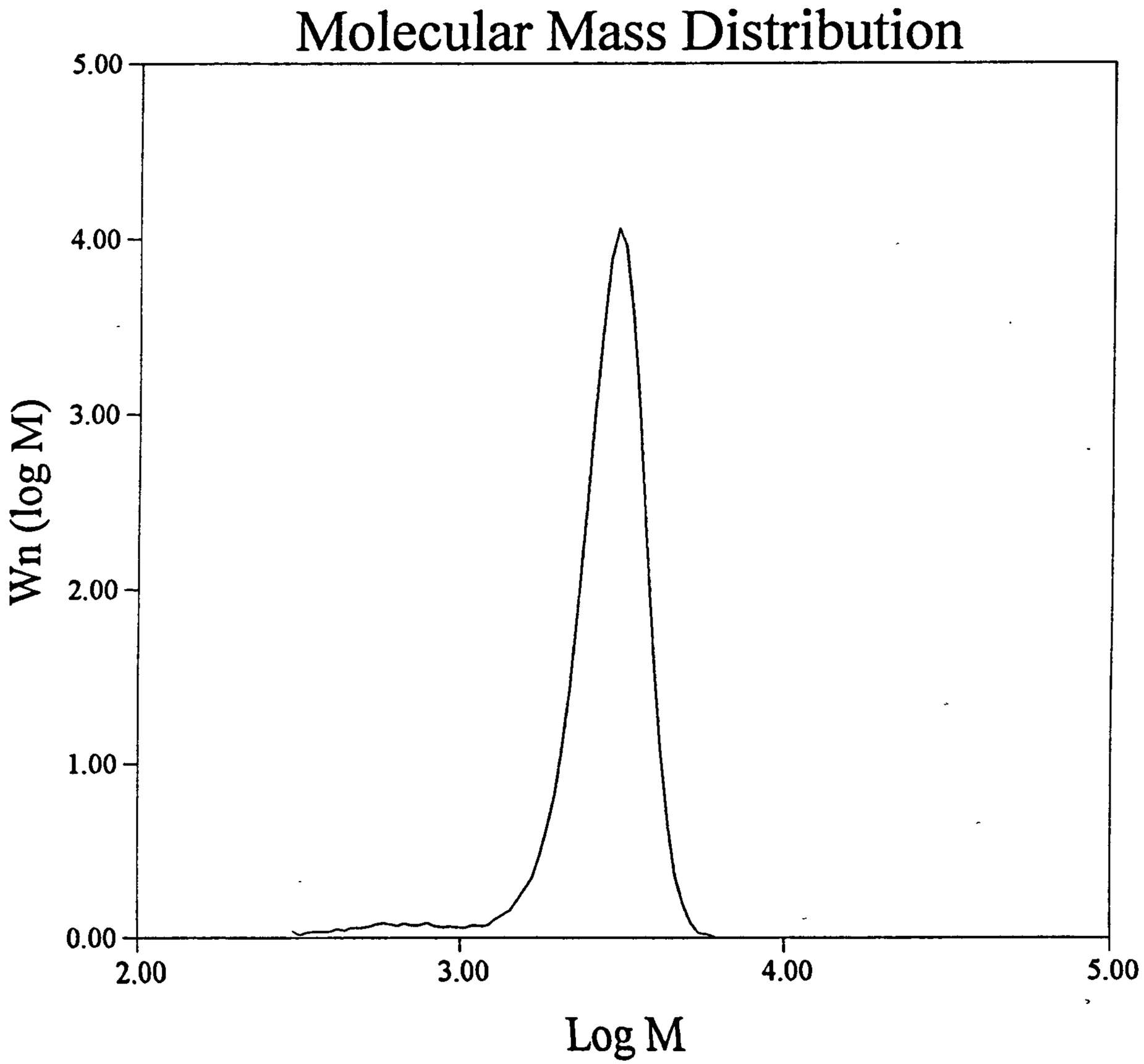


## Molecular Mass Values

| | |
|---|---|
| **Mw:** | 2880. |
| **Mn:** | 2510. |
| **Mp:** | 3030. |
| **Mw/Mn** | 1.15 |

## Parameters

| | |
|---|---|
| CONCENTRATION (mg/ml) | 2.280 |
| FLOW RATE (ml/min) | 0.993 |
| INJECTION VOLUME (ul) | 200.0 |
| SOLVENT | DMF |
| COLUMNS | B |
| DETECTOR | RI |
| PEAK AREA: | 12.716 |

| | |
|---|---|
| Calibration file: | DMF528.nar |
| Run date: | 07/11/9513:47 |
| Peak Parameters: | dmf528.pkp |
| Tau | 0.135 |
| Sigma | 0.133 |

**Baseline Sets:**

| | | |
|---|---|---|
| Int. limits: | 13.31 | 15.60 |
| baseline: | 12.37 | 22.44 |

**Operator:** JC

# GPC Summary Report

Run No: D820
Sample: 11 (9033)

**Calculation:** Standard Calc

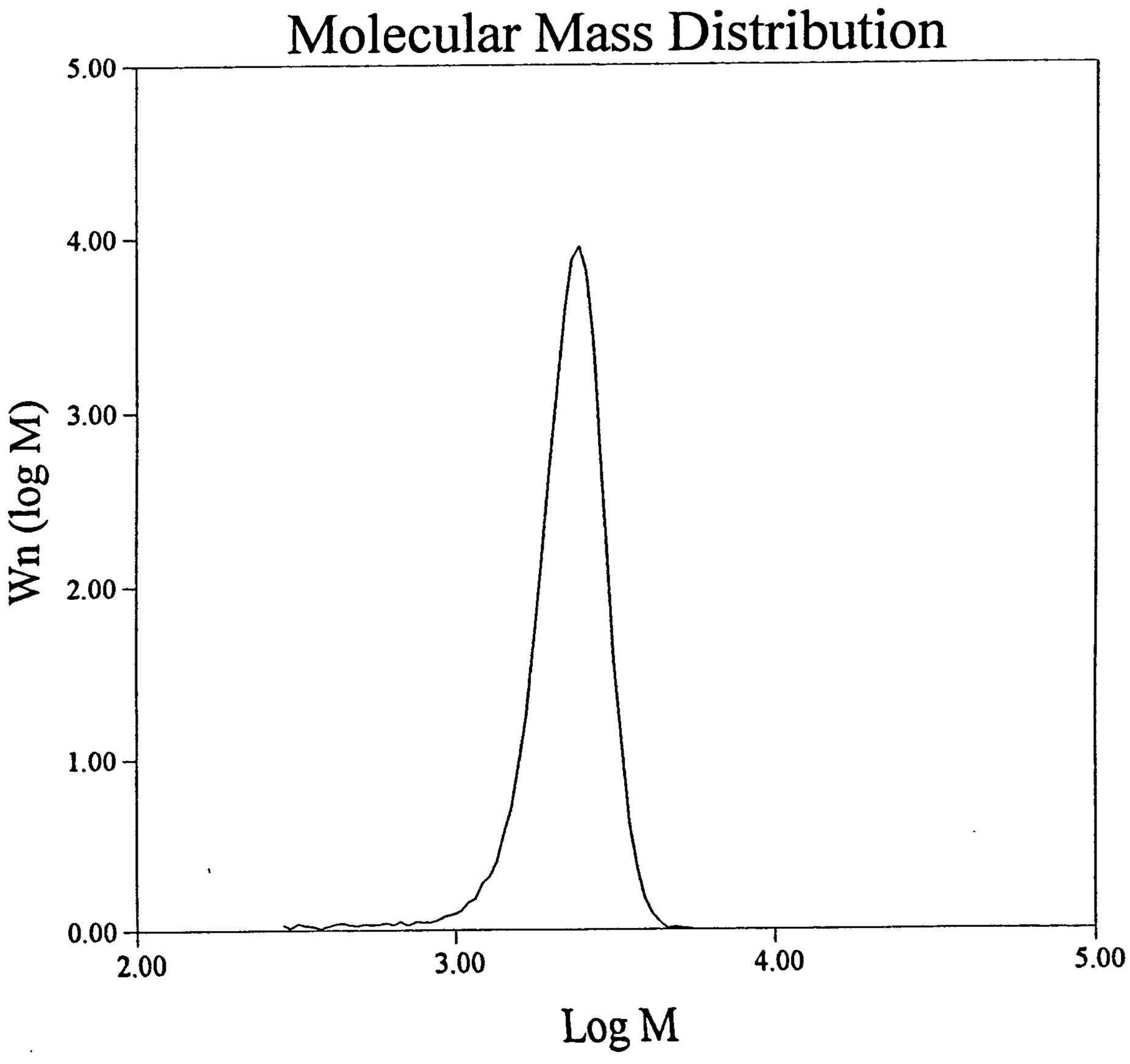


## Molecular Mass Values

| | |
|---|---|
| **Mw:** | 2320. |
| **Mn:** | 2120. |
| **Mp:** | 2440. |
| **Mw/Mn** | 1.09 |

## Parameters

| | |
|---|---|
| CONCENTRATION (mg/ml) | 2.060 |
| FLOW RATE (ml/min) | 0.993 |
| INJECTION VOLUME (ul) | 200.0 |
| SOLVENT | DMF |
| COLUMNS | B |
| DETECTOR | RI |
| PEAK AREA: | 11.005 |

| | |
|---|---|
| Calibration file: | dmf528.nar |
| Run date: | 07/11/9512:49 |
| Peak Parameters: | dmf528.pkp |
| Tau | 0.135 |
| Sigma | 0.133 |

**Baseline Sets:**

| | | |
|---|---|---|
| Int. limits: | 13.40 | 15.63 |
| baseline: | 12.85 | 22.85 |

**Operator:** JC

# GPC Summary Report

Run No: D824
Sample: 12 (9034)

**Calculation:** Standard Calc

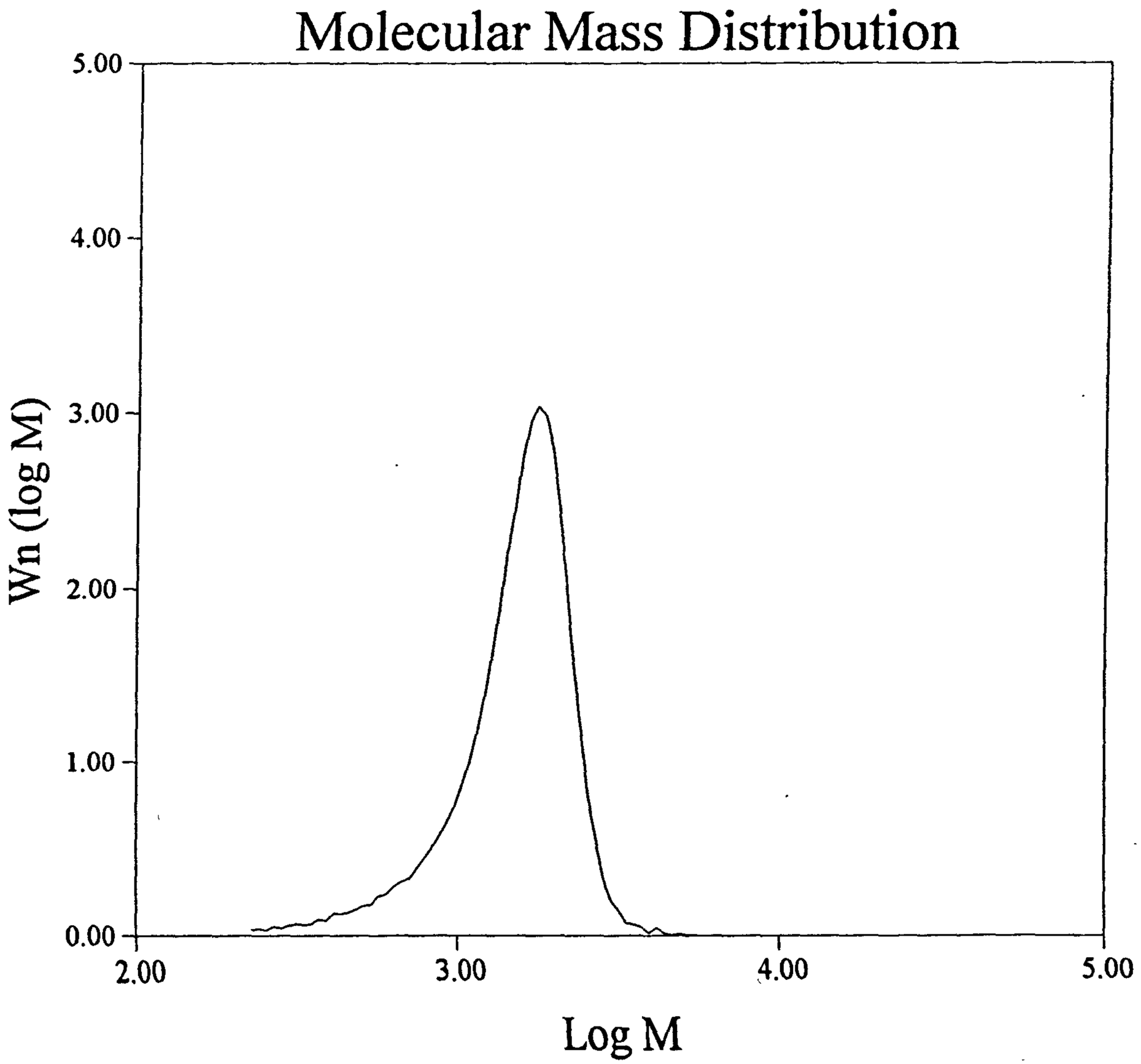


## Molecular Mass Values

| | |
|---|---|
| **Mw:** | 1610. |
| **Mn:** | 1360. |
| **Mp:** | 1770. |
| **Mw/Mn** | 1.18 |

## Parameters

| | |
|---|---|
| CONCENTRATION (mg/ml) | 2.100 |
| FLOW RATE (ml/min) | 0.993 |
| INJECTION VOLUME (ul) | 200.0 |
| SOLVENT | DMF |
| COLUMNS | B |
| DETECTOR | RI |
| PEAK AREA: | 11.525 |

| | |
|---|---|
| Calibration file: | DMF528.nar |
| Run date: | 07/11/9514:38 |
| Peak Parameters: | dmf528.pkp |
| Tau | 0.135 |
| Sigma | 0.133 |

**Baseline Sets:**

| | | |
|---|---|---|
| Int. limits: | 13.43 | 15.79 |
| baseline: | 12.81 | 22.51 |

**Operator:** JC

# GPC Summary Report

Run No: D819
Sample: 13 (9035)

**Calculation:** Standard Calc

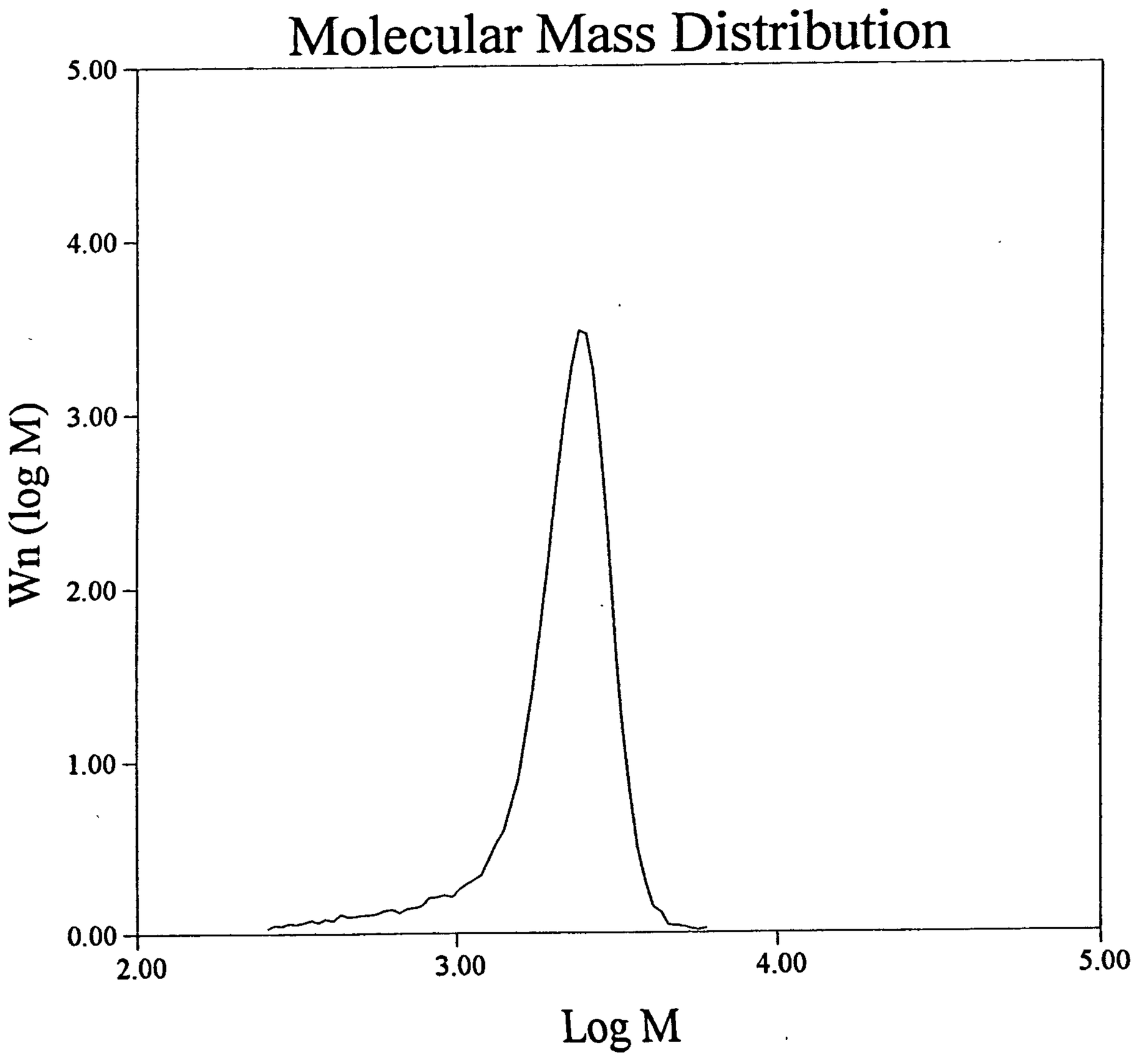


## Molecular Mass Values

| | |
|---|---|
| **Mw:** | 2250. |
| **Mn:** | 1850. |
| **Mp:** | 2420. |
| **Mw/Mn** | 1.22 |

## Parameters

| | |
|---|---|
| CONCENTRATION (mg/ml) | 1.940 |
| FLOW RATE (ml/min) | 0.991 |
| INJECTION VOLUME (ul) | 200.0 |
| SOLVENT | DMF |
| COLUMNS | B |
| DETECTOR | RI |
| PEAK AREA: | 9.508 |

| | |
|---|---|
| Calibration file: | DMF528.nar |
| Run date: | 07/11/9512:24 |
| Peak Parameters: | dmf528.pkp |
| Tau | 0.135 |
| Sigma | 0.133 |

**Baseline Sets:**

| | | |
|---|---|---|
| Int. limits: | 13.33 | 15.72 |
| baseline: | 13.01 | 21.91 |

**Operator:** JC

# GPC Summary Report

Run No: D827
Sample: 14 (9036)

**Calculation:** Standard Calc

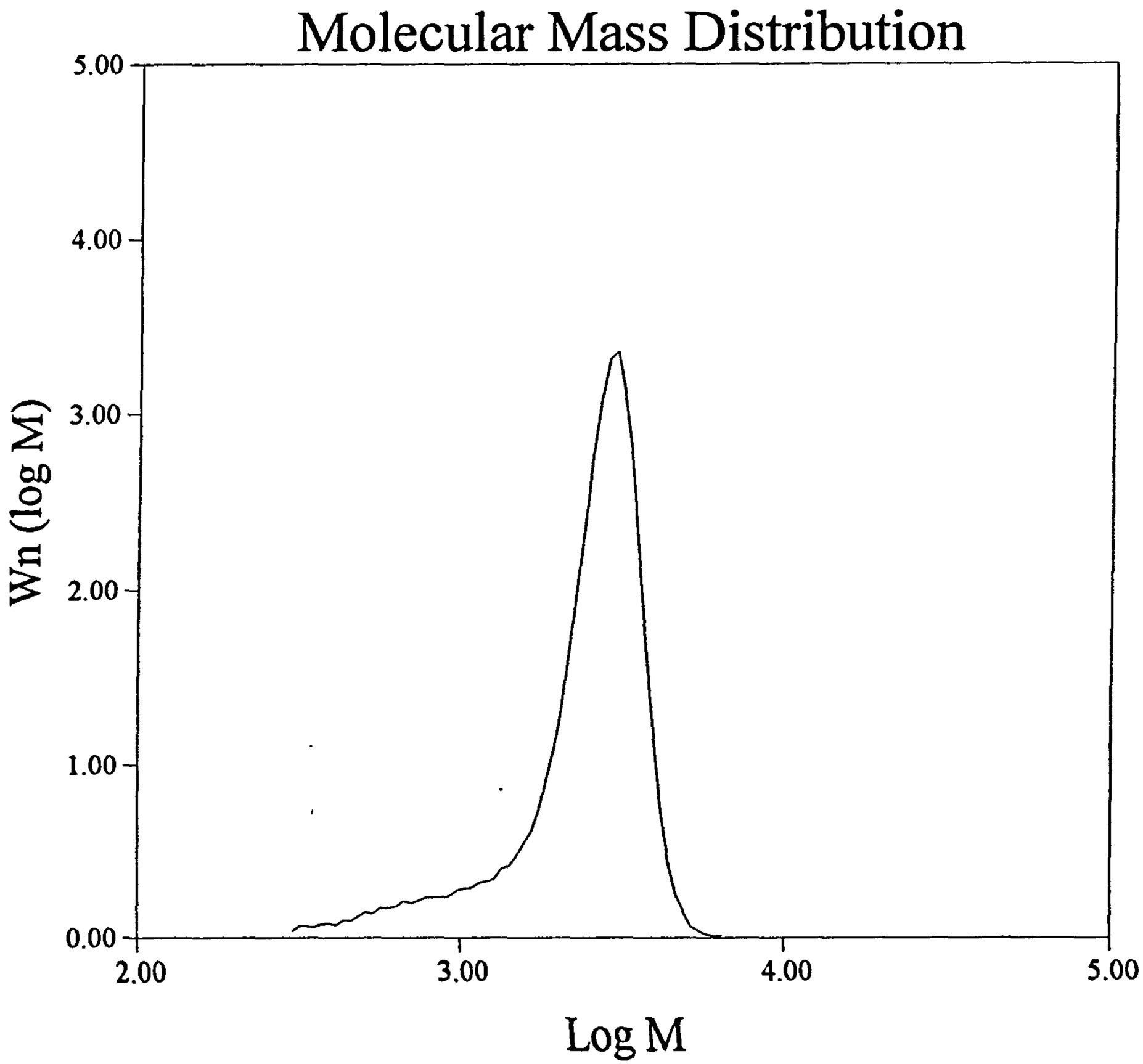


## Molecular Mass Values

| | |
|---|---|
| **Mw:** | 2580. |
| **Mn:** | 2020. |
| **Mp:** | 3030. |
| **Mw/Mn** | 1.28 |

## Parameters

| | |
|---|---|
| CONCENTRATION (mg/ml) | 2.100 |
| FLOW RATE (ml/min) | 0.993 |
| INJECTION VOLUME (ul) | 200.0 |
| SOLVENT | DMF |
| COLUMNS | B |
| DETECTOR | RI |
| PEAK AREA: | 9.212 |

| | |
|---|---|
| Calibration file: | dmf528.nar |
| Run date: | 07/11/9515:59 |
| Peak Parameters: | dmf528.pkp |
| Tau | 0.135 |
| Sigma | 0.133 |

**Baseline Sets:**

| | | |
|---|---|---|
| Int. limits: | 13.21 | 15.60 |
| baseline: | 13.28 | 21.61 |

**Operator:** JC

# GPC Summary Report

Run No: D826
Sample: 15 (9037)

**Calculation:** Standard Calc

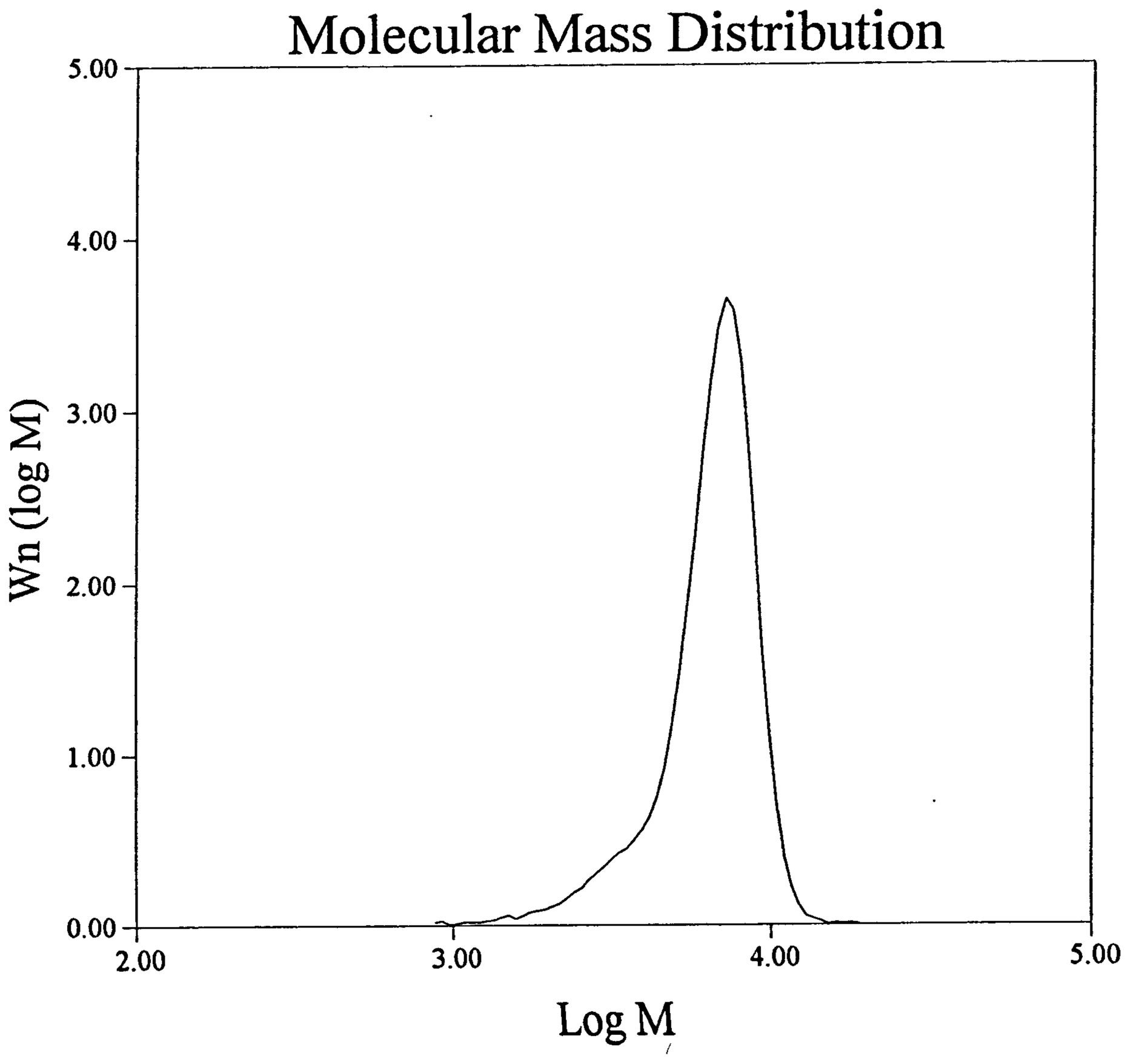


## Molecular Mass Values

| | |
|---|---|
| **Mw:** | 6660. |
| **Mn:** | 5900. |
| **Mp:** | 7150. |
| **Mw/Mn** | 1.13 |

## Parameters

| | |
|---|---|
| CONCENTRATION (mg/ml) | 2.290 |
| FLOW RATE (ml/min) | 0.993 |
| INJECTION VOLUME (ul) | 200.0 |
| SOLVENT | DMF |
| COLUMNS | B |
| DETECTOR | RI |
| PEAK AREA: | 14.799 |

| | |
|---|---|
| Calibration file: | dmf528.nar |
| Run date: | 07/11/9515:33 |
| Peak Parameters: | dmf528.pkp |
| Tau | 0.135 |
| Sigma | 0.133 |

**Baseline Sets:**

| | | |
|---|---|---|
| Int. limits: | 12.50 | 14.81 |
| baseline: | 12.50 | 21.80 |

**Operator:** JC

# GPC Summary Report

Run No: D836
Sample: 16 (9038)

**Calculation:** Standard Calc

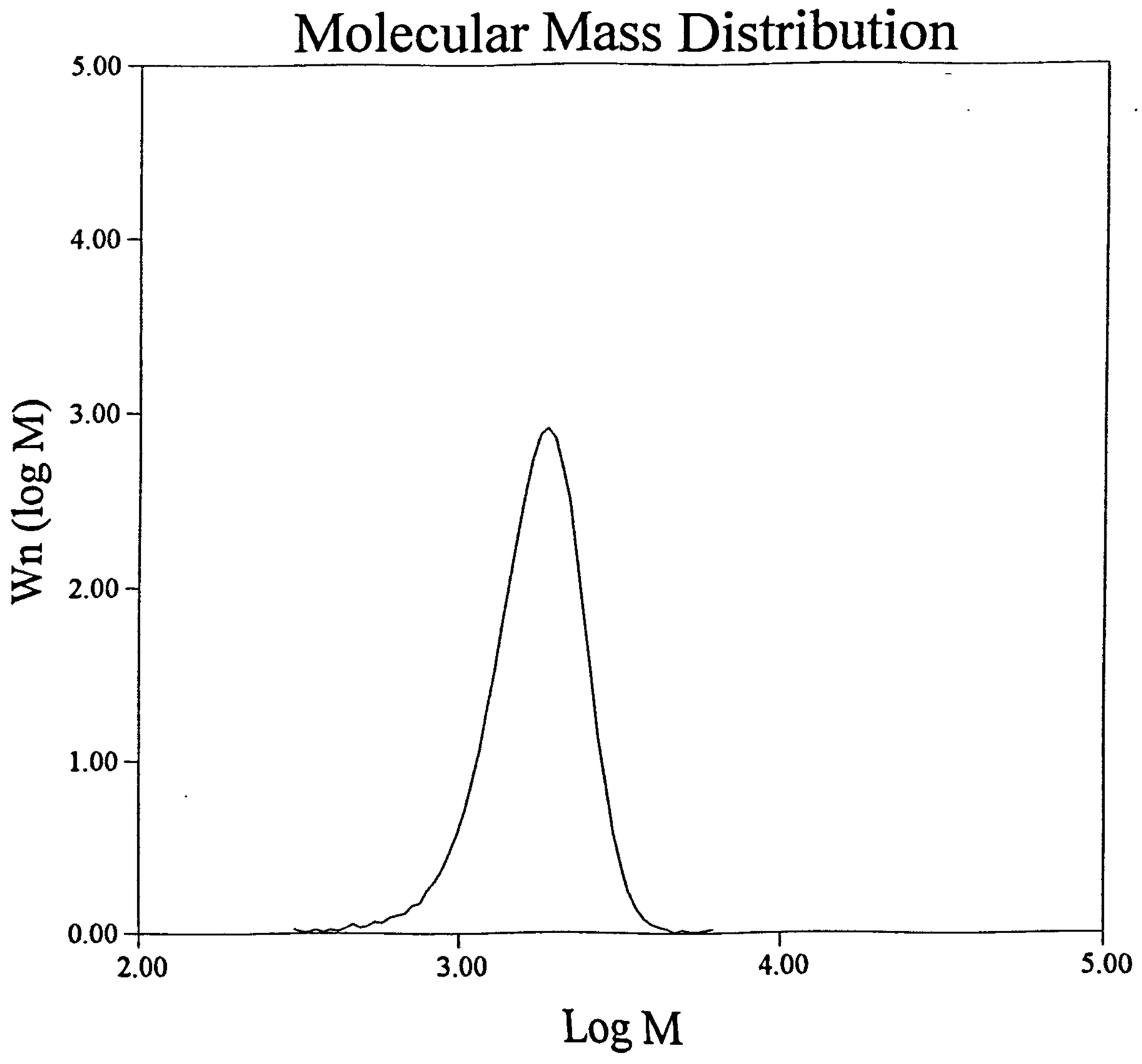


## Molecular Mass Values

| | |
|---|---|
| **Mw:** | 1830. |
| **Mn:** | 1630. |
| **Mp:** | 1890. |
| **Mw/Mn** | 1.12 |

## Parameters

| | |
|---|---|
| CONCENTRATION (mg/ml) | 2.080 |
| FLOW RATE (ml/min) | 0.996 |
| INJECTION VOLUME (ul) | 200.0 |
| SOLVENT | DMF |
| COLUMNS | B |
| DETECTOR | RI |
| PEAK AREA: | 10.638 |

| | |
|---|---|
| Calibration file: | dmf528.nar |
| Run date: | 07/12/9511:24 |
| Peak Parameters: | dmf528.pkp |
| Tau | 0.135 |
| Sigma | 0.133 |

**Baseline Sets:**

| | | |
|---|---|---|
| Int. limits: | 13.31 | 15.61 |
| baseline: | 12.68 | 22.31 |

**Operator:** JC

# GPC Summary Report

Run No: D844
Sample: 17 (9039)

**Calculation:** Standard Calc

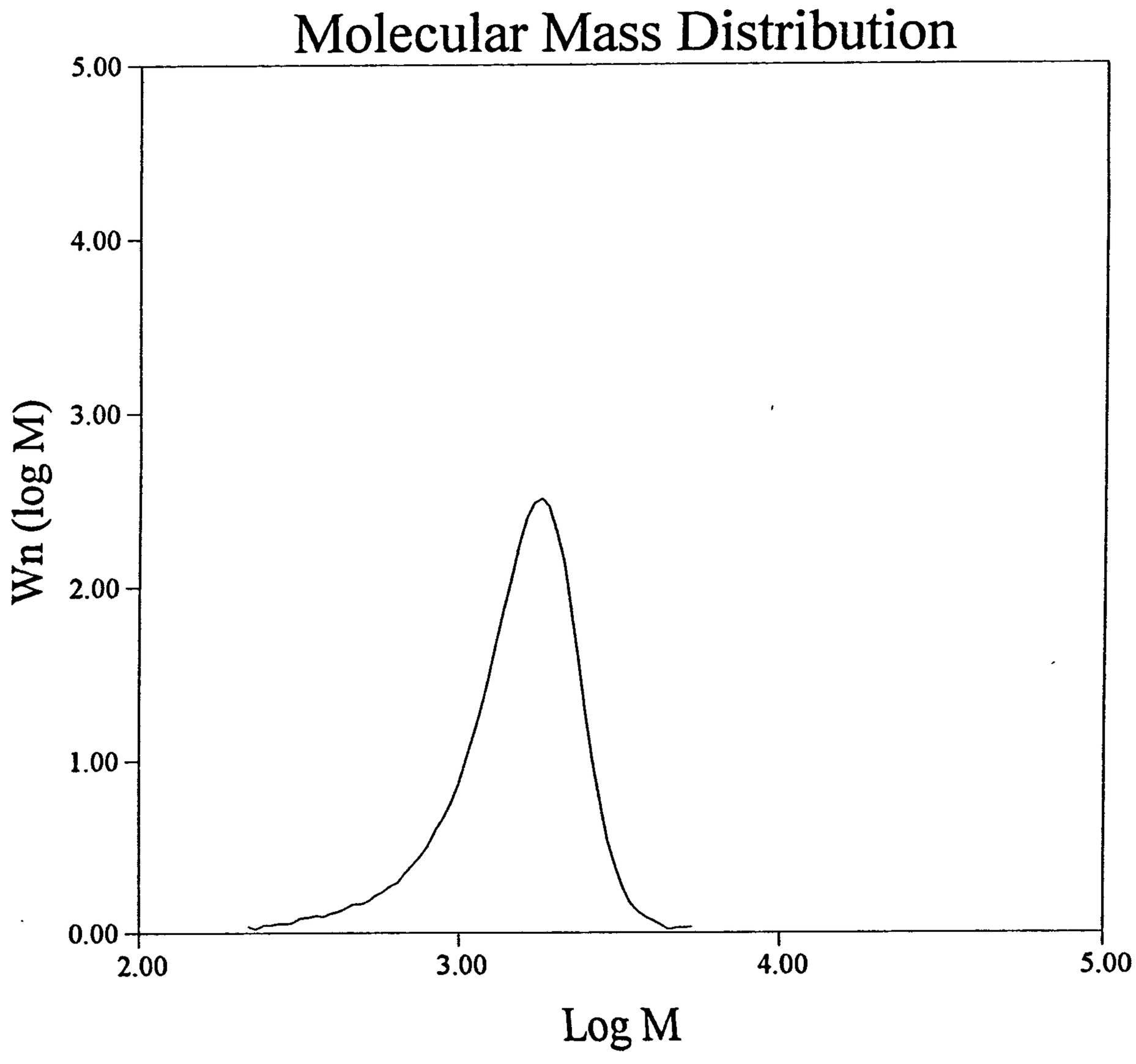


## Molecular Mass Values

| | |
|---|---|
| **Mw:** | 1650. |
| **Mn:** | 1330. |
| **Mp:** | 1810. |
| **Mw/Mn** | 1.24 |

## Parameters

| | |
|---|---|
| CONCENTRATION (mg/ml) | 1.880 |
| FLOW RATE (ml/min) | 0.998 |
| INJECTION VOLUME (ul) | 200.0 |
| SOLVENT | DMF |
| COLUMNS | B |
| DETECTOR | RI |
| PEAK AREA: | 10.433 |

| | |
|---|---|
| Calibration file: | DMF528.nar |
| Run date: | 07/12/9515:26 |
| Peak Parameters: | dmf528.pkp |
| Tau | 0.135 |
| Sigma | 0.133 |

**Baseline Sets:**

| | | |
|---|---|---|
| Int. limits: | 13.41 | 15.83 |
| baseline: | 12.32 | 21.01 |

**Operator:** JC

# GPC Summary Report

Run No: D830
Sample: 18 (9040)

**Calculation:** Standard Calc

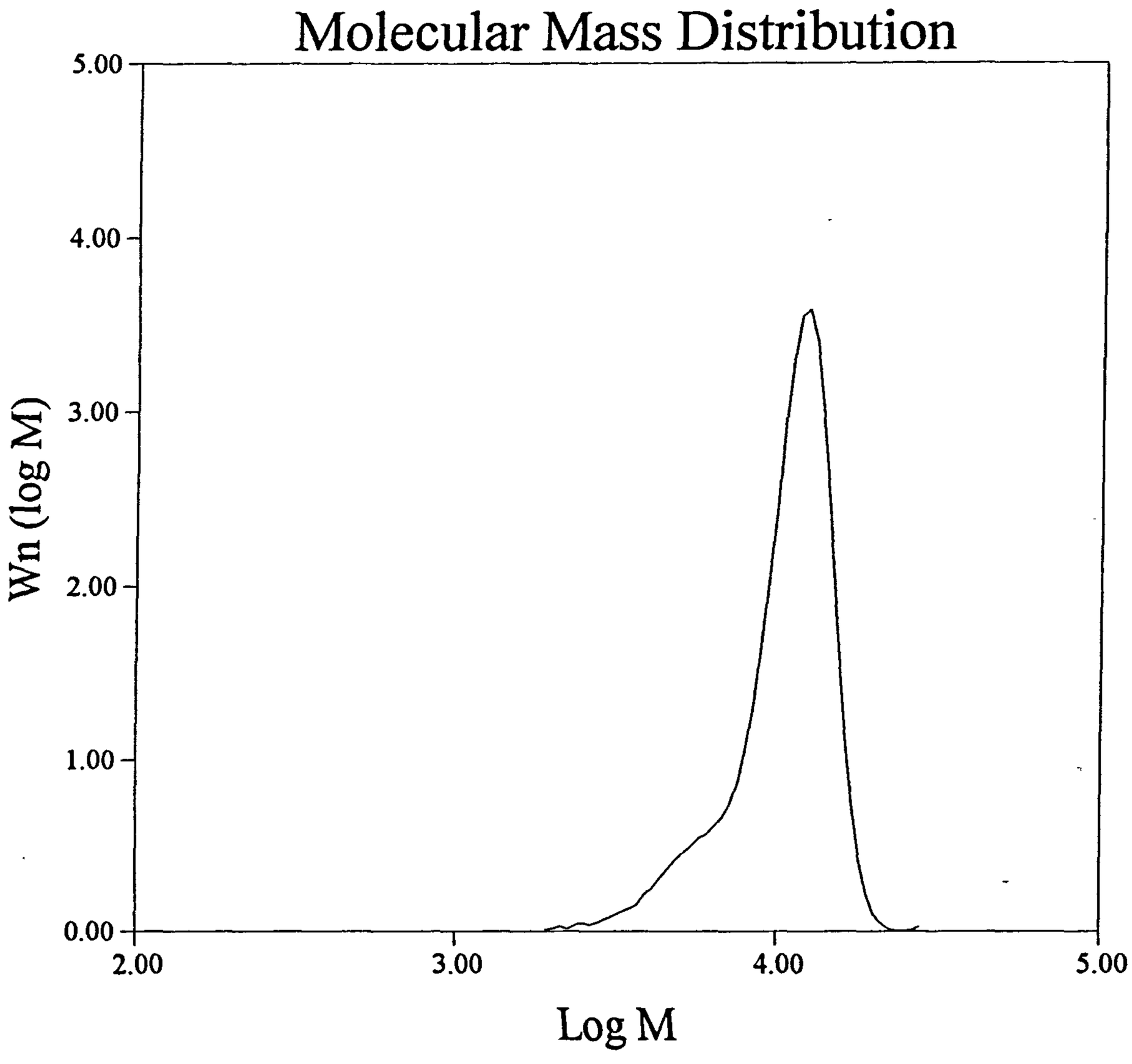


## Molecular Mass Values

| | |
|---|---|
| **Mw:** | 10900. |
| **Mn:** | 9700. |
| **Mp:** | 12300. |
| **Mw/Mn** | 1.12 |

## Parameters

| | |
|---|---|
| CONCENTRATION (mg/ml) | 1.940 |
| FLOW RATE (ml/min) | 0.993 |
| INJECTION VOLUME (ul) | 200.0 |
| SOLVENT | DMF |
| COLUMNS | B |
| DETECTOR | RI |
| PEAK AREA: | 12.401 |

| | |
|---|---|
| Calibration file: | dmf528.nar |
| Run date: | 07/11/9517:22 |
| Peak Parameters: | dmf528.pkp |
| Tau | 0.135 |
| Sigma | 0.133 |

**Baseline Sets:**

| | | |
|---|---|---|
| Int. limits: | 12.20 | 14.22 |
| baseline: | 12.16 | 22.12 |

**Operator:** JC

# GPC Summary Report

Run No: D846
Sample: 19 (9041)

**Calculation:** Standard Calc

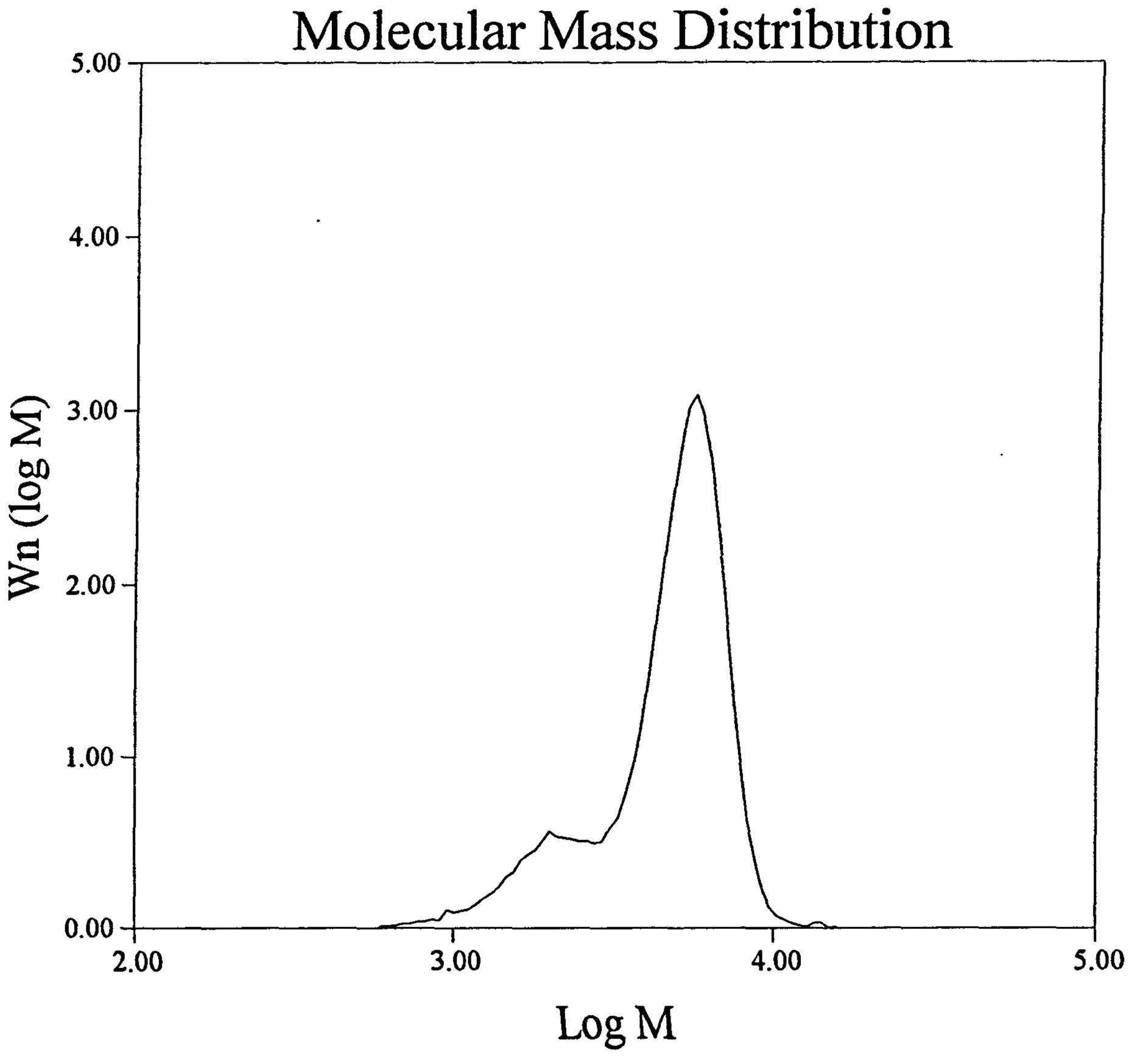


## Molecular Mass Values

| | |
|---|---|
| **Mw:** | 4910. |
| **Mn:** | 3920. |
| **Mp:** | 5680. |
| **Mw/Mn** | 1.25 |

## Parameters

| | |
|---|---|
| CONCENTRATION (mg/ml) | 1.850 |
| FLOW RATE (ml/min) | 1.000 |
| INJECTION VOLUME (ul) | 200.0 |
| SOLVENT | DMF |
| COLUMNS | B |
| DETECTOR | RI |
| PEAK AREA: | 10.595 |

| | |
|---|---|
| Calibration file: | DMF528.nar |
| Run date: | 07/12/9516:17 |
| Peak Parameters: | DMF528.pkp |
| Tau | 0.135 |
| Sigma | 0.133 |

**Baseline Sets:**

| | | |
|---|---|---|
| Int. limits: | 12.61 | 15.10 |
| baseline: | 12.22 | 22.90 |

**Operator:** JC

# GPC Summary Report

Run No: D848
Sample: 20 (9042)

**Calculation:** Standard Calc

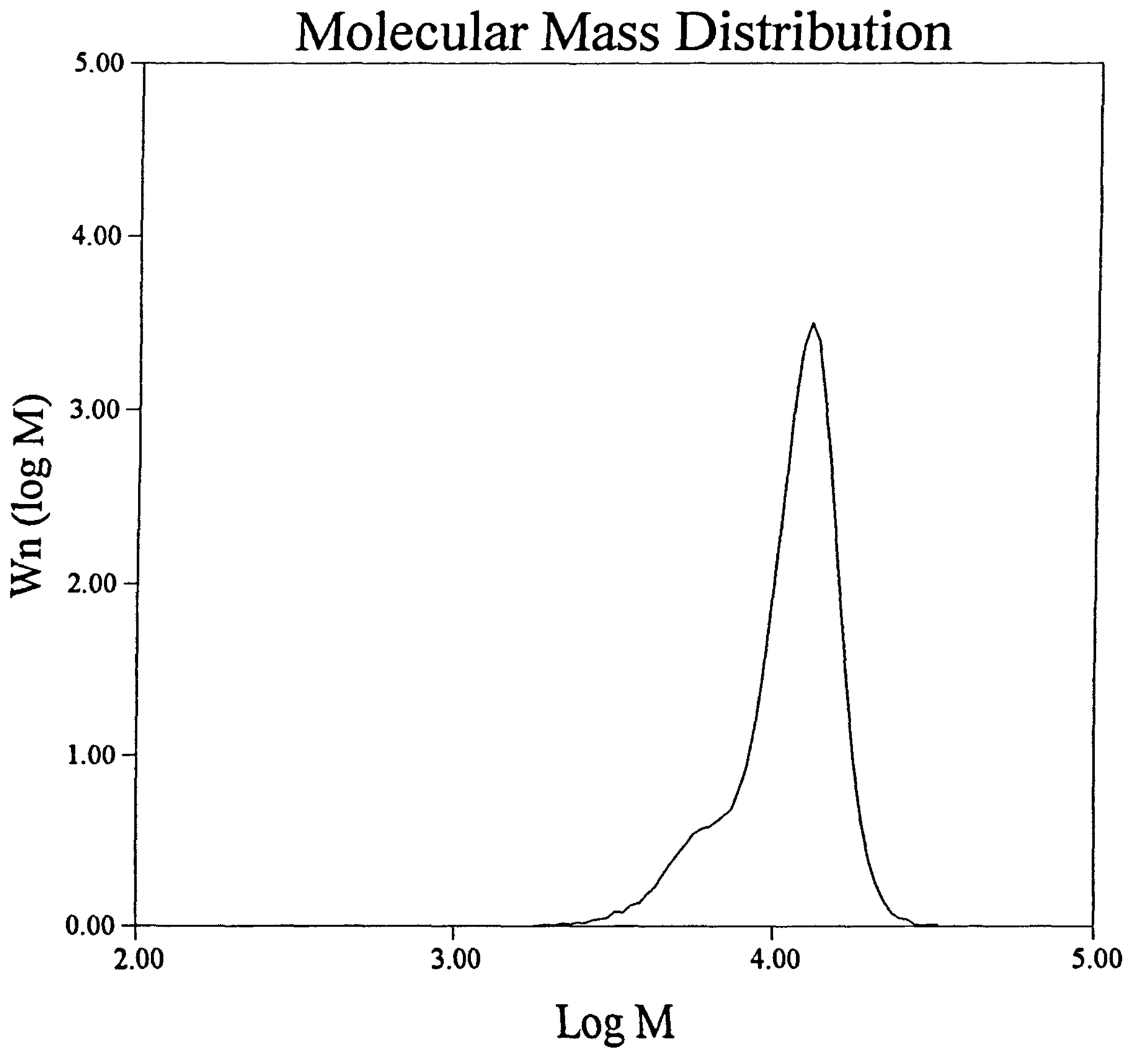


## Molecular Mass Values

| | |
|---|---|
| **Mw:** | 11800. |
| **Mn:** | 10400. |
| **Mp:** | 12900. |
| **Mw/Mn** | 1.13 |

## Parameters

| | |
|---|---|
| CONCENTRATION (mg/ml) | 2.220 |
| FLOW RATE (ml/min) | 1.000 |
| INJECTION VOLUME (ul) | 200.0 |
| SOLVENT | DMF |
| COLUMNS | B |
| DETECTOR | RI |
| PEAK AREA: | 14.328 |

| | |
|---|---|
| Calibration file: | dmf528.nar |
| Run date: | 07/12/9517:07 |
| Peak Parameters: | dmf528.pkp |
| Tau | 0.135 |
| Sigma | 0.133 |

**Baseline Sets:**

| | | |
|---|---|---|
| Int. limits: | 12.10 | 14.20 |
| baseline: | 11.54 | 21.01 |

**Operator:** JC

# GPC Summary Report

Run No: D847
Sample: 21 (9043)

**Calculation:** Standard Calc

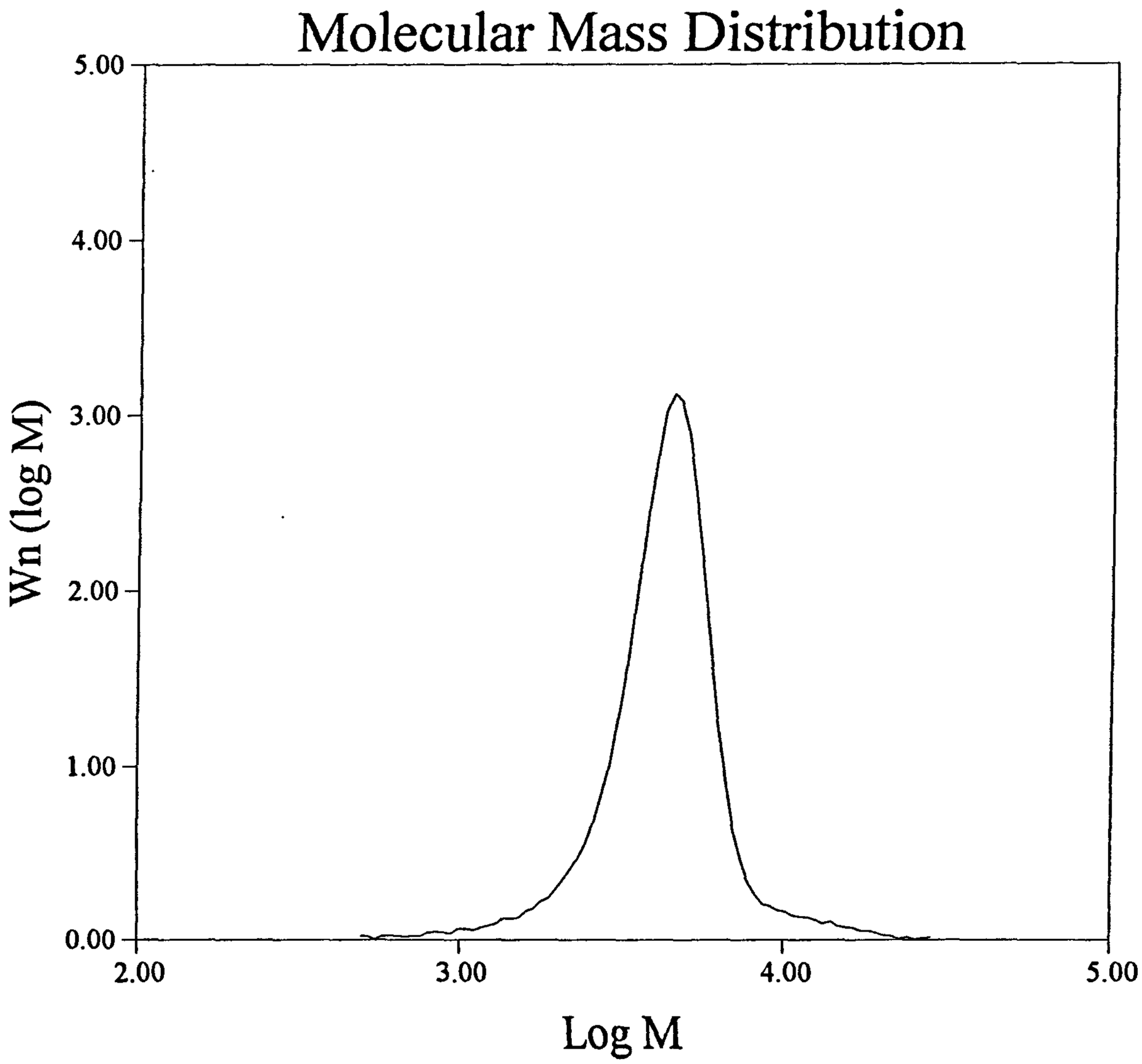


## Molecular Mass Values

| | |
|---|---|
| **Mw:** | 4660. |
| **Mn:** | 3860. |
| **Mp:** | 4510. |
| **Mw/Mn** | 1.21 |

## Parameters

| | |
|---|---|
| CONCENTRATION (mg/ml) | 2.150 |
| FLOW RATE (ml/min) | 0.998 |
| INJECTION VOLUME (ul) | 200.0 |
| SOLVENT | DMF |
| COLUMNS | B |
| DETECTOR | RI |
| PEAK AREA: | 14.050 |

| | |
|---|---|
| Calibration file: | dmf528.nar |
| Run date: | 07/12/9516:42 |
| Peak Parameters: | dmf528.pkp |
| Tau | 0.135 |
| Sigma | 0.133 |

**Baseline Sets:**

| | | |
|---|---|---|
| Int. limits: | 12.21 | 15.22 |
| baseline: | 11.24 | 22.01 |

**Operator:** JC

# GPC Summary Report

Run No: D857
Sample: 22 (9044)

**Calculation:** Standard Calc

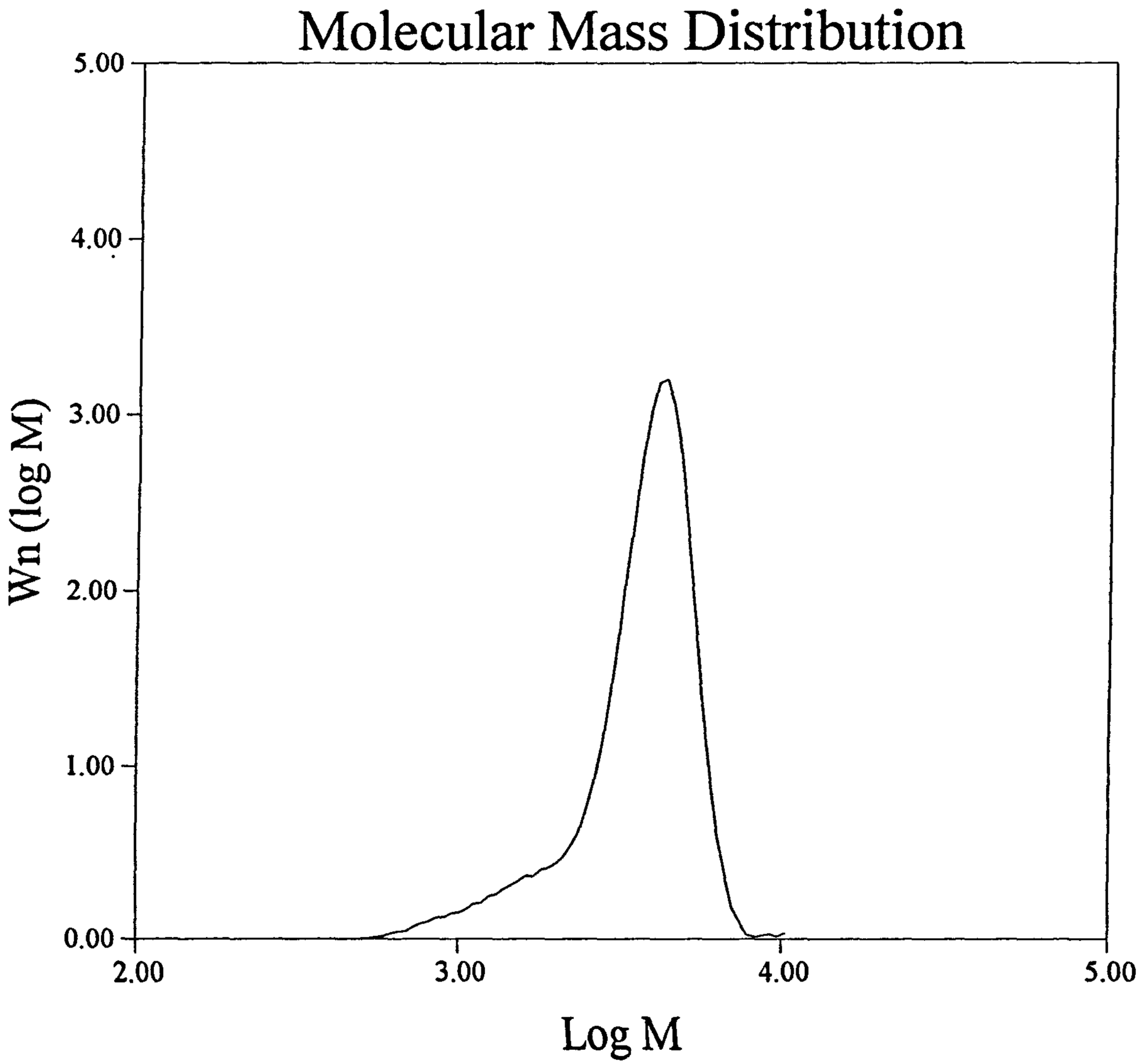


## Molecular Mass Values

| | |
|---|---|
| **Mw:** | 3810. |
| **Mn:** | 3190. |
| **Mp:** | 4330. |
| **Mw/Mn** | 1.19 |

## Parameters

| | |
|---|---|
| CONCENTRATION (mg/ml) | 2.270 |
| FLOW RATE (ml/min) | 1.000 |
| INJECTION VOLUME (ul) | 200.0 |
| SOLVENT | DMF |
| COLUMNS | B |
| DETECTOR | RI |
| PEAK AREA: | 12.562 |

| | |
|---|---|
| Calibration file: | dmf528.nar |
| Run date: | 07/13/9511:55 |
| Peak Parameters: | dmf528.pkp |
| Tau | 0.135 |
| Sigma | 0.133 |

**Baseline Sets:**

| | | |
|---|---|---|
| Int. limits: | 12.93 | 15.21 |
| baseline: | 12.62 | 21.83 |

**Operator:** JC

# GPC Summary Report

Run No: D958
Sample: SAMPLE 23 (0754)

**Calculation:** Standard Calc

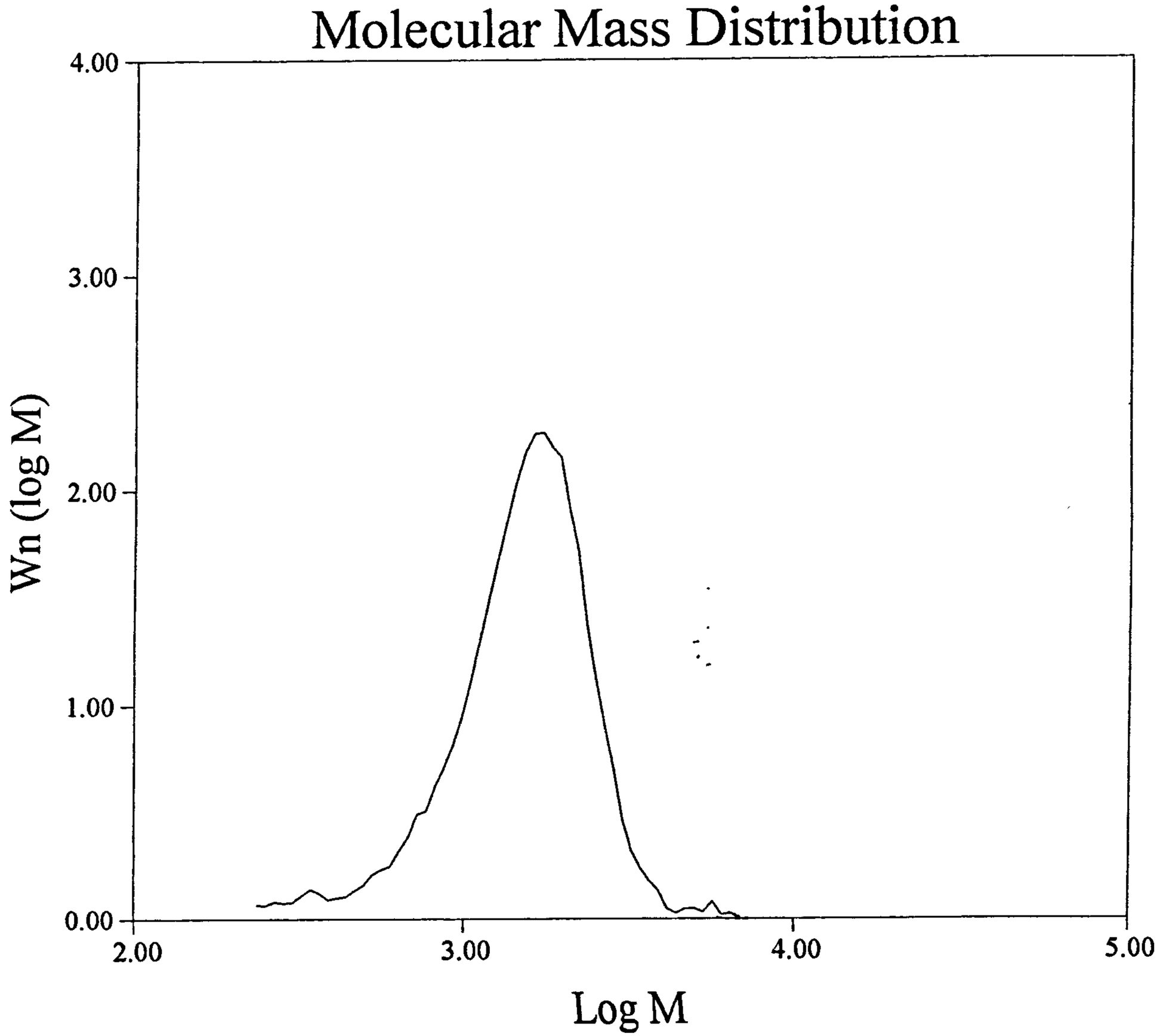


## Molecular Mass Values

| | |
|---|---|
| **Mw:** | 1630. |
| **Mn:** | 1290. |
| **Mp:** | 1750. |
| **Mw/Mn** | 1.26 |

## Parameters

| | |
|---|---|
| CONCENTRATION (mg/ml) | 2.330 |
| FLOW RATE (ml/min) | 1.002 |
| INJECTION VOLUME (ul)) | 200.0 |
| SOLVENT | DMF |
| COLUMNS | B |
| DETECTOR | RI |
| PEAK AREA: | 9.854 |

| | |
|---|---|
| Calibration file: | dmf610.nar |
| Run date: | 03/04/9617:09 |
| Peak Parameters: | dmf610.pkp |
| Tau | 0.143 |
| Sigma | 0.151 |

**Baseline Sets:**

| | | |
|---|---|---|
| Int. limits: | 13.29 | 15.49 |
| baseline: | 12.46 | 20.89 |

**Operator:** BS

# GPC Summary Report

Run No: D961
Sample: SAMPLE 24 (0755)

**Calculation:** Standard Calc

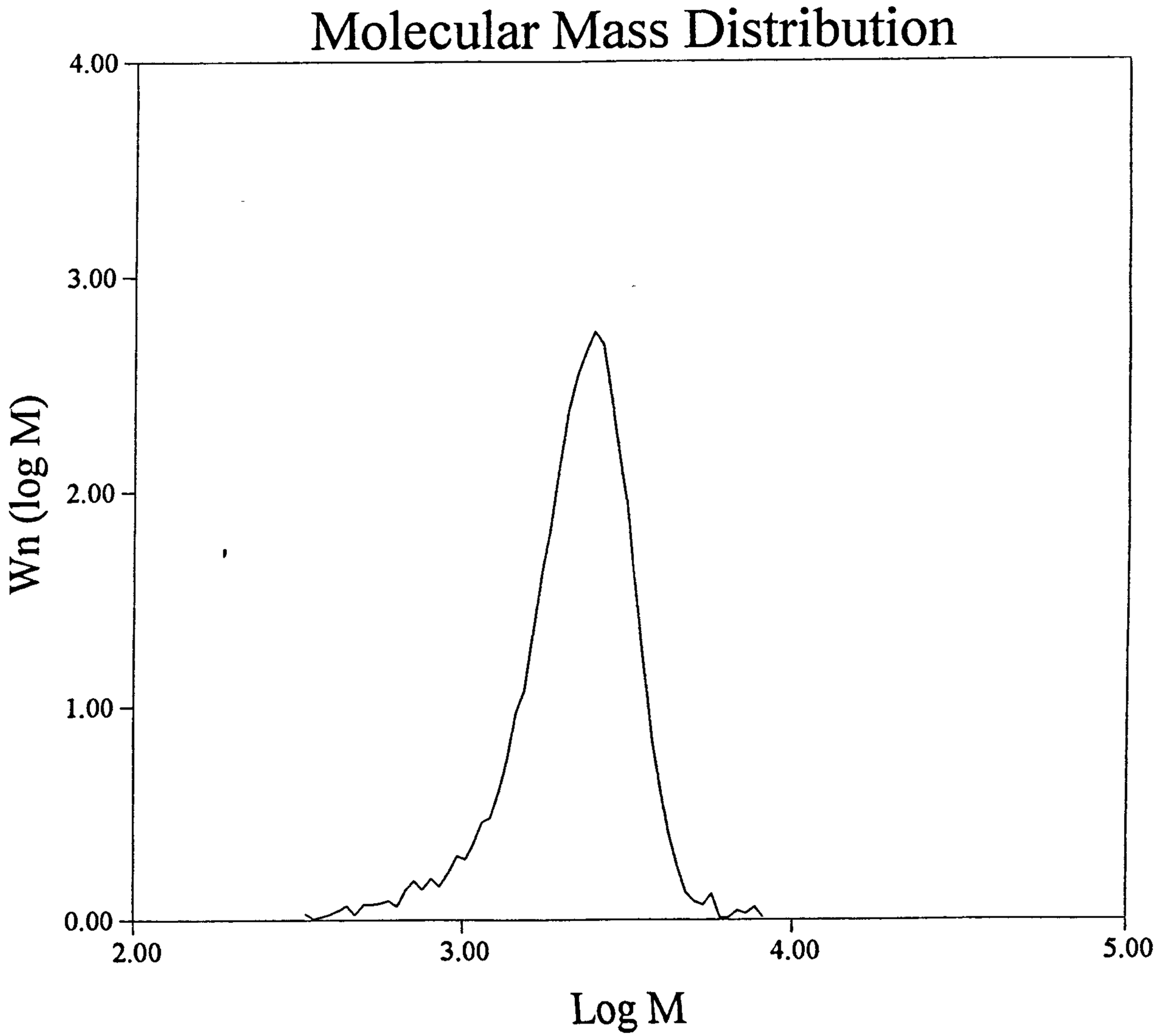


## Molecular Mass Values

| | |
|---|---|
| **Mw:** | 2350. |
| **Mn:** | 1990. |
| **Mp:** | 2500. |
| **Mw/Mn** | 1.18 |

## Parameters

| | |
|---|---|
| CONCENTRATION (mg/ml) | 2.030 |
| FLOW RATE (ml/min) | 0.993 |
| INJECTION VOLUME (ul)) | 200.0 |
| SOLVENT | DMF |
| COLUMNS | B |
| DETECTOR | RI |
| PEAK AREA: | 9.129 |

| | |
|---|---|
| Calibration file: | dmf610.nar |
| Run date: | 03/05/9610:28 |
| Peak Parameters: | dmf610.pkp |
| Tau | 0.143 |
| Sigma | 0.151 |

**Baseline Sets:**

| | | |
|---|---|---|
| Int. limits: | 13.13 | 15.31 |
| baseline: | 11.44 | 21.07 |

**Operator:** BS

# GPC Summary Report

Run No: D963
Sample: SAMPLE 25 (0756)

**Calculation:** Standard Calc

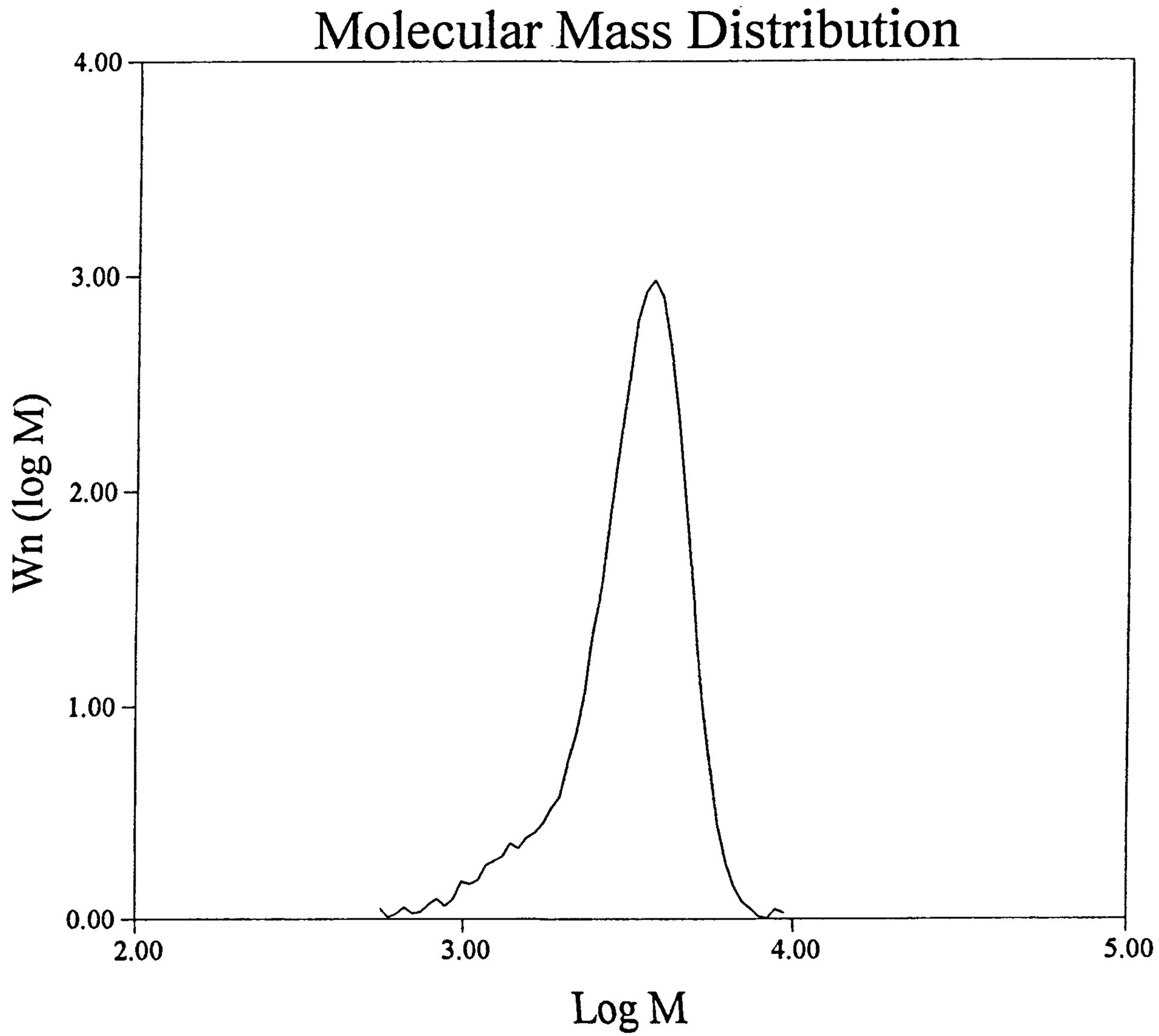


## Molecular Mass Values

| | |
|---|---|
| **Mw:** | 3390. |
| **Mn:** | 2920. |
| **Mp:** | 3740. |
| **Mw/Mn** | 1.16 |

## Parameters

| | |
|---|---|
| CONCENTRATION (mg/ml) | 2.210 |
| FLOW RATE (ml/min) | 0.996 |
| INJECTION VOLUME (ul)) | 200.0 |
| SOLVENT | DMF |
| COLUMNS | B |
| DETECTOR | RI |
| PEAK AREA: | 10.657 |

| | |
|---|---|
| Calibration file: | dmf610.nar |
| Run date: | 03/05/9611:25 |
| Peak Parameters: | dmf610.pkp |
| Tau | 0.143 |
| Sigma | 0.151 |

**Baseline Sets:**

| | | |
|---|---|---|
| Int. limits: | 13.01 | 15.01 |
| baseline: | 11.65 | 20.40 |

**Operator:** BS

# GPC Summary Report

Run No: D959
Sample: SAMPLE 26 (0757)

**Calculation:** Standard Calc

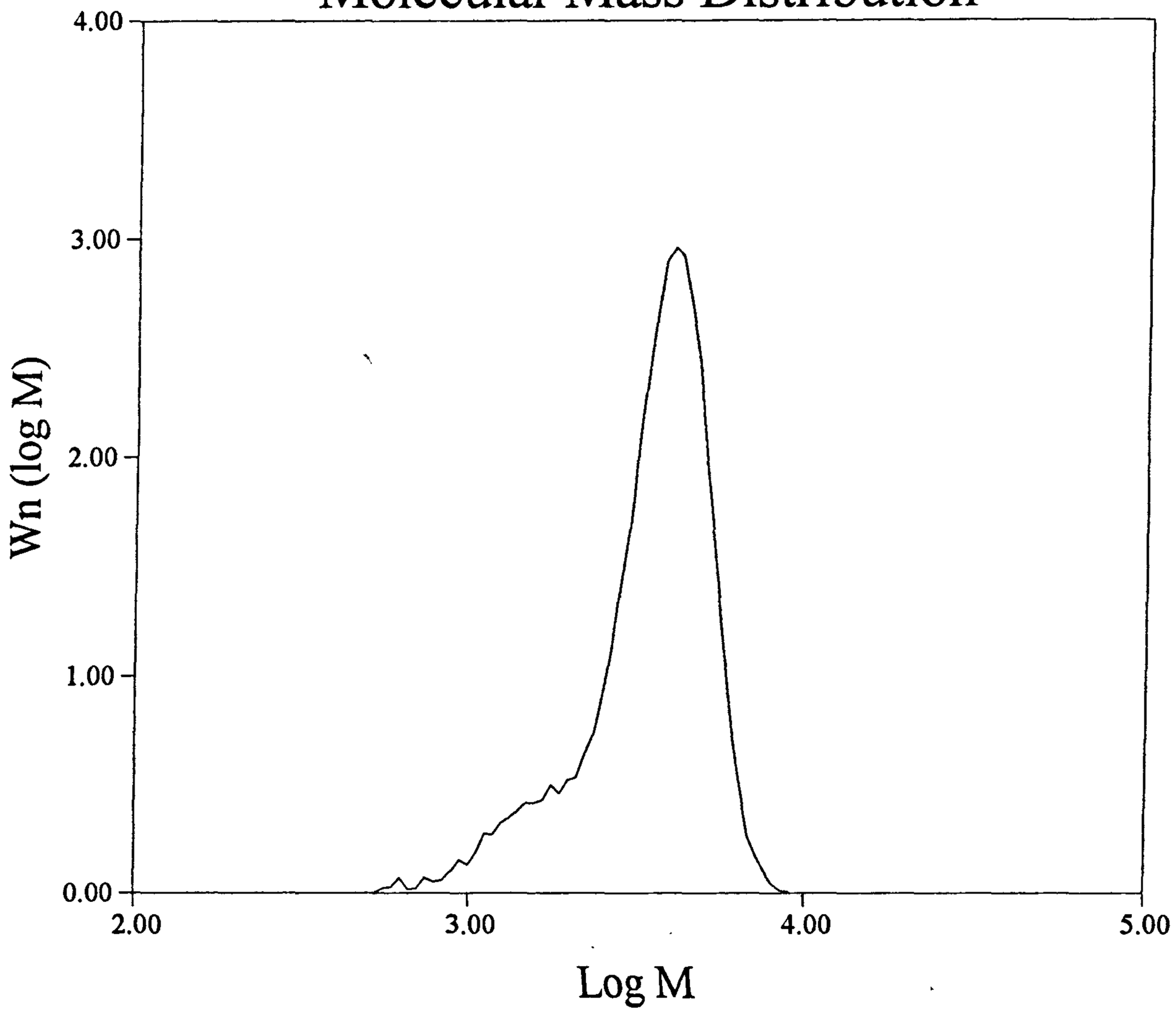


## Molecular Mass Values

| | |
|---|---|
| **Mw:** | 3620. |
| **Mn:** | 3030. |
| **Mp:** | 4010. |
| **Mw/Mn** | 1.19 |

## Parameters

| | |
|---|---|
| CONCENTRATION (mg/ml) | 2.170 |
| FLOW RATE (ml/min) | 1.004 |
| INJECTION VOLUME (ul)) | 200.0 |
| SOLVENT | DMF |
| COLUMNS | B |
| DETECTOR | RI |
| PEAK AREA: | 10.245 |

| | |
|---|---|
| Calibration file: | dmf610.nar |
| Run date: | 03/04/9617:36 |
| Peak Parameters: | dmf610.pkp |
| Tau | 0.143 |
| Sigma | 0.151 |

**Baseline Sets:**

| | | |
|---|---|---|
| Int. limits: | 13.03 | 15.03 |
| baseline: | 11.96 | 15.54 |

**Operator:** BS

# GPC Summary Report

Run No: D957
Sample: SAMPLE 27 (0758)

**Calculation:** Standard Calc

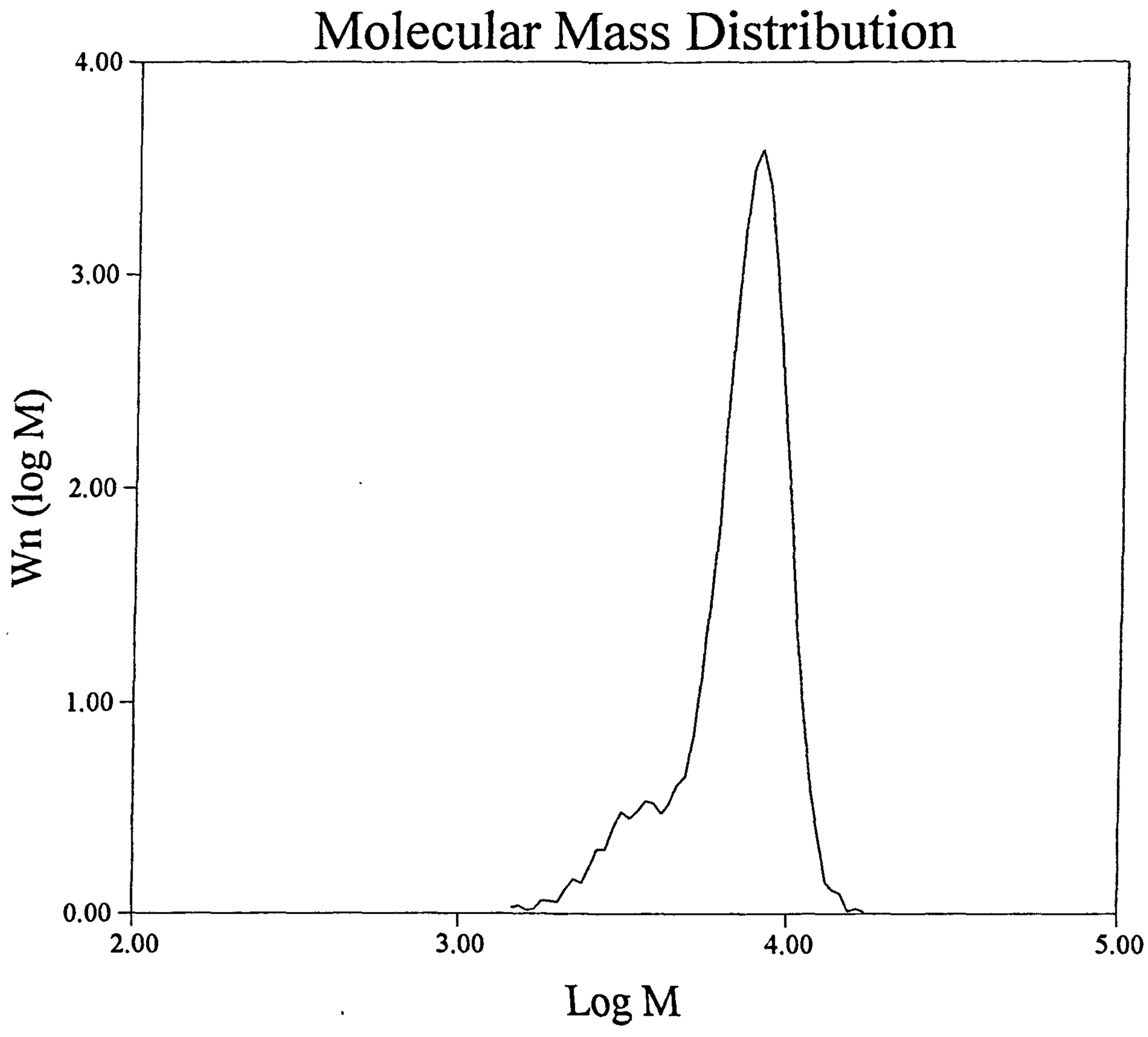


## Molecular Mass Values

| | |
|---|---|
| **Mw:** | 7250. |
| **Mn:** | 6410. |
| **Mp:** | 7980. |
| **Mw/Mn** | 1.13 |

## Parameters

| | |
|---|---|
| CONCENTRATION (mg/ml) | 2.350 |
| FLOW RATE (ml/min) | 1.002 |
| INJECTION VOLUME (ul)) | 200.0 |
| SOLVENT | DMF |
| COLUMNS | B |
| DETECTOR | RI |
| PEAK AREA: | 12.179 |

| | |
|---|---|
| Calibration file: | dmf610.nar |
| Run date: | 03/04/9616:42 |
| Peak Parameters: | dmf610.pkp |
| Tau | 0.143 |
| Sigma | 0.151 |

**Baseline Sets:**

| | | |
|---|---|---|
| Int. limits: | 12.52 | 14.38 |
| baseline: | 11.76 | 19.02 |

**Operator:** BS

# GPC Summary Report

Run No: D962
Sample: SAMPLE 28 (0759)

**Calculation:** Standard Calc

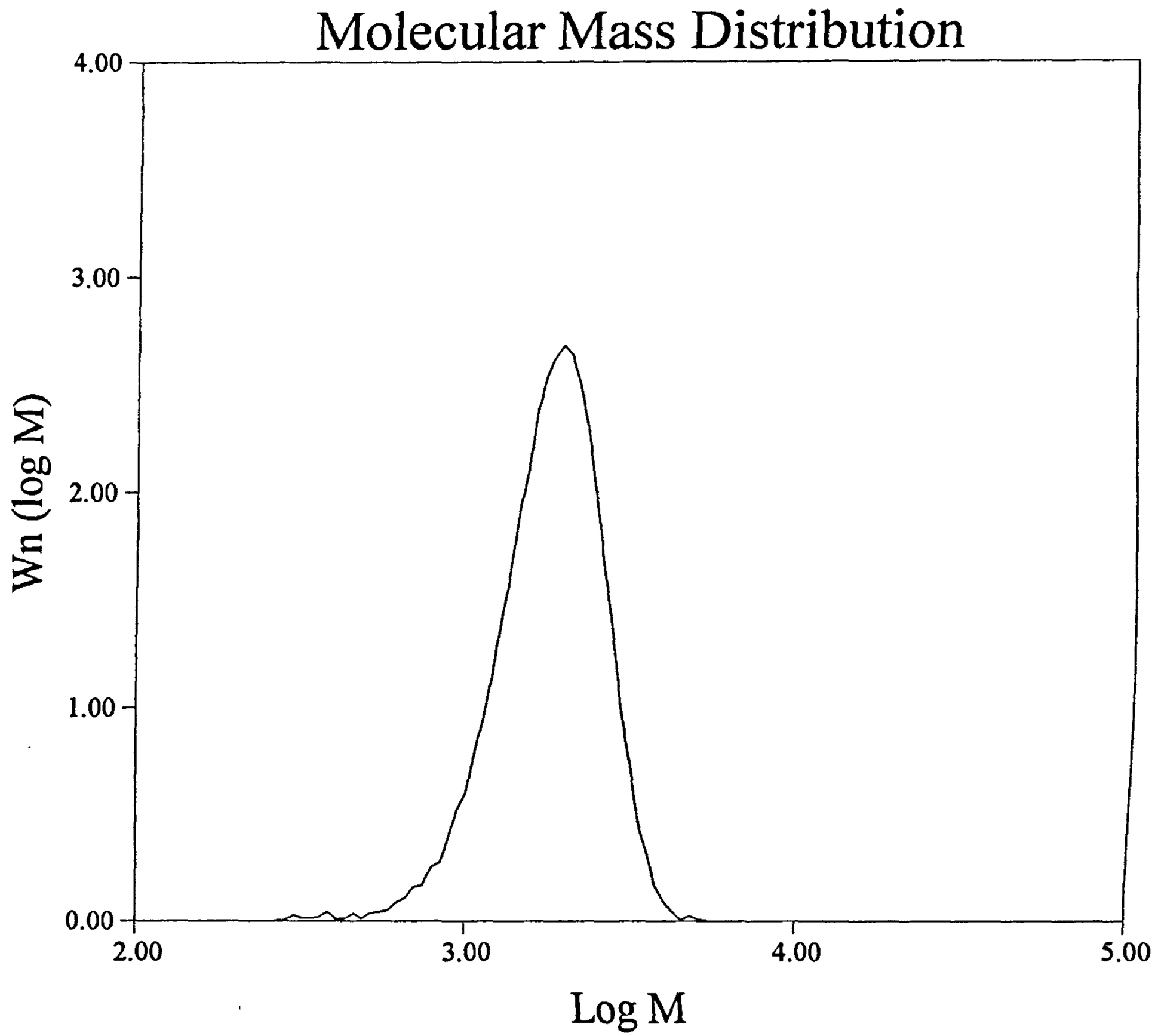


## Molecular Mass Values

| | |
|---|---|
| **Mw:** | 1870. |
| **Mn:** | 1670. |
| **Mp:** | 1960. |
| **Mw/Mn** | 1.12 |

## Parameters

| | |
|---|---|
| CONCENTRATION (mg/ml) | 2.010 |
| FLOW RATE (ml/min) | 0.994 |
| INJECTION VOLUME (ul)) | 200.0 |
| SOLVENT | DMF |
| COLUMNS | B |
| DETECTOR | RI |
| PEAK AREA: | 9.075 |

| | |
|---|---|
| Calibration file: | dmf610.nar |
| Run date: | 03/05/9610:55 |
| Peak Parameters: | dmf610.pkp |
| Tau | 0.143 |
| Sigma | 0.151 |

**Baseline Sets:**

| | | |
|---|---|---|
| Int. limits: | 13.41 | 15.46 |
| baseline: | 12.62 | 20.94 |

**Operator:** BS

# Molecular Mass Distribution

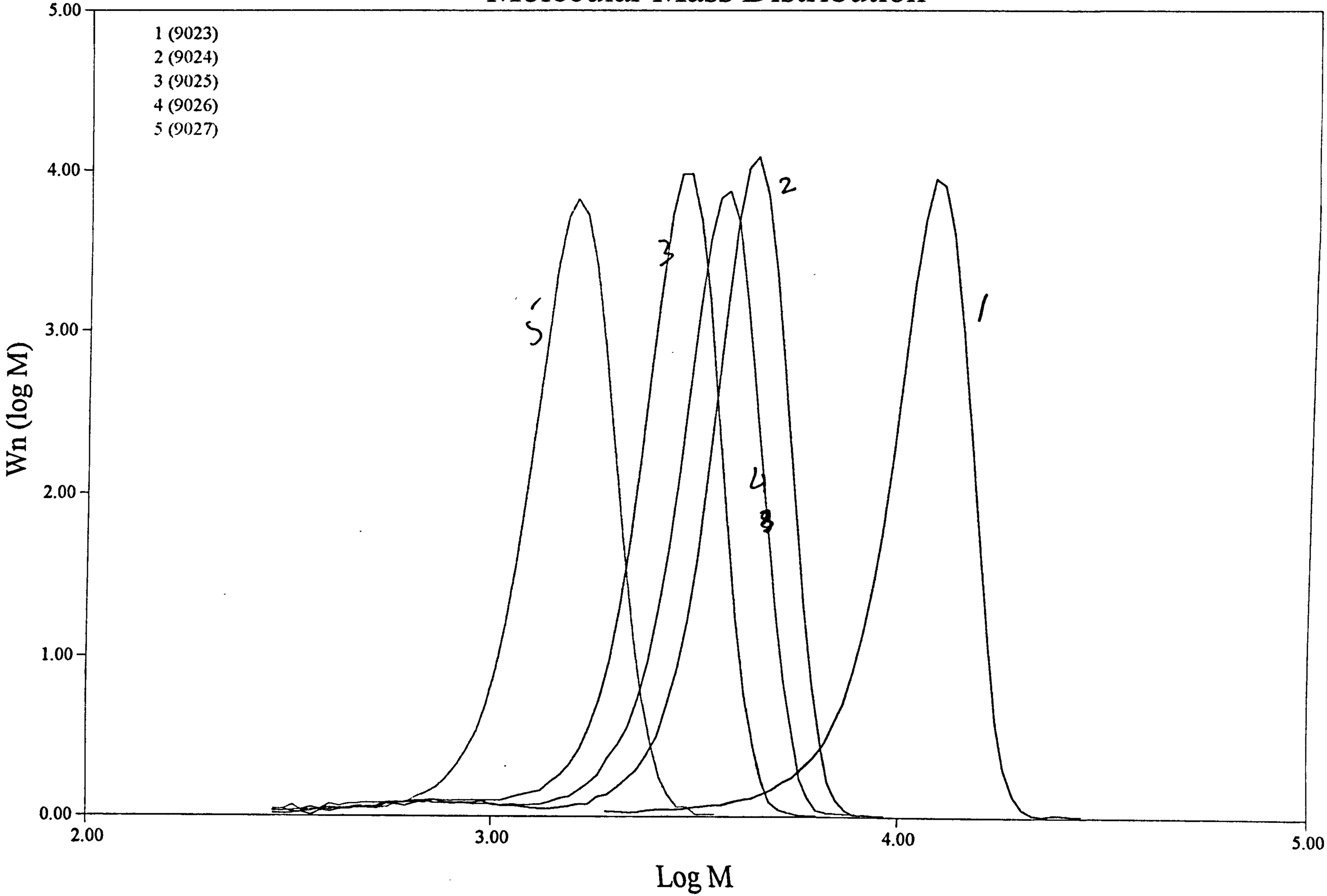

# Molecular Mass Distribution

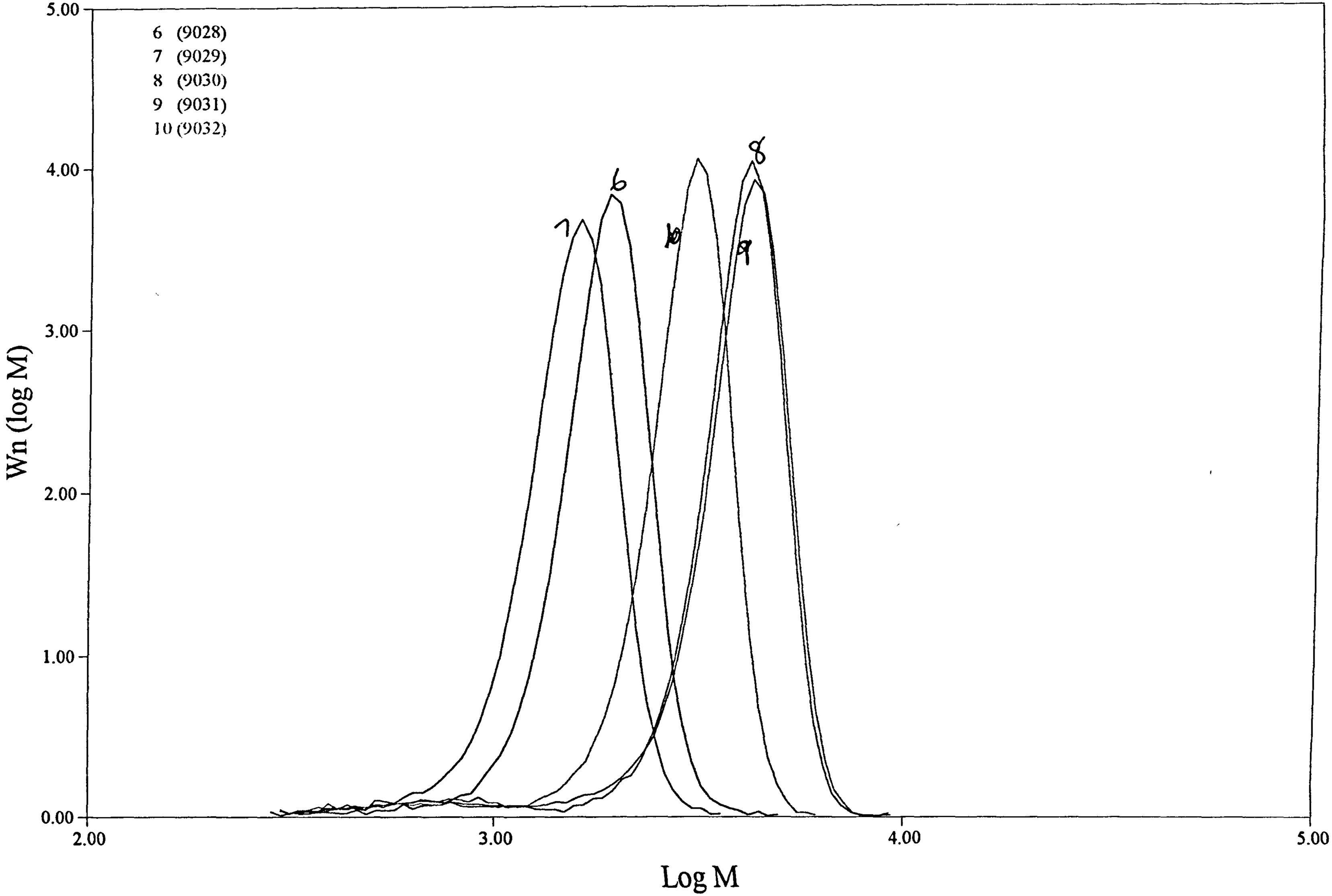

# Molecular Mass Distribution

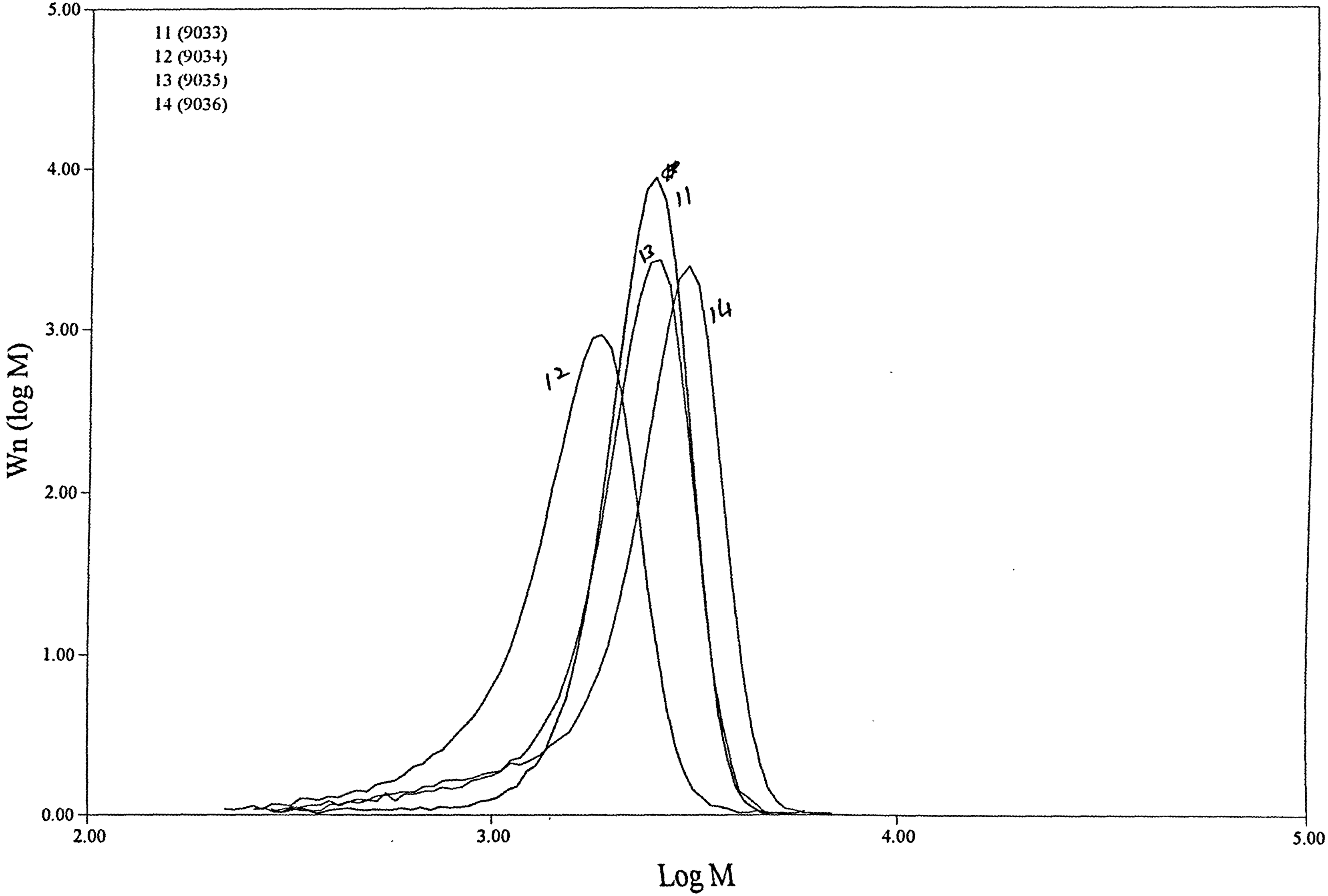

# Molecular Mass Distribution

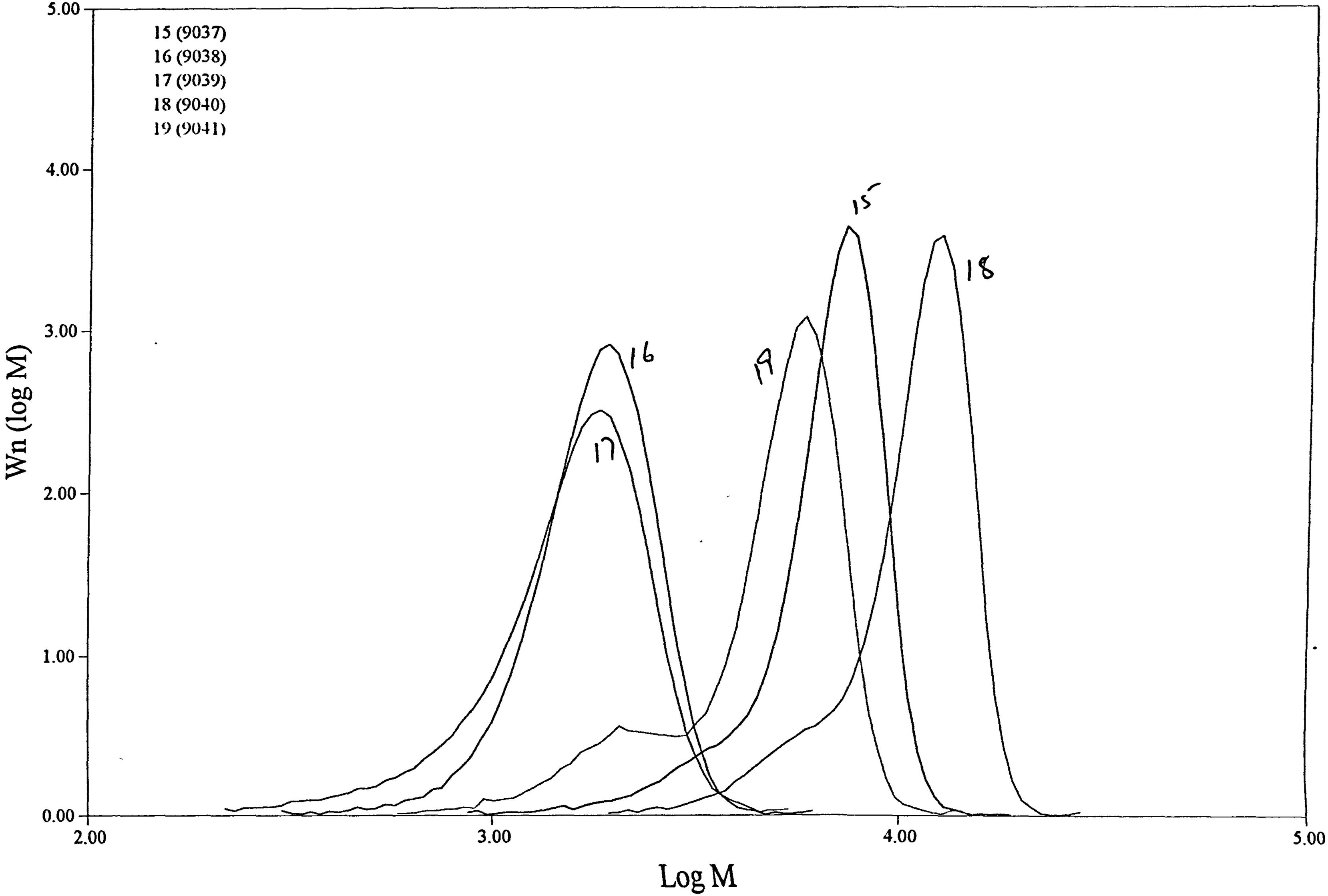

# Molecular Mass Distribution

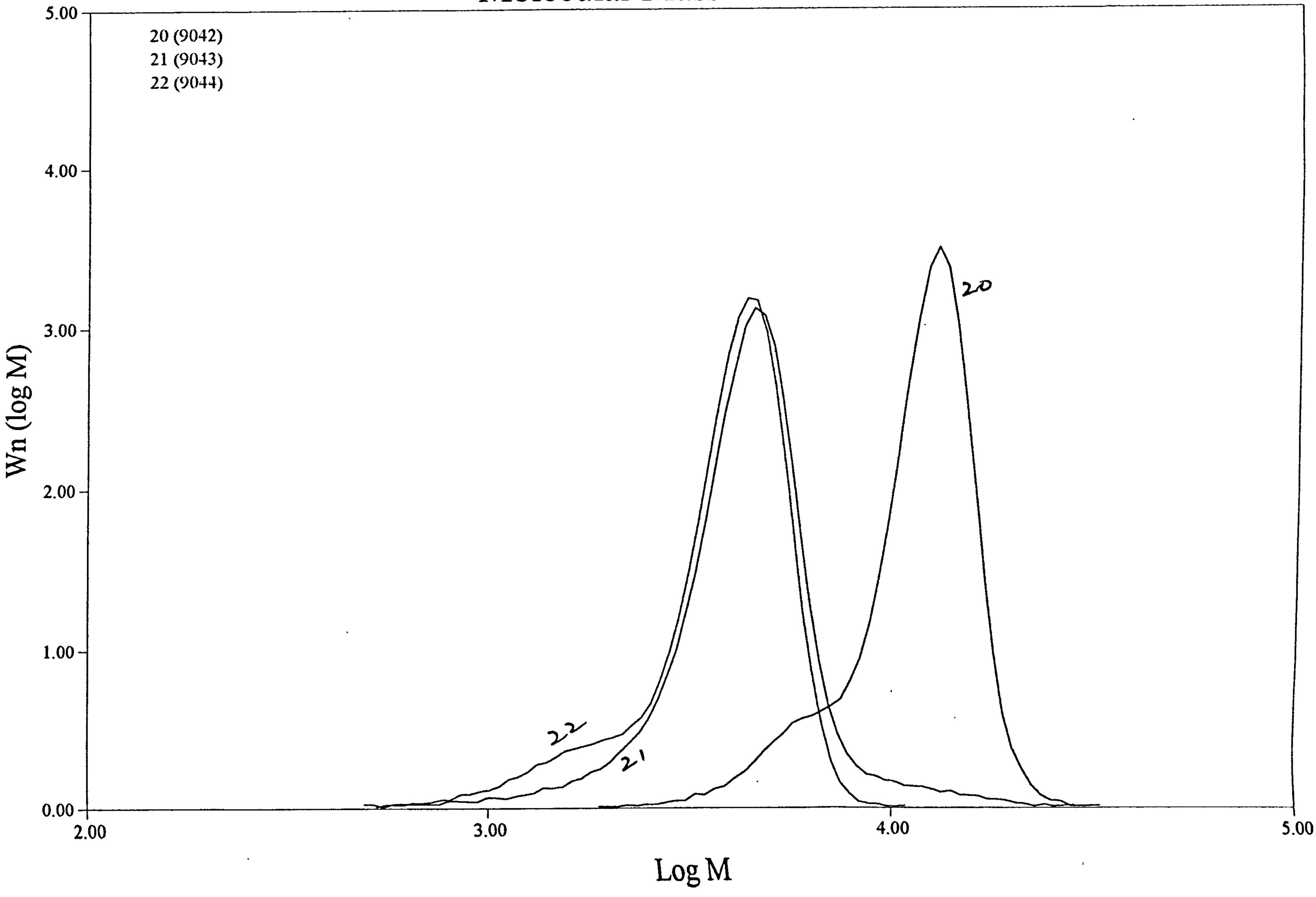

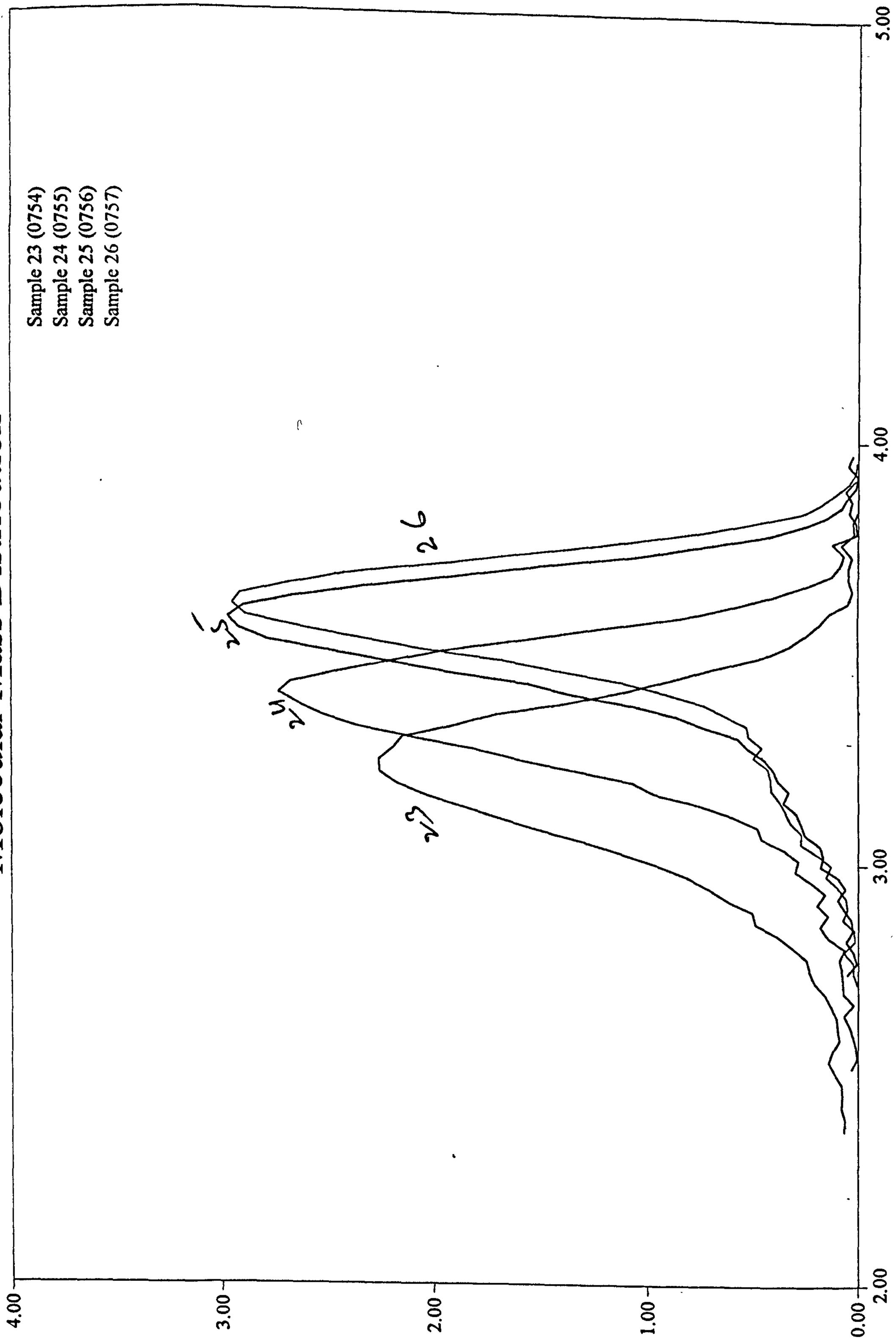
Molecular Mass Distribution
Sample 23 (0754)
Sample 24 (0755)
Sample 25 (0756)
Sample 26 (0757)
5.00
4.00
3.00
2.00
Log M
Wn (log M)
4.00
3.00
2.00
1.00
0.00

Sample 23 (0754)
Sample 27 (0758)
Sample 28 (0759)

Molecular Mass Distribution